INTERNATIONAL DOCTORAL
SCHOOL OF THE USC

Ana Filipa
Pereira da Mota

PhD Thesis

Design and development of soft contact lenses for diabetic eye

Santiago de Compostela, 2022

Doctoral Programme in Drug Research and Development

USC
UNIVERSIDADE
DE SANTIAGO
DE COMPOSTELA

DOCTORAL THESIS

DESIGN AND DEVELOPMENT OF SOFT CONTACT LENSES FOR DIABETIC EYE

Ana Filipa Pereira da Mota

INTERNATIONAL DOCTORAL SCHOOL OF THE UNIVERSITY OF SANTIAGO DE COMPOSTELA

DOCTORAL PROGRAM IN DRUG RESEARCH AND DEVELOPMENT

SANTIAGO DE COMPOSTELA

2022

USC
UNIVERSIDADE
DE SANTIAGO
DE COMPOSTELA

AUTHORIZATION OF THESIS SUPERVISOR

Design and development of soft contact lenses for diabetic eye

Prof. Carmen Álvarez Lorenzo

REPORT:

That the present Thesis, corresponds to the work carried out by Miss **Ana Filipa Pereira da Mota**, under my supervision, and that I authorize its presentation considering it gathers the necessary requirements of article 34 of the USC Doctoral Studies Regulation, and that as supervisor of this Thesis, it does not incur in the abstention causes established by the law 40/2015

In accordance with the Doctoral Studies Regulations, I also declare that this doctoral thesis is suitable to be defended as a Monographic with reproduction of publications, in which the participation of the doctoral student was decisive for its elaboration and the publications are in accordance with the Research Plan.

At **Santiago de Compostela**, on **December 19th, 2022**

USC UNIVERSIDADE DE SANTIAGO DE COMPOSTELA

USC
UNIVERSIDADE
DE SANTIAGO
DE COMPOSTELA

PhD CANDIDATE STATEMENT

Miss. **Ana Filipa Pereira da Mota**

PhD Thesis: **Design and development of soft contact lenses for diabetic eye**

I submit my Doctoral Thesis, following the procedure according to the Regulation, stating that:

1. This Thesis gathers the results corresponding to my work.
2. When necessary, explicit mention is given to the collaborations the work may have had.
3. The present document is the final version submitted for its defense and coincides with the document sent in electronic format.
4. I confirm that the Thesis does not incur in any plagiarism of any other authors or documents submitted by me for obtaining other degrees.

At **Santiago de Compostela**, on **December 19th, 2022**

Sgd. Ana Filipa Pereira da Mota

USC UNIVERSIDADE DE SANTIAGO DE COMPOSTELA

USC
UNIVERSIDADE
DE SANTIAGO
DE COMPOSTELA

Aos meus pais e irmã.

USC
UNIVERSIDADE DE SANTIAGO DE COMPOSTELA

USC
UNIVERSIDADE
DE SANTIAGO
DE COMPOSTELA

AGRADECEMENTOS

Chegado o final desta longa etapa, quero agradecer a todas as pessoas que ao longo deste caminho partilharam comigo o seu conhecimento, ideais, experiências e momentos.

Me gustaría empezar dando las gracias a mi directora de tesis, *Carmen Álvarez Lorenzo* por la oportunidad de realizar este trabajo en su grupo de investigación, por su supervisión, apoyo y consejos a lo largo de estos tres años.

To my co-supervisors, Professor *Angel Concheiro*, Professor *Ana Paula Serro*, Professor *Gonzalo Carracedo* and Professor *Lyndon Jones*, thank you for the suggestions, encouragement and moral support that contributed to my professional and personal growth. I would like to thank everyone from the labs where I did my three secondments, they made me feel like I was one of them since the first day. To the NanoMatLab colleagues, in particular, *Nadia, Ana, Diana, Sofia* and *Pedro*. To the Ocupharm colleagues, *María, Marisa, Bea, Fernando*, and *Cristina*. And, to the CORE colleagues, *Chau, Marilyn, Diane, Piyush, Chris, Megala, Manish* and *David*. Thank you all!

I would like to acknowledge the European Union's Horizon 2020 research and innovation program for the financial support through the Marie Skłodowska-Curie Actions grant agreement Nº 813440 (ORBITAL – Ocular Research by Integrated Training and Learning).

USC
UNIVERSIDADE DE SANTIAGO DE COMPOSTELA

To the ORBITAL team, in particular to *Tess*, *Larry*, *Simon* and the other supervisors thank you for providing me the knowledge and trainings necessary to complete this project. To the ESRs, thank you for the support, motivation and especially for understanding all the difficulties of this PhD work.

A todos mis compañeros de laboratorio, *Xián, Isa, Axel, Patri, Lucía, Miguel, María Pita, Alex,* y *Mariana*, gracias por llenar de alegría mis días! Y, en especial, a *Iago* y *María*, mis compañeros desde el primer día, gracias por todas las risas, por todos los consejos, por ayudarme a seguir adelante cuando todo parecía perdido, gracias por todo!

Às minhas "tugas" preferidas, *Inês, Rita, Diana* e *Carol*, por todo o carinho e companhia nestes últimos meses e, principalmente, por me fazerem sentir um bocadinho mais perto de casa.

A todos os meus amigos que Braga me deu, em especial às minhas "Muchachas", *Andreia, Raquel, Jéssica* e *Cristiana*, obrigada por nunca me deixarem desistir da concretização dos meus objetivos, por acreditarem sempre que eu ia conseguir, até mesmo quando eu já não acreditava! Por todas as longas conversas e, acima de tudo por me terem proporcionado os melhores anos da minha vida e continuarem a fazer parte dela! *Everybody has a home team*!

À minha família, um obrigado enorme por me fazerem perceber que a família é o mais importante e, a nossa é fantástica! Em especial aos meus avós, *Celeste* e *Júlio*, por toda a força que me deram!

Aos pilares da minha vida. Aos meus pais, *Ana Paula* e *Roberto*, e à minha irmã *Inês* obrigada por acreditarem sempre em mim e por me incentivarem a alcançar os meus objetivos, mesmo que sejam a quilómetros de distância. E, por fim, ao *Bruno*, ao meu melhor amigo e namorado, por acompanhar-me em todas as etapas desta tese, por me

USC
UNIVERSIDADE DE SANTIAGO DE COMPOSTELA

ajudar a enfrentar e descontrair nos momentos mais stressantes e complicados e, por celebrar comigo todas as conquistas. Obrigada por me ensinares que o amor é do tamanho do mundo!

A todos, um obrigado do fundo do coração!

USC
UNIVERSIDADE DE SANTIAGO DE COMPOSTELA

USC
UNIVERSIDADE
DE SANTIAGO
DE COMPOSTELA

INDEX

RESUMO **3**

1. INTRODUCTION **21**

1.1 MEDICATED CONTACT LENSES AS DRUG-DEVICE COMBINATION PRODUCTS 25

1.1.1 Regulatory Status *25*

1.1.2 Drug-Eluting CLs in Clinical Trials *28*

1.2 GUIDELINES AND PHARMACOPOEIA METHODS FOR TESTING OCULAR DRUG RELEASE 35

1.2.1 Determining Drug Bioavailability from Drug-CLs using Mathematical Models *35*

1.2.2 Current Official Methods for Testing Drug Release from Topical Ophthalmic Medicines *43*

1.3 *IN VITRO* TESTING OF DRUG RELEASE FROM MEDICATED CLS 49

1.4 *IN VIVO-IN VITRO* RELATIONSHIPS 54

1.4.1 Comparison of In vivo and In vitro Release Profiles *73*

1.4.2 Comparison of In vitro Release Profiles and Therapeutic Outcome *82*

1.4.3 Comparison of In vitro Release Profiles and Drug Accumulation into Anterior and Posterior Segments *91*

1.5 CONCLUSIONS AND FUTURE PERSPECTIVES 102

1.6 REFERENCES 128

2. AIMS **165**

USC UNIVERSIDADE DE SANTIAGO DE COMPOSTELA

3. ATORVASTATIN-ELUTING CONTACT LENSES: EFFECTS OF MOLECULAR IMPRINTING AND STERILIZATION ON DRUG LOADING AND RELEASE 175

3.1 INTRODUCTION.....175

3.2 MATERIALS AND METHODS.....181

3.2.1 Materials.....181

3.2.2 Computational Modeling.....182

3.2.3 Hydrogel Preparation.....183

3.2.4 Hydrogel Characterization.....185

3.2.5 Atorvastatin Loading and Release.....186

3.2.6 HET-CAM Test.....187

3.2.7 Sterilization.....187

3.2.8 FTIR-ATR Analysis.....188

3.2.9 Cytocompatibility Studies.....189

3.2.10 Cornea and Sclera Permeability and Accumulation.....190

3.2.11 Light Stability of Atorvastatin Calcium Solution.....191

3.2.12 Statistical Analysis.....192

3.3 RESULTS AND DISCUSSION.....192

3.3.1 Hydrogels Synthesis and Conditioning.....192

3.3.2 Hydrogels Characterization.....195

3.3.3 Atorvastatin Loading and Release.....197

3.3.4 HET-CAM Test and Cytocompatibility.....202

3.3.5 Effects of Sterilization.....204

3.3.6 Cornea and Sclera Permeability and Accumulation.....216

3.3.7 Stability of Atorvastatin Calcium Solution.....218

USC UNIVERSIDADE DE SANTIAGO DE COMPOSTELA

3.4 CONCLUSIONS 219
3.5 REFERENCES 220
4. CONTACT LENSES FOR PRAVASTATIN DELIVERY TO EYE SEGMENTS: DESIGN AND IN VIVO-IN VITRO CORRELATIONS 235
4.1 INTRODUCTION 235
4.2 MATERIALS AND METHODS 240
4.2.1 Materials 240
4.2.2 Synthesis of Hydrogel Discs and CLs 241
4.2.3 Hydrogel Characterization 242
4.2.4 Pravastatin Loading and Release 244
4.2.4.1 Pravastatin Release from Sterile CLs 245
4.2.5 HET-CAM Test 246
4.2.6 Cytocompatibility and Anti-inflammatory Activity 246
4.2.7 Ex vivo Cornea and Sclera Permeability 248
4.2.8 Sterilization and Stability of Pravastatin-Loaded Hydrogels 250
4.2.9 In vivo Experiments: Drug Release and Tissue Accumulation 250
4.2.9.1 In vivo Release 253
4.2.9.2 Quantification of Pravastatin in Tear Fluid 254
4.2.9.3 Quantification of Pravastatin in Ocular Tissues 254
4.2.10 Statistical Analysis 255
4.3 RESULTS AND DISCUSSION 256
4.3.1 Hydrogels Synthesis and Characterization 256

USC UNIVERSIDADE DE SANTIAGO DE COMPOSTELA

4.3.2 Pravastatin Loading and In vitro Release *259*

4.3.3 Cytocompatibility and HET-CAM *261*

4.3.4 Effects of Sterilization and Light Exposition on Drug Stability and Release *264*

4.3.5 Effects of SLF Volume and Proteins on In vitro Drug Release Profiles *266*

4.3.6 Ex vivo Corneal and Scleral Permeability *270*

4.3.7 Anti-inflammatory Activity *273*

4.3.8 In vivo Studies *276*

4.3.9 In vitro-in vivo Correlations *281*

4.4 CONCLUSIONS 284

4.5 REFERENCES 284

5. IN VITRO – IN VIVO CORRELATION OF DRUG RELEASE PROFILES FROM MEDICATED CONTACT LENSES USING AN IN VITRO EYE BLINK MODEL 299

5.1 INTRODUCTION 299

5.2 MATERIALS AND METHODS 303

5.2.1 Materials *303*

5.2.2 Contact Lens Preparation *304*

5.2.3 Drug Loading *305*

5.2.3.1 Pravastatin Sodium *305*

5.2.3.2 Resveratrol *306*

5.2.4 Eye Blink Model *306*

5.2.4.1 Eyeball and Collection Unit *307*

5.2.4.2 Eyelid *308*

USC UNIVERSIDADE DE SANTIAGO DE COMPOSTELA

5.2.4.3 Flow Rate and Blinking *309*
5.2.4.4 Temperature and Humidity *309*
5.2.4.5 Release Sampling *309*
5.2.4.6 Drug Extraction from the Eyelid and CLs *310*
5.2.5 Release in a Vial *310*
5.2.6 Drug Quantification Methods *311*
5.2.7 Statistical Analysis *312*
5.3 RESULTS AND DISCUSSION 312
5.3.1 3D Eye Blink Model *312*
5.3.1.1 Pravastatin *312*
5.3.1.2 Resveratrol *315*
5.3.2 In vivo Release – Eye Blink Model Comparisons *317*
5.3.2.1 Pravastatin *318*
5.3.2.2 Resveratrol *323*
5.4 CONCLUSIONS 326
5.5 REFERENCES 327
6. BIOINSPIRED MELANIN CONTACT LENSES WITH ANTIBACTERIAL PROPERTIES 335
6.1 INTRODUCTION 335
6.2 MATERIALS AND METHODS 340
6.2.1 Materials *340*
6.2.2 Silicone Hydrogel Discs Preparation *341*
6.2.3 Melanin Synthesis and Incorporation on the Hydrogels *342*
6.2.4 Characterization of Melanin Discs and CLs *343*
6.2.4.1 Raman Spectroscopy *343*

USC
UNIVERSIDADE DE SANTIAGO DE COMPOSTELA

6.2.5 Ciprofloxacin Loading and Release *343*
6.2.6 Light Transmittance and Photothermal Activity *344*
6.2.7 Antibacterial Performance by Isothermal Microcalorimetry *344*
6.3 RESULTS AND DISCUSSION 345
6.3.1 Melanin Incorporation *345*
6.3.2 Light Transmittance and Photothermal Activity *349*
6.3.3 Ciprofloxacin Loading and Release *354*
6.3.4 Antibacterial Performance *357*
6.4 CONCLUSIONS 360
6.5 REFERENCES 361
7. CONCLUSIONS 369
ANNEXES 375

USC
UNIVERSIDADE DE SANTIAGO DE COMPOSTELA

RESUMO

USC
UNIVERSIDADE DE SANTIAGO DE COMPOSTELA

USC
UNIVERSIDADE
DE SANTIAGO
DE COMPOSTELA

RESUMO

A visión é un dos sentidos que xoga un papel máis relevante na interacción social das persoas desde o momento do nacemento ata a vellez. Factores xenéticos, o envellecemento, determinados estilos de vida e comportamentos, as infeccións e unha serie de condicións de saúde son factores de risco importantes para ao desenvolvemento de afeccións oculares que poden comprometer a capacidade de visión.

A diabetes mellitus é un dos maiores desafíos de saúde e está a acadar proporcións epidémicas. A falta de control da glicemia provoca unha variedade de danos en múltiples estruturas dos segmentos anterior e posterior do ollo, desencadeando o desenvolvemento de queratopatía diabética, síndrome do ollo seco, cataratas, glaucoma, retinopatía diabética e edema macular. A concienciación pública sobre as enfermidades oculares está aumentando, o que permite un diagnóstico precoz e o início temprano do tratamento das patoloxías oculares, e xenera unha maior demanda de solucións máis eficaces e amigábeis para o paciente.

Atopar un tratamento eficaz a nivel ocular é un desafío, xa que hai moitos factores a ter en conta para que o fármaco alcance a súa diana. O ollo é un órgano complexo equipado con varias barreiras anatómicas e fisiolóxicas fronte a penetración de fármacos, incluíndo mecanismos de defensa dinámica (parpadeo ou lagrimeo), drenaxe nasolacrimal, os

USC
UNIVERSIDADE DE SANTIAGO DE COMPOSTELA

compoñentes e dinámica da película lacrimal e barreiras anatómicas estáticas (corneal, conxuntival e sanguínea). Un dos retos máis importantes da administración ocular é manter a concentración óptima do fármaco no lugar de acción durante períodos prolongados de tempo. Segundo a zona do ollo afectada (segmento anterior ou posterior), a administración presenta máis ou menos dificultades. A vía sistémica (oral, intramuscular ou intravenosa) úsase raramente, xa que son necesarias doses elevadas de fármaco para alcanzar niveis efectivos nas estruturas oculares, polo tanto asócianse cun un elevado risco de producir efectos secundarios.

A administración tópica en forma de colirios é a máis común entre os métodos clásicos de administración de fármacos ao ollo. Trátase dun procedemento de administración non invasivo, indoloro, cun aceptable grao de cumprimento, que permite conseguir un efecto inmediato. A súa principal desvantaxe é que a biodispoñibilidade ocular dos fármacos administrados é inferior ao 5%, por mor dás barreiras escritas con anterioridade. Isto obriga a efectuar instilacións repetidas de disolucións concentradas a intervalos de tempo curtos, coas consecuentes molestias para o doente e o incremento do risco de que aparezan efectos secundarios a nivel sistémico, xa que parte da dose instilada pode acceder ao torrente circulatorio a través da conxuntiva, mucosa nasal ou tracto gastrointestinal. Entre os enfoques que se propuxeron para dar resposta ao reto de manter concentracións de fármacos suficientemente elevadas na superficie corneal e promover a penetración nas estruturas oculares internas, o uso de lentes de contacto brandas está a gañar un interese cada vez maior.

As lentes de contacto están formadas por entramados poliméricos altamente biocompatibles e son usadas por máis de 100 millóns de persoas para corrixir problemas de visión. As lentes de contacto brandas

USC UNIVERSIDADE DE SANTIAGO DE COMPOSTELA

son hidroxeles altamente porosos e flexibles que poden absorber grandes cantidades de auga. O uso de lentes de contacto como plataformas para a cesión controlada de fármacos oftálmicos foi ideado en 1961 por Otto Wichterle e os seus colaboradores. A partires deste ano, e despois de case 60 anos, Johnson & Johnson Vision logrou a aprobación por parte das respectivas axencias reguladoras para a comercialización da primeira lente de contacto con propiedades antihistamínicas no Xapón e Canadá. Unha vez colocadas no ollo, a lente de contacto atrasa a renovación do fluido na película lacrimal posterior á lente, incrementando o gradiente de concentración de fármaco na córnea e favorecendo o fluxo no tecido. Como resultado, as lentes de contacto minimizan a perda improdutiva de fármacos ao tempo que aumentan a biodispoñibilidade ocular a máis do 50%. A personalización dos tratamentos, a mellora da adherencia do paciente o tratamento e mesmo o control da liberación de fármacos en resposta a estímulos son outras vantaxes potenciais.

A pesar das vantaxes aparentes dun dispositivo de administración de fármacos baseado en lentes de contacto fronte ás gotas tópicas, transformar unha lente de contacto nunha plataforma de liberación de fármacos afronta numerosos desafíos científicos, tecnolóxicos e regulatorios. A maioría dos materiais de lentes de contacto dispoñibles carecen de afinidade polos fármacos oftálmicos. Cando unha lente de contacto se mergulla nunha disolución de fármaco, as moléculas deste difunden á fase acuosa da lente de contacto ata que a concentración tanto na disolución de carga como na fase acuosa do hidroxel este en equilibrio. Se non hai ningunha interacción ou unión do fármaco á rede de polímeros das lentes de contacto, os fármacos libéranse rápidamente cando a lente de contacto cargada de fármacos é colocada na superficie ocular. Nesta situación, non hai vantaxes da combinación de lente de contacto-fármaco en comparación cun colirio. Exploráronse estratexias

USC
UNIVERSIDADE DE SANTIAGO DE COMPOSTELA

para aumentar a carga e limitar a liberación de fármacos, os cales inclúen a copolimerización con monómeros funcionais, a incorporación do fármaco a nanoportadores, a impresión molecular, e os recubrimentos con películas poliméricas e otras barreiras de difusión específicas.

A aplicación de estratexias biomiméticas, baseadas na enxeñaría inversa, permite abordar a selección de monómeros funcionais con criterios máis racionais. A enxeñaría inversa consiste en identificar os aminoácidos e a súa disposición espacial no sitio activo (o lugar onde o fármaco se une á biomacromolécula) e, a continuación, imitar ese sitio activo nos receptores sintéticos da estrutura da lente de contacto. Deste xeito, a estrutura do receptor na biomacromolécula natural serve de guía para deseñar o receptor artificial utilizando monómeros que conteñan grupos químicos similares aos dos aminoácidos do sitio activo do receptor natural. Se o fármaco actúa é porque interactúa con gran afinidade, pero de forma reversible, ca súa diana. Do mesmo modo, as lentes de contacto deben ter unha gran afinidade para que o fármaco sexa incorporado, sendo a interacción reversible para poder liberarse.

Nesta tese de doutoramento o enfoque empregado para aplicar criterios bioinspirados para dotar as lentes de contacto de recoñecemento de moléculas combinouse coa tecnoloxía de impresión molecular. A tecnoloxía de impresión molecular ten como obxectivo dispor os compoñentes do polímero nunha conformación adecuada para crear grupos específicos que actúen como receptores dunha determinada substancia. O enfoque baséase en utilizar as moléculas que se recoñecerán como molde durante a polimerización. Cando se engaden á sopa de monómeros, obrigan aos monómeros a organizarse segundo a súa afinidade. Esta organización faise permanente durante a polimerización, e despois da eliminación das moléculas modelo, o

USC UNIVERSIDADE DE SANTIAGO DE COMPOSTELA

polímero presenta cavidades co tamaño e grupos químicos máis adecuados para acoplar de novo as moléculas modelo.

O segundo reto a superar sobre os sistemas de liberación de fármacos baseados en lentes de contacto céntrase en como relacionar os perfís de liberación *in vitro* co comportamento *in vivo*. Aínda que os requisitos *in vivo* para a liberación do fármaco puidesen predicirse teóricamente a partires das demandas farmacolóxicas e do aclaramento do fármaco, faltan modelos de liberación *in vitro* estandarizados que poidan ser usados para predicir o desempeño das lentes de contacto cargadas con fármacos unha vez colocadas no ollo. A meirande parte dos artigos refírense a perfís de liberación *in vitro* rexistrados en viais, pero utilizando volumes, medios, axitación e substitución de medio moi variables. A selección do volume de cesión é unha cuestión moi relevante; se se escolle un volume demasiado pequeno, o proceso de liberación pode estar controlado pola solubilidade do fármaco e, polo tanto, a capacidade da lente de contacto de regular a liberación do fármaco estaría sendo sobreestimada. En comparación, se se escolle un volume demasiado grande ou se substitúe con frecuencia un volume pequeno, entón a creación dun gran gradiente de concentración pode acelerar forzosamente o proceso de liberación e a lente de contacto pode vaciarse moito máis rápido que en condicións *in vivo*.

Os intentos de imitar mellor o complexo escenario de liberación *in vivo* tense centrado ata o momento no deseño de cámaras microfluídicas que permitan regular tanto o fluxo como o volume total de medio que esta en contacto coa lente. Non obstante, estes dispositivos non foron capaces de reproducir outras condicións fisiolóxicas, incluíndo factores como a forma da córnea e das pálpebras, o grosor da película lacrimal ou o pestanexo. Recentemente empregáronse modelos de ollos *in vitro* impresos en 3D para avaliar *in vitro* as lentes de contacto para desta

USC UNIVERSIDADE DE SANTIAGO DE COMPOSTELA

forma poder superar algúns retos aos que se enfrontan o uso de dispositivos microfluídicos e simular de forma máis adecuada os efectos do fluxo e o volume lacrimal, a exposición ao aire e a frecuencia de pestanexo. Estes modelos 3D aínda están sen validar.

A Tese de Doutoramento formulouse co obxectivo xeral de deseñar e desenvolver lentes de contacto brandas mediante estratexias biomiméticas adecuadas para a carga e liberación de cantidades terapéuticas de fármacos útiles para o tratamento de enfermidades oculares. Dados os efectos positivos das estatinas a nivel ocular, desenvolvéronse dous tipos de produtos combinados: lentes de contacto brandas con atorvastatina e lentes de contacto brandas con pravastatina. O desenrolo deste obxectivo xeral, require facer fronte os retos de: seleccionar os monómeros máis adecuados para cada un dos fármacos, a posta a punto dun proceso de esterilización compatible coa lente de contacto e co fármaco, e a avaliación *in vivo* dos produtos de combinación. Un obxectivo relevante da Tese é avaliar a posibilidade de acadar correlacións *in vitro-in vivo* entre os perfís de cesión de fármaco obtidos no laboratorio empregando viais con volumen definido ou nun modelo de ollo impreso en 3D que simula o fluxo e o pestanexo ocular, e os perfis rexistrado no fluido lacrimal nun modelo animal (coello).

Na parte final deste traballo, abordouse o obxectivo de incorporar melanina as lentes de contacto coa dobre intencionalidade de: avaliar un procedimiento alternativo de incorporar fármacos as lentes de contacto a través da afinidade fármaco-melanina, e de tirar proveito da capacidade da melanina de absorber luz e dar lugar a incrementos localizados de temperatura para conseguir efectos fototérmicos. O traballo centrouse na incorporación de ciprofloxacino e na posible utilidade da terapia antimicrobiana combinada coa fototérmica no

USC UNIVERSIDADE DE SANTIAGO DE COMPOSTELA

tratamento de infeccións bacterianas asociadas ao uso de lentes de contacto en pacientes diabéticos.

De acordo con estes obxectivos, o traballo desenvolveuse en catro fases:

1. Deseño e síntese de lentes de contacto de hidroxel bioinspiradas con afinidade por atorvastatina

As estatinas úsanse amplamente por vía oral como tratamento de primeira liña da hipercolesterolemia e en redución dos riscos de enfermidades cardiovasculares ao inhibir a 3-hidroxi-3-metil-glutaril coenzima A (HMG-CoA) redutasa. Ademais, unha mellor comprensión das vías metabólicas sobre as que poden actuar revelou a súa capacidade pleiotrópica (por exemplo, propiedades anti-inflamatorias, neuroprotectoras e antiproliferativas). A administración oral prolongada de estatinas contribúe a efectos beneficiosos no tratamento dunha variedade de enfermidades oculares, incluíndo ollo seco, retinopatía diabética, dexeneración macular, glaucoma, entre outros.

A atorvastatina cálcica é unha estatina sintética con lipofilia relativamente moderada que pode penetrar nas estruturas oculares se se aplica tópicamente. Os estudos preliminares indican que as solucións oftálmicas de atorvastatina son ben toleradas no tratamento prolongado do ollo seco e da blefarite. A eficacia e seguridade do seu uso para o tratamento de patoloxías oculares podería mellorarse formulando as estatinas como formas de administración tópica ocular que permitan alcanzar concentracións suficientemente elevadas nas estruturas do ollo, evitando efectos sistémicos.

USC UNIVERSIDADE DE SANTIAGO DE COMPOSTELA

Nesta primeira parte da Tese prantexouse a hipótese de que a incorporación de monómeros funcionais no entramado polimérico da lente de contacto pode imitar o sitio activo da HMG-CoA reductasa, comunicando unha afinidade mellorada polas estatinas. Tendo en conta as funcionalidades dos aminoácidos implicados no sitio de unión da HMG-CoA redutase, EGPEM (etilenglicolfenileter metacrilato), AEMA (2-aminoetil metacrilamida) e APMA (N-(3-aminopropil) metacrilamida) foron escollidos como monómeros funcionais despois dun primeiro cribado da interacción coa atorvastatina mediante modelado computacional.

Preparáronse hidroxeles combinando AEMA, APMA e EGPEM en varias proporcións. Todos os monómeros disolvéronse rapidamente no medio de HEMA con excepción do monómero AEMA. Polo tanto, o segundo conxunto de hidroxeles non impresos e impresos preparouse con concentracións máis baixas de monómeros funcionais (30 mM). A cantidade de atorvastatina para impresión molecular correspondeu á proporción molar de fármaco:monómero funcional 1:4.

Os hidroxeles sintetizados caracterizáronse en termos de idoneidade como lentes de contacto (captación de auga, transmisión da luz, propiedades mecánicas e biocompatibilidade) e capacidade para cargar e liberar atorvastatina. Os hidroxeles de APMA foron os candidatos máis prometedores para ser usados como lentes de contacto de liberación de fármacos en canto á cantidade de fármaco cargada e liberada.

Desde o punto de vista da fabricación, a carga e a esterilización no mesmo procedemento é un paso crucial. Implementáronse tres protocolos de esterilización (autoclave, radiación gamma e alta presión hidrostática) e avaliáronse os seus efectos sobre as propiedades do hidroxel. A capacidade de carga dos hidroxeles e a estabilidade da

USC UNIVERSIDADE DE SANTIAGO DE COMPOSTELA

atorvastatina non se viron afectadas pola esterilización de alta presión hidrostática, que pode sustituir vantaxosamente o autoclave e a radiación gamma na esterilización de hidroxeles cargados con atorvastatina, mantendo a estabilidade da atorvastatina e o rendemento dos hidroxeles.

Estudos de permeabilidade a través de córnea e esclera porcinas revelaron que a cantidade de atorvastatina acumulada na córnea e na esclera podería ser eficaz para tratar as enfermidades da superficie ocular.

Os procedementos de esterilización realizáronse durante unha estadía no Centro de Química Estrutural, Departamento de Engenharia Química, Instituto Superior Técnico, Lisboa en colaboración coa Profesora Ana Paula Serro. Os resultados foron publicados na revista internacional Pharmaceutics (DOI: 10.3390/pharmaceutics13050606).

2. Optimizar as lentes de contacto bioinspiradas para administrar pravastatina

As lentes de contacto cargadas con atorvastatina demostraron unha mellora da acumulación de fármacos na córnea e na esclera, pero o fármaco non penetrou ata estratos mais profundos, probablemente debido ao seu elevado peso molecular e á súa hidrofobicidade. Así, o obxectivo desta segunda parte da tese foi incorporar unha estatina máis pequena e hidrófila, como a pravastatina sódica, nos hidroxeles de APMA/ EGPEM preparados anteriormente para mellorar a permeabilidade ocular.

Todos os hidroxeles caracterizáronse en termos de absorción de auga, transmisión de luz, propiedades mecánicas e capacidade de carga

USC UNIVERSIDADE DE SANTIAGO DE COMPOSTELA

e cesión de pravastatina. Tamén se avaliaron os efectos da esterilización mediante alta presión hidrostática e por calor húmido en autoclave. As lentes de contacto que mellores resultados ofreceron cargaron >6 mg/g *in vitro* e a esterilización a alta presión hidrostática non afectou a estabilidade do fármaco nen do entramado do hidroxel.

Fíxose unha análise preliminar de citocompatibilidade e tolerancia ocular con fibroblastos Balb/3T3 e un ensaio da membrana coroalantoidea de ovo de galiña fecundado (HET-CAM). A permeabilidade da pravastatina foi avaliada *ex vivo* usando tecidos de córnea e esclera porcina. Tamén se investigou a actividade anti-inflamatoria dos hidroxeles cargados con pravastatina, mostrando capacidade anti-inflamatoria (TNF-α).

A continuación, unha vez superados con éxito os ensaios preliminares de biocompatibilidade e cumprindo cos principios das 3Rs, planificouse un ensaio *in vivo* en coellos brancos de New Zealand para determinar a seguridade e a tolerancia ocular das lentes de contacto deseñadas e a acumulación de pravastatina nos distintos tecidos oculares. Como control empregouse unha disolucion de pravastatina coa mesma dose de fármaco que o liberado polas lentes de contacto. Esta parte do traballo levouse a cabo en colaboración co Profesor Gonzalo Carracedo en Ocupharm, Universidade Complutense de Madrid. Os protocolos foron aprobados polo Comité de Experimentación Animal da Universidade Complutense de Madrid, co correspondente permiso do Comité de Ética e cumprindo cas directrices ARVO e ARRIVE. Un obxectivo adicional dos estudos *in vivo* foi identificar as condicións de liberación *in vitro* que poidan proporcionar correlacións *in vitro-in vivo* (IVIVC).

As probas *in vivo* confirmaron que, en comparación cos colirios as lentes de contacto proporcionaron niveis significativamente máis altos

USC UNIVERSIDADE DE SANTIAGO DE COMPOSTELA

de pravastatina na lagrima entre 1 e 7 horas despois do uso. Ademais, despois de 8 h, a pravastatina estaba presente na córnea, esclera, humor acuoso e humor vítreo. Finalmente, a construcción do gráfico de Levy co fin de por de manifesto correlacións *in vivo-in vitro* (IVIVC), mostrou a existencia de fortes correlacións entre as porcentaxes de fármaco liberado *in vitro* e *in vivo*. A presenza de proteínas no medio de liberación *in vitro* favoreceu as IVIVC.

Os resultados desta segunda parte da Tese foron publicados na revista Journal of Controlled Release (DOI: 10.1016/j.jconrel.2022.06.001).

3. Predicir o comportamento *in vivo* de lentes de contacto medicadas mediante un modelo *in vitro* de ollo impreso en 3D que simula o fluxo e o pestanexo ocular

A maioría dos estudos *in vitro* para avaliar a cesión de fármacos das lentes de contacto empregan un modelo de vial de volume fixo sen protocolos estandarizados. Como consecuencia, non se dispón dunha guía normalizada para levar a cabo os ensaios *in vitro* nen se ten información sobre en qué medida os resultados *in vitro* poden servir para predicir os resultados *in vivo*. Isto significa que aínda son necesarios probas *in vivo* en modelos animais e estudos clínicos en humanos, mesmo para avaliar produtos combinados de fármacos-lentes de contacto en fase inicial, o que fai que o desenvolvemento sexa moi custoso en tempo e recursos.

Os modelos de ollos *in vitro* que imitan o escenario *in vivo* e os parámetros oculares chave teñen recibido atención nos últimos anos. Recentemente desenvolvéronse modelos de ollos *in vitro* impresos en

USC UNIVERSIDADE DE SANTIAGO DE COMPOSTELA

3D para avaliar o comportamento das lentes de contacto simulando os efectos do fluxo, volume do fluido lacrimal, a exposición ao aire e a frecuencia de pestanexo. O modelo de ollo impreso en 3D utilizado nesta terceira parte da Tese foi desenvolvido polo Profesor Lyndon Jones e o Doutor Chau Minh-Phan no CORE (Centre of Ocular Research and Education) da Universidade de Waterloo. O modelo consiste nun globo ocular feito de resina que simula a superficie ocular do ollo e unha pálpebra de alcohol polivinílico que se desliza sobre o globo ocular ou sobre as lentes de contacto adaptadas, espallando a solución lacrimal (subministrada a través dun tubo que está unido ao soporte da pálpebra). A solución de saída recóllese na unidade de recollida situada debaixo do globo ocular. No estudo desenvolvido, probouse a liberación *in vitro* no modelo de ollo a dous fluxos diferentes (5 e 10 µL/min) e unha velocidade de parpadeo de 1 pestanexo/10 s.

Para coñecer as correlacións *in vitro-in vivo*, o obxectivo deste traballo foi analizar os perfís de liberación das lentes de contacto cargadas con fármacos neste modelo *in vitro* impreso 3D e comparar os resultados obtidos coa liberación dun vial e cos niveis de fármaco detectados no fluido lacrimal *in vivo* en modelo animal. Probáronse lentes de contacto cargadas con dous fármacos, pravastatina e resveratrol, de propiedades fisicoquímicas distintas.

A cesión de ambos fármacos foi máis sostida e menor no modelo 3D en comparación coa liberación *in vitro* en viais. Ambos fármacos presentaron perfís de cesión similares no modelo 3D e *in vivo*, aínda que a cantidade total de fármaco liberado no modelo 3D foi significativamente menor que *in vivo*, especialmente para o resveratrol. Atopáronse fortes correlacións entre as porcentaxes de pravastatina liberada no modelo 3D (fluxo de 10 µl/min) e *in vivo*. A información recollida no presente estudo pode servir para coñecer os parámetros

USC UNIVERSIDADE DE SANTIAGO DE COMPOSTELA

fisiolóxicos relevantes que inflúen na liberación de fármaco a partir de lentes de contacto *in vivo*, como a composición do fluído lacrimal, o fluxo lacrimal, a temperatura do sistema e a composición da superficie do globo ocular. Os resultados obtidos poden servir de guía para mellorar o modelo 3D de pestanexo.

Os experimentos con modelos de ollo 3D realizáronse en colaboración co Profesor Lyndon Jones e o Doutor Chau Minh-Phan no CORE (Centre for Ocular Research & Education) na Universidade de Waterloo durante una estadía de tres meses, e o correspondente manuscrito foi aceptado para publicación na revista Drug Delivery and Translational Research (DOI: 10.1007/s13346-022-01276-6).

4. Uso de melanina para comunicar as lentes de contacto de afinidade por fármacos específicos e dotalas de capacidade de resposta fototérmica

A melanina é un pigmento natural que está presente en microorganismos, animais e plantas e presenta unha variedade de funcionalidades, incluíndo pigmentación, eliminación de radicais, protección contra a radiación e regulación térmica. A melanina a nivel ocular (eumelanina) actúa como un reservorio de unión química ao retener os fármacos dentro das células pigmentadas e influí na súa biodistribución. Ademais, a melanina ten unha característica importante para converter a luz absorbida en calor. O aumento rápido e local da temperatura através da melanina demostrou ser un método prometedor para matar bacterias sen risco de resistencia bacteriana o efectos secundarios.

USC UNIVERSIDADE DE SANTIAGO DE COMPOSTELA

A diabetes mellitus leva a cambios significativos en varios tecidos e estruturas do ollo. Os pacientes diabéticos teñen unha barreira epitelial corneal debilitada que pode levar a infeccións bacterianas da córnea e da conxuntiva. Na última parte da Tese, abordouse o obxectivo de incorporar melanina as lentes de contacto coa dobre intencionalidade de: avaliar un procedimiento alternativo de incorporar fármacos as lentes de contacto a través da afinidade fármaco-melanina, e de tirar proveito da capacidade da melanina de absorber luz e dar lugar a incrementos localizados de temperatura para conseguir efectos fototérmicos.

Incorporouse melanina en discos de hidroxel de silicona e dous tipos de lentes de contacto comerciais, e realizáronse probas adicionais para identificar a presenza de melanina nestes hidroxeles. A incorporación de melanina fíxose somerxendo os discos ou lentes nunha disolución de L-DOPA (L-3,4 dihidroxifenilalanina) oxidada por tirosinasa por distintos tempos de incubación.

Avaliouse a capacidade fototérmica da melanina nos discos e lentes e observouse un aumento máximo de 20 graos en 10 segundos na zona tratada nos discos incubados en melanina por 16 h.

Os discos de silicona e lentes de contacto foron cargados con ciprofloxacino, un antibiótico, e a cantidade de ciprofloxacino cedida foi maior nos discos de silicona con melanina incorporada. Ademais, a cantidade de ciprofloxacino liberada dos discos de hidroxel de silicona promoveu unha inhibición significativa do crecemento de *S. aureus* rexistrado mediante microcalorimetría isotérmica.

USC UNIVERSIDADE DE SANTIAGO DE COMPOSTELA

En conxunto, as estratexias bioinspiradas desenvolvidas nesta Tese de Doutoramento permiten obter produtos combinados fármaco-lente de contacto que proporcionan niveis sostidos de fármacos na superficie ocular e tamén permiten unha terapia fototérmica factible de enfermidades do segmento anterior do ollo. Ademais, identificáronse procedementos de ensaio *in vitro* que imitan a cesión de fármacos na superficie ocular, o que pode facilitar a implementación de metodoloxías cas que se poidan acadar correlacións *in vitro-in vivo* relevantes. Esta información debe server para simplificar o desenvolvemento de lentes de contacto medicadas.

USC
UNIVERSIDADE DE SANTIAGO DE COMPOSTELA

USC
UNIVERSIDADE
DE SANTIAGO
DE COMPOSTELA

INTRODUCTION

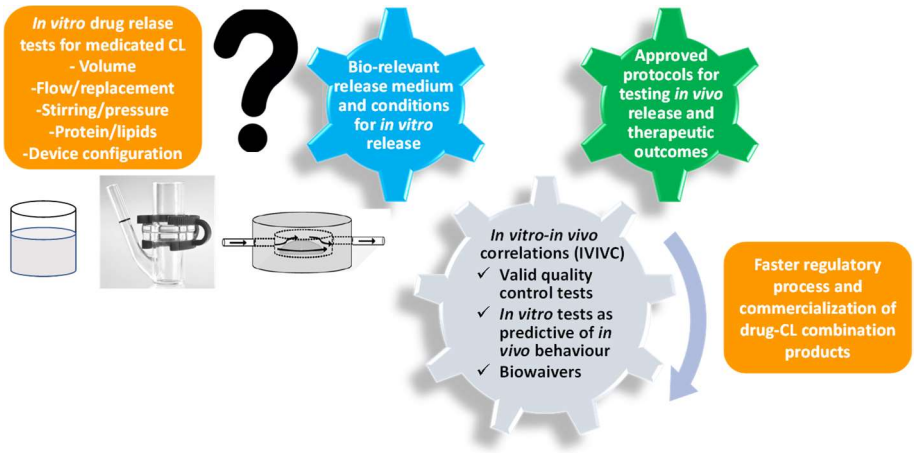

The work described in this chapter was published in **Testing drug release from medicated contact lenses: The missing link to predict *in vivo* performance**, *Journal of Controlled Release* 343, 2022, 672-702, authored by

Ana F. Pereira-da-Mota[a], Chau Minh-Phan[b,c], Angel Concheiro[a] Lyndon Jones[b,c], and Carmen Alvarez-Lorenzo[a]

[a]Departamento de Farmacología, Farmacia y Tecnología Farmacéutica, I+D Farma Group (GI-1645), Facultad de Farmacia, Instituto de Materiales (iMATUS) and Health Research Institute of Santiago de Compostela (IDIS), Universidade de Santiago de Compostela, 15782 Santiago de Compostela, Spain.

[b]Centre for Ocular Research & Education (CORE), School of Optometry and Vision Science, University of Waterloo, Waterloo, ON, Canada.

[c]Centre for Eye and Vision Research (CEVR), 17W, Hong Kong, Science Park, Hong Kong.

USC UNIVERSIDADE DE SANTIAGO DE COMPOSTELA

USC
UNIVERSIDADE
DE SANTIAGO
DE COMPOSTELA

1. INTRODUCTION

The world's first drug-releasing contact lens (CL) was recently approved by the appropriate regulatory bodies in both Japan and Canada [FDA News, 2021; Johnson & Johnson Vision Care, 2021. Although this approval was only specific to a drug (ketotifen)-CL combination, it nonetheless represents a significant milestone in the already long journey to obtain drug-CL combination products. Indeed, 2021 marked the 60th anniversary of the patent by Otto Wichterle and colleagues on the preparation of poly(2-hydroxyethylmethacrylate), pHEMA, soft CLs by the spin casting process [Wichterle, 1961]. pHEMA hydrogels revealed excellent optical properties and biocompatibility [Wichterle and Lim, 1960; Kopeček, 2009], and their moderate water content immediately caught the attention of Wichterle and Lim as a suitable compartment to host drugs, as stated in their US Patent 3,220,960 "*medicinally active substances (...) may be dissolved in the aqueous constituent of the hydrogels to provide medication over an extended period*" [Wichterle and Lim, 1965].

In these pioneering patents, the potential for using soft CL materials as drug delivery devices that can both act as an optical correction device and also provide therapeutic treatment for ocular diseases was implicit. However, the commercialization of both applications was not so straightforward. After the patent publication in 1961 it took Bausch + Lomb a further 10 years to bring soft CLs to the

USC UNIVERSIDADE DE SANTIAGO DE COMPOSTELA

market (SofLens in 1971, 50 years ago), and another 50 years for a company to obtain approval for a true drug delivering CL (Johnson & Johnson's ACUVUE Theravision) [FDA News, 2021; Johnson & Johnson Vision Care, 2022]. The enormous amount of time and research efforts invested up to this point are proof of how difficult it is to develop drug-releasing CLs (which are "combo devices" as they are considered both a device and a drug product), as opposed to just a CL device that solely corrects a visual deficit [González-Chomón et al., 2013].

There are several advantages to using CLs that elute drugs onto the ocular surface over conventional eye drops. It is known that a large number of patients prescribed drops are non-compliant with instilling them at the dosing frequency they are advised to, with non-adherence ranging from 5% to 80% for patients prescribed glaucoma medications [Olthoff et al., 2005]. A medicated CL that was inserted and worn for an extended period of time would overcome such an issue. Only a small and varying volume of an eye drop effectively contacts the ocular surface, which is then rapidly cleared from the eye due to rapid tear fluid turnover or absorbed through the conjunctiva. Combined with the low permeability of the cornea, it is estimated that less than 5% of the instilled drug is bioavailable [Hughes et al., 2005]. In contrast, a CL may provide more accurate dosing as a known amount of loaded drug (or drugs) is placed on the surface of the eye. The presence of a CL delays tear turnover in the post-lens tear film, thereby creating a higher drug concentration gradient towards the cornea and favoring flux into the tissue. As a result, the CL approach minimizes unproductive drug loss while increasing ocular bioavailability to more than 50% [Lanier et al., 2020]. Personalization of treatments, improved patient compliance, and even stimuli-responsive control of drug release are other potential advantages [Alvarez-Lorenzo et al., 2019]. Integration

USC UNIVERSIDADE DE SANTIAGO DE COMPOSTELA

of diagnosis components into the CLs may open the door to advanced ocular biosensors that can perceive changes of biorelevant biomarkers in real-time. These theranostic devices would not only alert the patients to potential worsening of their disease, but also be able to adjust the drug release rates to match the therapeutic amounts needed to treat the relevant disease [Jones et al., 2021; Shin et al., 2021; Savariraj et al., 2021].

Despite the apparent advantages of a CL-based drug delivering device over topical drops, transforming a CL into a drug-releasing platform faces numerous, formidable scientific, technological and regulatory challenges. To a large extent, these challenges are related to two major issues:

(a) the aqueous phase of the CL is insufficient by itself to host and control the release of the required dose;

(b) the drug release rate to maintain therapeutic levels for an extended period of time is unknown and cannot be directly extrapolated from previous data on eye drops.

Most commercially available CL materials lack affinity for ophthalmic drugs. When these materials are soaked in a drug solution, the drug molecules diffuse towards the aqueous phase of the CL until the concentration in both the loading solution and the aqueous phase of the hydrogel is at equilibrium. If there are no interactions or binding of the drug to the CL polymer network, then the drugs will be released very rapidly when the drug-loaded CL is applied onto the ocular surface. In this situation, there are no real advantages of the drug-CL combination in comparison to an eye drop. Strategies to address poor loading and limited control of drug release have been widely explored and include copolymerization with functional monomers, incorporation

USC UNIVERSIDADE DE SANTIAGO DE COMPOSTELA

of the drug into nanocarriers, and specific diffusional barriers [Alvarez-Lorenzo et al., 2019; Savariraj et al., 2021; Toffoletto et al., 2021].

The second issue of how to relate the *in vitro* release profiles with *in vivo* performance is even more complex and has been largely unexplored [Wuchte et al., 2021]. Even if the *in vivo* requirements for the drug release could be theoretically predicted from pharmacological demands and pharmacokinetic clearance, there are still a lack of standardized *in vitro* release models that can be used to predict the performance of drug-loaded CLs once placed onto the eye.

The purpose of this chapter is to shed light on biorelevant ways of evaluating *in vitro* drug release from CLs and the feasibility of establishing *in vitro-in vivo* correlations (IVIVC) to predict *in vivo* performance. First, the chapter will briefly address the regulatory status and specific opportunities and challenges of drug-releasing CLs. Regulatory agency guidelines and drug release tests collected in the Pharmacopoeias and specialized reports are examined and their possible adaptation to medicated CL discussed. The chapter covers the variety of *in vitro* release tests used to examine drug-CL interactions in the last two decades. Although the information available on *in vivo* drug release profiles from CL materials to tear fluid is still limited, IVIVC are attempted. Papers reporting both *in vitro* release profiles and either *in vivo* release or therapeutic response are analyzed in detail. Finally, key points to be considered for *in vitro* testing drug release from a medicated CL are highlighted. The information reviewed in this chapter may serve as a guide to harmonize drug-CLs *in vitro* testing and facilitate the translation of medicated CLs to the clinical arena.

USC UNIVERSIDADE DE SANTIAGO DE COMPOSTELA

1.1 MEDICATED CONTACT LENSES AS DRUG-DEVICE COMBINATION PRODUCTS

1.1.1 Regulatory Status

CLs are ocular prosthetic devices (i.e., ocular medical devices) used by approximately 150 million people worldwide, and they can be worn to correct vision impairment or for cosmetic or therapeutic reasons [Review of Cornea & Contact Lenses, 2021]. Regarding vision correction, CLs have some advantages over spectacles. Some patients report that their visual acuity is better with CLs than with glasses. CLs do not become foggy due to changes in temperature, humidity or when breathing through a protective mask. Additionally, they do not move or fall off during high-intensity activities. In contrast, the use of CLs poses increased risk of ocular infections, inflammation, and dry eyes. Also, as the age of the users increases, the chance of discontinuing lens wear increases due to CL associated dryness complaints [Pucker and Tichenor, 2020].

Regulatory agencies, such as the Food and Drug Administration (FDA) and the European Medicines Agency (EMA), classify CLs according to their intended use:

(1) non-therapeutic CLs – intended for correction of refractive ametropia, aphakia, and presbyopia;
(2) specialized use CLs – these include orthokeratology (ortho-K) lenses that cause a temporary change in corneal curvature to eliminate any refractive error and decorative (plano) lenses for fashion/cosmetic purposes;
(3) therapeutic CLs – these serve as a tool in the management of a wide variety of ophthalmic disorders refractory to other

USC UNIVERSIDADE DE SANTIAGO DE COMPOSTELA

treatment modalities, including pain relief, promotion of epithelial healing, corneal protection from mechanical damage,

(4) correction of an irregular corneal surface, and deliver medication [FDA, 2018a; Lim and Lim, 2020]. Drug release could be pursued for treatment of both general ocular diseases (e.g., seasonal allergies, as is the case for the approved ketotifen-releasing CL) and CL-related disorders (e.g., infection or dry-eye syndrome).

According to the FDA definition, a medical device is "*an instrument, apparatus, implement, machine (…) intended for use in the diagnosis of disease or other conditions, or in the cure, mitigation, treatment, or prevention of disease, in man or other animals, or intended to affect the structure or any function of the body of man or other animals, and which does not achieve its primary intended purposes through chemical action within or on the body of man or other animals and which is not dependent upon being metabolized for the achievement of any of its primary intended purposes*" [FDA, 2018b]. Therefore, a medical device is expected to achieve its purpose by means of physical or electronic actions. In contrast, drugs achieve their action by chemical actions. CLs as medical devices (as well as the lens care solutions) are under strict regulatory oversight from their design to postmarketing surveillance, with the aim to ensure patient safety and device efficacy. According to the risk profile that the patient may be exposed to, daily-wear CLs are labelled as Class II medical devices (moderate risk), while extended-wear CLs and ortho-K CLs are labelled as Class III medical devices (higher risk). Readers interested in a comparative analysis of FDA and European regulation on CLs should refer to a recent review [Zaki et al., 2019].

USC UNIVERSIDADE DE SANTIAGO DE COMPOSTELA

Overall, the many hurdles that should be solved to achieve the regulatory approval involve largely time (up to 31 months in USA) and investment (up to 77% of the total expenses required to bring the product to the market) [Hobson, 2017]. These expenditures cause substantial delays in the time a new product takes to become commercially available and may impede industrial innovations in CL materials and new designs. Transforming a CL into a drug-releasing CL requires changes in the composition and design that necessitate additional regulatory steps. Furthermore, if a drug-CL only addresses a small market segment, then commercialization may not be financially viable.

Even when CLs are only used as ophthalmic medical devices, the potential interactions of the polymer network to attract oppositely charged or hydrophobic drugs should be taken into consideration when the wearer has to apply eye drops with the lens *in situ*. Some reports have warned about the need to space the time between applying an eye drop and putting the CL onto the surface of the eye to avoid loss of drug by irreversible uptake by the CL [Kenley et al., 2013].

CLs designed for the purpose of drug-releasing platforms are considered as drug-device 'combination products'. As defined in 21 CFR 3.2(e), a combination product is comprised of two or more regulated components (i.e., in this case a drug and a device). Each component retains its regulatory identity, and additionally the combination product as a whole is subject to specialized regulatory requirements [FDA, 2013, 2016]. A drug-releasing CL is classified as the type of device coated/ impregnated/ otherwise combined with a drug in which the device has an additional function in addition to delivering the drug [FDA, 2018c]. In the USA, evaluation of a drug-releasing CL is assigned to a certain agency center depending on which component

USC UNIVERSIDADE DE SANTIAGO DE COMPOSTELA

provides the primary mode of action (PMOA). The agency center with the primary jurisdiction then works together with the other agency centers to carry out the adequate premarket review.

In the case of a drug-releasing CL used for vision correction that simultaneously delivers a drug for an ocular disease (device-led combination product), substantial equivalence to a predicate product (e.g., the CL device solely) does not apply, since the addition of the drug results in a new intended use and/or implies a change in the technological characteristics, which in turn raises additional questions regarding safety and effectiveness [FDA, 2019a]. If the drug makes the greatest contribution, for example, a plano power bandage CL that does not correct any residual refractive error but releases a drug onto the ocular surface, then the drug-led combination product would follow the "new drug application" pathway and demonstrate the safety and the effectiveness of the product in the new conditions of use. Although examples of drug releasing CLs are not included in the FDA guidelines, illustrative examples that refer to related device-led and drug-led combination products may be useful to understand the long regulatory pathway for a drug-CL combination product [FDA, 2019a].

1.1.2 Drug-Eluting CLs in Clinical Trials

The lack of predicate products implies that the safety and efficacy of a drug-releasing CL should be demonstrated in clinical trials. The search in ClinicalTrials.gov of "contact lens AND drug" (April 2021) led to 344 outcomes. Most clinical trials referred to safety studies of new CL or drugs after ocular or oral administration when they were administered sequentially, not as a combination product. Only 16 clinical trials referred to true drug-CL combination products (**Table**

USC UNIVERSIDADE DE SANTIAGO DE COMPOSTELA

1.1). In addition to the antihistamine/mast cell stabilizer ketotifen, other drugs of interest include those intended for the treatment of macular edema (dexamethasone), glaucoma and ocular hypertension (e.g., latanoprost, timolol and dorzolamide), pain management after photorefractive keratectomy, dry eye symptoms, and persistent epithelial defects.

Although in most clinical studies, the changes in CL composition or technologies to prepare the drug-releasing CL are not disclosed, the application of novel technologies is evident in some cases. As an example, NCT04747808 refers to a Phase 2a study of safety, tolerability, and efficacy of CLs that have been loaded with bimatoprost by means of a proprietary printing technology (MediPrint™). The company disclosed that using an FDA approved drug and an FDA approved CL led to a shorter regulatory course via a 505 (b) (2) pathway [MediPrint™, 2022]. Of note, the average age of the five patients in the trial was 77.4 years old and none had previously worn CLs. The bimatoprost-loaded CLs were well tolerated during the seven days of continuous wearing, which supports the short-term safety of these lenses [BusinessWire, 2021].

Patient and practitioner acceptability is a critical issue for the success of drug-releasing CLs in the marketplace. Physiological conditions associated with old age and vision disorders may hinder the insertion and removal of the CLs [Novack and Barnett, 2020]. In a recent survey, most patients suffering from an ophthalmic disease indicated that they would prefer to use drug releasing CLs instead of eye drops, if the combination product was less time consuming and reduced the required frequency of application [Ghazal et al., 2018]. Another important consideration is that CL-fitters in some countries are licensed to prescribe CLs but not drugs. Therefore, it is not entirely

USC UNIVERSIDADE DE SANTIAGO DE COMPOSTELA

clear who would be permitted to prescribe drug-releasing CLs, and the regulations will differ between various countries. In addition to legal issues, there are still many other issues to be solved, including the stability of the drug once loaded in the CL, the expiration date, the sterilization protocol for labile drugs, assurance of sterility, disposable procedures, and how to reload the drugs [Lanier et al., 2020; Tipnis and Burgess, 2018; Pereira-da-Mota et al., 2021].

USC UNIVERSIDADE DE SANTIAGO DE COMPOSTELA

USC

Table 1.1. Clinical trials of CLs loaded with a drug or an active substance according to a ClinicalTrials.gov search for "contact lens AND drug" after refinement for "not yet recruiting, recruiting, enrolling by invitation, active not recruiting, terminated, or completed" (April 2021).

Clinical Study	Status	Study Title	Contact Lens	Drug	Drug Loading	Condition/Outcome Measures	Phase
NCT04225611	Not yet recruiting	Therapeutic Contact Lens Drug Delivery System (TCL-DDS) in Patients With Recurrent Cystoid Macular Edema	Methafilcon (Kontur Kontact Lens Company, Hercules, CA)	Dexamethasone	TCL-DDS consisted of a Dexamethasone-polymer film encapsulated inside a CL	Cystoid macular edema. Occurrence of CL related ocular infection; corneal epithelial defect; ocular hypertension greater than 28; changes in OCT macular thickness; visual acuity.	1/2
NCT00432757	Completed	Evaluation of Efficacy and Safety of an Anti- Allergy Drug with a Contact Lens in Allergic Conjunctivitis.	Etafilcon A (1-Day ACUVUE, Vistakon, Florida, USA)	Ketotifen	CLs loaded 0.019 mg of Ketotifen	Allergic conjunctivitis. Ocular itching; conjunctival, ciliary, and episcleral redness; chemosis and mucous discharge; tearing and lid swelling.	3
NCT00445874	Completed	Evaluation of Efficacy and Safety of an Anti-Allergy Drug With a Contact Lens in the Treatment of Allergic Conjunctivitis	Etafilcon A (1-Day ACUVUE, Vistakon, Florida, USA)	Ketotifen	CLs loaded 0.019 mg of Ketotifen	Allergic conjunctivitis. Ocular itching; conjunctival, ciliary, and episcleral redness; chemosis and mucous discharge; tearing and lid swelling.	3
NCT04500574	Not yet recruiting	Latanoprost Eluting Contact Lens for Treating Glaucoma and Ocular Hypertension	Methafilcon (Kontur Kontact Lens Company, Hercules, California)	Latanoprost	Latanoprost eluting CLs consisted in a thin film of latanoprost-polymer film encapsulated	Glaucoma. Ocular hypertension. Adverse events as assessed by ocular infection, corneal epithelial defects, or cystoid macular edema; changes in intraocular	1

					within the periphery of the lens	pressure; tolerability and comfort.	
NCT04747808	Completed	Study of LL-BMT1 in Patients With Elevated Intraocular Pressure	7-days continuous wearing CLs	Bimatoprost	Drug-printed CLs	Primary open angle glaucoma and ocular hypertension. Adverse event rate; IOP elevation and changes.	2
NCT00889252	Completed	Safety Study of a Contact Lens With Ketotifen in Healthy,Normal Volunteers	-	Ketotifen	-	Allergic conjunctivitis. Ocular itching; conjunctival, ciliary, and episcleral redness; chemosis and mucous discharge; tearing and lid swelling.	3
NCT00569777	Completed	Safety Study of a Contact Lens With Ketotifen in Healthy, Normal Volunteers	-	Ketotifen	-	Allergic conjunctivitis. Ocular itching; conjunctival, ciliary, and episcleral redness; chemosis and mucous discharge; tearing and lid swelling.	3
NCT02852057	Recruiting	Effectiveness and Safety of Timolol and Dorzolamide Loaded Contact Lenses	Senofilcon A (ACUVUE Oasys, Vistakon, Fl, USA)	Timolol maleate and dorzolamide hydrochloride	CLs contained vitamin E as an additive for achieving extended release of the drugs	Glaucoma. IOP changes.	1
NCT03848221	Completed	Direct Application of Systane Complete to Contact Lenses	Daily disposable contact lens	Systane Complete; Sensitive Eyes Rewetting Drops	Direct application of Systane Complete to CL	Dry eye. Contact lens complication. Ocular surface damage; identifying dry eye disease.	4
NCT03026257	Completed	Clinical Assessment of a HYDRAGLYDE® Regimen.	Lotrafilcon B (AIR OPTIX® plus	Polyoxyethylene polyoxybutylene ;	CLs were packaged in a blister solution	Myopia. Hypermetropia. Refractive errors.	-

USC

			HYDRAGLYD E®, Alcon, A Novartis Division)	EOBO	containing the wetting agent polyoxyethylene polyoxybutylene	*Ex vivo* total cholesterol uptake.	
NCT03392532	Completed	Comparison of Two Silicone Hydrogel Toric Contact Lenses	Lotrafilcon B (AIR OPTIX® plus HYDRAGLYD E®, and AIR OPTIX® for Astigmatism , Alcon, A Novartis Division)	Polyoxyethylene polyoxybutylene ; EOBO	-	Astigmatism. Percentage of lenses with axis orientation within ±30 degrees from the 90 degree axis.	-
NCT01918410	Completed	Effect of Contact Lens With Alginic Acid in Dry Eye Patients	SEED 1dayPure moisture and SEED 2weekPure (SEED Co., Ltd., Tokyo, Japan)	Alginic acid	CLs were stored in a solution of alginic acid.	Dry eyes. Difference of visual analogue scale for the ocular discomfort; tear lipid layer thickness; schirmer and tear breakup time tests; corneal fluorescein staining, and tear proteomic analysis.	-
NCT04283331	Recruiting	Anesthetic Impregnated Bandage Soft Contact Lens (BSCL) in Pain Management After Photorefractive Keratectomy (PRK)	Bandage contact lens (BCL)	Proparacaine	The BSCL were soaked in proparacaine hydrochloride 0.5%	Myopia. Hypermetropia. Refractive errors. Astigmatism. Daily pain score; complete re-epithelialization and final refraction at post-operative.	4
NCT03388138	Completed	Clinical Evaluation of Etafilcon A With	Etafilcon A (1-Day	Ketotifen	CLs loaded 0.019 mg of	Visual acuity.	2

		Ketotifen	ACUVUE, Vistakon, Florida, USA)		ketotifen	Monocular contact lens corrected distance visual acuity; eyes with clinically significant slit lamp findings and with unacceptable lens fitting.	
NCT03653650	Recruting	Autologous Platelet-rich Plasma in the Treatment of Persistent Epithelial Defects	Bandage contact lens (BCL)	Autologous plateletrich plasma	Bandage CLs plus autologous platelet-rich plasma eye drops	Persistent epithelial defect. Persistent epithelial defect healing time; change in corneal sensitivity; uncorrected visual acuity, best corrected visual acuity; ocular pain; ocular surface symptoms, and frequency of adverse effects.	-
NCT04553432	Recruting	Dry Eye OmniLenz Application of Omnigen Research Study (DOORS)	OmniLenz® (NuVision®, Nottingham, UK)	Omnigen (Amnionic membrane)	OminLenz allows easy delivery and comfortable retention of Omnigen at the ocular surface	Dry eye. Change in dry eye symptoms, visual acuity, meniscus height, non-invasive tear breakup time, ocular surface staining and ocular redness.	4

1.2 GUIDELINES AND PHARMACOPOEIA METHODS FOR TESTING OCULAR DRUG RELEASE

The safety and efficacy of a drug product or a drug-device combo product are ultimately demonstrated in a clinical trial. However, studies with human participants are the final step after numerous preclinical studies involving laboratory testing and a variety of *in vivo* tests. *In vivo* testing in animal models should follow very strict ethical rules and adhere to the 3R´s principles; namely, 'replace' (search for alternatives), 'reduce' (minimize the experiments), and 'refine' (avoid distress) [European Commission, 2021]. Moreover, animal testing can be expensive and not suitable for early-stage testing. *In vitro* drug release tests are very valuable for quality assurance since they reveal the robustness and reproducibility of a drug product. Additionally, these tests help identify the critical elements of a drug-device that are important for *in vivo* performance [Kostewicz et al., 2014]. Therefore, *in vitro* models that better predict the performance of these devices may significantly facilitate the research and development process, thereby reducing both time and cost to bring these products to market.

1.2.1 Determining Drug Bioavailability from Drug-CLs using Mathematical Models

The advantages of drug-releasing CLs as ocular drug delivery systems are commonly compared with conventional eye drop administration. A simple mathematical model to explain the concentration of drugs on the ocular surface following an eye drop instillation was developed by Lang and Stiemke [Lang and Stiemke, 1996]. This model assumes that the tear fluid layer on the ocular surface behaves as a continuously stirred reactor (**Figure 1.1**). Once an eye drop

USC UNIVERSIDADE DE SANTIAGO DE COMPOSTELA

is deposited on the eye, the volume that cannot be contained in the tear layer spills over, and the rest of the volume is rapidly mixed with the tear fluid (**Figure 1.2**).

If no overflow occurs (i.e., drop volume is very small), the initial drug concentration on the ocular surface ($C_R(0)$) can be estimated as the ratio of the dose applied (Q_i) to the volume of the tear fluid layer (V_R). Since there is a hydrodynamic flow of tear fluid from temporal to the nasal segments of the eye ($\dot{V}$, the flow entrance of new tear fluid is the same as the flow of drainage) [Doane, 1989], the total amount of drug in the tear layer decreases exponentially according to

$$Q_R(t) = Q_i \cdot \exp\left(-\frac{\dot{V}}{V_R} \cdot t\right) \quad \text{(Eq. 1.1)}$$

In this equation $Q_R(t)$ represents the amount of drug at time t in the tear fluid, Q_i the initial amount (dose) instilled, $\dot{V}$ the tear flow, and V_R the volume of tear fluid.

Similarly, drug concentration in the tear fluid layer decreases along time as follows

$$C_R(t) = \frac{Q_R(t)}{V_R} = C_R(0) \cdot \exp\left(-\frac{\dot{V}}{V_R} \cdot t\right) \quad \text{(Eq. 1.2)}$$

In addition to drainage through the lacrimal puncta, tear film losses occur due to evaporation and absorption through the cornea, but the contributions of these two factors under healthy conditions are limited to 15-20% of total tear fluid losses [Joshi et al., 1996]. In other words, the amount of drug that is transported from the eye mostly enters into the nasolacrimal duct at a rate of

$$Q_{out}(t) = Q_i \cdot \left(1 - \exp\left(-\frac{\dot{V}}{V_R} \cdot t\right)\right) \quad \text{(Eq. 1.3)}$$

USC UNIVERSIDADE DE SANTIAGO DE COMPOSTELA

These equations do not consider drug penetration into eye tissue, but for most drugs that show poor ocular bioavailability, the model is still valid. Assuming that the drug penetrates through all ocular tissues by diffusion, the flux of drug from the tear fluid layer (J) depends on drug diffusion through the eye tissue (D), the oil-water partition coefficient (K), the drug concentration ($C_R(t)$), and the thickness of the diffusional barrier (h) as follows

$$J = \frac{DK}{h} \cdot C_R(t) \qquad \text{(Eq. 1.4)}$$

Thus, the rate of absorption can be calculated as

$$\dot{Q}_A(t) = J \cdot A = \frac{DKA}{h} \cdot C_R(t) \qquad \text{(Eq. 1.5)}$$

The amount absorbed at a given time is estimated by integration to be

$$\frac{Q_A(t)=\frac{DKA}{h\cdot\dot{V}}\cdot Q_{out}(t)=P\cdot A}{\dot{V}\cdot Q_{out}(t)} \qquad \text{(Eq. 1.6)}$$

The typical values of the permeability coefficient, P, of ophthalmic drugs are quite low [Loch et al., 2012], and therefore the fraction absorbed is predicted to also be minimal.

An example simulating the fate of the drug after instillation of 50 µL of a 0.1% drug solution is shown in **Figure 1.1**. Assumptions included that only 10 µL are effectively mixed with the tear fluid (Q_i = 0.01 mg), the drug has a quite high permeability coefficient ($0.5 \cdot 10^{-6}$ cm/s), the corneal surface available for absorption is 0.5 cm^2 [Cavas-Martínez et al., 2014], and that the tear flow is 1.2 µL/min [Lang and Stiemke, 1996]. **Figure 1.1** evidences the rapid clearance of the drug from the tear fluid layer and the small amount that can penetrate the ocular tissues. This model also explains that a drug-induced tearing

USC UNIVERSIDADE DE SANTIAGO DE COMPOSTELA

(e.g., tear flow 2.4 µL/min) causes a faster decrease in the drug levels in the tear fluid, consequently resulting in less drug being absorbed. In contrast, an excipient that increases the viscosity of the eyedrop may decrease the flow (e.g., tear flow 0.6 µL/min) and thus favors drug permanence on the ocular surface and subsequent drug absorption (**Figure 1.2B1**).

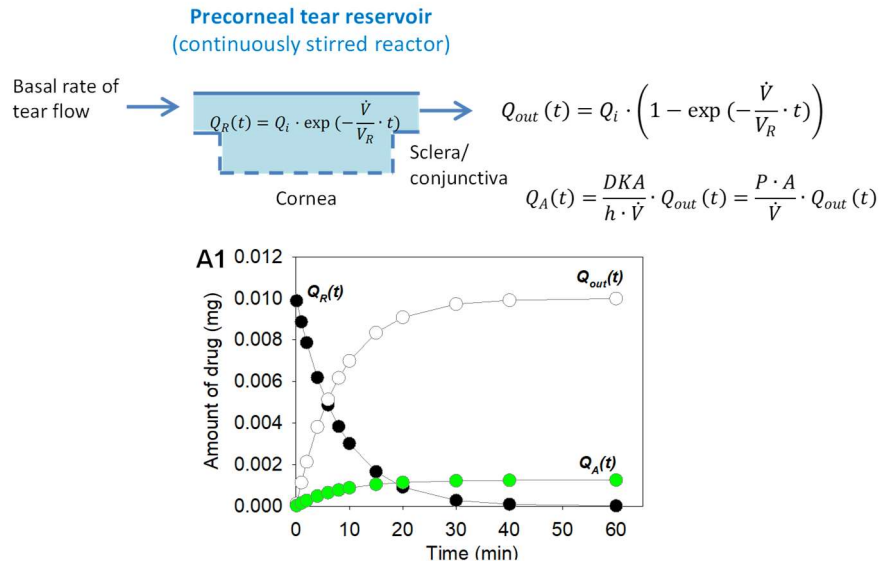

Figure 1.1. Modeling of the precorneal tear reservoir as a continuously stirred reactor consisting in a chamber with capability to contain a certain volume of tear fluid, V_R, which is under continuous flow, $\dot{V}$; and equations that predict, after one drop instillation, the amount of drug that remains in the precorneal tear reservoir, $Q_R(t)$ (black symbols), and the amount that is cleared in total, $Q_{out}(t)$ (white symbols), and through tissue permeation, $Q_A(t)$ (green symbols), at a certain time point. Equations adapted from Lang and Stiemke [Lang and Stiemke, 1996]. Plot A1 simulates the evolution of the drug levels after instillation of one drop (50 µL) of a 0.1% drug solution; assuming that only 10 µL are effectively mixed with the tear fluid (Q_i = 0.01 mg), the drug has a quite high permeability coefficient ($0.5 \cdot 10^{-6}$ cm/s), the corneal surface available for absorption is 0.5 cm^2, and tear flow is 1.2 µL/min.

USC UNIVERSIDADE DE SANTIAGO DE COMPOSTELA

Using microparticles that perform as drug-binding resins can notably prolong the time of permanence of the drug on the surface of the eye (**Figure 1.2**). An equilibrium between the drug that is inside the resin and the drug that is free in the tear fluid is established. The fraction of free drug (*F*, not bound to the microparticles) can vary depending on the affinity of the resin for the drug. In **Figure 1.2**, the *F* value was assumed to be 0.2; i.e., at each time point 20% of the drug is free and 80% of the drug remains in the formulation. The total amount of drug in the tear fluid layer is the sum of both free and bound drug, but the drug that can be absorbed or drained is only the free drug. Therefore, the equations should be modified accordingly, as follows

$$Q_{out}(t)_{resin} = Q_i \cdot \left(1 - \exp\left(-\frac{F \cdot \dot{V}}{V_R} \cdot t\right)\right) \quad \text{(Eq. 1.7)}$$

$$\frac{Q_A(t)_{resin} = \frac{DKA}{h \cdot \dot{V}} \cdot Q_{out}(t)_{resin} = P \cdot A}{\dot{V} \cdot Q_{out}(t)_{resin}} \quad \text{(Eq. 1.8)}$$

Sustained drug release attenuates the decrease in $Q_R(t)$, but also slows down the amount absorbed, and the amount drained. Therefore, the therapeutic advantage of formulating a drug into microparticles is not related to an increase in the concentration of drug available for absorption (which decreases if the dose remains constant), but due to the prolonged residence of the drug in the tear fluid. Assuming that the formulation does not alter drug permeability, it is clear that a decrease in free drug concentration diminishes the flux of drug into eye tissues (**Equation 1.5**) and thus the absorption rate. Therefore, the improvements in ocular bioavailability recorded for microparticle-based formulations are not due to an increase in permeability, but to a change in the pharmacokinetic profile. Slow drug release from microparticles means more contact time of the drug with the eye tissue. If the absorption rate is sufficient to reach the pharmacological

USC UNIVERSIDADE DE SANTIAGO DE COMPOSTELA

threshold, i.e., the minimum therapeutic concentration in the target tissue, then the pharmacological effects could be notably prolonged compared to eye drop instillation.

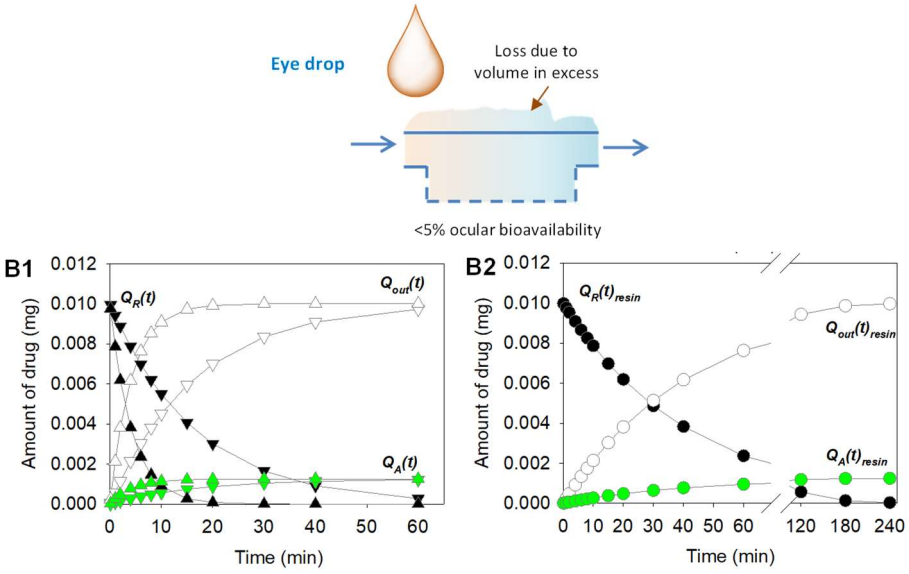

Figure 1.2. Plot B1 depicts the effect of a change in the tear flow from 0.6 µL/min (e.g., a decrease induced by a thickening excipient; down triangles) to 2.4 µL/min (e.g., tearing induced by the drug itself; up triangles). Plot B2 depicts the effect of formulating the drug in microparticles that perform as drug-binding resins and that during the release the fraction of drug released at each point (free drug) is 20% of the drug remaining in the microparticles. Only the free drug released to the tear fluid is absorbed or drained, which decreases both the rate of absorption and the clearance, but notably increased the time of permanence of the drug in the tear fluid for the same dose instilled as compared to Figure 1.1A1.

It seems clear that ocular drug absorption benefits from a decrease in tear flow and a sustained drug release. Interestingly, CLs may

USC UNIVERSIDADE DE SANTIAGO DE COMPOSTELA

simultaneously achieve both of these conditions. In the case of CLs, an equilibrium between free and bound drugs may not occur since the strength of the binding is less than for the ionic resins. F is expected to increase with time. Therefore, in the following equations F' is not a constant and may be a function of the release kinetics. $Q_R(t)$ depends also on the release kinetics. Additionally, placing a CL on the eye causes the tear film to divide into two layers, an outer 'pre-lens tear film' closest to the air and a layer beneath the CL and in front of the cornea designated as the 'post-lens tear film'. Drug release mainly occurs toward the post-lens tear film because, in the time interval between successive blinks, the external surface of the CL dries and thus drug diffusion stops. Therefore, an initial consequence of placing a CL on the surface of the eye is that the volume available for drug release is less than in the case of eye drops. Tear film thickness in the absence of a CL is estimated to be 6 μm, and the thickness below a CL is 1-2 μm [Nichols and King-Smith, 2003].

A second consequence is that the exchange of tear fluid beneath the CL, i.e., the hydrodynamic flow of the post-lens lachrymal fluid ($\dot{V}_{CL}$), is smaller than in the absence of the CL, particularly for soft CLs [Muntz et al., 2015]. Moreover, the dynamics of tear flow under the CL may follow a nonconstant rate, since blinking causes deformation of the CL, which in turn ejects the fluid when the CL is under pressure and suctions more fluid when the pressure vanishes [Maki and Ross, 2014]. Thus, $\dot{V}_{CL}$ should be considered as a mean value, and the blinking pressure may also alter drug release kinetics from the CL.

$$Q_{out}(t)_{CL} = Q_i \cdot \left(1 - \exp\left(-\frac{F' \cdot \dot{V}_{CL}}{V_R} \cdot t\right)\right) \qquad \text{(Eq. 1.9)}$$

$$Q_A(t)_{CL} = \frac{DKA}{h \cdot \dot{V}_{CL}} \cdot Q_{out}(t)_{CL} = \frac{P \cdot A}{\dot{V}_{CL}} \cdot Q_{out}(t)_{CL} \qquad \text{(Eq. 1.10)}$$

USC UNIVERSIDADE DE SANTIAGO DE COMPOSTELA

The complex dependence of the release rate, $Q_R(t)$ and F' on $\dot{V}_{CL}$ explains the difficulties in designing *in vitro* release tests for drug-eluting CLs that can mimic the physiological conditions on the eye surface, or at least that can provide values useful to predict *in vivo* behavior. It should be noted that CLs are not expected to increase drug permeability, because this parameter mainly depends on the drug-tissue pair, but CLs may notably enhance ocular bioavailability (at least $Q_A(t)_{CL}$) by regulating the concentration of drug in the tear fluid and the time of permanence (**Figure 1.3**). These two latter parameters can be tuned through an adequate design of the CL that considers not only drug-network interactions, but also the potential competitive binding of the drug to tear components (lipid, proteins) and also the binding of various tear components to the CL [Mahomed et al., 2016].

USC UNIVERSIDADE DE SANTIAGO DE COMPOSTELA

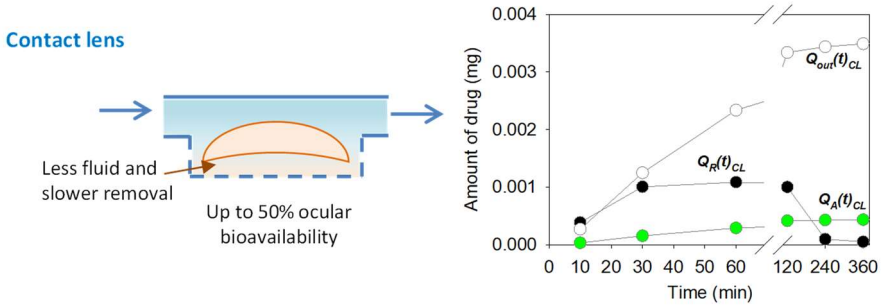

Parameters that may affect bioavailability

(i) Amount release and release rate from CLs
- Tear volume and flow
- Drug-CL interactions *
- Binding of tear componentes (lipid, proteins) *

(ii) Amount that can permeate the tissues
- Partition coeficiente
- Drug molecular weight
- Diffusion rate
- Time of permanence *
- Drug binding to tissue components

Figure 1.3. The use of drug-loaded CL alters the tear volume and slows down the flow beneath the lens. Also, the sustained release of the drug (in the plot $Q_R(t)_{CL}$ represents real data of free drug levels recorded *in vivo* by some of the authors) notably slows down drug clearance (attenuating the risk of collateral systemic effects) and may facilitate sustained absorption through ocular tissues. If the absorption rate is sufficient to induce pharmacological effects, the therapeutic efficiency of the treatment may be notably enhanced and prolonged. Among the listed parameters that may affect ocular drug bioavailability, CLs may preferentially act on those marked with *.

1.2.2 Current Official Methods for Testing Drug Release from Topical Ophthalmic Medicines

In the development of a drug product (medicine), drug release tests provide valuable information for quality control during manufacturing and regulatory review process and as predictive tools of *in vivo*

USC UNIVERSIDADE DE SANTIAGO DE COMPOSTELA

performance. Particularly, for ophthalmic non-solution products, traditional systemic pharmacokinetics studies (using blood sampling) do not inform on bioavailability at the site of action (inner eye structures) [Luke and Kozak, 2021]. Regulatory bodies have published recommendations on bioequivalence studies that involve clinical endpoint studies (mostly for glaucoma, ocular hypertension, and pain), pharmacokinetic studies in aqueous humor (e.g., topical corticosteroids prior to cataract extraction), microbial kill rate assay (e.g., antimicrobial drugs) and *in vitro* release studies [Choi and Lionberger, 2016]. Clinical endpoints provide semiqualitative information and may be affected by the patient health conditions. Since their capability to discriminate similar products is low, clinical endpoint assessment requires a fairly large sample size. Pharmacokinetic studies in the aqueous humor offer quantitative data of transcorneal ocular bioavailability, but usually only one sampling per patient is feasible. Moreover, drug levels in the aqueous humor may be affected by several interindividual differences (e.g., age, ethnicity, ocular illness) and thus a very large sample size is required for statistical significance [Luke and Kozak, 2021]. Therefore, so far, *in vitro* studies are considered more reliable to assess differences among ophthalmic formulations.

Researchers and regulatory bodies have been attempting to establish methods for *in vitro-in vivo* correlations (IVIVC). Strong efforts are being made to develop ocular physiologically relevant pharmacokinetic (PBPK) *in silico* models (i.e., via computer simulation) that can predict drug ocular bioavailability and tear film breakup time based on the physicochemical properties of the drug and the formulation. For instance, GastroPlus™ has recently been implemented with an Ocular Compartmental Absorption and Transit (OCAT™) model [FDA, 2019b]. Various other modeling approaches

USC UNIVERSIDADE DE SANTIAGO DE COMPOSTELA

to simulate drug transport through the cornea are also currently under investigation [Pak et al., 2018].

Some product-specific guidances are available for ophthalmic non-solution products, such as suspensions and ointments. A great deal of attention has been focused on identifying drug release tests that can detect changes in formulation or manufacturing process having the same drug and the same inactive ingredients. The most common apparatus to monitor drug release from non-solution ophthalmic products are those included in official pharmacopeias for oral dosage forms, with some modifications to be adapted to semisolid products. Some key examples of the apparatus include the Franz diffusion cell, USP apparatus 2 with enhancer cells, and USP apparatus 4 with semisolid adapters (**described in Figure 1.4**) [Bao and Burgess, 2018]. Nevertheless, non-compendial dissolution methods that can be more biorelevant are under investigation, such as devices simulating low-volume flow-through [Luke and Kozak, 2021].

USC UNIVERSIDADE DE SANTIAGO DE COMPOSTELA

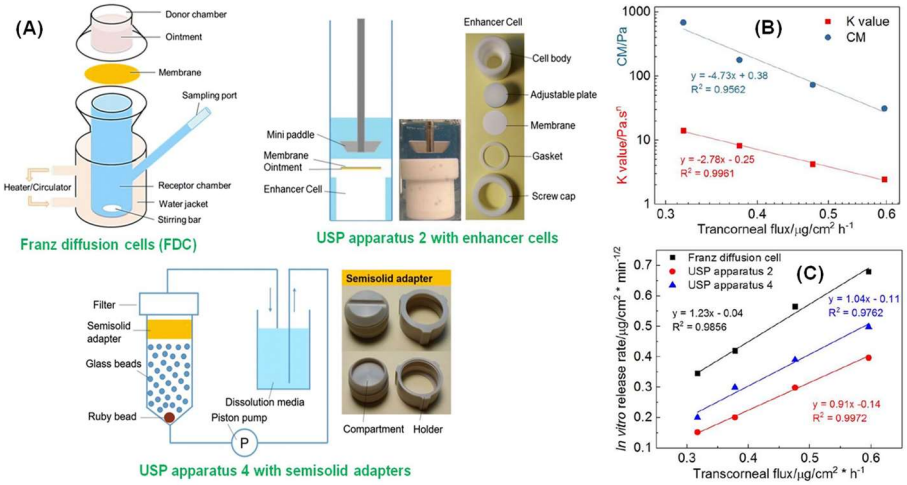

Figure 1.4. (**A**) Scheme of some of the apparatus considered in the USP chapter <1724> for *in vitro* drug release from semisolid drug products. Franz (vertical) diffusion cells consists of two compartments (donor and receptor) separated from each other by a membrane onto which, typically, 200 mg of the product under test is placed. A heating jacket is used to regulate the temperature and the experiment is carried out for 4-6 h. The modified USP apparatus 2 consists of a cell filled with the product (300 mg - 2 g covered with a permeable membrane) which is placed at the bottom of the glass flat vessel. The release medium is added and maintained under stirring with the help of a small paddle positioned at a certain distance from the product. The flow-through cell USP apparatus 4 consists of a reservoir (semisolid adapter) filled with the product (also covered with a permeable membrane) through which a sinusoidal flow of release medium is impelled. Reprinted from Bao and Burgess [Bao and Burgess, 2018] by permission from Springer Nature; (**B**) Linear correlation (semi-logarithmic mode) between critical parameters of loteprednol etabonate ophthalmic ointments (crossover modulus CM and power law consistency index K) and drug transcorneal flux; and (**C**) linear correlation between *in vitro* release rate recorded using the three apparatus described in (A) and *ex vivo* transcorneal flux (receptor filled with 5 mL of artificial lachrymal fluid with 9% hydroxypropyl-ß-cyclodextrin, 600 rpm). Reprinted from Bao et al. [Bao and Burgess, 2018] with permission from Elsevier.

USC UNIVERSIDADE DE SANTIAGO DE COMPOSTELA

There is an increasing number of reports devoted to identifying the apparatus and the release conditions that allow for improved discrimination among similar ophthalmic formulations of a given drug [Bao et al., 2017]. *In vitro* release tests in simulated lachrymal fluid and *ex vivo* transcorneal flux correlations have also been attempted. As an example, four loteprednol etabonate ophthalmic ointments considered as qualitatively and quantitatively equivalent formulations (the same components in the same concentration; Q1/Q2) were evaluated in terms of rheological behavior, *in vitro* drug release in artificial lachrymal fluid and *ex vivo* (rabbit) transcorneal flux [Bao et al., 2018]. The USP apparatus 4 (1.54 cm^2 exposed area, 50 mL medium capacity, flow rate 8 mL/min) clearly showed differences in release rate among the formulations, which were not detected or were less evident using the Franz diffusion cells (1.77 cm^2 exposed area, 12 mL receptor medium, 600 rpm) or the USP apparatus 2 with enhancer cells (4 cm^2 exposed area, 40 mL release medium, 150 rpm). The highest release rates, but the less reproducible ones, were recorded in the Franz diffusion cells. Inverse correlations were found between the rheological properties (crossover modulus and power law consistency index) and the release rate (Higuchi model) of the four ointments. Moreover, *ex vivo* transcorneal permeation coefficients recorded in Franz diffusion cells also revealed differences among the formulations, which correlated with their rheological features (**Figure 1.4A**). Compared to the drug release rates calculated *in vitro*, the drug permeation rates were lower, but the rank order of the formulations was the same; namely, a direct correlation was found between *in vitro* release rate and *ex vivo* release flux (**Figure 1.4B**). This study demonstrated the usefulness of the *in vitro* release tests as predictive tools of *ex vivo* drug transcorneal flux, which may correlate with the flux *in vivo*, although this has not been demonstrated yet. Additionally, particular attention should be paid to

USC UNIVERSIDADE DE SANTIAGO DE COMPOSTELA

the preservation of corneal structure and epithelium integrity during the test [Bao et al., 2018]. In any case, such *in vitro-ex vivo* correlations are particularly useful when a predicate product has already demonstrated safety and effectiveness, and a generic product is intended to be developed. Nevertheless, prediction of *in vivo* performance does not depend only on the release rate, but also on other formulation properties, such as retention time on the ocular surface.

Release tests carried out with solid ophthalmic formulations, namely inserts to be placed in the conjunctival fornix, are also quite heterogeneous [Del Amo and Urtti, 2018; Bertens et al., 2018; Miller and Eaton, 2021; Saettone and Salminen, 1995]. Ocusert-like inserts prepared with poly(lactic coglycolic) acid and polyethylene glycol (PEG) and loaded with brimonidine tartrate showed almost constant release rate for one month when placed in phosphate buffered saline (PBS) solution at 37 °C [Mealy et al., 2014]. The release medium was completely replaced at each sampling point, but total release medium volume and stirring conditions were not disclosed. There are few other inserts for drug delivery that are under preclinical or clinical phase. A bimatroprost ocular ring (formerly HeliosTM), which contains the drug onto a non-biodegradable support and coated with silicone, was reportedly 'safe' in preclinical tests, but the *in vitro* release profiles were not disclosed [Miller and Eaton, 2021]. Ciprofloxacin release from OphthaCoil inserts (stainless steel coated with SlipSkin®) was evaluated by placing the insert in a silicon tube (inner diameter of 1 mm), through which simulated lachrymal fluid was pumped at a rate of 100 μL/min. Fractions of 150 μL were collected for release kinetics evaluation. In general, the profiles showed fast release in the first minutes and decreased amount released in the next few hours [Pijls et al., 2007a]. Pradofloxacin-loaded OphthaCoil inserts were similarly tested *in vitro* and compared with the release *in vivo* in a dog model

USC UNIVERSIDADE DE SANTIAGO DE COMPOSTELA

after insertion in the lower conjunctival fornix of the eye [Pijls et al., 2007b]. The *in vivo* release was notably slower and thus more prolonged, which was attributed to the *in vitro* high flow of release medium (100 µL/min) compared to physiological tear turnover (1-5 µL/min). Overall, the information reported for topical ocular solid formulations also reveals a disparity of release media and testing conditions, without conclusive proposals on the *in vitro* test setup that may mimic *in vivo* release.

The lack of standardized *in vitro* test models has also been pointed out as a relevant concern for the development of ocular implants for posterior eye segment [Braga et al., 2010]. A variety of setups, including configurations similar to those depicted in **Figure 1.4**, have been tested, but finding IVIVC remains elusive. The high complexity of the ocular tissues, comprising a diversity of metabolic and physiological barriers, makes the *in vitro* mimicking of the *in vivo* processes of drug release, absorption and distribution much more challenging than for any other route.

1.3 *IN VITRO* TESTING OF DRUG RELEASE FROM MEDICATED CLS

Since there is not an officially approved method for testing drug release from CLs, authors have used a myriad of different approaches. A search was performed in Web of Science database with the keywords “drug AND contact lens” within the 2000 to 2021 time frame. The search was further refined using the word “release” and to papers published in English. In total, 455 results were generated. This search included ocular drugs and macromolecular demulcents. Further refinement manually removed contributions that did not match the

USC UNIVERSIDADE DE SANTIAGO DE COMPOSTELA

appropriate outcomes searched for, resulting in 251 original papers being analyzed.

The *in vitro* setups can be categorized into three main groups (**Figure 1.5)**:

- **(i)** release in a beaker with or without replacement of the release medium at a pre-stablished time;
- **(ii)** release under fluid flow in specially designed microfluidic chambers;
- **(iii)** release under blinking-mimic conditions

Most reports refer to *in vitro* release profiles recorded in small beakers, but using widely variable volume, medium composition, stirring and replacement. For exhaustive information the reader is referred to **Table 1.3**. Although analysis of this non-harmonized data is not easy, beakers in which the release medium is not replaced are usually filled with more volume than those that undergo partial or complete replacement of the release medium at each sampling time (**Figure 1.5A1**). The selection of the release medium volume is a highly relevant issue, as evidenced in a previous comprehensive report [Tieppo et al., 2014]. If a too small volume is chosen, then the release process may become controlled by drug solubility, and therefore the capability of the CL to regulate drug release is overestimated. In comparison, if too large a volume is chosen or a small volume is frequently replaced, then a sink effect accompanied by a large concentration gradient may forcedly accelerate the release process, and the CL may become exhausted much more rapidly than under *in vivo* conditions. Clearly, CLs that are able to sustain the release under the *in vitro* more challenging conditions are also expected to control the release under *in vivo* conditions. However, as evidenced in **section 1.4**, these *in vitro* conditions do not ensure IVIVC because the release *in vivo* may be

USC UNIVERSIDADE DE SANTIAGO DE COMPOSTELA

slower. Interestingly, an overall analysis of the time that CLs sustain drug release *in vitro* suggests that, disregarding whether the release medium is replaced or not, conventional commercially available CLs release the drug much faster than CLs designed ad hoc or coated with components that exhibit affinity for the drug. According to the data compiled in **Table 1.3**, for these latter CLs, the duration of the release could be prolonged for 149 (s.d. 99), 319 (s.d. 338), 226 (s.d. 278) and 290 (s.d. 328) hours in PBS without replacement, in PBS with replacement, in artificial tears without replacement, and in artificial tears with replacement, respectively. The box plot showing the median values and the upper and lower quartiles are depicted in **Figure1.5A2 and A3**. No *in vivo* release profiles are available for reports collected in **Table 1.3**.

Attempts to better mimic the complex scenario of *in vivo* release have mainly focused on the design of microfluidic chambers that allow for regulation of both the flow and the total volume of medium that bathes the CL (**Figure 1.5B**). The microfluidic device depicted in **Figure 1.5B1**, which may hold 175 µL in the inner chamber and pumps the release medium at a flow rate of 3 µL/min, has been shown to be useful for discrimination of the capability of silicone hydrogel CLs to sustain dexamethasone release [Kaczmarek et al., 2014]. Compared to the release in a large-volume beaker, CLs loaded with a variety of drugs and demulcents showed slower release profiles when tested in the microfluidic device, which were prolonged for weeks [Tieppo et al., 2012a; White et al., 2016; White et al., 2011]. The microfluidic device depicted in **Figure 1.5B2** consisted of two 3D printed molds resembling the corneal/scleral curvature and the eyelid. The CL is placed between these structures, and the space available for the release medium is 100 µL. For a flow rate of 3.3 µL/min, commercially available CLs sustained the release of ciprofloxacin, moxifloxacin and fluconazole for

USC UNIVERSIDADE DE SANTIAGO DE COMPOSTELA

several hours compared to the few minutes recorded when the test was carried out in a vial with 4.8 mL PBS, partially replaced at each sampling time [Bajgrowicz et al., 2015; Phan et al., 2016a].

The microfluidic device depicted in **Figure 1.5B3** is the one with the lowest volume in the inner chamber (45 μL, which is quite close to the maximum tear film volume in the eye) and has 8 outlets that converge in a common collector [Pimenta et al., 2016a]. Once again, release profiles recorded using this microfluidic device showed remarkably slower rates than the release in a beaker [Alvarez-Rivera et al., 2019; Silva et al., 2021]. At this time, the microfluidic devices are still to be validated with appropriate *in vivo* data.

The reports on devices that can mimic the pressure exerted by the eyelid on the CL are still incipient (**Figure 1.5C**). Repetitive load and friction cycles (16 kPa) onto CLs placed in a Simublink device (**Figure 1.5C1**) have been shown to accelerate the release of levofloxacin when directly loaded in the bulk of the CL [Galante et al., 2015], but the effect was negligible when the drug was encapsulated in liposomes coating the CL [Paradiso et al., 2017]. A whole *in vitro* eye model device constructed using 3D printing has recently been proposed to evaluate the effects of air exposure, flow rate, and blinking frequency on drug release rate (**Figure 1.5C2**) [Phan et al., 2021; Phan et al., 2016b; Phan et al., 2019a]. The model considers the coating of the front surface of the eyeball with a silicone material to prevent unspecific binding of the tested drug and allows for quantifying the amount of drug that penetrates into the polyvinyl alcohol (PVA)-mimicking eyelid [Phan et al., 2019a].

USC UNIVERSIDADE DE SANTIAGO DE COMPOSTELA

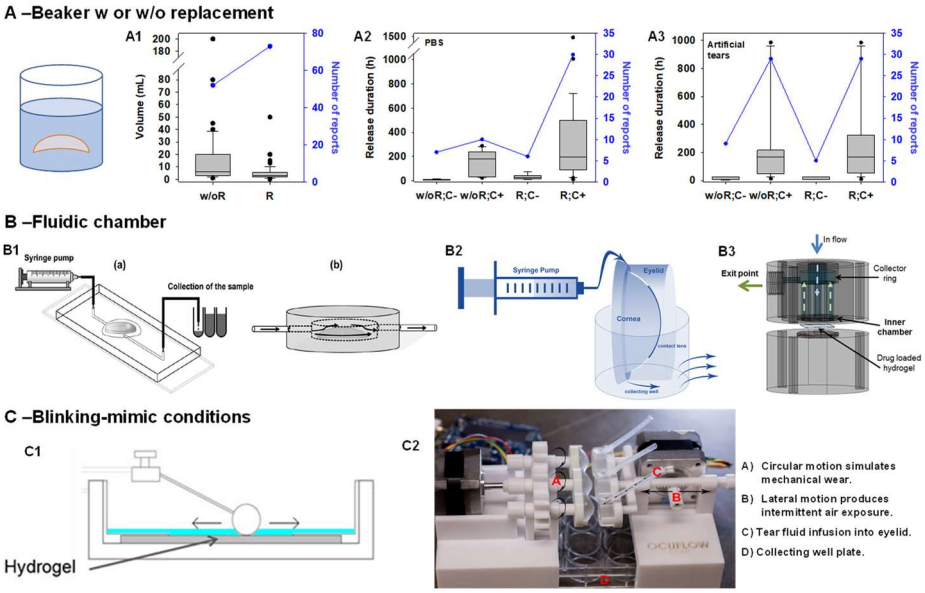

Figure 1.5. Main setups used to evaluate *in vitro* drug release from CLs. (**A**) Beaker of variable volume (from small well to large tube) with (R) or without (w/oR) replacement of the release medium at a pre-established time. The box plots constructed from the data compiled in **Table 1.3** demonstrate that (A1) tests made without replacement of the release medium (w/oR) usually involve large volumes, and (A2 and A3) CLs designed to control drug release (code C+) are more efficient in providing sustained release than conventional CLs (code C-) disregarding whether the release medium (PBS or artificial tears) is replaced or not during the *in vitro* test. (**B**) Devices proposed to evaluate drug release under fluid flow showing different configurations for inlet and outlet ports; (B1), (B2) and (B3) reprinted, respectively, from Tieppo et al. [Tieppo et al., 2012a] with permission from Elsevier, Bajgrowicz et al. [Bajgrowicz et al., 2015] with permission from ARVO, and Pimenta et al. [Pimenta et al., 2016a] with permission from Springer Nature. (**C**) Advanced prototypes in which CLs can be subjected to normal forces that may mimic the blinking conditions; (C1) reproduced from Galante et al. [Galante et al., 2015] by permission of Taylor & Francis Ltd., and (C2) reproduced from Phan et al. [Phan et al., 2021] (Creative Common CC BY license).

USC UNIVERSIDADE DE SANTIAGO DE COMPOSTELA

1.4 *IN VIVO-IN VITRO* RELATIONSHIPS

There is an increasing interest in using *in vitro* profiles to predict *in vivo* performance. Nearly 50 papers have been published since 2000 reporting *in vitro* release profiles from CLs together with either *in vivo* levels in tear fluid or therapeutic response (**Table 1.2**). Most studies have relied on the rabbit eye model, which has structural similarities with the human eyes. However, it is important to note that there are also marked differences in lacrimal fluid turnover (~7.1%/min in rabbits *vs.* ~16%/min in humans) and blinking frequency (every 15 min in rabbits *vs.* every 5 s in humans) [Chrai et al., 2016; Mishima et al., 1996]. Thus, drug release may be faster and drug residence time may be shorter in human eyes. Potential *in vivo-in vitro* (co-)relations are discussed in detail in this section as they can provide key information on the true potential of CLs as drug carriers, as well as feedback for improvements.

USC UNIVERSIDADE DE SANTIAGO DE COMPOSTELA

USC

Table 1.2. Drug-loaded CLs evaluated *in vivo* (animal model) in terms of drug release to tear fluid. Some studies also include the measurement of drug accumulation in eye tissues or therapeutic outcomes.

Entry	Drug	Lens Material	Loading Protocol	*In Vitro* Test	*In Vivo* Test	Outcome	Ref.
1	Timolol maleate	N,N-Diethylacrylamide (DEAA), Methacrylic acid (MAA) and Ethylene glycol dimethacrylate (EGDMA)	Soaking of imprinted and non-imprinted CLs in 10 ml of 1 mM timolol solution for 3 days. Then, autoclaved	10 ml of 0.9% NaCl at 37 ºC	Male Nippon albino rabbits. Imprinted (21 μg dose) and non-imprinted (34 μg) were applied on cornea. Timolol solutions (34 and 125 μg) were used as control. Drug levels in tear fluid were monitored.	*In vitro* release sustained for 24 h. *In vivo* release prolonged for 90 min.	Hiratani et al., 2005a
2	Ketotifen fumarate	Poly(HEMA-co-AA-co-AM-co-NVP-co-PEG200DMA)	Soaking of imprinted and non-imprinted CLs in 3 ml of 0.3 mg/mL drug solution. Then, autoclaved	300 mL of artificial lacrimal solution, at 30 rpm and 34 ºC	Male New Zealand white rabbits. Imprinted (110 μg dose) and non-imprinted (39 μg) were applied on right cornea. As control, one drop (50 μL) of commercially available 0.025% ketotifen eye drops was instilled in left cornea. Drug levels in tear fluid were monitored.	*In vitro* release from imprinted CLs was sustained for 72 h (85% released in 24h). *In vivo* release prolonged for 26 h.	Tieppo et al., 2012b
3	Ketotifen fumarate	MA-PDMS-MA macromonomer, DMA, TRIS, EGDMA	Soaking in 5 mL of 1.945 mg/mL drug solution for 5 days	5 mL of PBS, at 100 rpm and 37 ºC	Rabbits. One CL per animal (amount loaded ranged from 25 to 31 mg/g). As	*In vitro* release from more hydrophilic CLs was prolonged for 5 h, while less hydrophilic	Xu et al., 2011

					control, one drop (50 µL) of commercially available 0.050% ketotifen eye drops was instilled in the other cornea.	ones sustained the release for 12 h. These later CLs sustained *in vivo* release for 24 h.	
4	Bimatoprost	Dimethylacrylamide (DMA, 200 µL), Siloxane (50 µL); Methacrylic acid (MAA, 50 µL); Ethylene glycol dimethacrylate (EGDMA, 10 µL), and HEMA (up to 1 mL)	Immersion of imprinted and non-imprinted CLs in 2 ml of 10, 20 or 30 µg/mL drug solution in simulated tear fluid pH 7.4. The systems were autoclaved and soaking was prolonged for 10 days	2 mL simulated tear fluid at 34 ºC and 50 rpm; complete replacement of the release medium at each sampling point	New Zealand white rabbits of either sex. Imprinted (14.8) µg dose) and non-imprinted (16.2 µg) were applied on right cornea. As control, one drop (15 µg) of commercially available 0.025% ketotifen eye drops was instilled in left cornea. Drug levels in tear fluid were monitored.	*In vitro* release from imprinted CLs was sustained for 36 h. *In vivo* release prolonged for 12 h.	Yan et al., 2020
5	Puerarin	Poly(2-hydroxyethyl methacrylate-co-N-vinylpyrrolidone-co-methyl acrylate) (pHEMA-NVP-MA) (0.05 mm)	Soaking in 5 mL of 0.802 mg/mL drug solution in PBS at 37 ºC until equilibrium	5 mL PBS at 100 rpm and 37 ºC. At each sampling time, 100 µL of the volume was replaced by fresh medium	Rabbits. One CL per rabbit. In contralateral eye, one drop (50 µL) of 1% puerarin was instilled.	*In vitro*, drug release was complete in 4 h. *In vivo*, CLs with higher content in NVP (28 mg puerarin/g) showed MRT of 77.45 min, with quantifiable drug levels for 6 h. Eye drops had MRT of 12.88 min, with quantifiable drug levels for 90 min.	Xu et al., 2010a

USC

6	Puerarin	Copolymers of HEMA with mono-MA-β-CD and trimethylolpropane trimethacrylate	Soaking in 50 mL of 0.334 or 0.802 mg/mlof puerarin solution for 24 h	10 mL distilled water at 37 °C and 100 rpm. At each sampling time, 5 mL of the volume was replaced by fresh medium	Rabbits. One CL per rabbit. In contralateral eye, one drop (50 µL) of 1% puerarin was instilled.	CLs with MA-β-CD loaded more drug (32.6 mg/g) than without comonomer (13.3 mg/g). *In vitro* release profiles from both CLs showed a burst of ca. 60% in the first hour. CLs with MA-β-CD sustained the release for few hours more. *In vivo*, CLs with MA-β-CD sustained the release in tear fluid for 6 hours. They also provided relevant drug levels in aqueous humor for more than 12 h, with a maximum at 4-6 h. Eye drops were cleared in 50 min. from tear fluid.	Xu et al., 2010b
7	Diquafosol	Commercially available silicone hydrogel CLs (comfilcon A and balafilcon A)	Soaking in 1 mL of 1 mM drug solution for 12 h	1 mL NaCl 0.9%; complete replacement of the release medium every 24 h	Male New Zealand white rabbits. One loaded CL (approx. 0.02 mg) in one eye, and non-loaded CL in contralateral eye. As control, one drop (10 µL) of 0.1 mM drug was instilled.	*In vitro* release completed in 24 h. *In vivo*, eyedrops were completely drained in 5 min. CLs had maximum level at 30 min in tear fluid, but drug levels were detected for 240 min. *In vivo* CLs increased tear secretion for 300 min, while the effects of topical instillation	Dominguez-Godinez et al., 2018

						were maximum at 15 min and lasted for 90 min.	
8	Ketotifen	HEMA (up to 1 mL) with dimethacrylate acid (250 µL), siloxane (5 µL) and NVP (100 µL)	The drug directly or previously encapsulated in pegylated solid lipid nanoparticles (pSLNs) was added to monomer mixture before polymerization. Some hydrogels were loaded by soaking in drug solution or drug-encapsulated pSLNs for 10 days. After autoclaving, drug remaining in the CLs was quantified	2 mL of simulated tear fluid at 34 °C and 100 rpm; complete replacement of the release medium at each sampling time	New Zealand rabbits of either sex. One CL, either directly loaded with p-SLN (70.2 µg drug) or soaked in p-SLN (48.5 µg drug), placed on one eye. As control, two drops (25 µg) were instilled on one eye. Contralateral eyes were referred as control.	Directly loaded CLs provided lower Cmax (445.7 ± 85.3 µg/mL but higher drug levels in tear fluid along time than CLs that were loaded by soaking in ketotifen-encapsulated p-SLNs (581.6 ± 152.7 µg/mL).	Zhang et al., 2020
9	Ketotifen	HEMA (48% w/w), MAA (1% w/w), EGDMA (0.5% *w/w*) and water (50.5% *w/w*) mixed with 10% *w/w* silica shell nanoparticles	The drug directly or previously encapsulated in silica shell nanoparticles was added to monomer mixture before polymerization	2 mL of simulated tear fluid at 35 °C and 100 rpm; complete replacement of the release medium at each sampling time	New Zealand white rabbits. One CL on one eye. Contralateral eyes were referred as control.	*In vitro*, CLs loaded with the drug encapsulated in nanoparticles showed minor burst and sustained release for 9 days. Sustained drug levels in tear fluid were also recorded for a similar period of time.	Maulvi et al., 2016a

USC

10	Cyclosporine A	HEMA with methacrylic acid (MAA) (25:1 mol/mol)	The drug directly or previously encapsulated in a microemulsion was added to monomer mixture before polymerization. After boiling and autoclaving, drug remaining in the CLs was quantified	2 mL of simulated tear fluid at 34 ºC and 100 rpm; complete replacement of the release medium at each sampling time	New Zealand rabbits of either sex. One CL (100 μg drug) in one eye.	*In vitro* and *in vivo*, CLs loaded with the drug itself or encapsulated in unstable microemulsions showed more sustained release, but the release rate was too slow to provide therapeutic levels after few days. Differently, CLs with the drug encapsulated in stable microemulsions released the drug faster *in vivo* and provided therapeutic drug levels in tear fluid for some weeks. IVIV correlations were observed.	Maulvi et al., 2017a
11	Cyclosporine A	HEMA (60 %), MAA (2 %), EGDMA (0.5 %), NVP (1%), water (36.5 %)	The drug directly or previously encapsulated in Eudragit S100 nanoparticles was added to monomer mixture before polymerization. After boiling and autoclaving, drug remaining in the	2 mL of simulated tear fluid at 34 ºC and 100 rpm; complete replacement of the release medium at each sampling time	New Zealand rabbits of either sex. One CL (50 μg drug) in one eye.	*In vitro* and *in vivo*, CLs with the drug directly added showed a burst and completed the release in few days. CLs with the drug encapsulated in nanoparticles had lower burst and sustained for more time the release both *in vitro* and *in vivo*.	Maulvi et al., 2017b

			CLs was quantified				
12	Bimatoprost	Siloxane (100 µL), ethyleneglycol dimethacrylate (15 µL), dimethyl acrylamide (300 µL), and hydroxyl ethylmethacrylate (HEMA, up to 1 ml)	Soaking in bimatoprost microemulsion (ME) or solution (SM) containing 25, 50 or 75 µg drug per mL of simulated tear fluid for 7 days	2 mL of simulated tear fluid at 34 °C and 50 rpm; complete replacement of the release medium at each sampling point	New Zealand rabbits (male and female). SM (32.6 µg) and ME (46.4 µg) CL on one eye. As control, one drop (50 µL) of 0.03% *w/v* bimatoprost eye drop solution was instilled on one eye. Contralateral eyes were referred as control.	*In vitro*, SM and ME CLs showed a relevant burst and sustained drug release for 24 h and 48 h, respectively. *In vivo*, the release in tear fluid was prolonged for 12 and 24 h, respectively. The eye drop was cleared in less than 1 hour.	Xu et al., 2019
13	Travoprost	Silicone hydrogel CLs made of dimethyl acrylamide (250 µL), siloxane (150 µL), EGDMA (10 µL), and hydroxyethyl methacrylate (HEMA, up to 1000 µL)	Soaking in drug microemulsion (T-ME) or solution (T-SM) containing 25, 50 and 75 µg drug per mL of simulated tear fluid for 10 days	2 mL of simulated tear fluid at 34 °C and 100 rpm; complete replacement of the release medium at each sampling point	New Zealand rabbits (male and female). T-SM (13.9 µg) and T-ME (26.9 µg) CL on one eye. As control, one drop (50 µL) of 0.003% *w/v* travoprost eye drop solution was instilled on one eye. Contralateral eyes were referred as control.	*In vitro* and *in vivo*, T-SM CL and T-ME CL sustained drug release for 24 and 48 h, respectively. Eye drops showed a rapid decay in drug levels in the first two hours.	Xu and Liu, 2020
14	Olopatadine	EGDMA (10 µL), siloxane (100 µL), and HEMA (up to 1 mL)	Soaking (SM-OL), drug directly added during polymerization (DL-OL), or drug encapsulated in ethylcellulose microprarticles in	2 mL of simulated tear fluid at 34 °C and 100 rpm; complete replacement of the release medium at	New Zealand rabbits of either sex. One DNT-OL CL (260 µg dose). As control, one drop (50 µg olopatadine HCl) was instilled on one eye. Contralateral	*In vitro*, DNT-OL CL attenuated the burst but most drug was still released in the first 12 h. *In vivo*, olopatadine levels in tear fluid lasted few hours after eye drop	Xue et al., 2020

USC

			doughnut CLs (DNT-OL)	each sampling time	eyes were referred as control.	instillation and were prolonged for 24 h with the CLs.	
15	Betaxolol HCl	Silicone hydrogel CLs made of HEMA:NVP:TRIS 20:40:40 *w/w/w*	Drug loaded pH-responsive film (cellulose acetate-Eudragit S100) embedded in the CL	10 mL of simulated tear fluid or PBS at 35 ºC and 100 rpm; 2 mL replacement of the release medium at each sampling point	Male Nippon albino rabbit. Soaked CL (121 µg dose), film-embedded CL (700 µg dose), or one eye drop (100 µg dose) on one eye. Contralateral eyes were referred as control.	*In vitro*, drug release was minimum in PBS pH6.8 and prolonged for 10 h in simulated tear fluid. *In vivo*, drug levels in tear fluid were measurable for several days. IVIVC found.	Zhu et al., 2018a
16	Diclofenac sodium	HEMA and EGDMA (0.5 %)	Drug loaded pH-responsive film (ethylcellulose-Eudragit S100) embedded in the CL	10 mL of simulated tear fluid or PBS at 35 ºC and 100 rpm; 2 mL replacement of the release medium at each sampling point	Male Nippon albino rabbit. Soaked CL (100 µg dose), film-embedded CL (121 µg dose), or one eye drop (150 µg dose) on one eye. Contralateral eyes were referred as control.	*In vitro*, drug release was minimum in PBS pH6.8. The release rate in simulated tear fluid depended on thickness and molecular weight of polymer film. *In vivo*, drug levels in tear fluid were measurable for 12 h. IVIVC found.	Zhu et al., 2018b
17	Betaxolol HCl	Silicone hydrogel CLs made of HEMA:NVP:TRIS 20:40:40 *w/w/w*	Drug loaded ion-responsive film (poly(styrene-divinyl benzene) in cellulose acetate) embedded in the CL	10 mL of simulated tear fluid at 35 ºC and 100 rpm; 2 mL replacement of the release medium at each sampling point	Male Nippon albino rabbit. Film-embedded CL (700 µg dose), or one eye drop of drug-resin complex (100 µg dose) on one eye. Contralateral eyes were referred as control.	*In vitro*, drug release was sustained for one week. *In vivo*, drug levels in tear fluid were measurable for several days. The resin eye drops remained for 8h in tear fluid. IVIVC found.	Zhu et al., 2018c

18	Timolol	ACUVUE® TruEye™ (narafilcon A) silicone hydrogel contact lenses	Soaking in 3 mL of 20 or 50 mg/mL vitamin E in ethanol for 24 h, washed with water, and then placed in 3.5 ml of 8.0 mg/ml timolol maleate-PBS solution for 21 days. CLs without vitamin E were soaked in 2.5 mg/mL drug solution for 7 days	2 mL of PBS (room temperature)	Beagle dog model of glaucoma. One eye drop (150 μg) was applied to one eye twice a day for 4 days (total amount of timolol delivered 1200 μg). The other eye was referred as control. One control CL (60 μg dose) to be worn for 24 h, and replaced daily with a freshly drug-loaded CL for 4 days. One control CL (200 μg dose) to be worn for 4 days. One drug-loaded vit E-pretreated CL (200 μg dose) to be worn for 4 days.	*In vitro*, vit E-pretreated CLs sustained drug release up to 84 h compared to the 4 h of control CLs. *In vivo*, vit E-pretreated CLs were more efficient in regulating IOP than control CLs wore for 4 days.	Peng et al., 2012a
19	Timolol and dorzolamide	Senofilcon A	Soaking in 3 mL of 40 mg/mL vitamin E in ethanol for 24 h, washed with water, and then placed in 3.5 ml of 0.8 mg/ml timolol maleate-PBS solution or 3.5 ml of 0.75 mg/ml dorzolamide hydrochloride	2 mL of PBS (room temperature)	Beagle dog model of glaucoma. One eye drop (205 μg of timolol and 670 μg of dorzolamide) was applied to one eye twice a day for 4 days. The other eye was referred as control. One drug-loaded commercial CL	Dually-loaded commercial CLs released 90% timolol in 1.2 h, and 90% dorzolamide in 3 h. Vit E-pretreated CLs sustained drugs release for 42 h. Dually loaded CLs exhibited superior IOP reduction compared to eye drops with 4-	Hsu et al., 2015a

USC

			solution (4 days). For dual loading, vit E pretreated CLs were soaked in 3.5 ml of PBS containing timolol (12.75 mg/ml) and dorzolamide (20 mg/ml)		(non-pretreated with vitamin E) (60 μg of timolol and 220 μg of dorzolamide) was worn for 24 h and replaced daily for 5 days. One drug-loaded vit E-pretreated CL (200 μg of timolol and 680 μg of dorzolamide) was worn for 48 h and replaced once with a similar CL. The treatment was stopped at 96 h.	to 6-fold lower drug loading. Continuous wear of dually-loaded vitamin E-pretreated CLs reduced IOP during the 4 days of wear time and for another 8 days after removal of the CLs.	
20	Timolol and bimatoprost	EGDMA (10 μL), DMA (310 μL), NVP (10 μL), siloxane (100 μL), and HEMA (up to 1 mL)	Three small implants loaded with timolol (100 mg), bimatoprost (75 mg) and HA (60 mg), respectively, were included in the CLs	2 mL of simulated tear fluid at 34 ºC and 100 rpm; complete replacement of the release medium at each sampling time	New Zealand rabbits of either sex. One CL on one eye (50 μg bimatoprost and 85 μg timolol). As control, one drop (15 μg bimatoprost and 250 μg timolol) was instilled on one eye. Contralateral eyes were referred as control.	*In vitro* and *in vivo*, implant-loaded CLs sustained drug release for 24 h and lowered IOP for 72 h. CLs loaded by soaking showed higher burst release both *in vitro* and *in vivo*, although therapeutic levels were recorded in tear fluid for 12 h and low IOP was maintained 48 h.	Desai et al., 2020
21	Timolol	Acuvue Oasys	Soaking for 24 h in 3% (*w*/*w*) dispersion of timolol-loaded	Storage in 1 ml of packaging solution (PBS)	Beagle dog model of glaucoma. One CL in one eye. The other	*In vitro*, freshly loaded CLs sustained drug release for two weeks. CLs stored in	Jung et al., 2013

			propoxylated glyceryl triacrylate nanoparticles in ethanol	for 2 weeks at 4 ºC. Release was then tested in 1.75-3.5 mL PBS at room temperature and 40 ºC	eye was referred as control.	packaging solution evidenced leakage of drug-loaded nanoparticles, which led to lower amount released. *In vivo*, decrease in IOP was observed on days 2, 3 and 4 of wearing.	
22	Timolol	HEMA-based ring containing timolol-ethyl cellulose nanoparticles and sandwiched in HEMA-CL	During synthesis	2 mL of simulated tear fluid at 34 ºC under shaking; complete replacement of the release medium at each sampling time	New Zealand rabbits of either sex. One CL with ring (150 µg dose) placed on one eye. As control, one drop (250 µg) was instilled on one eye. Contralateral eyes were referred as control.	*In vitro*, the CLs sustained drug release for two days. *In vivo*, CL showed Cmax of 6.79 µg/mL in 5 min, followed by steady release for several days. The drop led to C_{max} of 132.6 µg/mL in 5 min and rapid decrease of drug in tera fluid.	Maulvi et al., 2016b
23	Timolol and hyaluronic acid	HEMA (669 µL), EGDMA (5 µL), DMA (310 µL), TRIS (1 µL), NVP (10 µL)	Semi-circular implants containing timolol or HA	2 mL of simulated tear fluid at 34 ºC and 100 rpm; complete replacement of the release medium at each sampling point	New Zealand white rabbits of either sex. One CL (148 µg timolol) for 7 days wearing. One drop of 0.5% timolol maleate (250 µg timolol). Contralateral eyes were referred as control.	CLs sustained the release of timolol and HA for 96 h *in vitro* and 72 h *in vivo* and decreased IOP during 144 h.	Desai et al., 2018
24	Timolol base and latanoprost	HEMA (580 µL) and EGDMA (15 µL)	Micelles containing both drugs (0.4 mL)	Franz diffusion cell. Donor compartment	Male Nippon albino rabbits, healthy and glaucoma model. One CL (100 µg	*In vitro*, CLs sustained timolol and latanoprost release for up to 120 h and 96	Xu et al., 2019

			were added to the monomers	with one CL and 1 mL STF, and receptor with 7 mL STF at 35 ºC and 50 rpm; 1 mL replacement of the release medium at each sampling point.	timolol and 1 µg latanoprost) on one eye. As reference, 50 µL of Xalacom® eye drops (250 µg timolol and 2.5 µg latanoprost) were instilled. Contralateral eyes were referred as control.	h, respectively. *In vivo*, CLs increased MRT (79.6-fold and 122.2-fold) and bioavailability (2.2-fold and 7.3-fold) for both timolol and latanoprost compared with eye drops. IOP reduction over 168 h.	
25	Timolol base	Silicone hydrogel CLs made of dimethyl acrylamide (350 µL), siloxane (100 µL), and hydroxyethyl methacrylate (HEMA, up to 1000 µL)	Soaking in timolol microemulsion (TB-ME-SM) or timolol solution (TB-SM) containing 1, 2 or 3 mg drug per mL of simulated tear fluid for 10 days	2 mL of simulated tear fluid at 34 ºC and 50 rpm; complete replacement of the release medium at each sampling point	New Zealand rabbits (male and female). TB-SM (234.3 ± 18.5 µg) and TB-ME-SM (215.3 ± 9.1 µg) CL on one eye. As control, one drop (50 µL) of 0.5% *w/v* timolol eye drop solution was instilled on one eye. Contralateral eyes were referred as control.	*In vitro*, TB-SM CL and TB-ME-SM CL released more than 90% drug in 12 h and in 48 h, respectively. *In vivo*, TB-SM CL and TB-ME-SM CL had Cmax at 5 min and provided measurable drug levels in tear fluid for 24 and 72 h, respectively. Eye drops showed a rapid decay in timolol levels in the first two hours. *In vivo* efficacy was evaluated regarding intraocular pressure (IOP). TB-ME-SM CL showed prolonged reduction in IOP values.	Wei et al., 2021
26	Sparfloxacin	EGDMA (10 µL), siloxane (100	Immersion in 2 mL of drug solution (2-6 mg/mL) in	2 mL of simulated tear fluid at 34 ºC	New Zealand rabbits of either sex. One CL with ring (129 µg	*In vitro*, the ring-loaded CLs were the only able to sustain	Ran et al., 2020

		μL), and HEMA (up to 1 mL)	0.5% PVP-simulated tear fluid medium, autoclaving and soaking for 7 days. Alternatively, a drug-loaded ring was adapted to the CL	under shaking; complete replacement of the release medium at each sampling time	drug) placed on one eye. As control, one drop (150 μg) was instilled on one eye. Contralateral eyes were referred as control. Efficacy in conjunctivitis model.	drug release for two days. *In vivo*, the ring-loaded CLs provided therapeutically useful drug levels in tear fluid for 12 h and favored conjunctivitis treatment.	
27	Ofloxacin	Silicone hydrogel CLs made of dimethyl acrylamide (250 μL), siloxane (100 μL), and hydroxyl ethylmethacrylate (HEMA, up to 1000 μL)	Soaking in ofloxacin microemulsion (Of-ME) or ofloxacin solution (Of-SM) containing 1, 2 or 3 mg drug per mL of simulated tear fluid for 7 days	2 mL of simulated tear fluid at 34 °C and 100 rpm; complete replacement of the release medium at each sampling point	New Zealand rabbits (male and female). Of-SM (191 μg) and Of-ME (358 μg) CL on one eye. As control, one drop (50 μL) of 0.3% *w/v* ofloxacin eye drop solution was instilled on one eye. Contralateral eyes were referred as control.	*In vitro*, Of-SM and Of-ME CLs showed a relevant burst and sustained drug release for 24 h and 72 h, respectively. *In vivo*, the release in tear fluid was prolonged for 24 and 48 h, respectively. The eye drop was cleared in less than 1 hour. *In vivo* efficacy was tested against *Staphylococcus aureus*-induced conjunctivitis. Of-ME CL improved the symptoms in 24 h. Complete healing was observed after 4 days of treatment with either one CL or 0.3% *w/v* ofloxacin eye	Li et al., 2020

						drop solution instilled every 4 h.	
28	Gatifloxacin	HEMA with methacrylic acid (MAA) (25:1 mol/mol)	Soaking in 0.5 mg/L drug solution in 0.9% NaCl medium at 37 °C until equilibrium	Non-disclosed volume of 0.9% NaCl medium	Sprague Dawley rats. Keratitis was induced on the right eye. Drug-loaded CLs (50 mg) were placed on the cornea and the eyelids were sutured. Saline and drug drops (5 µL; unknown concentration) were instilled every 4 h and used as controls.	*In vitro* P(HEMA-co-MAA) (11.8 µg/mg) released 70% drug in 24 h. *In vivo* efficacy in a rat model of bacterial keratitis. Wearing for 48 h of P(HEMA-co-MAA) favored the healing of cornea lesions caused by epithelial erosion and stromal ulceration, more efficiently than drug drops.	Shi et al., 2013
29	Gatifloxacin	Dimethyl acrylamide (31%), siloxane (2.5%), NVP (1%), EGDMA (1%) and hydroxyl ethylmethacrylate (HEMA, up to 1000 µL)	Drug directly added to the monomers solution, following by autoclaving and storage in 0.3% drug solution in Pluronic micelles packaging solution (GT-PL-CL). For comparison, CLs were soaked in the drug-containing packaging solution	2 mL of simulated tear fluid at 34 °C and 100 rpm; complete replacement of the release medium at each sampling point	New Zealand rabbits (male and female). GT-PL-CL (92 µg dose), SM-CL (53 µg dose) or one eye drop (150 µg dose) on eye. Contralateral eyes were referred as control.	*In vitro*, all CLs showed more than 60% burst release in the first 1 h. SM-CL completed 90% release in 6 h, while GT-PL-CL extended the release for 48 h. *In vivo*, SM-CL and GT-PL-CL prolonged the release 12 h and 24 h, respectively.	Maulvi et al., 2020

30	Hyaluronic acid	HEMA (46.7%), MAA (0.08%), EGDMA (0.5%) in water (52%) (0.1 mm)	Direct addition of HA to the monomer solution	2 mL simulated tear fluid at 100 rpm at 35 ºC; complete replacement of the release medium at each sampling point	New Zealand white rabbits. CL was placed on right eye. As control, one drop (50 µL) of 0.1% HA was instilled on the right eye. Left eye was referred as control.	*In vitro* release from CLs (200 µg HA) was prolonged for 10 days, without burst. *In vivo* showed a burst in the first day followed by therapeutically useful values for 10 days (MRT 128 h). Eye drops disappeared in the first 3 h of treatment (MRT 0.74 h).	Maulvi et al., 2015
31	Hyaluronic acid	DMA (200 µL), EGDMA (10 µL), siloxane (100 µL), HEMA (up to 1 mL)	HA and reduced graphene oxide (rGO) were added before polymerization in silicone CLs (HA-GO-DL) or loaded by soaking in 2 mg/mL HA in simulated tear fluid (HA-GO-SM)	2 mL simulated tear fluid at 100 rpm; complete replacement of the release medium at each sampling point	White New Zealand rabbits of either sex. CL was placed on right eye. As control, one drop (50 µL) of 0.1% HA was instilled on the right eye. Left eye was referred as control.	*In vitro* HA-GO-DL (10 µg HA loaded) sustained HA release for 96 h. *In vivo*, HA-GO-DL provided therapeutic levels for 48 h and promoted the production of tear fluid.	Huang et al., 2021
32	Hyaluronic acid	DMA (200 µL), EGDMA (10 µL), siloxane (100 µL), HEMA (up to 1 mL)	HA and Pluronic F127 were added before polymerization to obtain DL-HA-Pl CLs containing 20, 40 or 60 µg of HA and 20 µg of Pluronic F127. Alternatively, CLs were soaked in 1-	2 mL simulated tear fluid at 50 rpm; complete replacement of the release medium at each sampling point	White New Zealand rabbits of either sex. DL-HA-Pl CL (22.5 µg HA) and HA-SM CL (17.6 µg HA) was placed on right eye. As control, one drop (50 µL) of 0.1% HA was instilled on the right eye. Left eye	*In vitro*, HA-SM CL showed high burst and completed the release in 12-36 h. DL-HA-Pl CL sustained HA release for 48-96 h. *In vivo*, HA-SM CL and DL-HA-Pl CL provided therapeutically useful values for 4 and 48 h, respectively.	Wei et al., 2020a

USC

			3 mg/mL HA in simulated tear fluid for 7 days (HA-SM CLs)		was referred as control.		
33	Prednisolone and beclomethasone	Lidofilcon (HEMA-based)	Soaking in 1 mL of prednisolone (5 mg/mL) or beclomethasone (1 mg/mL) for 18 h at 4 ºC	1 mL of saline medium for injection (unknown temperature or stirring); complete replacement of the release medium every 3 h	New Zealand white rabbits. Drug-loaded CL on both eyes and the eyes were closed with surgical tape for four hours. The treatment was applied on days 1, 2, 5, 8 and 10. The amount of drug in plasma and anterior and posterior segment tissues was analyzed on day 11.	*In vitro*, CLs sustained drug release for 6 h. Both drugs were preferentially found in posterior segment tissues, with lower levels in vitreous humour.	Schultz et al., 2011
34	Pirfenidone	11 commercially available CLs	Soaking in 2 mL of 0.05%-0.5% drug solution	2 mL of PBS under shaking; complete replacement of the release medium at each sampling time	New Zealand rabbits. One polymacon CL on the right eye (1147 μg dose), one eye drop (30 μL of 0.5%; 150 μg dose) in the left eye.	*In vitro*, polymacon CL showed sustained release for 30 min. *In vivo*, significant levels in tear fluid were recorded for 60 min. CL wearing provided measurable drug levels in cornea, aqueous humor and sclera.	Yang et al., 2016
35	Pirfenidone	Silicone hydrogel CLs (Acuvue Oasys®) pre-treated with vitamin E	Soaking in 0.1% drug solution in PBS for 72 h	3 mL of PBS without replacement of the release medium	New Zealand White rabbits of either sex. An alkali burn was induced in one eye. One group received CLs.	*In vitro*, CLs sustained drug release up to 260 min. Gene expression of inflammatory cytokines IL-1β, TNF-α, and TGF-β1 was reduced.	Dixon et al., 2018

36	Pirfenidone	Silicone CLs made of silicone elastomer MED-6015 embedding a drug-containing polyvinyl alcohol insert	Loading during CLs preparation	2 mL of PBS under shaking at 37 °C; complete replacement of the release medium at each sampling time	Female New Zealand white rabbits. One CL on right eye (15.4 μg dose), one eye drop (30 μL of 0.5%; μg dose) in the left eye.	*In vitro*, CLs released 52 % dose in the first hour, followed by ten-times lower release rate in the next 15 hours. *In vivo*, CLs provided lower but more sustained drug levels in tear fluid and aqueous humor than eye drops.	Wu et al., 2021
37	Epalrestat	HEMA (up to 1 mL) with dimethacrylate acid (250 μL), siloxane (5 μL) and NVP (100 μL)	The drug directly or previously encapsulated in pegylated solid lipid nanoparticles (pSLNs) was added to monomer mixture before polymerization. Some hydrogels were loaded by soaking in drug solution or drug-encapsulated pSLNs for 7 days. After autoclaving, drug remaining in the CLs was quantified	2 mL of simulated tear fluid at 34 °C under shaking; complete replacement of the release medium at each sampling time	New Zealand rabbits of either sex. One CL, either directly loaded with p-SLN (98.1 μg drug) or soaked in p-SLN (110.8 μg drug), placed on one eye. As control, two drops (100 μg) were instilled on one eye. Contralateral eyes were referred as control.	*In vitro*, CLs loaded during synthesis with the drug encapsulated in pSLNs showed more sustained release, which led to measurable drug levels in tear fluid for prolonged time. CL wearing provided measurable drug levels in lens, cornea, aqueous humor and retina.	Zhu and Sheng, 2020
38	Ofloxacin	HEMA (99.5 wt%) and EGDMA (0.5 wt%) in the form of corneal CL, scleral/	Soaking in ofloxacin ophthalmic solution of 0.3% drug in 0.85% NaCl	*In vivo* release. Japanese albino rabbits without nictitating	Japanese albino rabbits without nictitating membrane. Each device was worn for 1 h and the amount	CLs released the drug faster and favored drug accumulation in cornea. S/CL led to high drug levels both in anterior and	Shikamur et al., 2016

USC

		corneal CL (S/CL) and rings	medium at 100 rpm for 24 h	membrane. Each device was worn for 0.25, 0.5, 1, 2, 4 and 8 h and the amount of drug remaining was quantified	of drug accumulated in ocular tissues was quantified. As control, 50 μL of ophthalmic solution was instilled. Ofloxacin concentration data collected from each rabbit were converted from actual tissue concentrations to ratios with respect to the administered drug dose. Contralateral eyes were also investigated.	posterior segment tissues. Rings facilitated drug accumulation in the posterior segment.	
39	Timolol	HEMA (62.5 %), DMA (31 %), TRIS (2.5%) and NVP (1 %) with and without gold nanoparticles (up to 0.1 mM)	Soaking in timolol base (2 mg/mL and 4 mg/mL; 2 mL) solution in simulated tear fluid containing or not gold nanoparticles (up to 0.1 mM), for 72 h	2 mL of simulated tear fluid at 34 ºC and 100 rpm; complete replacement of the release medium at each sampling time	New Zealand white rabbits. One CL with or without gold nanoparticles (277 and 253 μg of timolol, respectively) on one eye. As control, one drop (50 μL) of 0.5% *w/v* timolol maleate eye drop solution was instilled on one eye (250 μg of timolol). Contralateral eyes were referred as	*In vitro* all hydrogels released most dose in less than one hour. *In vivo*, timolol was detected in tear fluid for 60 h when administered in CLs and only for 2 h when instilled as eye drops. Timolol was quantifiable in eye tissues for 24 h.	Maulvi et al., 2019

					control. IOP was also recorded.		
40	Latanoprost	Latanoprost and PLGA 65:35 or 85:15 (high molecular weight) film was covered with methafilcon monomers. After polymerization, CLs were lathed	Three sets of CLs were prepared containing films of thickness 20, 40 and 45 μm	5 mL of PBS under shaking at 37 ºC; complete replacement of the release medium every 24 h	New Zealand rabbits of either sex. One CL under the nictitating membrane for one month wearing. One drop (30 μL) of 0.005% latanoprost solution.	*In vitro*, $CL_{65:35,\ 20}$, $CL_{65:35,\ 40}$ and $CL_{85:15,\ 45}$ released 90%, 48% and 45% drug dose in the first three days. *In vivo*, drug levels in aqueous humor were sustained for 4 weeks.	Ciolino et al., 2014
41	Dexamethasone	PLGA 85:15 (high molecular weight) film loaded with dexamethasone was covered with methafilcon monomers. After polymerization, CLs were lathed	One drug-loaded PLGA film ring was encapsulated in the CL (Dex-DS CL). Alternatively, CLs were soaked in dexamethasone base or phosphate solutions for 24 h	10 mL PBS and incubating at 37 °C; complete replacement of the release medium at each sampling time	Female New Zealand White rabbits. One CL (1.5 mg dose) for 7 days wearing. One drop of 0.1% dexamethasone solution every hour for 8 h.	*In vitro*, soaked CLs completed the release in less than 4 h. Dex-DS CL sustained drug release for 7 days. *In vivo*, continuous wearing of Dex-DS CL provided higher drug levels in all ocular tissues than the eye drops.	Ross et al., 2019
42	Cyclosporine A	HEMA with methacrylic acid (MAA)	The drug was impregnated into nanoporous silica using supercritical CO_2 and then added to the monomers solution	2 mL of PBS at 37.8 ºC; complete replacement of the release medium at each sampling time	Female New Zealand rabbits health and dry eye model. CL wearing in both eyes applied daily, or 0.05% drug eyes drops.	*In vitro*, CLs sustained drug release for 8 h. *In vivo*, high levels of drug were detected for 48 h in cornea and conjunctiva. CLs increased tear volume and stabilized tear film.	Choi et al., 2019

1.4.1 Comparison of *In vivo* and *In vitro* Release Profiles

Drug-containing molecularly imprinted CLs were among the first investigated CL *in vivo*. In 2005, Hiratani et al. [Hiratani et al., 2005a] pioneered the optimization of soft CLs with an ability to load timolol (**Table 1.2, entry 1**). Imprinted CLs loaded 34.7 (s.d. 0.3) μg while non-imprinted ones only hosted 21.2 (s.d. 0.2) μg. In 0.9% NaCl medium (*in vitro* tests) both CLs sustained the release for more than 24 h in spite of being extremely thin (**Figure 1.6A1**). *In vivo* release (rabbit model) was monitored by measuring timolol levels in the tear fluid (**Figure 1.6A2**). Topically instilled eyedrops were rapidly cleared (either 34 μg or 125 μg dose), and timolol levels in the tear fluid decreased exponentially in the first 30 min and disappeared within 60 min. In contrast, CLs enhanced the mean residence time (MRT) by two-fold. Imprinted CLs provided measurable timolol levels in tear fluid for 180 min, which was 2-fold longer than the time recorded for non-imprinted CLs. Remarkably, the area under the curve (AUC) obtained with the imprinted CLs was 8 and 3 times higher than those recorded for the eye drop containing the same dose and for the non-imprinted CLs, respectively. The sustained timolol levels in the tear fluid provided by the imprinted CLs are the result of an enhanced affinity for the polymer network by the drug, which in turn facilitates higher loading and more controlled release [Hiratani et al., 2005a]. However, the capability of these CLs to sustain timolol release *in vivo* was remarkably lower than *in vitro*, probably as a consequence of both the continuous replacement of the tear fluid and blinking. It should be noted that the composition of the CLs tested in this work was chosen in such a way that the main structural component had very low affinity for the drug, and thus the main drug binding site was formed by only the functional methacrylic acid (MAA) moieties [Hiratani et al., 2004], which may be too weak for efficient drug retention under the competitive *in vivo* environment.

USC UNIVERSIDADE DE SANTIAGO DE COMPOSTELA

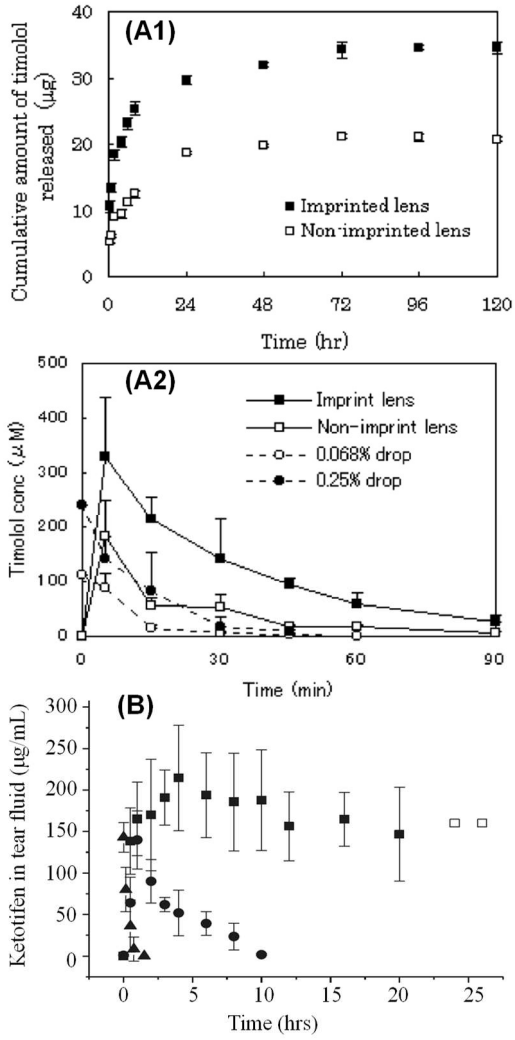

Figure 1.6. (**A1**) *In vitro* timolol release profiles (0.9% NaCl; 10 mL) and (**A2**) *in vivo* timolol levels in tear fluid after application of drug-loaded imprinted and nonimprinted CLs (0.08 mm center thickness). Timolol doses applied in each eye were 21 μg for non-imprinted CLs, 34 μg for imprinted CLs and 0.068% timolol eye drop, and 125 μg for 0.25% timolol eyedrop (*n* = 3-5). Reprinted from Hiratani et al. [Hiratani et al., 2005a] with permission from Elsevier. (**B**) Ketotifen fumarate levels in tear fluid during wearing of poly(HEMA-co-AA-co-AM-co-NVP-co-PEG200DMA)

imprinted (■, □) and non-imprinted (●) CLs and after instillation of eye drops (0.035% solution; ▲) (*n* = 3–5; hollow data points represent single run). Reprinted from Tieppo et al. [Tieppo et al., 2012b] with permission from Elsevier.

More prolonged *in vivo* release profiles were reported by Tieppo et al. [Tieppo et al., 2012b] for ketotifen-imprinted CLs (**Table 1.2, entry 2**). The multi-monomer composition of the CLs was chosen to attempt to mimic the human receptor of the drug. Ketotifen-imprinted poly(HEMA-co-AA-co-AM-co-NVP-co-PEG200DMA) showed 4 times higher loading than nonimprinted hydrogels and 19 times slower transport. Under dynamic infinite-sink *in vitro* release conditions, imprinted CLs released 85% of the drug in 24 h, while non-imprinted CLs completed the release in less than 6 h. Remarkably, imprinted CLs provided sustained release *in vivo* for an entire day (MRT 12.6 h) (**Figure 1.6B**). Non-imprinted CLs provided therapeutic drug levels (~ 30 μg/mL) for 7 h (MRT 3.4 h), and the eye drops only remained for a few minutes (MRT 0.25 h). The high capability of these drug-imprinted CLs to sustain ketotifen release may pave the way to clinical studies in humans [Wuchte et al., 2017]. Compared to conventional (non-imprinted) silicone hydrogel CLs (**Table 1.2, entry 3**) [Xu et al., 2011], the ketotifen-imprinted CLs provided higher drug levels for a more prolonged time. In the case of silicone hydrogel CLs, an increase in DMA enhanced ketotifen loading, but led to faster drug release both *in vitro* (complete release in 5 h) and *in vivo* (also 5 h with levels above the therapeutic concentration; MRT 1.9 h). Interestingly a clear correlation between capability to prolong drug release *in vitro* and *in vivo* was observed, although only two different compositions were evaluated [Xu et al., 2011]. Also, for ketotifen, it was confirmed that an increase in the concentration of the drug in the eye drops does not prolong the MRT.

USC UNIVERSIDADE DE SANTIAGO DE COMPOSTELA

Bimatoprost-imprinted silicone hydrogel CLs (**Table 1.2, entry 4**) showed minor improvements in drug loading compared to nonimprinted CLs, but more prolonged release *in vitro* (up to 36 h *vs.* 24 h) and slightly higher drug levels in tear fluid *in vivo* (rabbits) for 12 h [Yan et al., 2020]. Once again, although the capability of the CLs to sustain drug release *in vivo* was shown to be shorter than *in vitro*, the increase in residence time in tear fluid compared to eye drops was remarkable.

Comonomers with affinity for the drug, such as N-vinylpyrrolidone (NVP), have been used to improve the capability of HEMA-based CLs to uptake puerarin and to prolong its release *in vitro* and in tear fluid for 4 h (**Table 1.2, entry 5**) [Xu et al., 2010a]. Extended *in vitro* release up to 10 h was observed when β-cyclodextrin was copolymerized with HEMA, which in turn allowed for prolonged permanence in tear fluid, up to 6 h (**Table 1.2, entry 6**) [Xu et al., 2010b]. Favorable drug-CL interactions may also occur when using commercially available CLs, particularly silicone hydrogels, which are more prone to stablish hydrophobic interactions. As an example, diquafosol, a secretagogue for dry eye treatment, can be taken up by comfilcon A and balafilcon A (up to 0.02 mg) (**Table 1.2, entry 7**). In *in vivo* studies, CLs sustained drug release in tear fluid for 240 min and increased tear secretion for 300 min, while the effects of topical instillation only lasted for 90 min [Dominguez-Godinez et al., 2018].

Loading of hydrophobic drugs can be enhanced if the drug is encapsulated in lipid nanoparticles or microemulsions. Ketotifen was encapsulated in solid lipid nanoparticles, which were pegylated (p-SLNs) or not (SLNs) and then used for the drug loading of HEMA-based hydrogels (**Table 1.2, entry 8**) [Zhang et al., 2020]. Some hydrogels were loaded with ketotifen by addition of SLNs (DL-K-SLN-

USC UNIVERSIDADE DE SANTIAGO DE COMPOSTELA

100) or p-SLNs (DL-K-p-SLN-100) to the monomer solution before polymerization. Another batch of hydrogels was loaded by soaking into either ketotifen solution (SM-K-50 and SM-K-100) or ketotifen-encapsulated SLNs (SM-K-SLN-100) or p-SLNs (SM-K-p-SLN-100). All hydrogels were autoclaved before testing drug release. Hydrogels loaded by soaking showed a very intense burst in the *in vitro* release tests (**Figure 1.7A1**). Directly loaded CLs contained more drug and released it at slower rate. Interestingly, *in vivo*, these latter CLs (DL-K-p-SLN-100) provided lower C_{max} (445.7 ± 85.3 μg/mL *vs.* 581.6 ± 152.7 μg/mL) but more prolonged drug levels in tear fluid along time than CLs that were loaded by soaking in ketotifenencapsulated p-SLNs (SM-K-p-SLN-100) (**Figure 1.7A2**). This finding was related to stronger retention of the p-SLNs when they were incorporated into the bulk of the hydrogel. Similarly, prolonged ketotifen release in both *in vitro* and *in vivo* was recorded from CLs loaded with silica shell nanoparticles encapsulating the drug (**Table 1.2, entry 9**) [Maulvi et al., 2016a]. From a safety perspective, it should be noted that direct loading, in which the drugs are incorporated into a CL material before polymerization, has the inherent risk of leakage of unreacted monomers when the CL is inserted in the eye.

In vitro-in vivo correlations (IVIVC) have been attempted through Levy plot analysis. Mainly, the percentage of drug released *in vitro* at a certain time is reported on the X-axis, and the percentage of drug released in the tear fluid at the same time on the Y-axis. The methodology for the estimation of this latter parameter was not disclosed in most papers, but it can be assumed that the percentage of drug released *in vivo* was estimated as [Xu et al., 2019]

$$\text{Drug released } in\ vivo\ (\%) = \frac{Cumulative\ release\ amount_{0-t}}{Cumulative\ release\ amount_{0-last}} \times 100\% \quad \text{(Eq. 1.11)}$$

USC UNIVERSIDADE DE SANTIAGO DE COMPOSTELA

which can be calculated as

$$\text{Drug released } in\ vivo\ (\%) = \frac{AUC_{0-t}}{AUC_{0-las}} \times 100\% \qquad \text{(Eq. 1.12)}$$

In the case of ketotifen, the Levy plot suggests moderate IVIVC (**Figure 1.7A3**) [Zhang et al., 2020], although this plot should be read with caution, since only four data points of drug levels in tear fluid were used for the analysis.

CLs loaded with drugs encapsulated in microemulsions have also been investigated in detail. As an example, the effect of surfactant chain length (C8-sodium caprylate, C12-Tween 20, C18-Tween 80) and the molecular weight of Pluronic block copolymers (8400-PF68 and 12600-PF127) was investigated to elucidate how the stability of the microemulsion may determine cyclosporine A release kinetics from hydrogel CLs (**Table 1.2, entry 10**) [Maulvi et al., 2017a]. CLs loaded with cyclosporine A during polymerization (DL-100) were opaque due to drug precipitation. CLs loaded with cyclosporine A encapsulated in stable PF127-T80 microemulsions were transparent and released the drug *in vitro* faster than DL-100 and non-stable PF68-SC CLs (**Figure 1.7B1**). In this case, a prolonged release profile was not synonymous of prolonged efficacy since the release rate from drug-precipitated CLs was too slow to achieve therapeutic levels (**Figure 1.7B2**). Indeed, *in vivo* release tests showed that PF127-T80-containing CLs may supply higher drug levels and for more prolonged time than the other tested CLs. Although a dependence of the percentage of drug released to tear fluid on the percentage of drug released *in vitro* was observed (**Figure 1.7B3**), the correlation coefficients of Levy plots were far from 1, mostly because the cumulative amount released *in vivo* in the first time period was larger than that predicted from the *in vitro* release values. The authors pointed to the presence of lipophilic proteins in tears as a

USC UNIVERSIDADE DE SANTIAGO DE COMPOSTELA

cause of the Levy plot deviations, since they bind and solubilize hydrophobic drugs, promoting the release from the CL [Maulvi et al., 2017a]. Prolonged levels of cyclosporine A in tear fluid were also found when the drug was encapsulated in Eudragit S100 nanoparticles (**Table 1.2, entry 11**), but IVIVC were not investigated [Maulvi et al., 2017b].

Soaking in microemulsions has also been demonstrated as a useful method to load bimatoprost and to prolong both *in vitro* and *in vivo* drug release from CLs (**Table 1.2, entry 12**). Compared to the loading by soaking in a bimatoprost solution, the microemulsions doubled the amount loaded and the time required for complete release both *in vitro* (48 h *vs.* 24 h) and *in vivo* (24 h *vs.* 12 h) [Xu et al., 2019]. Similar results were reported for travoprost (**Table 1.2, entry 13**) [Xu et al., 2020].

Hydrophobic polymeric microparticles have been tested to encapsulate olopatadine and then applied as a doughnut ring on CLs (**Table 1.2, entry 14**). Compared to CLs loaded by soaking (SM-OL) or to which the drug was directly added during polymerization (DL-OL), the doughnut CLs (DNT-OL) avoided burst release *in vitro*, but still released most of the drug in the first 12 h. *In vivo*, DNT-OL CLs provided therapeutic levels in tear fluid for 24 h, but once again the Levy plot showed poor IVIVC as *in vivo* release was faster than predicted [Xue et al., 2020]. Also, bioinspired strategies for choosing the CL monomers have been shown able to enhance the affinity of CLs for olopatadine increasing the loading and providing 24 h almost constant rate release *in vitro* [González-Chomón et al., 2016]. Although these CLs were not tested *in vivo*, in cell culture they were able to efficiently inhibit the release of histamine and TNF-α from sensitized mast cells.

USC UNIVERSIDADE DE SANTIAGO DE COMPOSTELA

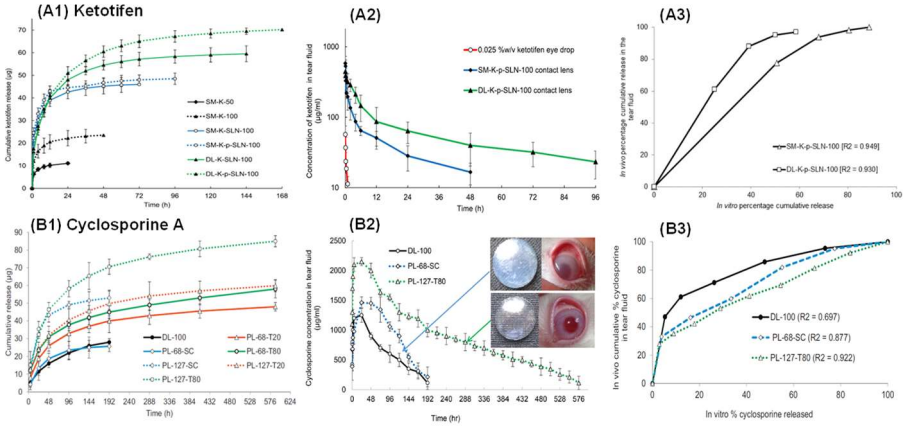

Figure 1.7. (**A1**) *In vitro* ketotifen release profiles from CLs loaded by soaking in drug solutions (SM-K-50 and SM-K-100) or drug-encapsulating non-pegylated solid lipid nanoparticles (SM-K-SLN-100) or pegylated solid lipid nanoparticles (SM-K-p-SLN-100), and CLs loaded by adding the drug-encapsulating nanoparticles directly to the monomer solution (DL-K-SLN-100 and DL-K-p-SLN-100), (**A2**) *in vivo* ketotifen profiles in tear fluid during CLs wearing and after eye drop instillation (n = 6), and (**A3**) Levy plot depicting the percentage of ketotifen released *in vivo vs. in vitro*. Reprinted from Zhang et al. [Zhang et al., 2020] with permission from Elsevier. (**B1**) *In vitro* cyclosporine A release profiles from CLs prepared with the drug directly added (DL-100) or previously encapsulated in a microemulsion, (**B2**) *in vivo* release profiles (n = 6) and, in the insert, the appearance of the CLs that were transparent when loaded with the drug encapsulated in stable microemulsions, and opaque when the drug was encapsulated in unstable microemulsions and precipitated in the CL network, and (**B3**) Levy plots for percentage of drug released *in vivo vs. in vitro*. Reprinted from Maulvi et al. [Maulvi et al., 2017a] with permission from Elsevier.

A variety of film-embedded CLs have also been designed. For example, pH-responsive films made of cellulose acetate and Eudragit S100 containing betaxolol hydrochloride were integrated into silicone hydrogels (**Table 1.2, entry 15**). The film prevented premature discharge during storage in PBS at pH 6.8 and provided sustained drug release for 10 days in simulated lachrymal fluid. Since the films

USC UNIVERSIDADE DE SANTIAGO DE COMPOSTELA

enhanced drug loading (700 μg dose) compared to commonly soaked CLs (100 μg) remarkably higher $AUC_{0\text{-}240h}$ (599 *vs.* 26 μg·h/mL) and MRT (88 *vs.* 1.7 h) were recorded in tear fluid (**Figure 1.8A1**). Improvements compared to eye drops were also evident ($AUC_{0\text{-}240h}$ 10.5 μg·h/mL and MRT 0.4 h). The Levy plot revealed that after a lag time, good IVIVC was obtained (R^2 0.9708) (**Figure 1.8A2**) [Zhu et al., 2018a]. In a related study, the same group evidenced the effects of the film components and thickness in controlling the release of diclofenac (**Table 1.2, entry 16**) and showed that for a similar amount of drug loaded, the film-embedded HEMA-based CL (121 μg dose) sustained the release both *in vitro* and *in vivo* for 12 h (**Figure 1.8B1**). In comparison, soaked CL (100 μg dose) rapidly discharged in 4 h. The improvement in the IVIVC according to the Levy plot was notably better in the case of the film-embedded CLs (**Figure 1.8B2**) [Zhu et al., 2018b]. The films were further modified to respond to ionic strength, preventing premature discharge when stored in water (**Table 1.2, entry 17**) [Zhu et al., 2018c] or to respond to both ionic strength and pH [Wei et al., 2020b]. Once again, the film-embedded CLs showed sustained release *in vivo* (**Figure 1.8C1**), which correlated quite well with the release pattern *in vitro* (**Figure 1.8C2**) [Zhu et al., 2018c].

USC UNIVERSIDADE DE SANTIAGO DE COMPOSTELA

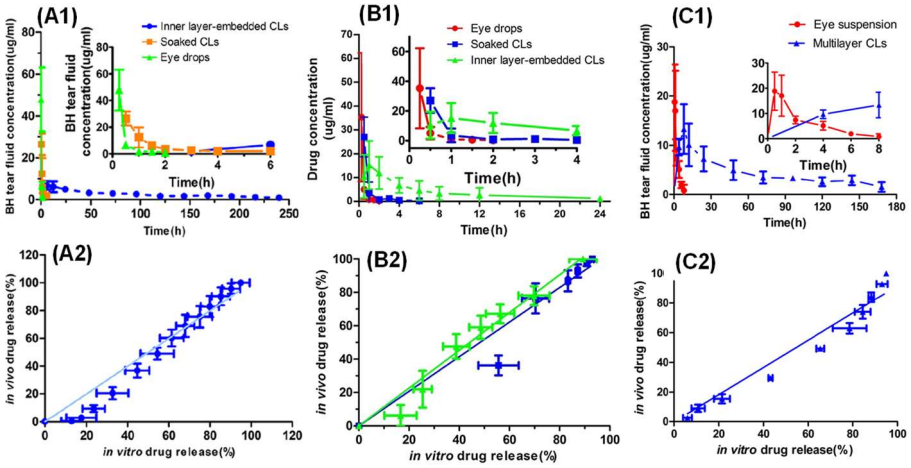

Figure 1.8. (**A1**) Betaxolol hydrochloride (BH) levels in tear fluid after instillation of eye drops (100 μg dose) or wearing of soaked CL (121 μg dose) and film-embedded CL (700 μg dose), and (**A2**) Levy plot for IVIVC (R^2= 0.9708). Reprinted from Zhu et al. [Zhu et al., 2018a] with permission from Elsevier. (**B1**) Diclofenac sodium levels in tear fluid after instillation of eye drops (150 μg dose) or wearing of soaked CL (100 μg dose) and film-embedded CL (121 μg dose), and (**B2**) Levy plot for IVIVC of soaked CL (R^2= 0.9019) and film-embedded CL (R^2= 0.9230). Reprinted from Zhu et al. [Zhu et al., 2018b] with permission from Elsevier. (**C1**) Betaxolol hydrochloride (BH) levels in tear fluid after instillation of suspension eye drops (100 μg dose) or wearing of dug-resin complex film-embedded CL (700 μg dose), and (**C2**) Levy plot for IVIVC obtained for the CL (R^2= 0.9406). Reprinted from Zhu et al. [Zhu et al., 2018c] with permission from Elsevier.

1.4.2 Comparison of *In vitro* Release Profiles and Therapeutic Outcome

Regulation of intraocular pressure (IOP) using timolol-loaded CLs has been the aim of various studies. Since most commercially available CLs lack sufficient affinity for ocular drugs, Chauhan and coworkers developed the strategy of creating biocompatible and optically transparent diffusion barriers that rely on the hydrophobic features of

USC UNIVERSIDADE DE SANTIAGO DE COMPOSTELA

vitamin E [Peng et al., 2012a; Peng et al., 2012b]. Both vitamin E-pretreated and non-pretreated silicone hydrogel CLs were loaded with 200 μg timolol with the aim of continuous wearing for 4 days (**Table 1.2, entry 18**). *In vitro*, non-pretreated CLs released 80% of the drug in the first 4 h, while vitamin E-pretreated CLs extended drug release for up to 84 h [Peng et al., 2012a]. The CLs were tested in a Beagle dog model of glaucoma. Daily-replaced non-pretreated CLs (60 μg timolol) led to a significant decrease in IOP from the first day of treatment until one day after. A similar pattern was observed for the eye drops, but the IOP decrease was more pronounced with the daily CLs in spite of containing only 20% of the drug dose instilled with the eye drops. Non-pretreated CLs worn for 4 days (200 μg timolol) caused a decrease in IOP during the first two days only, as expected from the limited capability of the CLs to sustain drug release *in vitro*. In comparison, vitamin E-pretreated CLs wore for 4 days (200 μg timolol) caused a progressive decrease in IOP from day 1 to day 4, and the decrease was maintained 24 h after CL removal. These findings clearly demonstrated the advantages of sustained drug release from CLs and their capability to enhance ocular bioavailability compared to eye drops.

Interestingly, commercially available senofilcon A CLs showed distinct release profiles depending on whether they were loaded with one antiglaucoma drug or simultaneously with two drugs (**Table 1.2, entry 19**) [Hsu et al., 2015a]. In separate, senofilcon A CLs loaded 20 μg timolol and sustained the release over 0.7 h, or loaded 122 μg of dorzolamide and sustained the release for 2.5 h. When both drugs were simultaneously loaded, the loading increased up to 60 μg timolol and 218 μg dorzolamide, and the release was extended to 1.2 h for timolol and 3.0 h for dorzolamide. The increase in drug affinity could be due to favorable drug-drug interactions through hydrogen bonding. Pre-treatment of CLs with vitamin E increased drug uptake and led to more

USC UNIVERSIDADE DE SANTIAGO DE COMPOSTELA

controlled release (**Figure 1.9A**). Timolol release was sustained for 24.6 h in single loaded CLs (18 μg dose) and for 42.2 h in dually loaded CLs (193 μg). Similarly, dorzolamide release was prolonged for 36.0 h in single loaded CLs (122 μg dose) and for 42.3 h in dually loaded CLs (680 μg) [Hsu et al., 2015a]. *In vivo* efficacy was evaluated in terms of decrease in IOP in a Beagle dog model of glaucoma. Compared to eye drops that required frequent administration to maintain low IOP values in the treated eye and that altered the IOP values in the contralateral eye (**Figure 1.9B**), dually-loaded CLs showed more pronounced and sustained decrease in IOP using a lower dose (4- to 6-fold lower) and avoiding effects on the control eye (**Figure 1.9C and D**). Dually-loaded vitamin E-pre-treated CLs maintained the therapeutic effect for two days and, after treatment, the decrease in IOP was maintained for approx. one week after the CLs were removed (**Figure 1.9D**). These findings confirm once again that CLs can increase ocular drug bioavailability and decrease systemic absorption of drugs through the conjunctiva and nasolacrimal duct, potentially avoiding side effects. These results also suggest a correlation between the time the drug can be released *in vitro* for a sustained period and the time that therapeutic effects can be maintained *in vivo*. It has been hypothesized that the prolonged IOP reduction may be a consequence of the creation of drug depots in the ocular tissues and, in particular, drug partition into corneal epithelial cells [Hsu et al., 2015a]. When hydrophilic drugs are administered as eye drops, the precorneal residence time is very short and the drug molecules may penetrate the epithelium by diffusion in between the cells (through the tight junctions), reach the stroma and then diffuse across the endothelium to the aqueous humor. In contrast, the transcellular pathway is slow and requires prolonged contact time for the drug to partition into the epithelium cells. Therefore, sustained release from CLs for several days may facilitate drug accumulation into

USC UNIVERSIDADE DE SANTIAGO DE COMPOSTELA

epithelium cells, which may subsequently act as drug depots. Once the CL is removed, the accumulated drug molecules may slowly release from the cells, maintaining the therapeutic effect.

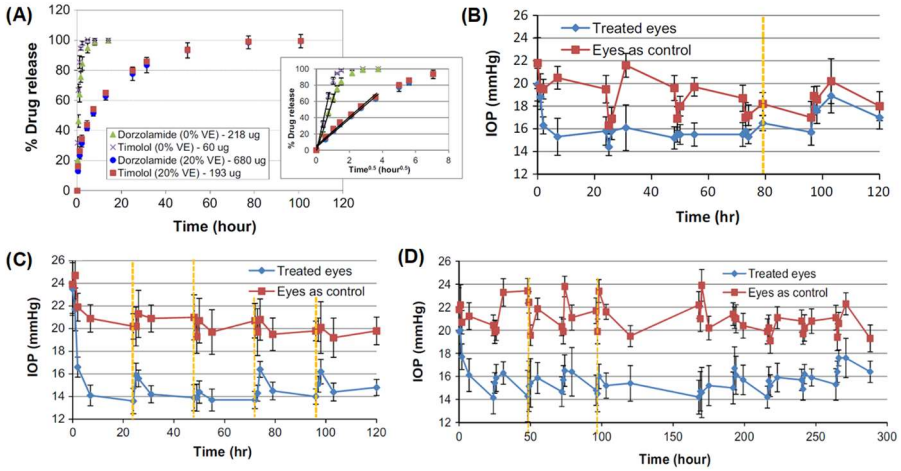

Figure 1.9. (**A**) Timolol and dorzolamide release profiles from dually loaded senofilcon A CLs that were pre-treated (20% VE) or not (0% VE) with vitamin E. In the insert the solid lines represent the fitting to the square root kinetics (n = 3). (B, C and D) Measurement of IOPs of 10 beagle dogs treated with (**B**) Cosopt® eye drops (one eye twice a day for 4 days) for 79 h (indicated by the dash line); (**C**) dually-loaded CLs worn for 24 h and replaced daily for 5 days; and (**D**) dually-loaded vitamin E pre-treated CLs worn for 48 h and replaced once with a similar CL (n = 10). Reprinted from Hsu et al. [Hsu et al., 2015a] with permission from Elsevier.

Dual delivery of timolol and bimatoprost has been investigated in the form of small implants (partial rings) attached to the outer periphery of silicone hydrogel CLs [Desai et al., 2020]. This approach had the drawback of rapid discharge during wet sterilization. Therefore, omplant-containing CLs could only be sterilized using radiation

USC UNIVERSIDADE DE SANTIAGO DE COMPOSTELA

sterilization and then hydrated for 24 h before wearing. The advantages of implant-containing CLs referred to attenuation of burst release and slow-release rate both *in vitro* and *in vivo* compared to CLs loaded by soaking in the solutions of both drugs (**Table 1.2, entry 20**) [Desai et al., 2020]. Implant-containing CLs provided therapeutic levels in tear fluid for 24 h and maintained IOP decrease for 72 h, while in the case of soaked CLs these times were limited to 12 h and 48 h, respectively.

Timolol encapsulation in nano or microstructures may also provide sustained release from extended wear (overnight) CLs. Nanoparticles of propoxylated glyceryl triacylate containing timolol linked through ester bonds could regulate drug release through the hydrolysis of the bond. CLs containing 5% nanoparticles sustained drug release *in vitro* for several weeks (**Table 1.2, entry 21**). *In vivo* testing in Beagle dogs revealed an efficient decrease in IOP on days 2, 3 and 4 of wearing, which means that the CLs required at least 24 h to supply therapeutic amounts of drug, and after 5 days of wearing they were exhausted [Jung et al., 2013]. An acrylate ring loaded with timolol-ethyl cellulose nanoparticles (150 μg dose) coupled to HEMA-based CLs has also been shown to enhance drug residence on the ocular surface and to decrease IOP levels for several days (**Table 1.2, entry 22**) [Maulvi et al., 2016b]. In this context, semi-circular rings of hyaluronic acid (HA) and timolol coupled to CLs sustained the release of both components for 96 h *in vitro* and 72 h *in vivo* and decreased IOP for 144 h (**Table 2, entry 23**) [Desai et al., 2018].

Co-delivery of timolol and latanoprost has been attempted by co-encapsulation of the drugs in mPEG-PLA micelles, which were directly added to HEMA before CL synthesis **(Table 1.2, entry 24**) [Xu et al., 2019]. *In vitro*, using a Franz diffusion cell, CLs showed a rapid release in the first 6 h followed by slower rate for up to several days. Compared

USC UNIVERSIDADE DE SANTIAGO DE COMPOSTELA

to eye drops, CLs led to lower C_{max} and more sustained levels of drug in tear fluid (**Figure 1.10A1 and A2**). In this case, the IVIVC was poor because the *in vivo* release rate was lower than predicted from the *in vitro* values (**Figure 1.10A3**). An impressive decrease in IOP was recorded for CLs compared to eye drops in a glaucoma model (**Figure 1.10A4**) [Xu et al., 2019].

Recently, silicone hydrogel CLs soaked in timolol microemulsion (TB-ME-SM) showed two-fold improvement in the loading compared to merely soaking in timolol solution (TB-SM) (**Table 1.2, entry 25**) [Wei et al., 2021]. *In vitro*, TB-ME-SM CLs released timolol more slowly (90% in 48 h) than TB-SM CLs (90% in 12 h) prepared containing similar drug doses (**Figure 1.10B1**). *In vivo*, TB-SM CL and TB-ME-SM CL had C_{max} at 5 min and provided measurable drug levels in tear fluid for 24 and 72 h, respectively (**Figure 1.10B2**). If instilled as eye drops, timolol levels in the tear fluid rapidly decayed in the first two hours, although the reduction in IOP was maintained for 6 h. Both TB-SM CL and TB-ME-SM CL caused more intense and prolonged reduction in IOP values (up to 72 h and 96 h, respectively) with a dose equivalent to a single eye drop (**Figure 1.10B3**).

USC UNIVERSIDADE DE SANTIAGO DE COMPOSTELA

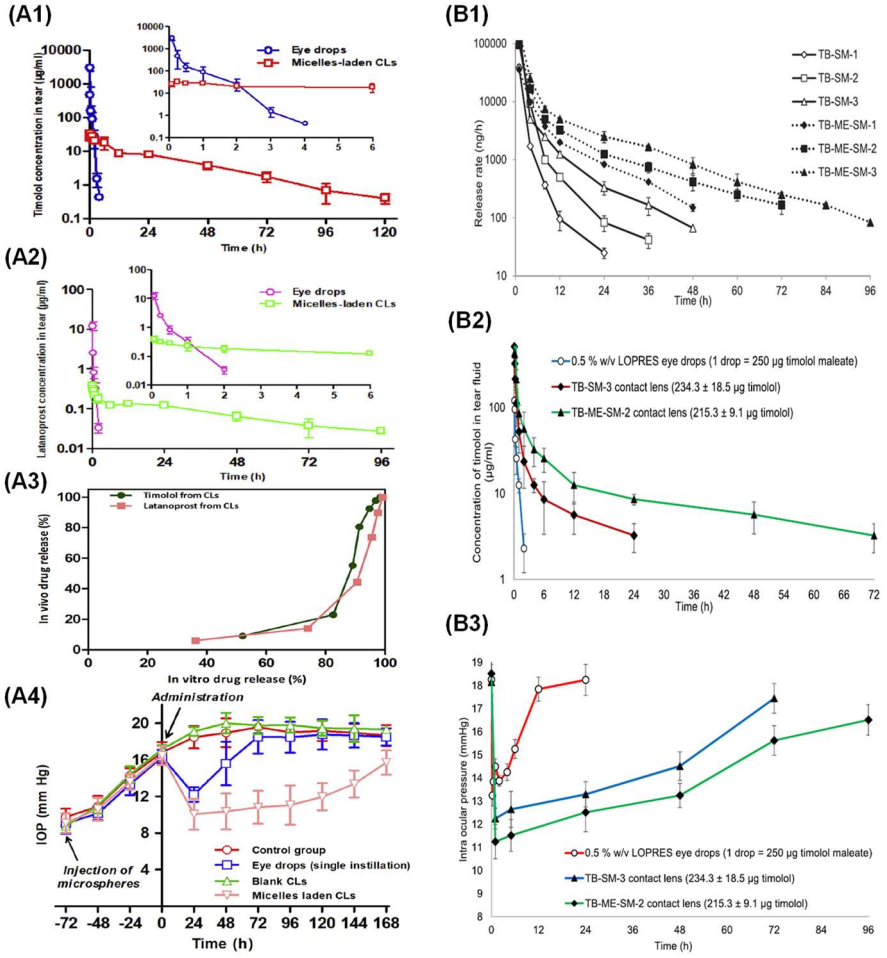

Figure 1.10. (**A1 and A2**) Timolol and latanoprost levels in tear fluid from rabbit eyes after instillation of Xalacom® eye drops (250 µg timolol and 2.5 µg latanoprost) and during wearing of CLs containing both drugs encapsulated in micelles (100 µg timolol and 1 µg latanoprost), (**A3**) Levy plot for timolol (R^2= 0.7613) and latanoprost (R^2= 0.7119); and (**A4**) increase in IOP after single injection of polystyrene microspheres three days before treatment and subsequent effect on IOP of the instillation of eye drops or wearing of CLs (drug dose as in former plots); (*n* = 4). Reprinted from Xu et al. [Xu et al., 2019] with permission from Elsevier. (**B1**) Timolol release rate in simulated lachrymal fluid from silicone hydrogel CLs loaded by soaking in timolol base solution (TB-SM) or in timolol base microemulsion (TB-ME-SM) (*n* = 3), (**B2**) timolol levels in tear fluid (rabbit model) (*n* = 6), and (**B3**)

effect of eye drop instillation or CL wearing on IOP values (n = 6). Timolol loaded in TB-SM-1, TB-SM-2 and TB-SM-3 was 48.5, 141.3 and 234.3 μg, respectively, and in TB-ME-SM-1, TB-ME-SM-2 and TB-ME-SM-3 was 108.5, 215.3 and 365.8 μg, respectively. Reprinted from Wei et al. [Wei et al., 2021] with permission by Taylor & Francis Ltd.

Delivery of antimicrobial agents using CLs has also been tested. For example, sparfloxacin cannot be directly added to silicone hydrogels (Sp-L method) because it causes phase separation and, thus, a loss in light transmission. This problem was overcome by co-loading of preformed CLs with sparfloxacin and polyvinylpyrrolidone (PVP) (Sp-S method) or applying the drug-PVP combination as a ring to be fixed in the periphery of the CL (Sp-R method) (**Table 1.2, entry 26**) [Ran et al., 2020]. In comparison to Sp-L and Sp-S CLs (which showed a high burst in the *in vitro* release test), Sp-R CLs sustained the release of both sparfloxacin and PVP for 48 h. In tear fluid (rabbit model), the Sp-R CLs released enough drug to achieve the minimum inhibitory concentration (MIC) for *Staphylococcus aureus* for 12 h. Furthermore, these CLs also notably shortened the time to treat the conjunctivitis. The Levy plot failed to correlate the percentage of drug released *in vivo* with that released *in vitro*; once again, the *in vivo* release was faster than predicted. In this case, the authors also suggested that sparfloxacin may be delivered quickly *in vivo* due to binding to lipids present in the tear film [Ran et al., 2020].

Microemulsions have also been advantageous to increase the loading of ofloxacin in HEMA-based CLs compared to conventional soaking (**Table 1.2, entry 27**) [Li et al., 2020]. Soaked (Of-SM, 191 μg dose) and emulsion-loaded (Of-ME, 358 μg dose) CLs were compared *in vivo* against eye drops (250 μg dose) in a rabbit model. The C_{max} were 334 ± 104 μg, 660 ± 255 μg and 446 ± 105 μg respectively, and drug

USC UNIVERSIDADE DE SANTIAGO DE COMPOSTELA

levels above the MIC of *S. aureus* were recorded for 24, 48 and 1 h respectively. The authors claimed good IVIVC, with Levy plot correlation coefficients of 0.966 for Of-SM CLs and 0.931 for Of-ME CLs. Importantly, two days wearing of one ofloxacin-loaded lens was shown to be as efficient as repeated eye drop instillation every 4 h for the treatment of conjunctivitis [Li et al., 2020].

Gatifloxacin was loaded in CLs using two different strategies: (i) to add functional monomers in the CLs that can attract the drug [Shi et al., 2013], and (ii) to soak the CLs into drug-micelle solutions [Maulvi et al., 2020]. The first strategy (**Table 1.2, entry 28**) revealed MAA as the most suitable monomer to enhance the affinity for gatifloxacin (loading from 2 to 12 μg/mg of CL). Although *in vivo* release was not investigated, two days of wear showed complete recovery from bacterial keratitis in a rat model [Shi et al., 2013]. The second strategy (**Table 1.2, entry 29**) consisted of a dual approach of adding gatifloxacin in the monomer solution before polymerization (at 0.3% *w/v*) and using drug dissolved (at 0.3% *w/v* also) in Pluronic micelles as a packaging solution [Maulvi et al., 2020]. The drug that had been added directly to the monomers precipitated in the CL, compromising the optical properties. Immersion in the packaging solution allowed drug resolubilization into the micelles and further enhanced drug loading. The resultant CLs (GT-PL-CL; 92 μg dose) showed slower release rates than soaked CLs (SM-CL; 53 μg dose), but both exhibited more than 60% burst release in the first 1 h. Compared to eye drops (150 μg dose) that rapidly disappeared from the ocular surface, SM-CL and GT-PL-CL provided measurable drug levels in tear fluid for 12 and 24 h, respectively [Maulvi et al., 2020].

The suitability of CLs as platforms for the sustained release of macromolecules such as HA for amelioration of dry eye syndrome has

USC UNIVERSIDADE DE SANTIAGO DE COMPOSTELA

also been demonstrated. Soaking of CLs in HA solution only allows for surface adsorption and thus leads to complete release in a few hours. In contrast, direct addition of HA to the monomer solution has been shown to render hydrogel CLs that provided therapeutically useful levels of HA both *in vitro* and in tear fluid for 10 days (**Table 1.2, entry 30**) [Maulvi et al., 2020]. Similarly, HA was added to silicone hydrogel monomers either solely or combined with reduced graphene oxide (rGO) (**Table 1.2, entry 31**) or Pluronic F127 (**Table 2, entry 32**). HA-rGO directly loaded CLs sustained the release for 96 h *in vitro* and for 48 h *in vivo*, and increased rabbit tear fluid volume for 96 h, being more efficient than eye drops or soaked CLs [Huang et al., 2021]. The combination of HA and Pluronic F127 improved CL wettability and tear production. Direct loading in the silicone monomers rendered CLs that sustained HA release for 48-96 h *in vitro* and 48 h *in vivo*, avoiding the huge burst recorded for CLs soaked in HA [Wei et al., 2020a]. Overall, as for small drug molecules, the achievement and the duration of therapeutic effects observed for HA-eluting CLs were the result of a fine equilibrium between enhanced loading and more controlled release. Thus, prolonged *in vitro* release had a direct correlation on the time the therapeutic outcome could be maintained.

1.4.3 Comparison of In vitro Release Profiles and Drug Accumulation into Anterior and Posterior Segments

Lidofilcon hydrogel CLs were shown to load steroids and provide sustained release for efficient drug penetration into the posterior segment [Schultz et al., 2011]. The CLs were soaked in either prednisolone suspension in saline for injection or beclomethasone dipropionate solution in dimethyl sulfoxide (DMSO):water 16:4 *v/v* mixture (**Table 1.2, entry 33**). After washing in saline solution for

USC UNIVERSIDADE DE SANTIAGO DE COMPOSTELA

injection, the release *in vitro* was sustained for 6 h. *In vivo* evaluation consisted of placing drug-loaded CLs on both eyes, which were kept closed with surgical tape for 4 h. Prednisolone was detected in the posterior segment ocular tissue of all rabbits, with concentrations ranging 26–166 ng/g. Prednisolone was found in the vitreous humor of three out of eight eyes and only detected in the plasma of one animal (out of six). Its metabolite prednisone (inactive) was below the quantification limit in all cases. Beclomethasone dipropionate was also detected in the posterior segment tissue, but not in vitreous humour and plasma. Its active metabolite, 17-beclomethasone, was detected in the posterior segment tissue and in most vitreous humor samples. Both prednisolone and beclomethasone dipropionate are small (< 600 g/mol) hydrophobic molecules. If they had penetrated the eye through the cornea and then migrated towards the macula and retina, the parent drugs should also be detected in the vitreous humor at similar levels. Since this was not the case, the drug molecules released from the CLs to the cornea and limbal areas may have entered through a non-corneal route. They could have reached the local vasculature and then been transported toward the posterior segment. The absence of drug in plasma discarded the notion that access to the posterior segment was via systemic circulation [Schultz et al., 2011].

Screening of eleven commercially available CL materials pointed to polymacon (polyHEMA) CLs as the most appropriate ones for loading of pirfenidone, an anti-inflammatory drug that favors the healing of the ocular surface (**Table 1.2, entry 34**) [Yang et al., 2016]. All tested CLs released the drug rapidly *in vitro* (**Figure 1.11A**), with polymacon having the best release profile (~30 min release duration). In rabbit eyes, the CLs (1147 μg dose) provided relevant pirfenidone levels in tear fluid for 60 min, while eye drops (150 μg dose) disappeared in the first 15 min (**Figure 1.11B**). Drug-loaded polymacon

USC UNIVERSIDADE DE SANTIAGO DE COMPOSTELA

CLs led to significantly higher drug levels in the cornea, aqueous humor and sclera at all data points assessed (**Figure 1.11C, D and F**). Importantly, the drug levels in the conjunctiva only showed a minor increase in the first 60 min (**Figure 1.11E**), which can be correlated with the preferential release of the drug towards the post-lens lachrymal fluid. Therefore, low levels in the conjunctiva may be the result of rapid clearance, as well as systemic absorption. Simultaneous improvements in pirfenidone loading and controlled release (80-260 min) were observed for silicone hydrogel CLs (Acuvue Oasys®) pre-treated with vitamin E (**Table 1.2, entry 35**). In an animal model of alkali burn, pirfenidone-loaded CLs efficiently down-regulated the gene expression of several inflammatory cytokines IL-1β, TNF-α, and TGF-β1 in the cornea [Dixon et al., 2018].

USC UNIVERSIDADE DE SANTIAGO DE COMPOSTELA

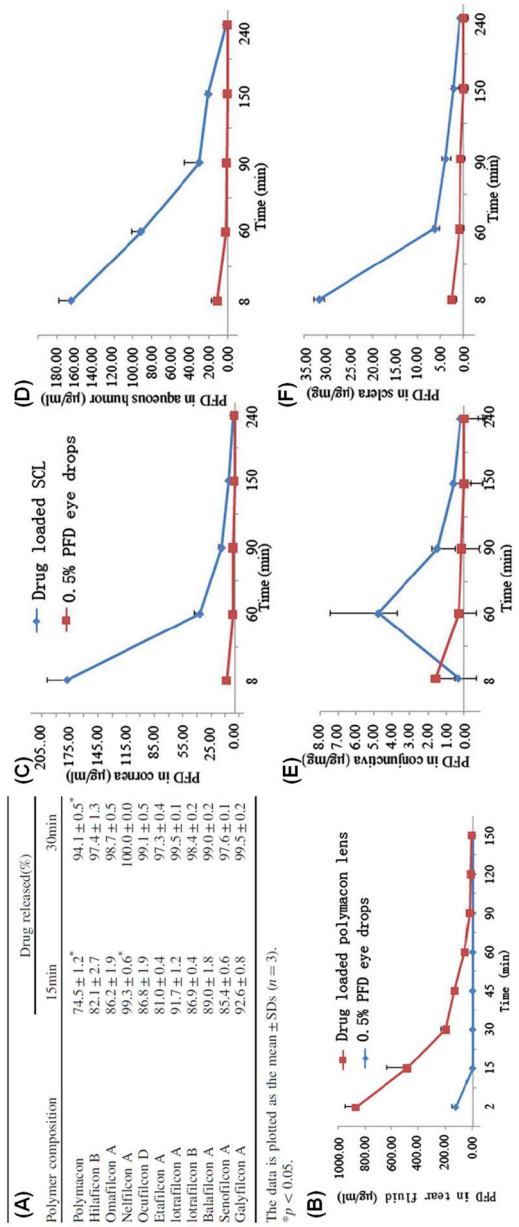

Figure 1.11. (**A**) Percentage of pirfenidone (PFD) released in PBS from commercially available CLs that were loaded by soaking in 2 mL of 0.5 mg/mL drug, (**B**) levels of PFD in tear fluid (rabbit model) after instillation of one drop of 0.5% PFD eye drop and during wearing of PFD-loaded polymacon CLs; (**C-F**) PFD levels in different ocular tissues at different times after eye drop instillation and CL wearing. Reprinted from Yang et al. [Yang et al., 2016] with permission by Taylor & Francis Ltd.

In a subsequent study, CLs showing prolonged release of pirfenidone were designed by embedding a drug insert into two layers of a silicone elastomer (**Table 1.2, entry 36**) [Wu et al., 2021]. The CLs exhibited a very low water content (11%) and 10-times lower dose (15 μg) than the amount instilled using eye drops. *In vitro*, CLs released 52% of the loaded dose in the first hour, followed by ten-times lower release rate in the next 15 hours. *In vivo*, CLs sustained drug levels for 8 h in tear fluid, which led to a higher drug concentration in the aqueous humor after 2 h of wear compared to the eye drop instillation, despite releasing less drug [Wu et al., 2021].

Pegylated (p-SLNs) and non-pegylated (SLNs) solid lipid nanoparticles have also been tested to enhance the loading of epalrestat (an aldose reductase inhibitor used for the treatment of diabetic neuropathy) for delivery to the retina (**Table 1.2, entry 37**). *In vitro* release profiles in simulated tear fluid revealed that CLs directly loaded with epalrestat encapsulated p-SLNs (DL-EP-p-SLN) had a smaller burst and sustained the release up to 196 h, compared to CLs loaded by soaking (SM-EP-p-SLN), which prolonged the release up to 144 h. DL-EP-p-SLN CLs and SM-EP-p-SLN CLs provided measurable drug levels in tear fluid (rabbit model) for 96 h and 48 h, respectively [Zhu and Sheng, 2020]. Epalrestat accumulation in various ocular tissues after wearing of DL-EP-p-SLN CLs for 24 h were in rank order of lens (7.28 μg/g) > cornea (6.34 μg/g) > aqueous humor (4.84 μg/g) > retina (0.21 μg/g). In contrast, after 24 h of an eye drop instillation, the only measurable levels of epalrestat were detected in the lens (0.87 μg/g) and aqueous humor (0.82 μg/g). These findings support that CLs may facilitate drug penetration to the back of the eye.

Efficient drug delivery to the posterior segment was investigated for the antibiotic ofloxacin loaded in HEMA-based corneal CL, scleral/

USC UNIVERSIDADE DE SANTIAGO DE COMPOSTELA

corneal CL (S/CL) and rings (**Table 1.2, entry 38**) [Shikamura et al., 2016]. The composition was the same in all cases; the only change referred to the size and shape of the device, which led to different weights: 44 mg CL, 261 mg S/CL, and 183 and 72 mg for ring 1 and 2, respectively. After soaking in the antibiotic solution, the amounts loaded were 282, 1715, 1200 and 565 μg per device, respectively. Drug release was evaluated *in vivo* (rabbit) in terms of the difference between dose and amount of drug remaining in the device after certain wearing periods (**Figure 1.12A1**). As expected from their higher loading, S/CL and ring 1 released more drug, although the percentage released after 1 h of wear was slightly lower (47.5% and 40.9%, respectively) than that recorded for the CL (59.6%). Preferential biodistribution of ofloxacin to anterior segment tissues was observed for CLs, which provided the highest drug accumulation in the cornea (**Figure 1.12A2**). S/CL led to high drug levels both in anterior and posterior segment tissues, while the rings facilitated drug accumulation in the posterior segment (**Figure 1.12A3**). All devices were much more efficient than eye drops in drug biodistribution and provided therapeutically useful drug levels in all tissues, including the retina-choroid after 1 h of wear (0.4 μg/g with CL, and ~4 μg/g with S/CL and rings) [Shikamura et al., 2016].

There are only a few studies that report on *in vitro* and *in vivo* release kinetics together with therapeutic outcomes and drug accumulation in ocular tissues [Maulvi et al., 2019]. HEMA-based CLs were used to test the potential value of using gold nanoparticles (65 nm) to increase the loading and slow the release of timolol (**Table 1.2, entry 39**). Two different approaches were investigated: (i) addition of gold nanoparticles to the monomers before polymerization and; (ii) addition of gold nanoparticles to the timolol solution in which the hydrogels were soaked. These approaches slightly increased the capability of the hydrogels to uptake timolol (284 and 277 μg, respectively) compared

USC UNIVERSIDADE DE SANTIAGO DE COMPOSTELA

to the same hydrogels processed in the absence of gold nanoparticles (253 μg). Regardless of the procedure, all hydrogels released most of the drugs within one hour when tested *in vitro*. Unexpectedly, *in vivo* (rabbit) results showed that timolol levels in tear fluid were quantifiable for 60 h. A significant decrease in IOP values were recorded in the first 24 h of wear. Thus, once again the therapeutic effect appears to be more prolonged than the release profiles recorded *in vitro* under sink conditions. This finding can be related to drug accumulation in various ocular tissues, as observed in **Figure 1.12B1 and B2** [Maulvi et al., 2019]. Specifically, accumulation of timolol in the ciliary muscle, where most β-receptors are located [Wax and Molinoff, 1987], may explain prolonged IOP decrease. Unfortunately, a similar analysis for the drug instilled using eye drops was not available.

USC UNIVERSIDADE DE SANTIAGO DE COMPOSTELA

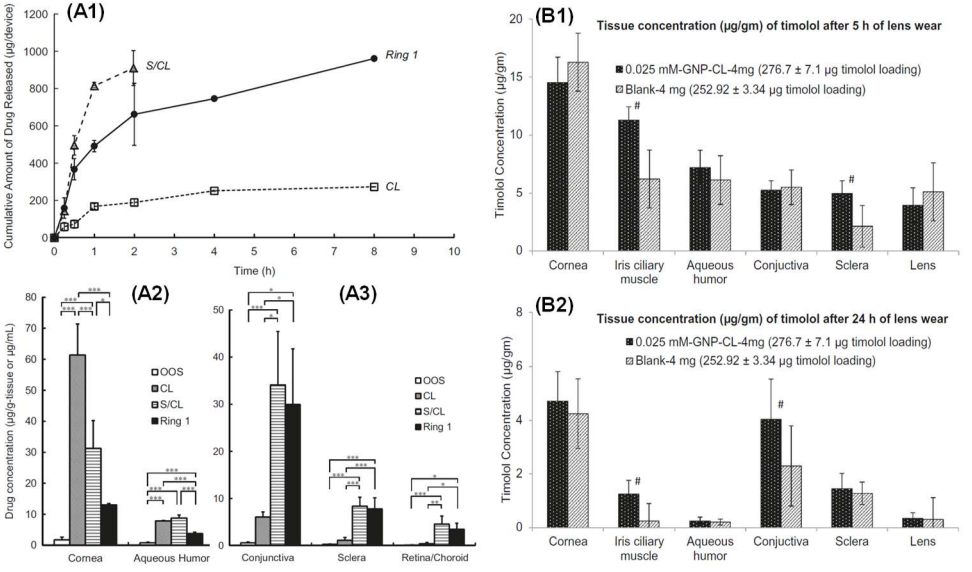

Figure 1.12. (**A1**) Ofloxacin released from HEMA-based corneal CL, scleral/corneal CL (S/CL) and rings once placed in Japanese albino rabbits (nictitating membranes were removed); the S/CL fell out of the eyes after 2 h; and (**A2 and A3**) ofloxacin levels in ocular tissues after 1 h wearing compared to the levels achieved after one drop instillation of ofloxacin ophthalmic solution (OOS) (n = 3; *p < 0.05, **p < 0.01, ***p < 0.005). Reprinted from Shikamura et al. [Shikamura et al., 2016] with permission from Taylor & Francis Ltd.; (**B1 and B2**) Evolution of timolol levels in various ocular tissues after wearing of CL with (0.025 mM-GNP-CL-4 mg; 277 µg of timolol) or without (Blank-4 mg; 253 µg of timolol) gold nanoparticles (mean ± SD; n = 3; # p < 0.05). Reprinted from Maulvi et al. [Maulvi et al., 2019] with permission from Elsevier.

Latanoprost-eluting CLs have been designed by encapsulating a drug-loaded poly(lactic-co-glycolic)acid (PLGA) film in methafilcon (**Table 1.2, entry 40**) [Ciolino et al., 2014]. Two high molecular weight (118 kDa) PLGA of 65 glycolide:35 L-lactide ratio and 85 glycolide:15 L-lactide ratio were used, and three sets of CLs were prepared containing films of thickness 20, 40 and 45 μm. CL65:35, 20, CL65:35, 40 and CL85:15, 45 contained 89, 178 and 178 μg latanoprost, respectively, and released *in vitro* 90%, 48% and 45% of the drug dose in the first three days. CL65:35, 400 and CL85:15, 45 sustained drug release for 20 days more (**Figure 1.13A1**). *In vivo* (rabbits) concentration of latanoprost was continuously monitored in the aqueous humor for 4 weeks (**Figure 1.13A2**). Compared to the low C_{max} (54 ng/mL) and the rapid concentration decrease recorded after one drop instillation, CL65:35, 20, CL65:35, 40 and CL85:15, 45 led to C_{max} of 970, 854 and 1473 ng/mL, respectively, and average steady concentration (Css) of 5.6, 39.6 and 21.0 ng/mL. Interestingly, good IVIVC was observed for the percentage of total drug absorbed *in vivo* (percentage of $AUC_{0\text{-}28}$ days in aqueous humor) with respect to the percentage of drug released *in vitro*. Moreover, the correlation coefficient became closer to 1 ($R^2 = 0.98$) when CL85:15, 45 was pre-soaked for 1 or 3 days in PBS to remove the drug released as a burst before wearing (**Figure 1.13A3**) [Ciolino et al., 2014]. This finding opens the possibility of predicting drug levels in the aqueous humor from the *in vitro* release values. Since latanoprost does not decrease IOP in rabbits, the therapeutic efficacy of similarly designed CLs (PLGA 50:50 and 147 μg drug) was demonstrated *in vivo* in glaucomatous eyes of cynomolgus monkeys [Ciolino et al., 2016] (**Figure 1.13A4**).

Recently, methafilcon CLs encapsulating PLGA 85:15 films loaded with dexamethasone were shown to sustain drug release *in vitro* over 7 days and to provide therapeutic levels in various ocular tissues,

USC UNIVERSIDADE DE SANTIAGO DE COMPOSTELA

including the retina (**Table 1.2, entry 41**); (**Figure 1.13B1 and B2**) [Ross et al., 2019]. In the aqueous humor (rabbit model) the drug levels were sustained for 7 days, and the CLs effectively prevented suture-induced corneal neovascularization and inflammation (**Figure 1.13B3**) and also lipopolysaccharide-induced anterior uveitis [Bengani et al., 2020].

Some other *in vivo* studies have been carried out with one optimized formulation and the drug concentration in tissues and the therapeutic response evaluated. Since only one CL type was reported, the effect of a change in the release rate on the *in vivo* levels and therapeutic outcomes cannot be evaluated. Nevertheless, all the studies evidenced that compared to eye drops, CLs favor drug accumulation and prolong the therapeutic levels, which in turn leads to improved therapeutic response with either less dose or less frequent administration. These findings have also been reported for CLs loaded with cyclosporine A impregnated in nanoporous silica by means of supercritical CO_2 (**Table 1.2, entry 42**) [Choi et al., 2019]. *In vitro*, CLs sustained drug release for 8 h, while *in vivo*, high levels of drug were detected for 48 h in cornea and conjunctiva. CLs increased tear volume and stabilized tear film after 1 and 2 weeks of treatment.

USC UNIVERSIDADE DE SANTIAGO DE COMPOSTELA

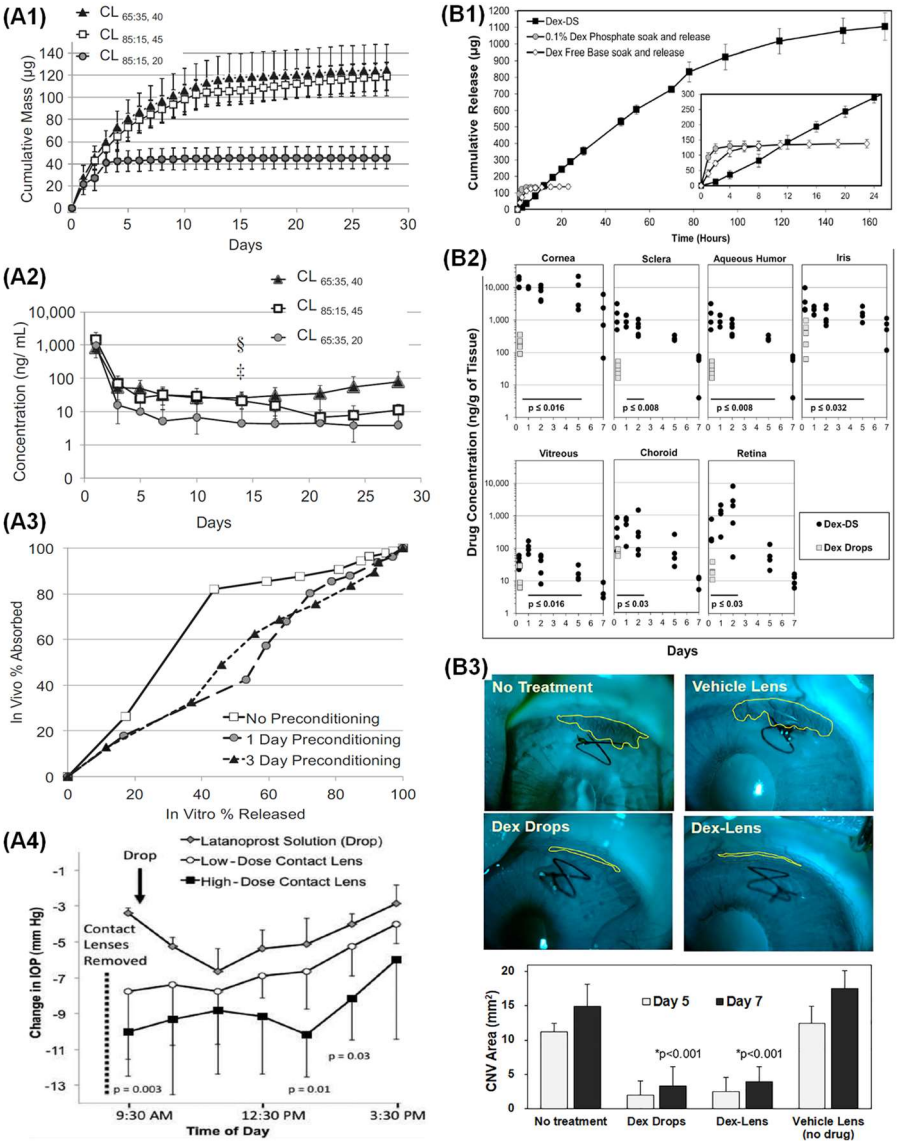

Figure 1.13. (**A1**) Latanoprost release profiles *in vitro* from CL embedding drug-loaded films of PLGA 65:35 of thickness 20 µm (CL65:35, 20) and 40 µm (CL65:35, 40) and PLGA 85:15 of thickness 45 µm (CL85:15, 45); (**A2**) latanoprost concentration in aqueous humor (rabbits) during CL wearing; and (**A3**) Levy plots for CL85:15, 45 without pre-conditioning (R^2 = 0.875) and with pre-conditioning for

1 day (R^2 = 0.979) or 3 days (R^2 = 0.982). Reprinted from Ciolino et al. [Ciolino et al., 2014] with permission from Elsevier. (**A4**) Decrease in IOP recorded in female cynomolgus monkeys (*n* = 4) after the fifth instillation of latanoprost eye drops (two 25 µL-drops of 0.005% drug per day) and after 7 days of continuous wearing of the drug-loaded CLs (97 µg and 147 µg dose), and IOP values recovering after CL removal. Reprinted from Ciolino et al. [Ciolino et al., 2016] with permission from The American Academy of Ophthalmology and Elsevier. (**B1**) Dexamethasone (Dex) release profiles *in vitro* from CLs soaked in either Dex phosphate or base solutions and from CLs embedding drug-loaded films of PLGA 85:15 (Dex-DS); (**B2**) Dex accumulation in ocular tissues after eye drop instillation and after Dex-DS CLs continuous wearing. Reprinted from Ross et al. [Ross et al., 2019] with permission from Elsevier. (**B3**) *In vivo* model of cornea neovascularization (CNV) induced by sutures placed along superior and inferior cornea; the pictures were taken 7 days after suture placement, and bar plots evidence that Dex-loaded CLs decreased the CNV invasion area compared to eyes that received no treatment or only blank CLs. Reprinted from Bengani et al. [Bengani et al., 2020] with permission from Elsevier.

1.5 CONCLUSIONS AND FUTURE PERSPECTIVES

Rapid release *in vitro* (even in the frame of hours) has resulted in researchers questioning the capability of CLs to really act as drug depots *in vivo*. However, the many examples gathered in previous sections reveal that most *in vitro* tests are not good predictors of *in vivo* performance and indeed CLs that show fast release *in vitro* may lead to sustained levels in tear fluid and remarkably high drug accumulation in key ocular tissues. CLs favor drug accumulation on eye surface tissues, which in turn leads to improved therapeutic response, with either fewer doses or less frequent administration than eye drops. Prolonged supply of drug to the post-lens tear fluid has been demonstrated as a key factor to increase drug ocular bioavailability, consequently leading to favorable drug binding to ocular tissues, drug penetration to the posterior segment, the formation of drug depots ("tissue reservoir effect"), and decreased side effects by minimizing drug spillover to the conjunctiva and nasolacrimal duct and systemic circulation.

USC UNIVERSIDADE DE SANTIAGO DE COMPOSTELA

In most reports on *in vitro* drug release, regardless of whether the test fulfils sink conditions, the volume of medium to which the drug-loaded CL is exposed is much larger than the 10 μL of tear fluid available on the ocular surface. A large volume in the *in vitro* release medium may generate a concentration gradient that is much more intense than the one that can be established *in vivo*, which in turn may trigger a faster drug discharge. Small release volume in *in vitro* studies may be not a shortcoming, but composition and dynamics may be more critical. Indeed, some of the best IVIVC have been obtained when the *in vitro* release medium consisted of 2 mL of simulated tear fluid at 34 °C and 100 rpm, and the medium was completely replaced at each sampling time. This was the case for CLs loaded with ketotifen [Zhang et al., 2020], cyclosporine [Maulvi et al., 2017a], ofloxacin [Li et al., 2020] and timolol [Maulvi et al., 2019]. Nevertheless, this finding should be interpreted with caution, since the drug was encapsulated in or associated with nanostructures. The situation may be different for drugs directly interacting with the CL. The reasoning behind the use of a 2 mL release medium is that this value approximately matches the daily tear turnover.

Interestingly, CLs that release the drug at slower rate *in vivo* than *in vitro* have also been reported. This is the case for drugs encapsulated in pH- or ionic strength-sensitive coatings, which were tested *in vitro* in 10 mL of simulated tear fluid or PBS at 35 °C and 100 rpm, with replacement of 2 mL at each sampling point [Zhu et al., 2018a; Zhu et al., 2018b]. Slower release *in vivo* was also recorded for timolol and latanoprost encapsulated in micelles and directly added to the monomers before CL polymerization. The release *in vitro* was evaluated in Franz diffusion cells with 1 mL medium in the donor compartment and 7 mL in the receptor kept at 35 °C and 50 rpm, with

USC UNIVERSIDADE DE SANTIAGO DE COMPOSTELA

1 mL replacement of the release medium at each sampling point [Xu et al., 2019].

In addition to volume and dynamics of the release medium, composition is also a key aspect. Biorelevant release medium may require a decrease in polarity of simulated lachrymal fluid (with the addition of organic miscible solvents that resemble lipid components in tear fluid) or an increase in binding substances that could mimic proteins that bind the specific drug. Addition of enzymes typically present in tears may be needed when the drug is linked to the CL or nanoparticles using labile bonds. Such a need was evidenced, for example, in the case of timolol loaded into CLs after being linked to nanoparticles through ester bonds; the *in vitro* release in PBS was sustained for weeks, while the IOP decrease *in vivo* was only maintained for 4 days [Jung et al., 2013].

Application of 3D printing and microfluidics may enable the design of devices that can tune the composition and flow of the release medium through the drug-loaded CLs in a more biomimetic way. The development of versatile microfluidic devices may help in the progress towards more accurate ways of evaluating *in vitro* drug release from CLs, although strong efforts for validation *in vivo* are still needed. Increasing feasibility of producing a variety of testing devices may lead to more biorelevant testing conditions, but it also has the risk of proliferation of too many models which would not help results comparison.

Currently, improved *in vitro* release tests are demanded as predictive tools of the capability of the CLs to sustain drug release *in vivo*. With the approval of the first drug-loaded CLs, one can envision that in the next years generic drug-releasing CLs may appear and therefore *in vitro* studies that can be used as predictive of

USC UNIVERSIDADE DE SANTIAGO DE COMPOSTELA

bioequivalence will be highly demanded. Therefore, advances in the identification of specific setups for *in vitro* release testing of CLs are becoming an urgent demand. Ideally, experts in the field and regulatory agencies should reach consensus on *in vitro* test conditions and devices. Standardization is very much needed.

USC UNIVERSIDADE DE SANTIAGO DE COMPOSTELA

Table 1.3. *In vitro* release studies of drug-loaded CLs with indication of release medium composition, volume, replacement and agitation conditions used as well as time the release was sustained.

Drug	Lens material and thickness	Loading protocol	Release medium (volume, replacement)	Release conditions (temp., agitation)	Release duration	Ref.
Acetazolamide	Commercially available silicone hydrogel CL (Balafilcon A) (Thickness – 0.05 – 0.5 mm)	CLs were impregnated using supercritical solvent impregnation methodology at 17 MPa, 40 ºC, 1, 2, 3 h, 0.06-0.15 MPa/min of depressurization rate	Saline water (10 mL, 6% of total volume was replaced at predetermined timepoints)	37 ºC, under orbital stirring	8 hours	Braga et al., 2010
Acetazolamide	HEMA, HEA, NMBA, KPS, and water (Thickness – 2 mm)	Soaking in 25 mL of 100 mg/l of acetazolamide solution for 4 days at 25 ºC	0.9% NaCl solution (50 mL, completely replaced at predetermined timepoints)	37 ºC (Rotation not specified)	About 10 days	Oucif et al., 2020
Acetazolamide, ethoxzolamide	HEMA, $ZnMA_2$, HEAA, 1VI, 4VI, and EGDMA (Thickness – 0.9 mm)	Soaking in 5 mL of 0.2 g/L of acetazolamide solution or 0.23 g/L of ethoxzolamide suspension for 48 h	0.9% NaCl solution (5 mL, without replacement)	25 ºC (Rotation not specified)	8 days	Ribeiro et al., 2011a
Acetazolamide and timolol	Commercially available silicone hydrogel CLs (Balafilcon A) (Thickness – 0.089 cm)	CLs were impregnated using supercritical solvent impregnation methodology at 17 MPa, 40 ºC, 90 min, 0.06 MPa/min of depressurization rate	Physiological serum (10 mL, without replacement)	37 ºC, 100 rpm	8 hours	Costa et al., 2010a
Acetazolamide, ethoxzolamide	NVP, DMA, GMA, and EGDMA (Thickness – 0.9 mm)	Soaking in 5 mL of 0.2 mg/mL of acetazolamide and 0.23 mg/mL of ethoxzolamide for 2 days at 25 ºC	0.9% NaCl solution (7.5 mL, without replacement)	25 ºC, (Rotation not specified)	24 hours	Ribeiro et al., 2012
Acetazolamide, ethoxzolamide	NVP, DMA, 1VI, 4VI, HEAA, Zinc salt, and	Soaking in 5 mL of 0.20 or 0.23 g/l of acetazolamide,	0.9% NaCl solution (10 mL, without replacement)	25 ºC (Rotation	Until 72 hours	Ribeiro et al., 2011b

	EGDMA (Thickness – 0.9 mm)	or ethoxzolamide, respectively for 48 h		not specified)		
Acetazolamide, riboflavin, sodium fluorescein, and theophylline	HEMA, MAA, and EGDMA (Thickness – 0.4 mm)	Soaking in sodium fluorescein solution of 1 x 10^{-5} M in PBS, and 1 x 10^{-7} in HCl. And, soaking in riboflavin, theophylline, acetazolamide solution of 1 x 10^{-5} M, 6 x 10^{-3} M, and 2 x 10^{-3} M, respectively, in PBS and HCl until equilibrium	PBS or HCl (Volume not specified) (Without replacement)	400 rpm	Not specified	Liu et al., 2016
Acyclovir, valacyclovir	HEMA, MAA, and EGDMA (Thickness – 0.45 mm)	Soaking in 5 or 15 mL of 0.3 mg/mL of acyclovir or 5 mL of 0.3 mg/mL of valacyclovir for 4 days at 25 ºC	STF (10 or 15 mL, without replacement)	35 ºC, 300 rpm	24 hours	Varela-Garcia et al., 2020a
Alexa Fluor 488 dye, timolol, brimonidine	HEMA, EGD, GMA, and NVP (Thickness – not specified)	Soaking in 1.5 mL of ethanol solution containing 0.1 mg of Alexa Fluor 488 dye, or 0.5 mg of timolol or brimonidine	PBS pH 7.4 (3 mL, without replacement)	Not specified	Until 6 hours	Lee et al., 2016
Aloe vera Extracts	Commercially available hydrogel CLs (Filcon IV3, and Methafilcon A) (Thickness – not specified)	Soaking in an *Aloe vera* pharmacological eye drop	0.9% NaCl solution (1 mL) (Replacement not specified)	Not specified	24 hours	Pulliero et al., 2020
Amphotericin B	Hydrogel Su 60 15, poly-ε-lysine, tween 80, octanedioic acid, n-methylmorpholine, and n-hydroxysuccinimide	Soaking in 30 µg/mL of amphotericin B solution for 2 h	PBS (0.1 mL, replaced completely at predetermined timepoints)	Not specified	96 hours	Gallagher et al., 2017
Ascorbic acid	HEMA, and EGDMA (Thickness – not specified)	Soaking in 1 mL of 4 mg/mL ascorbic acid for 24 h	PBS (1 mL, without replacement)	25 ºC, mild agitation	10 days	Ashtiani et al., 2020

Atropine and roscovitine	DMA, TRIS, TRIS-OH, EGDMA (Thickness - 1 mm)	Incorporation the drugs during the synthesis of the hydrogel materials or soaking in 1 mL of 2 mg/mL of roscovitine solution for 7 days	PBS pH 7.4 (1 mL, replaced completely at predetermined timepoints)	37 °C (Rotation not specified)	Atropine – about 23 days. Roscovitine – about 50 days	Lasowski and Sheardown, 2016
Atropine, pirenzepine	Commercially available silicone (Narafilcon A), and conventional hydrogel CLs (Etafilcon A, Oculfilcon B, Omafilcon A) (Thickness – mean of 0.08 mm)	Soaking in 2 mL of 10 mg/mL of atropine, and 1 mg/mL of pirenzepine for 24 h	PBS (4 mL, 100 µl removed at predetermined timepoints)	34 °C, shaking	24 hours	Hui et al., 2017
Azulene	HEMA, MAPTAC, anionic monomer, and EDMA (Thickness – not specified)	Soaking in 5 mL of 0.2 wt.% azulene for 48 h	Physiological saline solution pH 7.0 (5mL, replaced completely every 2 hours)	37 °C (Rotation not specified)	8 hours	Uchida et al., 2003
Betaine, dexpanthenol	Commercially available silicone hydrogel CLs (Narafilcon A, Senofilcon A) (Thickness – not specified)	Soaking in 3 mL of 8 or 80 mg/mL of dexpanthenol or betaine, respectively for 1 or 2 days	PBS (2 mL) (Replacement not specified)	Not specified	Until 40 hours	Hsu et al., 2015b
Betamethasone	Commercially available silicone hydrogel CLs (Lotrafilcon B, Senofilcon A, Comfilcon A) (Thickness – 0.07 and 0.08 mm)	Soaking in 2 mL of 2 mM of betamethasone until achieve the equilibrium at 25 °C	Artificial tear solution pH 8 (2 mL, replaced completely at predetermined timepoints)	37 °C (Rotation not specified)	Until 41 days	Rad et al., 2016a

USC

Bimatoprost and latanoprost	Commercially available silicone hydrogel CL (Senofilcon A, Narafilcon A) (Thickness – 0.1 mm)	Soaking in 3 mL of 0.125 mg/mL of bimatoprost, and 62.4 µg/mL of latanoprost until achieve the equilibrium	PBS (Volume and replacement not specified)	Not specified	About 10 days	Sekar et al., 2019
Brimonidine	HEMA, MAA, MAAM, 4VP, and EGDMA (Thickness – 0.4 mm)	Soaking in 10 mL of 0.2 mM of brimonidine aqueous solution for 24 h at room temperature	0.9% NaCl and artificial tear solutions (10 mL, 1 mL replaced at predetermined timepoints)	37 ºC (Rotation not specified)	48 h	Omranipour et al., 2015
Bupivacaine, lidocaine, tetracaine	Commercially available silicone hydrogel CL (Lotrafilcon B). TRIS, DMA, DBE-U12, NVP, and EGDMA (Thickness – 0.2 mm).	Soaking in 3 mL of 5.0, 2.5, and 1.0 mg/mL of lidocaine, bupivacaine, and tetracaine solutions, respectively for 7 days	PBS (2 mL, without replacement)	Not specified	Until about 90 hours	Peng et al., 2012c
Chlorhexidine, levofloxacin, and diclofenac	HEMA, PVP, TRIS, NVP, EGDMA (Thickness – 0.25 and 0.3 mm)	Soaking in 1 mL of 1 mg/mL of chlorhexidine, levofloxacin, and diclofenac until achieve the equilibrium at 25 ºC	PBS or water (3 mL, 200 µl replaced at predetermined timepoints)	38 ºC, 180 rpm	4 days	Pimenta et al., 2016b
Ciprofloxacin	Ciprofloxacin - PLGA films coated with pHEMA (Thickness – 450 µm)	Ciprofloxacin films were created by solvent casting, using a 1:1 ratio of medication to PLGA	PBS pH 7.4 (15 mL, replaced completely at each sampling point)	37 ºC, continuous shaking	4 weeks	Ciolino et al., 2009
Ciprofloxacin	HEMA, TRIS, EGDMA, acetic acid or acrylic acid (Thickness – not specified)	Soaking in 2 mL of ciprofloxacin (9.06 mM, 0.10 mM and 0.025 mM) for one week	Artificial tear solution (2 mL, without replacement)	34 ºC, with continuous shaking	14 days	Hui et al., 2012
Ciprofloxacin	Commercially available conventional hydrogels CLs (Ocufilcon D), and silicone hydrogel CLs (Delefilcon A,	Soaking in 1 mL of drug solutions for 18 h	PBS (1 mL, completely replaced every hour)	25 ºC (Rotation not specified)	Until 16 hours	Qin et al., 2017

	Comfilcon A, Lotrafilcon B, Narafilcon A) (Thickness – not specified)					
Ciprofloxacin	Commercially available silicone hydrogel CLs (Lotrafilcon B, Comfilcon A, Senofilcon A) (Thickness – 0.07/ 0.08 mm)	Soaking in 2 mL of ciprofloxacin solution for 24 h	Artificial tear solution (2 mL, completely replaced at predetermined timepoints)	37 ºC (Rotation not specified)	960 hours	Rad et al., 2017
Ciprofloxacin	HEMA, MEHQ, and PEGDM (thickness not specified)	Ciprofloxacin was encapsulated into nanospheres and mixed with the monomer's solution	Buffer (2 mL, completed replaced every 24 h for 3 days, then at 2 to 4 days for 14 days)	37 ºC (Rotation not specified)	14 days	Garhwal et al., 2012
Ciprofloxacin	Commercially available silicone (Balafilcon A, Lotrafilcon B, Lotrafilcon A, Senfilcon A, Galyfilcon A, Comfilcon A), and conventional hydrogel CLs (Polymacon, Alphafilcon A, Etafilcon A) (Thickness – mean of 0.08 mm)	Soaking in 2 mL of 0.3% of ciprofloxacin solution for 24 h at 34 ºC	Unisol4 pH 7.4 (2 mL, 5 or 10 µl was taken at predetermined timepoints)	34 ºC, gently shaking	24 hours	Hui et al., 2008
Ciprofloxacin, betamethasone	Commercially available silicone hydrogel CLs (Lotrafilcon B, Comfilcon A, Senfilcon	Soaking in 2 mL of 2 mM of ciprofloxacin-betamethasone solution at 25 ºC until achieve the equilibrium	STF pH 8 (2 mL, completely replaced at predetermined timepoints)	37 ºC (Rotation not specified)	About 38 days	Rad et al., 2016b

USC

	A) (Thickness – 0.08 mm)					
Ciprofloxacin, dexamethasone	HEMA, DMAA, TRIS, hyaluronic acid, and EGDMA (Thickness – 0.93-1.84 mm)	Soaking in 3 mg/mL of ciprofloxacin, or 1 mg/mL of dexamethasone for 24 h at 25 °C	PBS pH 7.4 (Volume and replacement not specified)	34 °C, 100 rpm	Until 7 days	Nguyen et al., 2012
Cisplatin	HEMA, APS, MAAc, NN-MBA, and TEMED (Thickness – not specified)	Cisplatin was mixed with the monomer's solution	Not specified	37 °C (Rotation not specified)	96 hours	Singh et al., 2011
Cromolyn sodium, ketotifen fumarate, ketorolac tromethamine,dexamethasone sodium phosphate	Commercially available silicone (Balafilcon A, Lotrafilcon A), and conventional hydrogel CLs (Polymacon, Omafilcon A, Etafilcon A, Vifilcon A, Alphafilcon A) (Thickness – not specified)	Soaking in 2 mL of 20 mg/mL of cromolyn, 0.2 mg/mL of ketotifen, 0.3 mg/mL of ketorolac, and 0.845 mg/mL of dexamethasone for 50 h	Saline solution (2 mL, without replacement)	25 °C (Rotation not specified)	24 hours	Karlgard et al., 2003
Cyclosporine A	HEMA, and EGDMA (Thickness – not specified)	Cyclosporine cholesterol-hyaluronate micelles were mixed with the monomer's mixture before polymerization	PBS (1 mL, replaced completely at predetermined timepoints)	37 °C (Rotation not specified)	288 hours	Mun et al., 2019
Cyclosporine A	Commercially available silicone hydrogel CLs (Lotrafilcon A, Lotrafilcon B, Senofilcon A, Balafilcon A), a conventional hydrogel CL (Etafilcon A)	Soaking in 10 mL of 15/17 µg/mL of cyclosporine A solution	PBS (1.75 mL, completely replaced at predetermined timepoints)	Not specified	Until 170 hours	Peng et al., 2011

	(Thickness – not specified)					
Cyclosporine A	HEMA, and EGDMA (Thickness – 0.2 mm)	Cyclosporine A was mixed with the monomer's solution	PBS (3.5 mL, completely replaced every 24 h)	25 °C (Rotation not specified)	Until 30 days	Kapoor et al., 2017
Cyclosporine A	HEMA, and EGDMA (Thickness – 0.1 or 0.2 mm)	Cyclosporine A microemulsions were mixed with monomer solution	PBS (3.5 mL, completely replaced every 24 h or without replacement)	25 °C (Rotation not specified)	Until 25 days	Kapoor et al., 2008a
Cyclosporine A, Brij 98	HEMA, and EGDMA (Thickness – not specified)	Surfactant solution was added to the monomer's mixture before polymerization	PBS (3.5 mL, without, and completely replacement every 24 h)	Not specified	About 42 days	Kapoor et al., 2008b
Cyclosporine A, dexamethasone, dexamethasone acetate	HEMA, and EGDMA (Thickness – 0.1/ 0.2/ 0.4/ 0.8 mm)	Drug solutions were mixed with the monomer solution	PBS (3.5 mL, without replacement, or completely replaced every 24 h)	Not specified	Until 55 days	Kapoor et al., 2009
Cysteamine	Commercially available silicone hydrogel CLs (Senofilcon A, Narafilcon A, Lotrafilcon B, Balafilcon A), and conventional hydrogel CLs (Etafilcon A) (Thickness – mean of 0.04 mm)	Soaking in 3 mL of 50 mg/mL of cysteamine for 24 h in the refrigerator	PBS (2 mL, without replacement)	24 °C (Rotation not specified)	Until 6 hours	Hsu et al., 2013
Dexamethasone	HEMA, and EGDMA (Thickness – 0.1 or 0.2 mm)	Soaking in 3 mL of dexamethasone solution for 3 h	Deionized water or PBS (3 mL, completely replacement at the end of the release)	25 °C (Rotation not specified)	35 hours	Kim et al., 2008a
Dexamethasone	γCD, HPMC,and EGDE (Thickness –	Soaking in 10 mL of 1 mg/mL of aqueous suspension of	Water (5 mL, without replacement)	25 °C (Rotation	72 hours	Moya-Ortega et al., 2010

USC

	cylindrical tube with 5 mm)	dexamethasone for 1 week at 25 °C		not specified)		
Dexamethasone	HEMA, DMA, TRIS(OH), ACR, mPDMS, and EGDMA (Thickness – 0.5 mm)	Soaking in 1.5 mL of 1 mg/mL of dexamethasone for 48 h	PBS pH 7.4 (1.5 mL, completely replaced at predetermined timepoints)	37 °C (Rotation not specified)	About 16 days	Guidi et al., 2014a
Dexamethasone	Commercially available silicone hydrogel CLs (Galyfilcon A, Senofilcon A, Lotrafilcon A, Lotrafilcon B, Balafilcon A) (Thickness – 0.08-0.1 mm)	Soaking in 2 mL of dexamethasone in PBS for 1 or 7 days and drug-ethanol for 3 h	PBS (2 mL, without replacement)	Not specified	Until 7 days	Kim et al., 2010
Dexamethasone 21-disodium phosphate	HEMA, and EGDMA (Thickness – 0.05-0.015 mm)	Soaking in 0.1 mg/mL of dexamethasone 21-disodium phosphate solution (140 mL solution per gram of CL) until equilibrium	PBS (6 mL, without replacement)	Not specified	About 41 days	Bengani and Chauhan, 2013
Dexamethasone acetate	HEMA, MA, and EGDMA (Thickness – 0.2 mm)	Soaking in 1.35 mg/mL of dexamethasone acetate-ethanol solution for 15 h	PBS pH 7.4 (4.5 mL, aliquots removed and replaced with equivalent volume at predetermined timepoints)	37 °C, constant stirring	30 days	Lu et al., 2013
Dexamethasone sodium phosphate	HEMA, and EGDMA (Thickness – 0.05 mm)	Dexamethasone nanoparticles were mixed with the monomer's solution	PBS pH 7.4 (5 mL, 100 µl replaced at predetermined timepoints)	37 °C, 50 rpm	About 20 days	Behl et al., 2016
Dexamethasone, cyclosporine, timolol, levofloxacin	Commercially available silicone hydrogel CL (Delefilcon A) (Thickness – not specified)	Soaking in 3, 4 or 10 mL of 1.5, 5.0, 0.05, 0.015 mg/mL of timolol, levofloxacin, dexamethasone, cyclosporine, respectively for 24, 48 or 72 h at 4 or 35 °C	PBS pH 7.4 (2 mL, without replacement)	25 °C (Rotation not specified)	Until 30 hours	Dixon and Chauhan, 2017

Dexamethasone, ketotifen fumarate, timolol maleate, and diclofenac sodium	HEMA, AA, AM, NVP, DEAEM, MAA, PDMS, TRIS, DMA, EGDMA and ethanol (Thickness – 0.145 mm)	Soaking in 5 mL of 0.30 mg/mL ketotifen, 0.20 mg/mL diclofenac, 0.08 mg/mL dexamethasone, and 0.20 mg/mL timolol maleate	Deionized water pH 6.4 (2, 5, 30, 200, 300, 400 mL, replaced completely every 24 hours for small volumes)	20 °C or 34 °C, 30 or 160 rpm	96 hours	Tieppo et al., 2014
Diclofenac	HEMA, NVP, TRIS, and EGDMA (Thickness – 0.25 mm)	Soaking in 3 mL of 1 mg/mL of diclofenac solution for 38 h at 4 °C	Saline solution 130 mM NaCl pH 6.9 (3 mL, 200 µl replaced at redetermined timepoints)	36 °C (Rotation not specified)	24 hours	Silva et al., 2020
Diclofenac sodium	HEMA, and EGDMA (Thickness – 0.12 mm)	Soaking in 3 mL of 0.2 mg/mL of diclofenac sodium for 7 days	PBS pH 7.4 (3 mL, 1 mL replaced at predetermined timepoints)	25 °C (Rotation not specified)	About 100 hours	Torres-Luna et al., 2019a
Diclofenac sodium	HEMA, glycerol, deionized water, and EGDMA (Thickness – 0-1 mm)	Soaking in 1 mL of 2 mg/mL of diclofenac sodium for 2 days at 37 °C	PSB (10 mL, 2 mL replaced at predetermined timepoints)	37 °C (Rotation not specified)	About 70 hours	Li et al., 2020
Diclofenac sodium	HEMA, GMA, and EGDMA (Thickness – 0.9 mm)	Soaking in 10 mL of 80 mg/l of diclofenac sodium solution for 4 days at 25 °C	STF (10-20 mL, without replacement)	25 °C (Rotation not specified)	20 days	Dos Santos et al., 2009
Diclofenac sodium, betaxolol	HEMA, and EGDMA (Thickness – 0.1 mm)	Soaking in 1 mL of drug solutions for 3 days at 25 °C	STF (10 mL, 2 mL replaced at predetermined timepoints)	35 °C, 100 rpm	About 10 hours	Zhu and Mao, 2019
Diclofenac sodium, flurbiprofen sodium, naproxen sodium	HEMA, and EGDMA (Thickness – 0.12 mm)	Drug-surfactant solutions were mixed with monomer's solution	PBS pH 7.4 (3 mL, 1 mL replaced at predetermined timepoints)	25 °C (Rotation not specified)	About 10 days	Torres-Luna et al., 2019b
Diclofenac, and cefepime	HEMA, DMAEMA, DMAA, and EGDMA (Thickness – not specified)	Soaking in 5.0% of cefepime, and 2.5% of diclofenac solutions	Water (Volume and replacement not specified)	Not specified	Not specified	Primachenko et al., 2014

USC

Diclofenac, ketorolac, chlorohexidine, and moxifloxacin	1.8 M of HEMA, 0.8 M of TRIS, 3.9 M of NVP, and 30 mM of EGDMA (Thickness – 0.3 mm)	Soaking in 3 mL of 1 mg/mL of diclofenac and ketorolac for 38 h, and 2.5 mg/mL of chlorohexidine, 5 mg/mL of moxifloxacin for 72 h at 4 ºC	Saline solution 130 mM NaCl (3 mL, 200 µl replaced at predetermined timepoints)	36 ºC, 150 rpm	10 days	Silva et al., 2016
Dorzolamide	HEMA, MAA, and EGDMA (Thickness – 0.4 mm)	Soaking in 50 mL of 0.005-0.1 mM of dorzolamide solutions for 48 h at 25 ºC	0.9% NaCl solution or STF pH 8 (10 mL, without replacement)	37 ºC (Rotation not specified)	48 hours	Malaekeh-Nikouei et al., 2013
Econazole	Econazole -PLGA films coated with pHEMA (Thickness – 450 µm)	Econazole films were created by solvent casting, adding 200 mg to 100 mg of PLGA dissolved in 4 mL of ethyl acetate	PBS (1 mL, replaced completely every 24 hours)	37 ºC, 100 rpm	10 days	Ciolino et al., 2011
Epalrestat	HEMA, MCS-MC12, APMA, and EGDMA (Thickness – 0.5 mm)	Soaking in 50 mL of 6.14 µg/mL of epalrestat for 6 days at 25 ºC	0.9% NaCl solution (45 mL, without replacement)	25 ºC, 200 rpm	7 days	Alvarez-Rivera et al., 2018
Epidermal growth factor	Commercially available silicone hydrogel CLs (Vasurfilcon A and Lotrafilcon A) (Thickness – not specified)	Soaking in 25 mL of 0.4 ppm of epidermal growth factor for 7 h	PBS (25 mL, 1 mL was taken at predetermined timepoints but replacement is not specified)	Not specified	7 hours	Schultz and Morck, 2010
Ethoxzolamide	HEMA, APMA, and EGDMA (Thickness – 0.9 mm)	Soaking in 2 mL of ethoxzolamide solution for 24 h	STF pH 8.0 (2 mL, and progressively increased up to 10 mL in the first 48 h)	25 ºC (Rotation not specified)	About 7 days	García-Fernández et al., 2013
Fe_3O_4-PEG-Dy_2O_3 nanocomposites and $Dy(OH)_3$ nanorods	Commercially available silicone hydrogel CL (Etafilcon A) (Thickness – not specified)	Soaking in the nanaoparticules solutions for 24 h at 37 ºC	PBS pH 7.4 (Volume and replacement not specified)	Not specified	24 hours	Kusrini et al., 2021
Fluorescent glucose (2-(N-(7-nitrobenz-2-oxa-	PEG, DMA, and EGDMA (Thickness – 0.79 mm)	Soaking in $1x10^{-3}$, $5x10^{-4}$, $1x10^{-4}$, and $1x10^{-5}$ mg/mL of 2-NBDG	Deionized water (50 mL, completely replaced at predetermined timepoints)	25 ºC, 25 rpm	About 20 days	Byrne et al., 2008

1,3-diazol-4-yl)amino)-2-deoxy-glucose) or 2-NBDG						
Flurbiprofen	Commercially available conventional hydrogel CLs (Hilafilcon B) (Thickness – not specified)	Soaking in 20 mL of $3.3x10^{-5}$ M of flurbiprofen for 14 h, or supercritical solvent impregnation at 40 ºC, 12 MPa for 2.5 h	Purified water (80 mL, without replacement)	37 ºC, 100 rpm	8 hours	Yañez et al., 2011a
Flurbiprofen and timolol maleate	Commercially available conventional hydrogels CL (Methafilcon A) (Thickness – not specified)	CLs were impregnated using supercritical solvent impregnation methodology at 9 MPa, 40 ºC, 120 min, 0.1/0.2 MPa/min of depressurization rate	Physiological serum (6 or 10 mL, 300 or 400 µl replaced at predetermined timepoints)	37 ºC (Rotation not specified)	8 hours	Costa et al., 2010b
G2-C Peptide	Commercially available conventional hydrogel CL (Ocufilcon D) (Thickness – not specified)	Soaking in 100 µL of 1o mg/mL of G2-C peptide for 5 days at 37 ºC	PBS (1 mL, completely replaced at predetermined timepoints)	37 ºC (Rotation not specified)	8 days	Jaishankar et al., 2016
Gatifloxacin and moxifloxacin	HEMA, MPTS, MAA, EGDMA, and 1,9-NDA. Commercially available silicone and conventional hydrogel CLs (Etafilcon A, Polymacon) (Thickness – not specified)	Soaking in 3 mL of drug solutions and sterilized by moist heat (121 ºC, 30 min)	PBS (2 mL, replaced completely at predetermined timepoints)	37 ºC (Rotation not specified)	72 hours	Kakisu et al., 2013
Hyaluronic Acid	Commercially available silicone hydrogel CL (Nelfilcon A) and hydrogels prepared with MA,	Hyaluronic acid was mixed with the monomer's solution	Artificial tear solution pH 8 (20 mL, replaced completely at predetermined timepoints)	35 ºC, 30 rpm	120 hours	Ali and Byrne, 2009

	NVP, and DEAEM (Thickness – 0.127 mm)					
Hyaluronic acid	HEMA, DMAA TRIS, and EGDMA (Thickness – not specified)	Hyaluronic acid was mixed with the monomer solution	PBS pH 7.4 (1 mL, samples were taken and replenished at predetermined timepoints)	37 ºC, circular shaking	Until 41 days	Weeks et al., 2013
Hydrocortisone, acetazolamide	HEMA, and EGDMA (Thickness – 0.9 mm)	Soaking in 10 or 5 mL of 100 mg/l of hydrocortisone, and acetazolamide, respectively followed by autoclaving	STF (10-20 mL, without replacement)	25 ºC (Rotation not specified)	1 month	Dos Santos et al., 2008
Hydroxypropyl methylcellulose	HEMA, TRIM, NVP, MAA, MMA, and EGDMA (Thickness – not specified)	Soaking in 1% of hydroxypropyl methylcellulose	PBS pH 5.80-8.03 (200 µl) (Replacement not specified)	25 ºC (Rotation not specified)	12 hours	Kim et al., 2019
Ibuprofen sodium, diclofenac sodium	HEMA, APMA, VP, and EGDMA (Thickness – 0.9 mm)	Soaking in 10-30 mL of different concentrations of ibuprofen and diclofenac solutions for 1 week at 25 ºC	PBS pH 5.8 or 8.0, or NaCl solutions (10, 50, 100, or 150mM) (6 or 30 mL, without replacement)	37 ºC (Rotation not specified)	Until 26 hours	Andrade-Vivero et al., 2007
Ketorolac tromethamine, flurbiprofen sodium, diclofenac sodium	Commercially available silicone hydrogel CLs (Senofilcon A, Narafilcon A) (Thickness – not specified)	Soaking in 3 mL of 1.2 mg/mL of ketorolac, 0.2 mg/mL of diclofenac, and flurbiprofen for 24 h at 25 ºC	Dulbecco PBS pH 7.4 (3 mL, 1 mL replaced at predetermined timepoints)	25 ºC (Rotation not specified)	Until 200 hours	Torres-Luna et al., 2019c
Ketotifen fumarate	AA, AM, HEMA, and NVP (Thickness – 0.4-0.7 mm)	Soaking in concentrated solutions of ketotifen fumarate until achieve the equilibrium	Artificial lachrymal fluid, deionized water, and lysozyme in artificial lachrymal fluid (30 mL, without replacement)	(Temperature not specified) 120 rpm	7 days	Venkatesh et al., 2007
Ketotifen fumarate	Commercially available conventional hydrogel CLs (etafilcon A,	Soaking in 6 mL of 0.25 mg/mL of ketotifen fumarate for 24 h at 34 ºC	Commercially available saline solution (Unisol 4) (6 mL, 30 µl were taken at	34 ºC (Rotation not specified)	24 hours	Soluri et al., 2012

	polymacon, and alphafilcon A), and silicone hydrogel CLs (lotrafilcon B, balafilcon A, comfilcon A, galyfilcon A, and senofilcon A) (Thickness – 0.035-0.1 mm)		predetermined timepoints without replacement)			
Ketotifen fumarate	HEMA, DMA, siloxane, NVP, and EGDMA (Thickness – not specified)	Soaking in 2 mL of 50 or 100 µg/mL of solid lipid nanoparticles of ketotifen followed by autoclaving	STF (2 mL, completely replaced at predetermined timepoints)	34 °C, 100 rpm	Until 7 days	Zhang et al., 2020
Latanoprost	Commercially available silicone (Balafilcon A, Comfilcon A, Delefilcon A, Lotrafilcon B, Galyfilcon A), and conventional hydrogel CLs (Polymacon) (Thickness – not specified)	Soaking in 5 mL of 0.125 g/l of latanoprost for 4 min	STF (completely replaced at 24, 48, 96, and 144 h) Volume not specified	Not specified	8 days	Home et al., 2020
Latanoprost	Commercially available silicone hydrogel CL (Delefilcon A) (Thickness – not specified)	Soaking in 5 mL of latanoprost solution in n-propanol for 60, 120, 240 sec	STF or water (3 mL, completely replaced at 24, 48, 96, 144, 192, and 240 h)	Not specified	10 days	Home et al., 2017
Levobunolol	Commercially available conventional hydrogel CL (Omafilcon A)	Soaking in 5 mL of levobunolol nanoparticules (5 mg/ mL) for 24 h	STF pH 7.4 (3 mL, 1 mL replaced every 24 h)	25 °C, 100 rpm	Until 12 days	Kumar et al., 2020

USC

	(Thickness – not specified)					
Levofloxacin	Commercially available hydrogel CLs (Hioxifilcon B) (Thickness – not specified)	Immobilization of levofloxacin lypossomes onto the surfaces of soft CLs using a multilayer immobilization strategy	Saline solution, 150 mM NaCl pH 7.4 (3 mL, without replacement)	37 °C (Rotation not specified)	6 days	Danion et al., 2007
Levofloxacin, chlorhexidine	HEMA, PVP, TRIS, NVP, EGDMA (Thickness – 0.3-0.35 mm)	Soaking in 13 mL of 1.5, 2.5, and 5 mg/mL of chlorhexidine, and 5 mg/mL of levofloxacin for 14 or 36 h at 4 °C	Saline solution 130 mM NaCl (13 mL, 1 mL replaced at predetermined timepoints)	35 °C, 150 rpm	24 hours	Paradiso et al., 2014
Levofloxacin, chlorhexidine	Commercially available silicone hydrogel CLs (Senofilcon A, Narafilcon A) (Thickness – not specified)	Soaking in 3 mL of 5 mg/mL of chlorhexidine for 7 days, and 5 and 25 mg/mL of levofloxacin for 7 and 14 days, respectively	PBS (3 mL, without replacement)	25 °C (Rotation not specified)	About 7 days	Paradiso et al., 2016
Levofloxacin, chlorhexidine	HEMA, PVP, and EGDMA (Thickness – 0.3 mm)	Soaking in 5 mL of 5 mg/mL and 10 mg/mL of levofloxacin, and 1 mg/mL and 2.5 mg/mL of chlorhexidine for 5 days at 4 °C	Saline solution 130 mM NaCl (5 mL, 0.5 mL replaced at predetermined timepoints)	37 °C, 180 rpm	60 hours	Pimenta et al., 2016c
Levofloxacin, chlorhexidine	HEMA, PVP, TRIS, NVP, and EGDMA (Thickness – 0.3-0.35 mm)	Soaking in levofloxacin and chlorhexidine solution of 5 and 10 mg/mL for 14 h at 4 °C (2.6 mL/cm^2 of surface area)	0.9% NaCl solution (2.6 mL/cm^2 of surface area, ~8% of total volume was replaced at predetermined timepoints)	35 °C, 150 rpm	32 hours	Paradiso et al., 2015
Levofloxacin, diclofenac sodium, timolol maleate, chlorhexidine diacetate	HEMA, TRIS, NVP, and EGDMA (Thickness – 0.35 mm)	Soaking in 6 mL of 1 mg/mL of levofloxacin, diclofenac sodium, timolol maleate, and chlorhexidine diacetate for 5 days at 35 °C	0.9% NaCl solution (6 mL, 0.65 mL replaced at predetermined timepoints)	35 °C, 150 rpm	96 hours	Galante et al., 2018

Lidocaine	HEMA, and EGDMA (Thickness – 1 mm)	Liposomal mixture was added to the monomer's solution before polymerization	Water (20 mL, without replacement)	26 °C (Rotation not specified)	About 8 days	Gulsen et al., 2005
Lidocaine	HEMA, and EGDMA (Thickness – 0.2 or 1.2 mm)	Microemulsions were added to the monomer's solution before polymerization	Water (40 mL, without replacement)	26 °C (Rotation not specified)	About 8 days	Gulsen and Chauhan, 2005
Lidocaine	HEMA and EGDMA (Thickness – 1 mm)	Soaking in 40 mL of 0.3 to 4.3mM of lidocaine at 25 °C until achieve the equilibrium	Water (40 mL, without replacement)	Not specified	4 days	Gulsen and Chauhan, 2006
Lidocaine	HEMA, and EGDMA (Thickness – 1 mm)	Lidocaine microemulsions were mixed with monomer's solution	Water (Volume and replacement not specified)	Not specified	Until 10 days	Gulsen and Chauhan, 2004
Loteprednol etabonate	HEMA, NVP, and PEG-DA (Thickness – 0.2 mm)	Loteprednol etabonate nanoparticles were mixed with the monomer's solution	PBS pH 7.4 /3.5 mL, without replacement)	35 °C (Rotation not specified)	About 12 days	Nasr et al., 2016
Meloxicam	HEMA, TEGDMA, water, ethylene glycol (Thickness – 0.4 mm)	BSA-NX-NA gels were prepared using acid-base neutralization in aqueous solutions and dispersed in pHEMA	PBS (200 mL, without replacement)	34 °C, 50 rpm	Until 10 days	Zhang et al., 2014
Miconazole	HEMA, GMA, and EGDMA (Thickness – 0.9 mm)	Soaking in 60 mL of miconazole aqueous suspension, and autoclaved for 20 min at 121 °C	0.3% SDS medium (10-35 mL, without replacement)	25 °C (Rotation not specified)	14 days	Dos Santos et al., 2010
Moxifloxacin	Commercially available intraocular lens (CI26Y and Definitive 50) (Thickness – 1 mm)	Soaking in 1 mL of 5 mg/mL of moxifloxacin solution from 4 days to 3 months at 4 or 60 °C	PBS (3 mL, 0.3 mL replaced at predetermined timepoints)	36 °C, 180 rpm	7 days	Topete et al., 2018

USC

Moxifloxacin	Commercially available silicone hydrogel CL (Lotrafilcon A). Soft Shield Collagen Shield (Oasis Medical Inc, Glendora, CA)	Soaking in 0.5% of moxifloxacin solution for 10 min at 25 ºC	PBS (1mL, without replacement)	25 ºC (Rotation not specified)	2 hours	Zhou et al., 2018
Moxifloxacin	HMW-PDMS, PHMS-co-PDMS, and THF (Thickness – mean of 0.08 mm)	Soaking in 5 mL of 50 µg/mL of moxifloxacin for 2 days at 25 ºC	PBS (5 mL, completely replaced at predetermined timepoints)	37 ºC, 100 rpm	10 hours	Guzman et al., 2017
Moxifloxacin, chlorhexidine, and diclofenac	0 TRIS, NVP, HEMA, and EGDMA (Thickness – 0.25 mm)	Soaking in 3 mL of 1 mg/mL of diclofenac for 38 h, 2.5 mg/mL of chlorhexidine for 72 h and 5 mg/mL of moxifloxacin for 72 h at 4 ºC	Saline solution 130 mM NaCl pH 6.9 (3 mL, 200 µl replaced at predetermined timepoints)	38 ºC, 180 rpm	120 hours	Silva et al., 2018
N-acetylcysteine, N-acetylcysteine amide	Commercially available conventional hydrogel CLs (Hilafilcon B, Narafilcon A, Methafilcon B) (Thickness – not specified)	Soaking in 10 mL of 3 mM of N-acetylcysteine, or N-acetylcysteine amide for 72 h at 25 ºC	PBS (5 mL, samples were taken and replaced at predetermined timepoints)	37 ºC (Rotation not specified)	72 hours	Yigit and Ercal, 2013
Naltrexone	HEMA, BzMA, AAc, and EGDMA (Thickness – 0.5 mm)	Soaking in 3 mL of 0.3 mg/mL of naltrexone solution for 2 days at 25 ºC	0.9% NaCl solution (3 mL, without replacement)	36 ºC, 50 rpm	8 days	Alvarez-Rivera et al., 2019
Naphazoline	MOEP, MAm, EDMA, and HEMA (Thickness – 0.3 mm)	Soaking in 0.5% of naphazoline at 25 ºC for 2 days	0.9% NaCl solution (10 mL, replacement not specified)	37 ºC (Rotation not specified)	40 hours	Sato et al., 2005
Natamycin	HEMA, DMMA, TRIS, MβCD, MHP-βCD, and EGDMA (Thickness – 1.2 mm)	Soaking in 2 mL of 100 mg/mL of natamycin suspension for 48 h	PBS (2 mL, without replacement)	32 ºC, constant rotation	24 hours	Phan et al., 2014a

Natamycin	HEMA, TRIS, DMAA, and EGDMA (Thickness – 1.2 mm)	Soaking in 4 mL of natamycin encapsulated within poly(D,L-lactide)-dextran nanoparticles solution for 7 days at 25 ºC	Borate buffered saline pH 7.4 (2 mL, completely replaced every 24 h)	32 ºC, constant rotation	7 days	Phan et al., 2014b
Natamycin	Commercially available silicone (Balafilcon A, Comfilcon A, Senofilcon A, Lotrafilcon A, Galyfilcon A), and conventional hydrogel CLs (Polymacon, Omafilcon A, Etafilcon A, Vifilcon A) (Thickness – mean of 0.08 mm)	Soaking in 2 mL of 2.6 mg/mL of natamycin in DMSO, for 24 h at 32 ºC	Unisol 4 solution pH 7.4 (5 or 8 mL, completely replaced every 24 h)	32 ºC, constant rotation	24 hours	Phan et al., 2013
Nitric oxide	N- diazeniumdiolate functionalized poly-ε-lysine (pεK) contact lens gels	CLs gels were pressurized to 5 bar with nitric oxide for 3 days	PBS, cell culture media, Luria–Bertani broth (LB) pH 7 (5 mL, without replacement)	Not specified	15 hours	Aveyard et al., 2019
Norfloxacin	HEMA, AA, VP, and EGDMA (Thickness – 0.4 or 0.9 mm)	Soaking in 10 mL of different concentrations of norfloxacin solution at 25 ºC	STF (10-15 mL, without replacement)	37 ºC (Rotation not specified)	1 week	Alvarez-Lorenzo et al., 2006
Ofloxacin	HEMA, MAA, MOESA, MAPTAC, and EGDMA or 1,9-NDA (Thickness – not specified)	Soaking in 0.3 wt % of ofloxacin for 3 h	0.9% NaCl solution (2 mL, completely replaced at predetermined timepoints)	25 ºC (Rotation not specified)	24 hours	Yamazaki et al., 2013
Ofloxacin	Commercially available silicone hydrogel CLs (Senofilcon A, Narafilcon A) (Thickness – 0.08 mm)	Soaking in 2 mL of 3 mg/mL of ofloxacin solution for 48 h at 25 ºC	PBS (3 mL, without replacement)	25 ºC (Rotation not specified)	Until 4 days	Ubani-Ukomaa et al., 2019

USC

Ofloxacin, neomycin	HEMA, GMA, NVP, MAA, AA, MPA, and EGDMA	Soaking in 1.5 mL containing 0.5 mg of ofloxacin, and 5.0 mg of neomycin for 24 h	PBS pH 7.4 (3 mL, without replacement)	25 ºC (Rotation not specified)	Until 6 hours	Lee et al., 2018
Olopatadine	HEMA, AAc, BzMA, AAm, AMPSA, and EGDMA (Thickness – 0.4 mm)	Soaking in 20 mL of 0.2 or 10 mg/mL of olopatadine solution for 20 days	Artificial lachrymal fluid (2 or 20 mL, 500 or 50 µl replaced at predetermined timepoints)	37 ºC, 25 rpm	48 or 72 hours	González-Chomón et al., 2016
Orfloxacin, puerarin	HEMA, MPC, APS, and TEMED (Thickness – 1.2 mm)	Soaking in 2 mL of 1 mg/mL of orfloxacin, or puerarin for 48 h	PBS (4 mL, 2 mL replaced at predetermined timepoints)	37 ºC, 100 rpm	24 hours	Hu et al., 2016
Phomopsidione	Commercially available silicone hydrogel CLs (Narafilcon A) (Thickness – not specified)	CLs were coated by soaking in 2% of phomopsidione nanoparticle solution for 24 h at 4 ºC	PBS 0.1 M pH 7.4 (1 mL was removed every 24 h) (Total volume not specified)	25 ºC (Rotation not specified)	6 days	Sahadana et al., 2019
Poly(vinyl pyrrolidone)	HEMA, Kollidon® 30, Kollidon® 90F, and EGDMA (Thickness – 0.9 mm)	PVP was mixed with the monomer's solution	Water (20 mL, 10 mL replaced every 24 h)	Not specified	30 days	Yañez et al., 2008
Polymyxin B, vancomycin	HEMA, AAc, water, and EGDMA (Thickness – 0.4 mm)	Soaking in 2 mL of 4 mg/mL of polymyxin B for 3 days or vancomycin solution for 2 days	0.9% NaCl solution (2 mL, completely replaced after 174 h for polymyxin B and 47 h for vancomycin)	25 ºC (Rotation not specified)	14 days	Malakooti et al., 2015
Polyvinyl alcohol	Commercially available conventional hydrogel CLs (Omafilcon A, Nelfilcon A, Etafilcon A) (Thickness – mean of 0.09 mm)	Soaking in 1 mL of 10 mg/mL of polyvinyl alcohol solution for 24 h at 25 ºC	PBS (2 mL, without replacement)	34 ºC, gently shaking	24 hours	Phan et al., 2019b
Prednisolone	Commercially available conventional hydrogel CLs (Alphafilcon A)	Soaking in 2 mL of prednisolone-loaded nanocapsules for 8 h	PBS pH 7.4 (7 mL, 1 mL replaced at predetermined timepoints)	34 ºC, stirring	8 hours	Katzer et al., 2017

	(Thickness – not specified)					
Prednisolone	HEMA, MAA, and EGDMA (Thickness – not specified)	Soaking in 0.4 g of prednisolone nanoparticles for 24 h	PBS (10 mL, 0.5 mL replaced at predetermined timepoints)	35.5 ºC, 80 rpm	24 hours	ElShaer et al., 2016
Prednisolone Acetate	HEMA, MAA, and EGDMA (Thickness – 0.4 mm)	Soaking in 10 mL of 0.01, 0.025, and 0.05 mM of prednisolone acetate at 25 ºC for 48 h	0.9% NaCl or artificial lachrymal solution pH 8 (10 mL, without replacement)	37 ºC (Rotation not specified)	48 hours	Malaekeh-Nikouei et al., 2012
Rhodamine B	Commercially available silicone (Balafilcon A, Lotrafilcon B, Lotrafilcon A, Senfilcon A, Galyfilcon A), and conventional hydrogel CLs (Filcon 1 a, Vifilcon A, Etafilcon A, Filcon 3 a, Nelfilcon A) (Thickness – not specified)	Soaking in 2 mL of 10 or 100 µg/mL of Rhodamine B until achieve the equilibrium	PBS pH 7.4 (5 mL, completed replaced every hour)	37 ºC, 200 rpm	24 hours	Mahomed and Tighe, 2014
Salicylic acid	Commercially available conventional hydrogel CL (Hilafilcon B) (Thickness – not specified)	CLs were impregnated using supercritical CO_2 impregnation methodology at 11 MPa, 40 ºC, 0.1 MPa/min of depressurization rate	PBS (10 mL, 0.3 mL replaced at predetermined timepoints)	37 ºC (Rotation not specified)	8 hours	Yokozaki et al., 2015
Tetracaine, diclofenac sodium, flurbiprofen sodium, bupivacaine,	Commercially available silicone hydrogel CLs (Senofilcon A, Narafilcon A), and conventional hydrogel CLs (Etafilcon A)	Soaking in 5 mL of 0.2 mg/mL of tetracaine, diclofenac sodium, flurbiprofen sodium, and 1.0 mg/mL of bupivacaine, and 0.3 mg/mL of ketotifen fumarate for 24 h at 25 ºC	Dulbecco PBS pH 7.4 (3 mL, 1 mL replaced at predetermined timepoints)	25 ºC, without rotation	Until 62 days	Torres-Luna et al., 2020

ketotifen fumarate	(Thickness – 0.07-0.09 mm)					
Thiosemicarbazone	HEMA, 2,3-di-O-methacrylated-6-O-methacrylated-ß-cyclodextrin monomer, and EGDMA (Thickness – 0.4 mm)	Soaking in 10 mL of thiosemicarbazone suspensions for 1 day at 25 ºC	STF (10 mL, 2-3 mL replaced at predetermined timepoints)	25 ºC (Rotation not specified)	About 350 hours	Glisoni et al., 2013
Timolol	HEMA, MAA, and EGDMA (Thickness – not specified)	Soaking in 5 mL of 0.1 mM of timolol solution at 25 ºC until achieve the equilibrium	STF pH 8.0 (5 mL, without replacement)	Not specified	12 hours	Deng et al., 2018
Timolol maleate	DMAA, TRIS, MAA, and EGDMA (Thickness – 0.3 mm)	Soaking in 10 mL of 0.001 M of timolol for 3 days at 25 ºC	0.9% NaCl solution (10 mL, without replacement)	25 ºC (Rotation not specified)	Until 72 hours	Hiratani et al., 2005b
Timolol maleate	Commercially available silicone hydrogel CL (Balafilcon A) (Thickness – not specified)	Exterior surface of the CLs was coated by electrospinning technique	PBS pH 7.4 (10 mL, 1 mL replaced at predetermined timepoints)	37 ºC, 90 rpm	About 23 hours	Mehta et al., 2017a
Timolol maleate	Commercially available silicone hydrogel CL (Balafilcon A) (Thickness – not specified)	Coating the CL surface using a electrohydrodynamic process based on ejected droplet charge and timolol	PBS pH 7.4 (10 mL, completely replaced at predetermined timepoints)	37 ºC, constantly stirring	About 24 hours	Mehta et al., 2017b
Timolol maleate	TRIS, DMAA, DBE-U12, and EGDMA (Thickness – 0.13 mm)	Soaking in 2 mL of 5 mg/mL of timolol for 12 h at 25 ºC. Vitamin E was loaded by supercritical impregnation in high-pressure CO_2	PBS (5 mL, without replacement)	37 ºC, gently stirring	About 8 hours	Yokozaki and Shimoyama, 2018
Timolol maleate	HEMA, DMA, TRIS, and EGDMA (Thickness – 1 mm)	Soaking in 1 mL of 0.2 or 1 mg/mL of timolol for 6 days	PBS pH 7.4 (1 mL, completely replaced at predetermined timepoints)	37 ºC, 90 rpm	8 days	Guidi et al., 2014b

Timolol maleate	HEMA, and EGDMA (Thickness – 0.2 mm)	Timolol was mixed with the monomer solution	Deionized water (3 mL, completely replaced every 24 h)	37 °C, minimal stirring	About 40 days	Li et al., 2007
Timolol maleate	DEAA, MAA, and EGDMA (Thickness – 0.3 mm)	Soaking in 10 mL of 1mM of timolol solution for 3 days at 37 °C	0.9% NaCl solution (10 mL, 0.6 mL replaced at predetermined timepoints)	37 °C (Rotation not specified)	1 week	Hiratani and Alvarez-Lorenzo, 2002
Timolol maleate	HEMA, AAc, and EGDMA (Thickness – 0.2/ 0.9 mm)	Soaking in 2 or 8 mL of 0.04, 0.06, 0.08, and 0.100 mM of timolol solutions	0.9% NaCl solution (2 or 8 mL, without replacement)	25 °C, gently shaking	Until 2 weeks	Yañez et al., 2011b
Timolol maleate	HEMA, MAA, and EGDMA (Thickness – 0.1 mm)	Soaking in 0.02 µM of timolol maleate solution for 72-120 h	STF pH 7.2 (2 mL, without replacement)	37 °C (Rotation not specified)	100 hours	Anirudhan et al., 2016
Timolol maleate	HEMA, MAA, MMA, and EGDMA (Thickness – 0.7 mm)	Soaking in 5 mL of 0.5 mg/mL of timolol solution adjusted to pH 1.5, 3.5, 5.5, 7.5, 10	0.9% NaCl solution pH 5.5, or PBS pH 7.4, or STF pH 8 (15 mL, without replacement)	37 °C (Rotation not specified)	48 hours	Alvarez-Lorenzo et al., 2002
Timolol maleate	HEMA, DEAA, MMA, SiMA, DMAA, MAA, and EGDMA (Thickness – 0.3 mm)	Soaking in 10 mL of 1 mM of timolol solution for 3 days at 37 °C	0.9% NaCl solution (10 mL, 0.6 mL replaced at predetermined timepoints)	37 °C (Rotation not specified)	1 week	Hiratani and Alvarez-Lorenzo, 2004
Timolol maleate	HEMA, TRIS, DMA, and EGDMA (Thickness – 1 mm)	Timolol was mixed with the monomer solution	PBS pH 7.4 (1 mL, completed replaced at predetermined timepoints)	37 °C, 90 rpm	About 14 days	Korogiannaki et al., 2015
Timolol maleate and brimonidine tartrate	Commercially available hydrogel CLs (vasurfilcon A) (Thickness – not specified)	Soaking in 25 mL of timolol maleate (0.65 mg/mL) or brimonidine tartrate (0.2 mg/mL) prepared in PBS	PBS (25 mL, without replacement)	Not specified	420 minutes	Schultz et al., 2009
Timolol maleate, dexamethasone 21-disodium	Commercially available silicone hydrogel CLs (Galyfilcon A,	Soaking in 3 mL of drug solutions in PBS and drug-ethanol for 3 h	PBS (2 mL, without replacement)	Not specified	Until 7 days	Peng et al., 2010

USC

phosphate, fluconazole	Senofilcon A, Lotrafilcon A, Lotrafilcon B, Balafilcon A) (Thickness – 0.08-0.1 mm)					
Timolol maleate, dexamethasone, and dexamethasone 21-acetate	TRIS, DMA, NVP, and EGDMA (Thickness – 0.1/ 0.2/ 0.4 mm)	Soaking in 2 or 2.5 mL of drug solutions for 3 h	PBS (Volume and replacement not specified)	Not specified	About 150 days	Kim et al., 2008b
Tobramycin and Amikacin	TRIS, PEG (M_n of 500 or 300), EGDMA, and isopropyl alcohol (Thickness – not specified)	Soaking in 1 mL of 5 mg/mL tobramycin or amikacin in PBS for 24 h	PBS pH 7.4 (0.5 mL, replaced at predetermined timepoints)	37 °C, 100 rpm	24 hours	Postic and Sheardown, 2019
Transferulic acid	HEMA, GMA, EGPEM, and EGDMA (Thickness – 0.45 mm)	Soaking in 5 mL of 0.01 mg/mL of transferulic acid for 48 h at 25 °C	SLF (5 mL, without replacement)	35 °C, 300 rpm	24 hours	Varela-Garcia et al., 2020b
Triamcinolone acetonide	HEMA, NVP, MA, and EGDMA (Thickness – 1 mm)	Soaking in 10 mL of 8-19 µg/mL of triamcinolone acetonide solution for 4 days at 25 °C	Artificial lachrymal fluid pH 7.4 (5 mL, 1 mL replaced at predetermined timepoints)	37 °C, 100 rpm	3 days	García-Millán et al., 2015
Triamcinolone acetonide	HEMA, MA, and EGDMA (Thickness – 1 mm) Commercially available conventional hydrogel CLs (Hilafilcon B) (Thickness – mean of 0.257 mm)	Soaking in 10 mL of triamcinolone acetonide saturated solutions or 5 mL of triamcinolone acetonide nanosuspension for 2 days at 25 °C	STF pH 8 (5 mL, 1 mL replaced at predetermined timepoints)	37 °C, 100 rpm	4 days	García-Millán et al., 2017
Vancomycin, gentamicin	Commercially available CLs from Acuity Contact Lenses, Hoddesdon, UK	Filled the concave surface of the contact lens with 25 mg/mL of vancomycin or 40 mg/mL of gentamicin	PBS (200 µl, completely replaced at predetermined timepoints)	37 °C (Rotation not specified)	72 hours	Hyatt et al., 2012

1.6 REFERENCES

Adrianto, M.F.; Annuryanti, F.; Wilson, C.G.; Sheshala, R.; Thakur, R.R.S. (**2022**). In vitro dissolution testing models of ocular implants for posterior segment drug delivery. *Drug Deliv. and Transl. Res.* 12(6), 1355-1375.

Ali, M.; Byrne, M.E. (**2009**). Controlled release of high molecular weight hyaluronic acid from molecularly imprinted hydrogel contact lenses. *Pharm. Res.* 26, 714–726.

Alvarez-Lorenzo, C.; Anguiano-Igea, S.; Varela-Garcia, A.; Vivero-Lopez, M.; Concheiro, A. (**2019**). Bioinspired hydrogels for drug-eluting contact lenses. *Acta Biomater.* 84, 49–62.

Alvarez-Lorenzo, C.; Hiratani, H.; Gómez-Amoza, J.L.; Martínez-Pacheco, R.; Souto, C.; Concheiro, A. (**2002**). Soft contact lenses capable of sustained delivery of timolol. *J. Pharm. Sci.* 91(10), 2182–2192.

Alvarez-Lorenzo, C.; Yañez, F.; Barreiro-Iglesias, R.; Concheiro, A. (**2006**). Imprinted soft contact lenses as norfloxacin delivery systems. *J. Control. Release.* 113(3), 236–244.

Alvarez-Rivera, F., Concheiro, A.; Alvarez-Lorenzo, C. (**2018**). Epalrestat-loaded silicone hydrogels as contact lenses to address diabetic eye complications. *Eur. J. Pharm. Biopharm.* 122, 126–136.

Alvarez-Rivera, F.; Serro, A.P; Silva, D.; Concheiro, A.; Alvarez-Lorenzo, C. (**2019**). Hydrogels for diabetic eyes: Naltrexone loading, release profiles and cornea penetration. *Mater. Sci. Eng. C.* 105, 110092.

USC UNIVERSIDADE DE SANTIAGO DE COMPOSTELA

Andrade-Vivero, P.; Fernandez-Gabriel, E.; Alvarez-Lorenzo, C.; Concheiro, A. (**2007**). Improving the loading and release of NSAIDs from pHEMA hydrogels by copolymerization with functionalized monomers. *J. Pharm. Sci.* 96(4), 802–813.

Anirudhan, T.S.; Nair, A.S.; Parvathy, J. (**2016**). Extended wear therapeutic contact lens fabricated from timolol imprinted carboxymethyl chitosan-g-hydroxy ethyl methacrylate-g-polyacrylamide as a onetime medication for glaucoma. *Eur. J. Pharm. Biopharm.* 109, 61–71.

Ashtiani, M.K.; Zandi, M.; Shokrollahi, P.; Ehsani, M.; Baharvand, H. (**2020**). Chitosan surface modified hydrogel as a therapeutic contact lens. *Polym. Adv. Technol.* 31, 741–748.

Aveyard, J.; Deller, R.C.; Lace, R.; Williams, R.L.; Kaye, S.B.; Kolegraff, K.N.; Curran, J.M.; D'Sa, R.A. (**2019**). Antimicrobial Nitric Oxide Releasing Contact Lens Gels for the Treatment of Microbial Keratitis. *ACS Appl Mater Interfaces.* 11(41), 37491-37501.

Bajgrowicz, M.; Phan, C.M.; Subbaraman, L.N.; Jones, L. (**2015**). Release of ciprofloxacin and moxifloxacin from daily disposable contact lenses from an in vitro eye model. *Invest. Ophthalmol. Vis. Sci.* 56(4), 2234–2242.

Bao, Q.; Burgess, D.J. (**2018**). Perspectives on physicochemical and in vitro profiling of ophthalmic ointments. *Pharm. Res.* 35(12), 234.

Bao, Q.; Jog, R.; Shen, J.; Newman, B.; Wang, Y.; Choi, S.; Burgess, D.J. (**2017**). Physicochemical attributes and dissolution testing of ophthalmic ointments. *Int. J. Pharm.* 523(1), 310–319.

USC UNIVERSIDADE DE SANTIAGO DE COMPOSTELA

Bao, Q.; Newman, B.; Wang, Y.; Choi, S.; Burgess, D.J. (**2018**). In vitro and ex vivo correlation of drug release from ophthalmic ointments. *J. Control. Release.* 276, 93–101.

Behl, G.; Iqbal, J.; O'Reilly, N.J.; McLoughlin, P.; Fitzhenry, L. (**2016**). Synthesis and characterization of poly(2-hydroxyethylmethacrylate) contact lenses containing chitosan nanoparticles as an ocular delivery system for dexamethasone sodium phosphate. *Pharm. Res.* 33(7), 1638–1648.

Bengani, L.C.; Chauhan, A. (**2013**). Extended delivery of an anionic drug by contact lens loaded with a cationic surfactant. *Biomaterials.* 34(11), 2814–2821.

Bengani, L.C.; Kobashi, H.; Ross, A.E.; Zhai, H.; Salvador-Culla, B.; Tulsan, R.; Kolovou, P.E.; Mittal, S.K.; Chauhan, S.K.; Kohane, D.S.; Ciolino, J.B. (**2020**). Steroid-eluting contact lenses for corneal and intraocular inflammation. *Acta Biomater.* 116, 149-161.

Bertens, C.J.F.; Gijs, M.; van den Biggelaar, F.J.H.M.; Nuijts, R.M.M.A. (**2018**). Topical drug delivery devices: A review. *Exp. Eye Res*. 168, 149-160.

Bin Sahadan, M.Y.; Tong, W.Y.; Tan, W.N.; Leong, C.R.; Bin Misri, M.N.; Chan, M.; Cheng, S.Y.; Shaharuddin, S. (**2019**). Phomopsidione nanoparticles coated contact lenses reduce microbial keratitis causing pathogens. *Exp. Eye Res.* 178, 10-14.

Braga, M.E.; Costa, V.P.; Pereira, M.J.; Fiadeiro, P.T.; Gomes, A.P.; Duarte, C.M.; de Sousa, H. C. (**2010**). Effects of operational conditions on the supercritical solvent impregnation of acetazolamide in Balafilcon A commercial contact lenses. *Int. J. Pharm.* 420(2), 231-43.

USC UNIVERSIDADE DE SANTIAGO DE COMPOSTELA

BusinessWire (**2021**). MediPrint™ Ophthalmics Announces Successful Completion of Its SIGHT-1 Phase 2a Clinical Study. https://www.businesswire.com/news/home/20210316005609/en/ (accessed November 2021).

Byrne, M.E.; Hilt, J.Z.; Peppas, N.A. (**2008**). Recognitive biomimetic networks with moiety imprinting for intelligent drug delivery. *J. Biomed. Mater. Res. A.* 84(1), 137–147.

Cavas-Martínez, F.; Fernandez-Pacheco, D.G.; De la Cruz-Sanchez, E.; Nieto Martinez, J.; Fernandez Cañavate, F.J.; Vega-Estrada, A.; Plaza-Puche, A.B.; Alio, J.L. (**2014**). Geometrical custom modeling of human cornea in vivo and its use for the diagnosis of corneal ectasia. *PLoS One. 9*, e110249.

Choi, S.H.; Lionberger, R.A. (**2016**). Clinical, pharmacokinetic, and in vitro studies to support bioequivalence of ophthalmic drug products. *AAPS J.* 18(4), 1032–1038.

Choi, J.H.; Li, Y.; Jin, R.; Shrestha, T.; Choi, J.S.; Lee, W.J.; Moon, M.J.; Ju, H.T.; Choi, W.; Yoon, K.C. (**2019**). The Efficiency of Cyclosporine A-Eluting Contact Lenses for the Treatment of Dry Eye. *Curr. Eye Res.* 44(5), 486-496.

Chrai, S.S.; Patton, T.F.; Metha, A.; Robinson, J.R. (**1973**). Lacrimal and instilled fluid dynamics in rabbit eyes. *J. Pharm. Sci.* 62(7), 1112–1121.

Ciolino, J.B.; Hoare, T.R.; Iwata, N.G.; Behlau, I.; Dohlman, C.H.; Langer, R.; Kohane, D.S. (**2009**). A drug-eluting contact lens. *Invest. Ophthalmol. Vis. Sci.* 50(7), 3346-3352.

USC UNIVERSIDADE DE SANTIAGO DE COMPOSTELA

Ciolino, J.B.; Hudson, S.P.; Mobbs, A.N.; Hoare, T.R.; Iwata, N.G.; Fink, G.R.; Kohane, D.S. (**2011**). A prototype antifungal contact lens. *Invest. Ophthalmol. Vis. Sci.* 52(9), 6286–6291.

Ciolino, J.B.; Ross, A.E.; Tulsan, R.; Watts, A.C.; Wang, R.F.; Zurakowski, D.; Serle, J.B.; Kohane, D.S. (**2016**). Latanoprost-Eluting Contact Lenses in Glaucomatous Monkeys. *Ophthalmol.* 123(10), 2085-2092.

Ciolino, J.B.; Stefanescu, C.F.; Ross, A.E.; Salvador-Culla, B.; Cortez, P.; Ford, E.M.; Wymbs, K.A.; Sprague, S.L.; Mascoop, D.R.; Rudina, S.S.; Trauger, S.A.; Cade, F.; Kohane, D.S. (**2014**). In vivo performance of a drug-eluting contact lens to treat glaucoma for a month. *Biomaterials.* 35(1), 432-439.

Costa, V.P.; Braga, M.E.M.; Duarte, C.M.M.; Alvarez-Lorenzo, C.; Concheiro, A.; Gil, M.H.; de Sousa, H.C. (**2010a**). Anti-glaucoma drug-loaded contact lenses prepared using supercritical solvent Impregnation. *J. Supercrit. Fluids.* 53, 165–173.

Costa, V.P.; Braga, M.E.M.; Guerra, J.P.; Duarte, A.R.C.; Duarte, C.M.M.; Leite, E.O.B.; Gil, M.H.; de Sousa, H.C. (**2010b**). Development of therapeutic contact lenses using a supercritical solvent impregnation method. *J. Supercrit. Fluids.* 52, 306–316.

Danion, A.; Arsenault, I.; Vermette, P. (**2007**). Antibacterial activity of contact lenses bearing surface-immobilized layers of intact liposomes loaded with levofloxacin. *J. Pharm. Sci.* 96(9), 2350–2363.

Del Amo, E.M.; Urtti, A. (**2008**). Current and future ophthalmic drug delivery systems. A shift to the posterior segment. *Drug Discov. Today.* 13(3-4), 135–143.

USC UNIVERSIDADE DE SANTIAGO DE COMPOSTELA

Deng, J.; Chen, S.; Chen, J.; Ding, H.; Deng, D.; Xie, Z. (**2018**). Self-reporting colorimetric analysis of drug release by molecular imprinted structural color contact lens. *ACS Appl. Mater. Interfaces.* 10(40), 34611–34617.

Desai, A.R.; Maulvi, F.A.; Desai, D.M.; Shukla, M.R.; Ranch, K.M.; Vyas, B.A.; Shah, S.A.; Sandeman, S.; Shah, D.O. (**2020**). Multiple drug delivery from the drug-implants-laden silicone contact lens: Addressing the issue of burst drug release. *Mater. Sci. Eng. C.* 112, 110885.

Desai, A.R.; Maulvi, F.A.; Pandya, M.M.; Ranch, K.M.; Vyas, B.A.; Shah, S.A.; Shah, D.O. (**2018**). Co-delivery of timolol and hyaluronic acid from semi-circular ring implanted contact lenses for the treatment of glaucoma: in vitro and in vivo evaluation. *Biomater. Sci.* 6, 1580.

Dixon, P.; Chauhan, A. (**2017**). Effect of the surface layer on drug release from delefilcon-A (Dailies Total 1®) contact lenses. *Int. J. Pharm.* 529(1-2), 89–101.

Dixon, P.; Ghosh, T.; Mondal, K.; Konar, A.; Chauhan, A.; Hazra, S. (**2018**). Controlled delivery of pirfenidone through vitamin E-loaded contact lens ameliorates corneal inflammation. *Drug Deliv. Transl. Res.* 8(5), 1114–1126.

Doane, M.G. (**1989**). An instrument for in vivo tear film interferometry. *Optom. Vis. Sci.* 66(6), 383–388.

Dominguez-Godinez, C.; Carracedo, G.; Pintor, J. (**2018**). Diquafosol delivery from silicone hydrogel contact lenses: improved effect on tear secretion. *J. Ocular Pharm. Ther.* 34(1-2), 170–176.

USC UNIVERSIDADE DE SANTIAGO DE COMPOSTELA

Dos Santos, J.R.; Alvarez-Lorenzo, C.; Silva, M.; Balsa, L.; Couceiro, J.; Torres-Labandeira, J.; Concheiro, A. (**2009**). Soft contact lenses functionalized with pendant cyclodextrins for controlled drug delivery. *Biomaterials.* 30(7), 1348–1355.

Dos Santos, J.R.; Couceiro, R.; Concheiro, A.; Torres-Labandeira, J.; Alvarez-Lorenzo, C. (**2008**). Poly(hydroxyethyl methacrylate-co-methacrylated-b-cyclodextrin) hydrogels: Synthesis, cytocompatibility, mechanical properties and drug loading/ release properties. *Acta Biomater.* 4(3), 745–755.

Dos Santos, J.R.; Torres-Labandeira, J.; Matthijs, N.; Coenye, T.; Concheiro, A.; Alvarez-Lorenzo, C. (**2010**). Functionalization of acrylic hydrogels with α-, β- or γ-cyclodextrin modulates protein adsorption and antifungal delivery. *Acta Biomater.* 6(10), 3919–3926.

ElShaer, A.; Mustafa, S.; Kasar, M.; Thapa, S.; Ghatora, B.; Alany, R.G. (**2016**). Nanoparticle-laden contact lens for controlled ocular delivery of prednisolone: formulation optimization using statistical experimental design. *Pharmaceutics.* 8(2), 14.

European Comission (**2021**). Replacement, Reduction and Refinement – the "Three Rs"; https://ec.europa.eu/environment/chemicals/lab_animals/3r/alternative_en.htm (accessed November 2021).

FDA (**2018c**). Combination Product Definition Combination Product Types; https://www.fda.gov/combination-products/about-combination-products/combination-product-definition-combination-product-types (accessed November 2021).

FDA (**2013, 2016**). Current Good Manufacturing Practice Requirements for Combination Products, published January 22, 2013

USC UNIVERSIDADE DE SANTIAGO DE COMPOSTELA

(21 CFR Part 4, Subpart A; 78 FR 4307-22) and Postmarketing Safety Reporting for Combination Products, 2021 published December 20, 2016 (21 CFR Part 4, Subpart B; 81 FR 92603-26.

FDA (**2019b**). FY2019 GDUFA Research Report: Ophthalmic; https://www.fda.gov/media/135187/download#page=50 (accessed November 2021).

FDA (**2018b**). Importing Medical Devices; https://www.fda.gov/industry/regulated-products/medical-device-overview (accessed October 2021).

FDA News (**2021**). Johnson & Johnson Vision's Drug-Releasing Contact Lens Approved in Japan; https://www.fdanews.com/articles/202045-johnson-johnson-visions-drug-releasing-contact-lens-approved-in-japan (accessed October 2021).

FDA (**2019a**). Principles of Premarket Pathways for Combination Products Guidance for Industry and FDA Staff; https://www.fda.gov/media/119958/download (accessed November 2021).

FDA (**2018a**). Types of Contact Lenses; https://www.fda.gov/medical-devices/contact-lenses/types-contact-lenses (accessed October 2021).

Galante, R.; Oliveira, A.S.; Topete, A.; Ghisleni, D.; Braga, M.; Pinto, T.J.A.; Colaço, R.; Serro, A.P. (**2018**). Drug-eluting silicone hydrogel for therapeutic contact lenses: Impact of sterilization methods on the system performance. *Colloids Surf. B: Biointerfaces.* 161, 537–546.

Galante, R.; Paradiso, P.; Moutinho, M.G.; Fernandes, A.I.; Mata, J.L.; Matos, A.P.; Colaço, R.; Saramago, B.; Serro, A.P. (**2015**). About the

USC UNIVERSIDADE DE SANTIAGO DE COMPOSTELA

effect of eye blinking on drug release from pHEMA-based hydrogels: an in vitro study. *J. Biomater. Sci. Polym. Ed.* 26(4), 235-251.

Gallagher, A.G.; McLean, K.; Stewart, R.M.K.; Wellings, D.A.; Allison, H.E.; Williams, R.L. (**2017**). Development of a poly-ε-lysine contact lens as a drug delivery device for the treatment of fungal keratitis. *Investig. Ophthalmol. Vis. Sci.* 58(11), 4499–4505.

Ghazal, H.; Ahmadouk, J.; Dhanji, S.; El-Bushra, A.; Kayyali, R.; ElShaer, A. (**2018**). Patients' and prescribers' perception of contact lenses as a potential ocular drug delivery system. *Contact Lens Ant. Eye.* 42(2), 190–195.

García-Fernández, M.J.; Tabary, N.; Martel, B.; Cazaux, F.; Oliva, A.; Taboada, P.; Concheiro, A.; Alvarez-Lorenzo, C. (**2013**). Poly-(cyclo)dextrins as ethoxzolamide carriers in ophthalmic solutions and in contact lenses. *Carbohydr. Polym.* 98(2), 1343–1352.

García-Millán, E.; Koprivnik, S.; Otero-Espinar, F.J. (**2015**). Drug loading optimization and extended drug delivery of corticoids from pHEMA based soft contact lenses hydrogels via chemical and microstructural modifications. *Int. J. Pharm.* 487, 260–269.

García-Millán, E.; Quintáns-Carballo, M.; Otero-Espinar, F.J. (**2017**). Improved release of triamcinolone acetonide from medicated soft contact lenses loaded with drug nanosuspensions. *Int. J. Pharm.* 525(1), 226–236.

Garhwal, R.; Shady, S.F.; Ellis, E.J.; Ellis, J.Y.; Leahy, C.D.; McCarthy, S.P.; Crawford, K.S.; Gaines, P. (**2012**). Sustained ocular delivery of ciprofloxacin using nanospheres and conventional contact lens materials. *Invest. Ophthalmol. Vis Sci.* 53(3), 1341-1352.

USC UNIVERSIDADE DE SANTIAGO DE COMPOSTELA

Glisoni, R.J.; García-Fern´andez, M.J.; Pino, M.; Gutkind, G.; Moglioni, A.G.; Alvarez-Lorenzo, C.; Concheiro, A.; Sosnik, A. (**2013**). β-Cyclodextrin hydrogels for the ocular release of antibacterial thiosemicarbazones. *Carbohydr. Polym.* 93(2), 449–457.

González-Chomón, C.; Concheiro, A.; Alvarez-Lorenzo, C. (**2013**). Soft contact lenses for controlled ocular delivery: 50 years in the making. *Ther. Deliv*. 4(9), 1141–1161.

González-Chomón, C.; Silva, M.; Concheiro, A.; Alvarez-Lorenzo, C. (**2016**). Biomimetic contact lenses eluting olopatadine for allergic conjunctivitis. *Acta Biomater.* 41, 302–311.

Guidi, G.; Hughes, T.C.; Whinton, M.; Brook, M.A.; Sheardown, H. (**2014a**). The effect of silicone hydrogel contact lens composition on dexamethasone release. *J. Biomater. Appl.* 29(2), 222–233.

Guidi, G.; Korogiannaki, M.; Sheardown, H. (**2014b**). Modification of timolol release from silicone hydrogel model contact lens materials using hyaluronic acid. *Eye Contact Lens.* 40(5), 269–276.

Gulsen, D.; Chauhan, A. (**2005**). Dispersion of microemulsion drops in HEMA hydrogel: a potential ophthalmic drug delivery vehicle. *Int. J. Pharm*. 292(1-2), 95–117.

Gulsen, D.; Chauhan, A. (**2006**). Effect of water content on transparency, swelling, lidocaine diffusion in p-HEMA gels. *J. Membr. Sci.* 269(1-2), 35–48.

Gulsen, D.; Chauhan, A. (**2004**). Ophthalmic drug delivery through contact lenses. *Invest. Ophthalmol. Vis. Sci.* 45(7), 2342–2347.

USC UNIVERSIDADE DE SANTIAGO DE COMPOSTELA

Gulsen, D.; Li, C.; Chauhan, A. (**2005**). Dispersion of DMPC liposomes in contact lenses for ophthalmic drug delivery. *Curr. Eye Res.* 30(12), 1071–1080.

Guzman, G.; Es-haghi, S.S.; Nugay, T.; Cakmak, M. (**2017**). Zero-order antibiotic release from multilayer contact lenses: nonuniform drug and diffusivity distributions produce constant-rate drug delivery. *Adv. Healthcare Mater.* 6(3), 1600775.

Hiratani, H.; Alvarez-Lorenzo, C. (**2004**). The nature of backbone monomers determines the performance of imprinted soft contact lenses as timolol drug delivery systems. *Biomaterials.* 25(6), 1105–1113.

Hiratani, H.; Alvarez-Lorenzo, C. (**2002**). Timolol uptake and release by imprinted soft contact lenses made of N,N-diethylacrylamide and methacrylic acid. *J. Control. Release.* 83(2), 223–230.

Hiratani, H.; Fujiwara, A.; Tamiya, Y.; Mizutani, Y.; Alvarez-Lorenzo, C. (**2005a**). Ocular release of timolol from molecularly imprinted soft contact lenses. *Biomaterials.* 26(11), 1293–1298.

Hiratani, H.; Mizutani, Y.; Alvarez-Lorenzo, C. (**2005b**). Controlling drug release from imprinted hydrogels by modifying the characteristics of the imprinted cavities, *Macromol. Biosci.* 5(8), 728–733.

Hobson, A. (2**017**). Regulatory barriers are stifling the contact lens industry; https://thehill.com/blogs/pundits-blog/technology/330856-regulatory-barriers-and-stifling-the-contact-lens-industry (accessed October 2021).

Horne, R.R.; Judd, K.E.; Pitt, W.G. (**2017**). Rapid loading and prolonged release of latanoprost from a silicone hydrogel contact lens. *J. Drug Deliv. Sci. Technol.* 41, 410–418.

USC UNIVERSIDADE DE SANTIAGO DE COMPOSTELA

Horne, R.R.; Rich, J.T.; Bradley, M.W.; Pitt, W.G. (**2020**). Latanoprost uptake and release from commercial contact lenses. *J. Biomater. Sci. Polym. Ed.* 31(1), 1–19.

Huang, C.; Zhang, X.; Li, Y.; Yang, X. (**2021**). Hyaluronic acid and graphene oxide loaded silicon contact lens for corneal epithelial healing. *J. Biomater. Sci. Polym. Ed.* 32(3), 372–384.

Hughes, P.M; Olejnik, O.; Chang-Lin, J.E.; Wilson, C.G. (**2005**). Topical and systemic drug delivery to the posterior segments. *Adv. Drug Deliv. Rev.* 57(14), 2010–2032.

Hui, A.; Bajgrowicz-Cieslak, M.; Phan, C.; Jones, L. (**2017**). In vitro release of two antimuscarinic drugs from soft contact lenses. *Clin. Ophthalmol.* 11, 1657–1665.

Hui, A.; Boone, A.; Jones, L. (**2008**). Uptake and release of ciprofloxacin-HCl from conventional and silicone hydrogel contact lens materials. *Eye Contact Lens.* 34(5), 266–271.

Hui, A.; Sheardown, H.; Jones, L. (**2012**). Acetic and acrylic acid molecular imprinted model silicone hydrogel materials for ciprofloxacin-HCl delivery. *Materials.* 5(1), 85–107.

Hsu, K.H.; Carbia, B.E.; Plummer, C.; Chauhan, A. (**2015a**). Dual drug delivery from vitamin E loaded contact lenses for glaucoma therapy. *Eur. J. Pharm. Biopharm*. 94, 312–321.

Hsu, K.; De la Jara, P.L.; Ariyavidana, A.; Watling, J.; Holden, B.; Garrett, Q.; Chauhan, A. (**2015b**). Release of betaine and dexpanthenol from vitamin E modified silicone-hydrogel contact lenses. *Curr. Eye Res.* 40(3), 267–273.

USC UNIVERSIDADE DE SANTIAGO DE COMPOSTELA

Hsu, K.; Fentzke, R.C.; Chauhan, A. (**2013**). Feasibility of corneal drug delivery of cysteamine using vitamin E modified silicone hydrogel contact lenses. *Eur. J. Pharm. Biopharm.* 85(3 Pt A), 531–540.

Hu, X.; Tan, H.; Chen, P.; Wang, X.; Pang, J. (**2016**). Polymer micelles laden hydrogel contact lenses for ophthalmic drug delivery. *J. Nanosci. Nanotechnol.* 16(6), 5480–5488.

Hyatt, A.J.T.; Rajan, M.S.; Burling, K.; Ellington, M.J.; Tassoni, A.; Martin, K.R. (**2012**). Release of vancomycin and gentamicin from a contact lens versus a fibrin coating applied to a contact lens. *Investig. Ophthalmol. Vis. Sci.* 53(4), 1946–1952.

Jaishankar, D.; Buhrman, J.S.; Valyi-Nagy, T.; Gemeinhart, R.A.; Shukla, D. (**2016**). Extended release of an anti–heparan sulfate peptide from a contact lens suppresses corneal herpes simplex virus-1 infection. *Investig. Ophthalmol. Vis. Sci.* 57(1), 169–180.

Johnson & Johnson Vision Care (**2021**). ACUVUE® Theravision®; https://www.jnjvisionpro.ca/products/acuvue-theravision (accessed October 2021).

Jones, L.; Hui, A.; Phan, C.M.; Read, M.L.; Azar, D.; Buch, J.; Ciolino, J.B.; Naroo, S.A.; Pall, B.; Romond, K.; Sankaridurg, P.; Schnider, C.M.; Terry, L.; Willcox, M. (**2021**). CLEAR-Contact lens technologies of the future. *Contact Lens Ant. Eye.* 44(2), 398–430.

Joshi, A.; Maurice, D.M.; Paugh, J.R. (**1996**). A new method for determining corneal epithelial barrier to fluorescein in humans. *Invest. Ophthalmol. Vis. Sci.* 37(6), 1008–1016.

Jung, H.J.; Abou-Jaoude, M.; Carbia, B.E.; Plummer, C.; Chauhan, A. (**2013**). Glaucoma therapy by extended release of timolol from

USC UNIVERSIDADE DE SANTIAGO DE COMPOSTELA

nanoparticle loaded silicone hydrogel contact lenses. *J. Control. Release.* 165(1), 82–89.

Kaczmarek, J.C.; Tieppo, A.; White, C.J.; Byrne, M.E. (**2014**). Adjusting biomaterial composition to achieve controlled multiple-day release of dexamethasone from an extended-wear silicone hydrogel contact lens. *J. Biomater. Sci. Polym. Ed.* 25(1), 88–100.

Kakisu, K.; Matsunaga, T.; Kobayakawa, S.; Sato, T.; Tochikubo, T. (**2013**). Development and efficacy of a drug-releasing soft contact lens. *Investig. Ophthalmol. Vis. Sci.* 54(4), 2551–2561.

Kapoor, Y.; Chauhan, A. (**2008b**). Drug and surfactant transport in Cyclosporine A and Brij 98 laden p-HEMA hydrogels. *J. Colloid Interface Sci.* 322(2), 624–633.

Kapoor, Y.; Chauhan, A. (**2008a**). Ophthalmic delivery of Cyclosporine A from Brij-97 microemulsion and surfactant-laden p-HEMA hydrogels. *Int. J. Pharm.* 361(1-2), 222–229.

Kapoor, Y.; Dixon, P.; Sekar, P.; Chauhan, A. (**2017**). Incorporation of drug particles for extended release of cyclosporine A from poly-hydroxyethyl methacrylate hydrogels. *Eur. J. Pharm. Biopharm.* 120, 73–79.

Kapoor, Y.; Thomas, J.C.; Tan, G.; John, V.T.; Chauhan, A. (**2009**). Surfactant-laden soft contact lenses for extended delivery of ophthalmic drugs. *Biomaterials.* 30(5), 867–878.

Karlgard, C.C.S.; Wong, N.S.; Jones, L.W.; Moresoli, L. (**2003**). In vitro uptake and release studies of ocular pharmaceutical agents by silicon-containing and p-HEMA hydrogel contact lens materials. *Int. J. Pharm.* 257(1-2), 141–151.

USC UNIVERSIDADE DE SANTIAGO DE COMPOSTELA

Katzer, T.; Chaves, P.S.; Pohlmann, A.R.; Guterres, S.S.; Beck, R.C.R. (**2017**). Loading a drug on contact lenses using polymeric nanocapsules: effects on drug release, transparency, and ion permeability. *J. Nanosci. Nanotechnol.* 17, 9286–9294.

Kenley, R.A.; Filippone, H.; Giske, M.; Beidler, D.; Vehige, J.; Fleitman, J. (**2013**). Equilibrium binding interactions between Lotrafilcon a soft contact lenses and the two prostaglandin antiglaucoma drugs bimatoprost and tafluprost. *Eye Contact Lens.* 39(4), 295–302.

Kim, G.; Kim, H.J.; Noh, H. (**2019**). Influence of solution pH on drug release from ionic hydrogel lens. *Macromol. Res.* 27, 191–197.

Kim, J.; Chauhan, A. (**2008a**). Dexamethasone transport and ocular delivery from poly (hydroxyethyl methacrylate) gels. *Int. J. Pharm.* 353(1-2), 205–222.

Kim, J.; Conway, A.; Chauhan, A. (**2008b**). Extended delivery of ophthalmic drugs by silicone hydrogel contact lenses. *Biomaterials.* 29(14), 2259–2269.

Kim, J.; Peng, C.; Chauhan, A. (**2010**). Extended release of dexamethasone from silicone hydrogel contact lenses containing vitamin E. *J. Control. Release.* 148(1), 110–116.

Kopeček, J. (**2009**). Hydrogels from soft contact lenses and implants to self-assembled nanomaterials. *J. Polym. Sci. A Polym. Chem.* 47(22), 5929–5946.

Korogiannaki, M.; Guidi, G.; Jones, L.; Sheardown, H. (**2015**). Timolol maleate release from hyaluronic acid-containing model silicone hydrogel contact lens materials. *J. Biomater. Appl.* 30(3), 361–376.

USC UNIVERSIDADE DE SANTIAGO DE COMPOSTELA

Kostewicz, E.S.; Abrahamsson, B.; Brewster, M.; Brouwers, J.; Butler, J.; Carlert, S.; Dickinson, P.A.; Dressman, J.; Holm, R.; Klein, S.; Mann, J.; McAllister, M.; Minekus, M.; Muenster, U.; Müllertz, A.; Verwei, M.; Vertzoni, M.; Weitschies, W.; Augustijns, P. (**2014**). In vitro models for the prediction of in vivo performance of oral dosage forms. *Eur. J. Pharm. Sci.* 57, 342-366.

Kumar, N.; Aggarwal, R.; Chauhan, M.K. (**2020**). Extended levobunolol release from Eudragit nanoparticle-laden contact lenses for glaucoma therapy. *Future J. Pharm. Sci.* 6(109), 109.

Kusrini, E.; Sabira, K.; Hashim, F.; Abdullah, N.A.; Usman, A.; Putra, N.; Prasetyanto, E.A. (**2021**). Design, synthesis and antiamoebic activity of dysprosium-based nanoparticles using contact lenses as carriers against Acanthamoeba sp. *Acta Ophthalmol.* 99(2), e178-e188.

Lang, J.C.; Stiemke, M.M. (**1996**). Biological barriers to ocular delivery. In *Ocular Therapeutics and Drug Delivery*; Reddy, I.K. (Ed.), Technomic Publishing Co. Inc, Lancaster, PA, USA, 63–93.

Lanier, O.L.; Christopher, K.G.; Macoon, R.M.; Yu, Y.; Sekar, P.; Chauhan, A. (**2020**). Commercialization challenges for drug eluting contact lenses. *Expert Opin. Drug Deliv.* 17(8), 1133–1149.

Lasowski, F.; Sheardown, H. (**2016**). Atropine and roscovitine release from model silicone hydrogels. *Optom. Vis. Sci.* 93(4), 404–411.

Lee, D.; Cho, S.; Park, H.S.; Kwon, I. (**2016**). Ocular drug delivery through pHEMA-hydrogel contact lenses co-loaded with lipophilic vitamins. *Sci. Rep.* 6, 34194.

USC UNIVERSIDADE DE SANTIAGO DE COMPOSTELA

Lee, D.; Lee, N.; Kwon, I. (**2018**). Efficient loading of ophthalmic drugs with poor loadability into contact lenses using functional comonomers. *Biomater. Sci.* 6(10), 2639–2646.

Li, C.; Abrahamson, M.; Kapoor, Y.; Chauhan, A. (**2007**). Timolol transport from microemulsions trapped in HEMA gels. *J. Colloid Interface Sci.* 315(1), 297–306.

Lim, L.; Lim, E.W.L. (**2020**). Therapeutic contact lenses in the treatment of corneal and ocular surface diseases—A Review. *Asia-Pac. J. Ophthalmol.* 9(6), 524–553.

Li, R.; Guan, X.; Lin, X.; Guan, P.; Zhang, X.; Rao, Z.; Du, L.; Zhao, J.; Rong, J.; Zhao, J. (**2020**). Poly(2-hydroxyethyl methacrylate)/β-cyclodextrin-hyaluronan contact lens with tear protein adsorption resistance and sustained drug delivery for ophthalmic diseases. *Acta Biomater.* 110, 105-118.

Li, Y.; Huang, C.; Yang, X.; Zhang, X. (**2020**). Ofloxacin laden microemulsion contact lens to treat conjunctivitis. *J. Biomater. Sci. Polym. Ed.* 31(12), 1566–1579.

Liu, D.E.; Dursch, T.J.; Taylor, N.O.; Chan, S.Y.; Bregante, D.T.; Radke, C.J. (**2016**). Diffusion of water-soluble sorptive drugs in HEMA/MAA hydrogels. *J. Control. Release.* 239, 242–248.

Loch, C.; Zakelj, S.; Kristl, A.; Nagel, S.; Guthoff, R.; Weitschies, W.; Seidlitz, A. (**2012**). Determination of permeability coefficients of ophthalmic drugs through different layers of porcine, rabbit and bovine eyes. *Eur. J. Pharm. Sci.* 47(1), 131-138.

USC UNIVERSIDADE DE SANTIAGO DE COMPOSTELA

Lu, C.; Yoganathan, R.B.; Kociolek, M.; Allen, C. (**2013**). Hydrogel containing silica shell cross-linked micelles for ocular drug delivery. *J. Pharm. Sci*. 102(2), 627–637.

Luke, M.C.; Kozak, D. (**2021**). Regulating generic ophthalmologic drug bioequivalence—envisioning accessibility for patients. *J. Ocul. Pharmacol. Ther.* 37(3), 157–161.

Mahomed, A.; Tighe, B.J. (**2019**). The design of contact lens based ocular drug delivery systems for single-day use: Part (I) Structural factors, surrogate ophthalmic dyes and passive diffusion studies. *J. Biomater. Appl.* 29(3), 341–353.

Mahomed, A.; Wolffsohn, J.S.; Tighe, B.J. (**2016**). Structural design of contact lens-based drug delivery systems; in vitro and in vivo studies of ocular triggering mechanisms. *Contact Lens Ant. Eye.* 39(2), 97–105.

Maki, K.L.; Ross, D.S. (**2014**). Exchange of tears under a contact lens is driven by distortions of the contact lens. *Integr. Comp. Biol.* 54(6), 1043–1050.

Malaekeh-Nikouei, B.; Atefeh Vahabzadeh, S.; Ahmad Mohajeri, S. (**2013**). Preparation of a molecularly imprinted soft contact lens as a new ocular drug delivery system for dorzolamide. *Current Drug Deliv.* 10(3), 279–285.

Malaekeh-Nikouei, B.; Ghaeni, F.A.; Motamedshariaty, V.S.; Mohajeri, S.A. (**2012**). Controlled release of prednisolone acetate from molecularly imprinted hydrogel contact lenses. *J. Appl. Polym. Sci.* 126, 387–394.

USC UNIVERSIDADE DE SANTIAGO DE COMPOSTELA

Malakooti, N.; Alexander, C.; Alvarez-Lorenzo, C. (**2015**). Imprinted contact lenses for sustained release of polymyxin B and related antimicrobial peptides. *J. Pharm. Sci.* 104(10), 3386–3394.

Maulvi, F.A.; Choksi, H.H.; Desai, A.R.; Patel, A.S.; Ranch, K.M.; Vyas, B.A.; Shah, D.O. (**2017b**). pH triggered controlled drug delivery from contact lenses: Addressing the challenges of drug leaching during sterilization and storage. *Colloids Surf. B: Biointerfaces*. 157, 72–82.

Maulvi, F.A.; Desai, A.R.; Choksi, H.H.; Patil, R.J.; Ranch, K.M.; Vyas, B.A.; Shah, D.O. (**2017a**). Effect of surfactant chain length on drug release kinetics from microemulsion-laden contact lenses. *Int. J. Pharm.* 524 (1-2), 193–204.

Maulvi, F.A.; Lakdawala, D.H.; Shaikh, A.A.; Desai, A.R.; Choksi, H.H.; Vaidya, R.J.; Ranch, K.M.; Koli, A.R.; Vyas, B.A.; Shah, D.O. (**2016**). In vitro and in vivo evaluation of novel implantation technology in hydrogel contact lenses for controlled drug delivery. *J. Control. Release.* 226, 47-56.

Maulvi, F.A.; Mangukiya, M.A.; Patel, P.A.; Vaidya, R.J.; Koli, A.R.; Ranch, K.M.; Shah, D.O. (**2016**). Extended release of ketotifen from silica shell nanoparticle-laden hydrogel contact lenses: in vitro and in vivo evaluation. *J. Mater. Sci. Mater. Med.* 27(6), 113.

Maulvi, F.A.; Parmar, R.J.; Desai, A.R.; Desai, D.M.; Shukla, M.R.; Ranch, K.M.; Shah, S.A.; Shah, D.O. (**2020**). Tailored gatifloxacin Pluronic® F-68-loaded contact lens: Addressing the issue of transmittance and swelling. *Int. J. Pharm.* 581, 119279.

Maulvi, F.A.; Patil, R.J.; Desai, A.R.; Shukla, M.R.; Vaidya, R.J.; Ranch, K.M.; Vyas, B.A.; Shah, S.A.; Shah, D.O. (**2019**). Effect of gold

USC UNIVERSIDADE DE SANTIAGO DE COMPOSTELA

nanoparticles on timolol uptake and its release kinetics from contact lenses: In vitro and in vivo evaluation. *Acta Biomater.* 86, 350-362.

Maulvi, F.A.; Soni, T.G.; Shah, D.O. (**2015**). Extended release of hyaluronic acid from hydrogel contact lenses for dry eye syndrome. *J. Biomater. Sci. Polym. Ed.* 26(15), 1035–1050.

Mealy, J.E.; Fedorchak, M.V.; Little, S.R. (**2014**). In vitro characterization of a controlled release ocular insert for delivery of brimonidine tartrate. *Acta Biomater.* 10(1), 87–93.

MediPrintTM Ophtalmics (**2022**). https://mediprintlens.com/glaucoma/ (accessed November 2021).

Mehta, P.; Al-Kinani, A.A.; Arshad, M.S.; Chang, M.-G.; Alany, R.G.; Ahmada, Z. (**2017b**). Development and characterisation of electrospun timolol maleate-loaded polymeric contact lens coatings containing various permeation enhancers. *Int. J. Pharm.* 532(1), 408–420.

Mehta, P.; Al-Kinani, A.A.; Haj-Ahmad, R.; Arshad, M.S.; Chang, M.W.; Alany, R.G.; Ahmad, Z. (**2017a**). Electrically atomised formulations of timolol maleate for direct and on-demand ocular lens coatings. *Eur. J. Pharm. Biopharm.* 119, 170-184.

Miller, P.E.; Eaton, J.S. (**2021**). Medical anti-glaucoma therapy: Beyond the drop. *Vet. Ophthalmol.* 24 (Suppl. 1), 2–15.

Mishima, S.; Gasset, A.; Klyce, S.D.; Baum, J.L. (**1996**). Determination of tear volume and tear flow. *Investig. Ophthalmol.* 5(3), 264–276.

Moya-Ortega, M.D.; Alvarez-Lorenzo, C.; Sigurdsson, H.H.; Concheiro, A.; Loftsson, T. (**2010**). γ-Cyclodextrin hydrogels and semi-interpenetrating networks for sustained delivery of dexamethasone. *Carbohydr. Polym.* 80(3), 900–907.

USC UNIVERSIDADE DE SANTIAGO DE COMPOSTELA

Mun, J.; Won Mok, J.; Jeong, S.; Cho, S.; Joo, C.; Hahn, S.K. (**2019**). Drug-eluting contact lens containing cyclosporine-loaded cholesterol-hyaluronate micelles for dry eye syndrome. *RSC Adv.* 9, 16578–16585.

Muntz, A.; Subbaraman, L.N.; Sorbara, L.; Jones, L. (**2015**). Tear exchange and contact lenses: A review. *Aust. J. Optom.* 8(1), 2–11.

Nasr, F.H.; Khoee, S.; Dehghan, M.M.; Chaleshtori, S.S.; Shafiee, A. (**2016**). Preparation and evaluation of contact lenses embedded with polycaprolactone-based nanoparticles for ocular drug delivery. *Biomacromolecules.* 17(2), 485–495.

Nichols, J.J.; King-Smith, P.E. (**2003**). Thickness of the pre- and post-contact lens tear film measured in vivo by interferometry. *Invest. Ophthalmol. Vis. Sci.* 44(1), 68–77.

Nguyen, D.; Hui, A.; Weeks, A.; Heynen, M.; Joyce, E.; Sheardown, H.; Jones, L. (**2012**). Release of ciprofloxacin-HCl and dexamethasone phosphate by hyaluronic acid containing silicone polymers. *Materials.* 5(4), 684–698.

Novack, G.D.; Barnett, M. (**2020**). Ocular drug delivery systems using contact lenses. *J. Ocul. Pharmacol. Ther.* 36, 595–601.

Olthoff, C.M.; Schouten, J.S.; van de Borne, B.W; Webers, C.A. (**2005**). Noncompliance with ocular hypotensive treatment in patients with glaucoma or ocular hypertension an evidence-based review. *Ophthalmology.* 112(6), 953–961.

Omranipour, H.M.; Tabassi, S.A.S.; Kowsari, R.; Rad, M.S.; Mohajeri, S.A. (**2015**). Brimonidine imprinted hydrogels and evaluation of their binding and releasing properties as new ocular drug delivery systems. *Current Drug Deliv.* 12(6), 717–725.

USC UNIVERSIDADE DE SANTIAGO DE COMPOSTELA

Oucif, A.; Haddadine, N.; Zakia, D.; Bouslah, N.; Benaboura, A.; Beyaz, K.; Guedouar, B.; El Shall, M.S. (**2022**). Poly (hydroxyethyl methacrylate-co-hydroxyethyl acrylate) soft contact lenses for acetazolamide release. *Polym. Bull.* 79, 1535-1554.

Pak, J.; Chen, Z.N.; Sun, K.; Przekwas, A.; Walenga, R.; Fan, J. (**2018**). Computational modeling of drug transport across the in vitro cornea. *Comput. Biol. Med*. 92, 139–146.

Paradiso, P.; Chu, V.; Santos, L.; Serro, A.P.; Colaço, R.; Saramago, B. (**2015**). Effect of plasma treatment on the performance of two drug-loaded hydrogel formulations for therapeutic contact lenses. *J. Biomed. Mater. Res. B Appl. Biomater.* 103, 1059–1068.

Paradiso, P.; Colaço, R.; Mata, J.L.G.; Krastev, R.; Saramago, B.; Serro, A.P. (**2017**). Drug release from liposome coated hydrogels for soft contact lenses: the blinking and temperature effect. *J. Biomed. Mater. Res. B Appl. Biomater.* 105(7), 1799–1807.

Paradiso, P.; Galante, R.; Santos, L.; Alves de Matos, A.P.; Colaço, R.; Serro, A.P.; Saramago, B. (**2014**). Comparison of two hydrogel formulations for drug release in ophthalmic lenses. *J. Biomed. Mater. Res. B Appl. Biomater.* 102(6), 1170–1180.

Paradiso, P.; Serro, A.P.; Saramago, B.; Colaço, R.; Chauhan, A. (**2016**). Controlled release of antibiotics from vitamin E-loaded silicone-hydrogel contact lenses. *J. Pharm. Sci.* 105(3), 1164–1172.

Peng, C.; Burke, M.T.; Chauhan, A. (**2012c**). Transport of topical anesthetics in vitamin E loaded silicone hydrogel contact lenses. *Langmuir.* 28(2), 1478–1487.

USC UNIVERSIDADE DE SANTIAGO DE COMPOSTELA

Peng, C.C.; Ben-Shlomo, A.; Mackay, E.O.; Plummer, C.E.; Chauhan, A. (**2012a**). Drug delivery by contact lens in spontaneously glaucomatous dogs. *Curr. Eye Res.* 37(3), 204–211.

Peng, C.C.; Burke, M.T.; Carbia, B.E.; Plummer, C.; Chauhan, A. (**2012b**). Extended drug delivery by contact lenses for glaucoma therapy. *J. Control. Release*. 162(1), 152–158.

Peng, C.; Chauhan, A. (**2011**). Extended cyclosporine delivery by silicone–hydrogel contact lenses. *J. Control. Release.* 154(3), 267–274.

Peng, C.; Kim, J.; Chauhan, A. (**2010**). Extended delivery of hydrophilic drugs from silicone-hydrogel contact lenses containing vitamin E diffusion barriers. *Biomaterials*. 31(14), 4032–4047.

Pereira-da-Mota, A.F.; Vivero-Lopez, M.; Topete, A.; Serro, A.P.; Concheiro, A.; Alvarez-Lorenzo, C. (**2021**). Atorvastatin-eluting contact lenses: effects of molecular imprinting and sterilization on drug loading and release. *Pharmaceutics.* 13, 606.

Phan, C.M.; Bajgrowicz, M.; Gao, H.; Subbaraman, L.N.; Jones, L.W. (**2016a**). Release of fluconazole from contact lenses using a novel in vitro eye model. *Optom. Vis. Sci.* 93(4), 387–394.

Phan, C.M.; Shukla, M.; Walther, H.; Heynen, M.; Suh, D.; Jones, L. (**2021**). Development of an in vitro blink model for ophthalmic drug delivery. *Pharmaceutics.* 13(3), 300.

Phan, C.; Subbaraman, L.; Liu, S.; Gu, F.; Jones, L. (**2014b**). In vitro uptake and release of natamycin Dex-b-PLA nanoparticles from model contact lens materials. *J. Biomater. Sci. Polym. Ed.* 25(1), 18–31.

Phan, C.; Subbaraman, L.N.; Jones, L. (**2014a**). In vitro drug release of natamycin from β-cyclodextrin and 2-hydroxypropyl-β-cyclodextrin-

USC UNIVERSIDADE DE SANTIAGO DE COMPOSTELA

functionalized contact lens materials. *J. Biomater. Sci. Polym. Ed.* 25(17), 1907–1919.

Phan, C.; Subbaraman, L.N.; Jones, L. (**2013**). In vitro uptake and release of natamycin from conventional and silicone hydrogel contact lens materials. *Eye Contact Lens.* 39(2), 162–168.

Phan, C.; Subbaraman, L.N.; Jones, L.W. (**2019b**). Uptake and release of polyvinyl alcohol from hydrogel daily disposable contact lenses. *Optom. Vis. Sci.* 96(3), 180–186.

Phan, C.M.; Walther, H.; Gao, H.; Rossy, J.; Subbaraman, L.N.; Jones, L. (**2016b**). Development of an in vitro ocular platform to test contact lenses. *J. Vis. Exp.* 110, e53907.

Phan, C.M.; Walther, H.; Qiao, H.; Shinde, R.; Jones, L. (**2019a**). Development of an eye model with a physiological blink mechanism. *Trans. Vis. Sci. Tech.* 8, 1.

Pijls, R.T.; Cruysberg, L.P.; Nuijts, R.M.; Dias, A.A.; Koole, L.H. (**2007a**). Capacity and tolerance of a new device for ocular drug delivery. *Int. J. Pharm.* 341(1-2), 152-61.

Pijls, R.T.; Lindemann, S.; Nuijts, R.M.M.A.; Daube, G.W.; Koole, L.H. (**2007b**). Pradofloxacin release from the OphthaCoil: a new device for sustained delivery of drugs to the eye. *J. Drug Del. Sci. Tech.* 17(1), 87–91.

Pimenta, A.F.R.; Ascenso, J.; Fernandes, J.C.S.; Colaço, R.; Serro, A.P.; Saramago, B. (**2016b**). Controlled drug release from hydrogels for contact lenses: Drug partitioning and diffusion. *Int. J. Pharm.* 515(1-2), 467-475.

USC UNIVERSIDADE DE SANTIAGO DE COMPOSTELA

Pimenta, A.F.R.; Serro, A.P.; Paradiso, P.; Saramago, B.; Colaço, R. (**2016c**). Diffusion-based design of multi-layered ophthalmic lenses for controlled drug release. *PLoS One.* 11(12), e0167728.

Pimenta, A.F.; Valente, A.; Pereira, J.M.; Pereira, J.C.; Filipe, H.P.; Mata, J.L.; Colaço, R.; Saramago, B.; Serro, A.P. (**2016a**). Simulation of the hydrodynamic conditions of the eye to better reproduce the drug release from hydrogel contact lenses: experiments and modeling. *Drug Deliv. Transl. Res.* 6(6), 755-762.

Postic, I.; Sheardown, H. (**2019**). Altering the release of tobramycin by incorporating poly(ethylene glycol) into model silicone hydrogel contact lens materials. *Aust. J. Biol. Sci.* 30(13), 1115–1141.

Primachenko, O.N.; Marinenko, E.A.; Ivanchev, S.S. (**2014**). Polymer hydrogels with the memory effect for immobilization of drugs. *Polymer Sci. Ser. B.* 56, 863–870.

Pucker, A.D.; Tichenor, A.A. (**2020**). A review of contact lens dropout. *Clin. Optom.* 12, 85–94.

Pulliero, A.; Profumo, A.; Izzotti, A.; Saccà, S.C. (**2020**). Release of Aloe vera extracts from therapeutic lenses. *Appl. Sci.* 10, 9055.

Qin, G.; Zhu, Z.; Li, S.; McDermott, A.M.; Cai, C. (**2017**). Development of ciprofloxacin loaded contact lenses using fluorous chemistry. *Biomaterials.* 124, 55–64.

Rad, M.S.; Mohajeri, S.A. (**2017**). Extended ciprofloxacin release using vitamin E diffusion barrier from commercial silicone-based soft contact lenses. *Eye Contact Lens.* 43(2), 103–109.

USC UNIVERSIDADE DE SANTIAGO DE COMPOSTELA

Rad, M.S.; Mohajerib, S.A. (**2016b**). Simultaneously load and extended release of betamethasone and ciprofloxacin from vitamin E-loaded silicone-based soft contact lenses. *Curr. Eye Res.* 41(9), 1185–1191.

Rad, M.S.; Tabassi, S.A.S.; Moghadam, M.H.; Mohajeri, S.A. (**2016a**). Controlled release of betamethasone from vitamin E-loaded silicone-based soft contact lenses. *Pharm. Dev. Technol*. 21(7), 894–899.

Ran, W.; Ma, H.; Li, M. (**2020**). In vitro and in vivo studies of polyvinyl pyrrolidone-coated sparfloxacin-loaded ring contact lens to treat conjunctivitis. *J. Pharm. Sci.* 109(6), 1951–1957.

Review of Cornea & Contact Lenses. (**2021**). Material Gains: 50 Years of the Soft Contact Lens; Material Gains: 50 Years of the Soft Contact Lens; https://www.reviewofcontactlenses.com/article/material-gains-50-years-of-the-soft-contact-lens (accessed November 2021).

Ribeiro, A.; Veiga, F.; Santos, D.; Torres-Labandeira, J.J.; Concheiro, A.; Alvarez-Lorenzo, C. (**2011b**). Bioinspired imprinted pHEMA-hydrogels for ocular delivery of carbonicanhydrase inhibitor drugs. *Biomacromolecules.* 12(3), 701–709.

Ribeiro, A.; Veiga, F.; Santos, D.; Torres-Labandeira, J.J.; Concheiro, A.; Alvarez-Lorenzo, C. (**2012**). Hydrophilic acrylic hydrogels with built-in or pendant cyclodextrins for delivery of anti-glaucoma drugs. *Carbohydr. Polym.* 88, 977–985.

Ribeiro, A.; Veiga, F.; Santos, D.; Torres-Labandeira, J.J.; Concheiro, A.; Alvarez-Lorenzo, C. (**2011a**). Receptor-based biomimetic NVP/DMA contact lenses for loading/ eluting carbonic anhydrase inhibitors. *J. Membr. Sci.* 383, 60–69.

USC UNIVERSIDADE DE SANTIAGO DE COMPOSTELA

Ross, A.E; Bengani, L.C.; Tulsan, R.; Maidana, D.E.; Salvador-Culla, B.; Kobashi, H.; Kolovou, P.E.; Zhai, H.; Taghizadeh, K.; Kuang, L.; Mehta, M.; Vavvas, D.G.; Kohane, D.S.; Ciolino, J.B. (**2019**). Topical sustained drug delivery to the retina with a drug eluting contact lens. *Biomaterials*. 217, 119285.

Saettone, M.F.; Salminen, L. (**1995**). Ocular inserts for topical delivery. *Adv. Drug Deliv. Rev.* 16(1), 95–106.

Sato, T.; Uchida, R.; Tanigawa, H.; Uno, K.; Murakami, A. (**2005**). Application of polymer gels containing side-chain phosphate groups to drug-delivery contact lenses. *J. Appl. Polym. Sci.* 98, 731–735.

Savariraj, A.D.; Salih, A.; Alam, F.; Elsherif, M.; AlQattan, B.; Khan, A.A.; Yetisen, A.K.; Butt, H. (**2021**). Ophthalmic sensors and drug delivery. *ACS Sensors.* 6(6), 2046–2076.

Schultz, C.; Breaux, J.; Schentag, J.; Morck, D. (**2011**). Drug delivery to the posterior segment of the eye through hydrogel contact lenses. *Clin. Exp. Optom.* 94(2), 212–218.

Schultz, C.L.; Morck, D.W. (**2010**). Contact lenses as a drug delivery device for epidermal growth factor in the treatment of ocular wounds. *Clin. Exp. Optom.* 93(2), 61–65.

Schultz, C.L.; Poling, T.R.; Mint, J.O. (**2009**). A medical device/drug delivery system for treatment of glaucoma. *Clin. Exp. Optom.* 92(4), 343–348.

Sekar, P.; Chauhan, A. (**2019**). Effect of vitamin-E integration on delivery of prostaglandin analogs from therapeutic lenses. *J. Colloid Interface Sci.* 539, 457–467.

USC UNIVERSIDADE DE SANTIAGO DE COMPOSTELA

Shikamura, Y.; Yamazaki, Y.; Matsunaga, T.; Sato, T.; Ohtori, A.; Tojo, K. (**2016**). Hydrogel ring for topical drug delivery to the ocular posterior segment. *Curr. Eye Res.* 41(5), 653–661.

Shin, H.; Seo, H.; Chung, W.G.; Joo, B.G.; Jang, J.; Park, J.U. (**2021**). Recent progress on wearable point-of-care devices for ocular systems. *Lab Chip.* 21(7), 1269–1286.

Shi, Y.; Lv, H.; Fu, Y.; Lu, Q.; Zhong, J.; Ma, D.; Huang, Y.; Xu, W. (**2013**). Preparation and characterization of a hydrogel carrier to deliver gatifloxacin and its application as a therapeutic contact lens for bacterial keratitis therapy. *Biomed. Mater.* 8(5), 055007.

Silva, D.; de Sousa, H.C.; Gil, M.H.; Santos, L.F.; Moutinho, G.M.; Serro, A.P.; Saramago, B. (**2018**). Antibacterial layer-by-layer coatings to control drug release from soft contact lenses material. *Int. J. Pharm.* 553(1-2), 186–200.

Silva, D.; De Sousa, H.C.; Gil, M.H.; Santos, L.F.; Amaral, R.A.; Saraiva, J.A.; Salema-Oom, M.; Alvarez-Lorenzo, C.; Serro, A.P.; Saramago, B. (**2021**). Imprinted hydrogels with LbL coating for dual drug release from soft contact lenses materials. *Mater. Sci. Eng. C.* 120, 111687.

Silva, D.; De Sousa, H.C.; Gil, M.H.; Santos, L.F.; Moutinho, G.M; Salema-Oom, M.; Alvarez-Lorenzo, C.; Serro, A.P.; Saramago, B. (**2020**). Diclofenac sustained release from sterilised soft contact lens materials using an optimised layer-by-layer coating. *Int. J. Pharm.* 585, 119506.

Silva, D.; Pinto, L.F.V.; Bozukova, D.; Santos, L.F.; Serro, A.P.; Saramago, B. (**2016**). Chitosan/alginatebased multilayers to control

USC UNIVERSIDADE DE SANTIAGO DE COMPOSTELA

drug release from ophthalmic lens. *Colloids Surf. B: Biointerfaces.* 147, 81–89.

Singh, B.; Chauhan, N.; Sharma, V. (**2011**). Design of molecular imprinted hydrogels for controlled release of cisplatin: evaluation of network density of hydrogels. *Ind. Eng. Chem. Res.* 50, 13742–13751.

Soluri, A.; Hui, A.; Jones, L. (**2012**). Delivery of ketotifen fumarate by commercial contact lens materials. *Optom. Vis. Sci.* 89(8), 1140–1149.

Tieppo, A.; Boggs, A.C.; Pourjavad, P.; Byrne, M.E. (**2014**). Analysis of release kinetics of ocular therapeutics from drug releasing contact lenses: Best methods and practices to advance the field. *Contact Lens Ant. Eye.* 37(4), 305–313.

Tieppo, A.; Pate, K.M.; Byrne, M.E. (**2012a**). In vitro controlled release of an anti-inflammatory from daily disposable therapeutic contact lenses under physiological ocular tear flow. *Eur. J. Pharm. Biopharm*. 81(1), 170–177.

Tieppo, A.; White, C.J.; Paine, A.C.; Voyles, M.L.; McBride, M.K.; Byrne, M.E. (**2012b**). Sustained in vivo release from imprinted therapeutic contact lenses. *J. Control. Release.* 157(3), 391-397.

Tipnis, N.P.; Burgess, D.J. (**2018**). Sterilization of implantable polymer-based medical devices: A review. *Int. J. Pharm.* 544(2), 455–460.

Toffoletto, N.; Saramago, B.; Serro, A.P. (**2021**). Therapeutic ophthalmic lenses: a review. *Pharmaceutics.* 13(1), 36.

Topete, A.; Oliveira, A.S.; Fernandes, A.; Nunes, T.G.; Serro, A.P.; Saramago, B. (**2018**). Improving sustained drug delivery from

USC UNIVERSIDADE DE SANTIAGO DE COMPOSTELA

ophthalmic lens materials through the control of temperature and time of loading. *Eur. J. Pharm. Sci*. 117, 107–117.

Torres-Luna, C.; Hu, N.; Fan, X.; Domszy, R.; Yang, J.; Briber, R.M.; Yang, A. (**2020**). Extended delivery of cationic drugs from contact lenses loaded with unsaturated fatty acids. *Eur. J. Pharm. Biopharm.* 155, 1–11.

Torres-Luna, C.; Hu, N.; Koolivand, A.; Fan, X.; Zhu, Y.; Domszy, R.; Yang, J.; Yang, A.; Wang, N.S. (**2019a**). Effect of a cationic surfactant on microemulsion globules and drug release from hydrogel contact lenses. *Pharmaceutics.* 11, 262.

Torres-Luna, C.; Hu, N.; Tammareddy, T.; Domszy, R.; Yang, J.; Wang, N.S.; Yang, A. (**2019c**). Extended delivery of non-steroidal anti-inflammatory drugs through contact lenses loaded with Vitamin E and cationic surfactants. *Contact Lens Ant. Eye.* 42(5), 546–552.

Torres-Luna, C.; Koolivand, A.; Fan, X.; Agrawal, N.R.; Hu, N.; Zhu, Y.; Domszy, R.; Briber, R.M.; Wang, N.S.; Yang, A. (**2019b**). Formation of Drug-Participating Catanionic Aggregates for Extended Delivery of Non-Steroidal Anti-Inflammatory Drugs from Contact Lenses. *Biomolecules.* 9(10), 593.

Ubani-Ukomaa, U.; Gibsonb, D.; Schultz, G.; Silva, B.O.; Chauhan, A. (**2019**). Evaluating the potential of drug eluting contact lenses for treatment of bacterial keratitis using an ex vivo corneal model. *Int. J. Pharm.* 565, 499–508.

Uchida, R.; Sato, T.; Tanigawa, H.; Uno, K. (**2003**). Azulene incorporation and release by hydrogel containing methacrylamide propyltrimenthylammonium chloride, and its application to soft contact lens. *J. Control. Release.* 92(3), 259–264.

USC UNIVERSIDADE DE SANTIAGO DE COMPOSTELA

Varela-Garcia, A.; Concheiro, A.; Alvarez-Lorenzo, C. (**2020b**). Cytosine-functionalized bioinspired hydrogels for ocular delivery of antioxidant transferulic acid. *Biomater. Sci.* 8, 1171–1180.

Varela-Garcia, A.; Gomez-Amoza, J.L.; Concheiro, A.; Alvarez-Lorenzo, C. (**2020a**). Imprinted contact lenses for ocular administration of antiviral drugs. *Polymers.* 12(9), 2026.

Venkatesh, S.; Sizemore, S.P.; Byrne, M.E. (**2007**). Biomimetic hydrogels for enhanced loading and extended release of ocular therapeutics. *Biomaterials.* 28(4), 717–724.

Wax, M.; Molinoff, P.B. (**1987**). Distribution and properties of beta-adrenergic receptors in human iris-ciliary body. *Invest. Ophthalmol. Vis. Sci.* 28(3), 420–430.

Weeks, A.; Subbaraman, L.N.; Jones, L.; Sheardown, H. (**2013**). Physical entrapment of hyaluronic acid during synthesis results in extended release from model hydrogel and silicone hydrogel contact lens materials. *Eye Contact Lens.* 39(2), 179–185.

Wei, N.; Dang, H.; Huang, C.; Sheng, Y. (**2021**). Timolol loaded microemulsion laden silicone contact lens to manage glaucoma: in vitro and in vivo studies. *J. Dispers. Sci. Technol.* 42, 742–750.

Wei, N.; Xu, X.; Huang, C.; Cao, L. (**2020a**). Hyaluronic acid-Pluronic®F127-laden soft contact lenses for corneal epithelial healing: in vitro and in vivo studies. *AAPS PharmSciTech.* 21(5), 162.

Wei, Y.; Hu, Y.; Shen, X.; Zhang, X.; Guan, J.; Mao, S. (**2020b**). Design of circular-ring film embedded contact lens for improved compatibility and sustained ocular drug delivery. *Eur. J. Pharm. Biopharm.* 157, 28–37.

USC UNIVERSIDADE DE SANTIAGO DE COMPOSTELA

White, C.J.; DiPasquale, S.A.; Byrne, M.E. (**2016**). Controlled release of multiple therapeutics from silicone hydrogel contact lenses. *Optom. Vis. Sci.* 93(4), 377–386.

White, C.J.; McBride, M.K.; Pate, K.M.; Tieppo, A.; Byrne, M.E. (**2011**). Extended release of high molecular weight hydroxypropyl methylcellulose from molecularly imprinted, extended wear silicone hydrogel contact lenses. *Biomaterials.* 32(24), 5698–5705.

Wichterle, O.; Lim, D. (**1965**). Cross-linked hydrophilic polymers and articles made therefrom. Patent US3220960.

Wichterle, O.; Lim, D. (**1960**). Hydrophilic gels for biological use. *Nature.* 185, 117–118.

Wichterle O. (**1961**). U.S. Patents. 3,660,545; 3,408,429; 3,496,254; 3,499,862.

Wuchte, L.D.; DiPasquale, S.A.; Byrne, M.E. (**2021**). In vivo drug delivery via contact lenses: The current state of the field from origins to present. *J. Drug Deliv. Sci. Tech.* 63, 102413.

Wu, C.; Or, P.W.; Chong, J.I.T.; Pathirage Don, I.K.K.; Lee, C.H.C.; Wu, K.; Yu, M.; Lam, D.C.C.; Yang, Y. (**2021**). Extended Delivery of Pirfenidone with Novel, Soft Contact Lenses In Vitro and In Vivo. *J. Ocul. Pharmacol. Ther.* 37(2), 75-83.

Xu, B.; Liu, T. (**2020**). Travoprost loaded microemulsion soaked contact lenses: Improved drug uptake, release kinetics and physical properties. *J. Drug Deliv. Sci. Tech.* 57, 101792.

Xue, Y.; Zhang, W.; Lei, Y.; Dang, M. (**2020**). Novel polyvinyl pyrrolidone-loaded olopatadine HCl-laden doughnut contact lens to treat allergic conjunctivitis. *J. Pharm. Sci.* 109 (5), 1714–1724.

USC UNIVERSIDADE DE SANTIAGO DE COMPOSTELA

Xu, J.; Ge, Y.; Bu, R.; Zhang, A.; Feng, S.; Wang, J.; Gou, J.; Yin, T.; He, H.; Zhang, Y.; Tang, X. (**2019**). Co-delivery of latanoprost and timolol from micelles-laden contact lenses for the treatment of glaucoma. *J. Control. Release.* 305, 18–28.

Xu, J.; Li, X.; Sun, F. (**2011**). In vitro and in vivo evaluation of ketotifen fumarate-loaded silicone hydrogel contact lenses for ocular drug delivery. *Drug Deliv.* 18(2), 150–158.

Xu, J.; Li, X.; Sun, F. (**2010b**). Cyclodextrin-containing hydrogels for contact lenses as a platform for drug incorporation and release. *Acta Biomater*. 6(2), 486–493.

Xu, J.; Li, X.; Sun, F. (**2010a**). Preparation and evaluation of a contact lens vehicle for puerarin delivery. *J. Biomater. Sci. Polym. Ed.* 21(3), 271–288.

Xu, W.; Jiao, W.; Li, S.; Tao, X.; Mu, G. (**2019**). Bimatoprost loaded microemulsion laden contact lens to treat glaucoma. *J. Drug Deliv. Sci. Technol.* 54, 101330.

Yamazaki, Y.; Matsunaga, T.; Syohji, K.; Arakawa, T.; Sato, T. (**2013**). Effect of anionic/ siloxy groups on the release of ofloxacin from soft contact lenses. *J. Appl. Polym. Sci.* 127, 5022–5027.

Yañez, F.; Chauhan, A.; Concheiro, A.; Alvarez-Lorenzo, C. (**2011b**). Timolol-imprinted soft contact lenses: influence of the template: functional monomer ratio and the hydrogel thickness. *J. Appl. Polym. Sci.* 122, 1333–1340.

Yañez, F.; Concheiro, A.; Alvarez-Lorenzo, C. (**2008**). Macromolecule release and smoothness of semi-interpenetrating PVP–pHEMA

USC UNIVERSIDADE DE SANTIAGO DE COMPOSTELA

networks for comfortable soft contact lenses. *Eur. J. Pharm. Biopharm.* 69(3), 1094–1103.

Yañez, F.; Martikainen, L.; Braga, M.E.M.; Alvarez-Lorenzo, C.; Concheiro, A.; Duarte, C.M.M.; Gil, M.H.; de Sousa, H.C. (**2011a**). Supercritical fluid-assisted preparation of imprinted contact lenses for drug delivery. *Acta Biomater.* 7(3), 1019–1030.

Yan, F.; Liu, Y.; Han, S.; Zhao, Q.; Liu, N. (**2020**). Bimatoprost imprinted silicone contact lens to treat glaucoma. *AAPS PharmSciTech.* 21(2), 63.

Yang, M.; Yang, Y.; Lei, M.; Ye, C.; Zhao, C.; Xu, J.; Wu, K.; Yu, M. (**2016**). Experimental studies on soft contact lenses for controlled ocular delivery of pirfenidone: in vitro and in vivo. *Drug Deliv.* 23(9), 3538–3543.

Yigit, E.A.; Ercal, N. (**2013**). Release of N-acetylcysteine and N-acetylcysteine amide from contact lenses. *Eye Contact Lens.* 39(5), 335–340.

Yokozaki, Y.; Sakabe, J.; Shimoyama, Y. (**2015**). Enhanced impregnation of hydrogel contact lenses with salicylic acid by addition of water in supercritical carbon dioxide. *Chem. Eng. Res. Design*. 104, 203–207.

Yokozaki, Y.; Shimoyama, Y. (**2018**). Loading of vitamin E into silicone hydrogel by supercritical carbon dioxide impregnation toward controlled release of timolol maleate, *J. Supercrit. Fluids.* 131, 11–18.

Zaki, M.; Pardo, J.; Carracedo, G. (**2019**). A review of international medical device regulations: Contact lenses and lens care solutions. *Contact Lens Ant. Eye.* 42(2), 136–146.

USC UNIVERSIDADE DE SANTIAGO DE COMPOSTELA

Zhang, T.; Zhu, T.; Wang, F.; Peng, L.; Lai, M. (**2020**). Ketotifen loaded solid lipid nanoparticles laden contact lens to manage allergic conjunctivitis. *J. Drug Deliv. Sci. Technol*. 60, 101949.

Zhang, W.; Zu, D.; Chen, J.; Peng, J.; Liu, Y.; Zhang, H.; Li, S.; Pan, W. (**2014**). Bovine serum albumin–meloxicam nanoaggregates laden contact lenses for ophthalmic drug delivery in treatment of postcataract endophthalmitis. *Int. J. Pharm.* 475(1-2), 25–34.

Zhou, S.; Hunt, K.M.; Grewal, A.S.; Brothers, K.M.; Dhaliwal, D.K.; Shanks, R.M.Q. (**2018**). Release of moxifloxacin from corneal collagen shields. *Eye Contact Lens.* 44(Suppl 2), S143–S147.

Zhu, Q.; Cheng, H.; Huo, Y.; Mao, S. (**2018a**). Sustained ophthalmic delivery of highly soluble drug using pH-triggered inner layer-embedded contact lens. *Int. J. Pharm.* 544(1), 100–111.

Zhu, Q.; Liu, C.; Sun, Z.; Liang, N.; Mao, S. (**2018b**). Inner layer-embedded contact lenses for pH-triggered controlled ocular drug delivery. *Eur. J. Pharm. Biopharm.* 128, 220–229.

Zhu, Q.; Mao, S. (**2019**). Enhanced drug loading efficiency of contact lenses via saltinduced modulation. *Asian J. Pharm. Sci.* 14(2), 204–215.

Zhu, Q.; Wei, Y.; Li, C.; Mao, S. (**2018c**). Inner layer-embedded contact lenses for ion-triggered controlled drug delivery. *Mater. Sci. Eng. C.* 93, 36–48.

Zhu, Y.; Sheng, Y. (**2020**). Sustained delivery of epalrestat to the retina using PEGylated solid lipid nanoparticles laden contact lens. *Int. J. Pharm.* 587, 119688.

USC UNIVERSIDADE DE SANTIAGO DE COMPOSTELA

AIMS

USC
UNIVERSIDADE
DE SANTIAGO
DE COMPOSTELA

USC
UNIVERSIDADE
DE SANTIAGO
DE COMPOSTELA

2. AIMS

Efficient ocular drug delivery for the treatment of various anterior and posterior eye diseases is still a challenging task. Considering the complexity and particularity of the anatomy of the eye, the design of successful ophthalmic pharmaceutical formulations can be quite demanding as the static and dynamic barriers of the eye restrict drug delivery into the target site.

Contact lenses (CLs) are being positioned as advantageous platforms for the sustained release of ophthalmic drugs, by improving drug bioavailability in the eye, minimizing the systemic absorption and possible side effects, avoiding frequent instillation which might compromise patient compliance. However, most commercially available CL materials lack affinity for ophthalmic drugs. The amount of drug loaded by these materials is very low and if there are no interactions or binding of the drug to the CL network, then the drugs are released very rapidly. Strategies to address poor loading and limited control of drug release have been widely explored and include copolymerization with functional monomers. Bioinspired strategies to create artificial receptors for the drug inside the CL network by mimicking the human natural binding site of the drug were used in the present Thesis.

USC UNIVERSIDADE DE SANTIAGO DE COMPOSTELA

Additionally, the difficulties to achieve biorelevant ways of evaluating *in vitro* drug release from CLs and the feasibility of establishing *in vitro-in vivo* correlations (IVIVC) to predict *in vivo* performance have been highlighted in the introduction.

The main objective of the present PhD Thesis was to design and develop soft CLs applying biomimetic strategies suitable for the loading and release of therapeutic amounts of drugs useful for the treatment of ocular diseases related with diabetes. The main design criterion was to obtain CLs that show high affinity for the drugs of interest and still preserve the properties required for any contact lens, mainly in terms of ocular tolerance, light transmission, and mechanical properties.

According to this general aim, four specific aims were identified and developed as follows.

1. To design and prepare bioinspired hydrogel contact lenses with affinity for atorvastatin

Statins are widely used orally as first line treatment of hypercholesterolemia and reduction of cardiovascular disease risks by inhibiting 3-hydroxy-3-methyl-glutaryl coenzyme A (HMG-CoA) reductase. Additionally, a better understanding of the metabolic pathways on which they can act has revealed their pleiotropic capacity (e.g., anti-inflammatory, neuroprotective and antiproliferative properties). Prolonged oral administration of statins contributes to beneficial effects on the treatment of a variety of eye conditions including dry eye, diabetic retinopathy, macular degeneration, glaucoma, among others.

Atorvastatin calcium is a synthetic statin with relatively moderate lipophilicity, which may be able to penetrate the ocular structures if

USC UNIVERSIDADE DE SANTIAGO DE COMPOSTELA

topically applied. Preliminary studies indicate that atorvastatin ophthalmic solutions are well tolerated in prolonged treatment of dry eye and blepharitis. The efficacy and safety of its use for the treatment of ocular pathologies could be improved by formulating statins as forms of ocular topical administration that allow sufficiently high concentrations to be reached in the structures of the eye, avoiding systemic effects.

This part of the Thesis relies on the hypothesis that the incorporation of functional monomers in the CL network that can mimic the active site of HMG-CoA reductase might exhibit enhanced affinity for statins. Taking into account the functionalities of the amino acids involved in the binding site of HMG–CoA reductase, ethylene glycol phenyl ether methacrylate (EGPEM), 2-aminoethyl methacrylate hydrochloride (AEMA), and N-(3-aminopropyl) methacrylamide hydrochloride (APMA) were chosen as functional monomers after a first screening of the interaction with atorvastatin using computational modeling.

Several sets of hydrogels were prepared varying the contents of AEMA, EGPEM and APMA. Some hydrogels were synthetized in the presence of atorvastatin to verify if the drug molecules could contribute to a better arrangement of the monomers for a more efficient formation of ad hoc artificial receptors. The hydrogels were then characterized in terms of suitability to be used as CLs (solvent uptake, light transmission, mechanical properties, biocompatibility) and capability to load and sustain the release of atorvastatin in simulated lachrymal fluid. The most promising hydrogels were evaluated regarding cytocompatibility with Balb/3T3 fibroblasts, ocular tolerance, and *ex vivo* accumulation/permeability of atorvastatin through the porcine cornea and sclera tissues.

USC UNIVERSIDADE DE SANTIAGO DE COMPOSTELA

Since sterilization is a mandatory step in conditioning of contact lenses, one specific aim of this step was to elucidate the effects that steam heat, high hydrostatic pressure and gamma radiation sterilization techniques may have on both the drug and the CLs. The sterilization procedures were implemented during a research secondment at Centro de Química Estrutural, Departamento de Engenharia Química, Instituto Superior Técnico, Lisbon in collaboration with Prof. Ana Paula Serro.

2. To optimize HMG-CoA bioinspired hydrogels to deliver pravastatin

CLs soaked in atorvastatin calcium solution demonstrated improved drug accumulation in cornea and sclera, but the drug did not penetrate further probably because its large molecular weight and hydrophobicity. Thus, the aim of this part of the Thesis was to incorporate a smaller and hydrophilic statin, like pravastatin sodium, in the former prepared APMA/ EGPEM hydrogels to improve drug ocular permeability.

To carry out this work, successfully designed APMA/ EGPEM hydrogels were loaded with pravastatin and characterized in terms of solvent uptake, light transmission, mechanical properties as well as drug release profiles. Loaded-hydrogels stability against steam heat and high hydrostatic pressure sterilization was also monitored. Preliminary screening of cytocompatibility and ocular tolerance was carried out with Balb/3T3 fibroblasts and HET-CAM (Hen's Egg Test – Chorioallantoic Membrane) assay. Pravastatin permeability was assessed *ex vivo* using porcine cornea and sclera. Finally, the anti-inflammatory capacity of the loaded-hydrogels was evaluated.

USC UNIVERSIDADE DE SANTIAGO DE COMPOSTELA

After *in vitro*, *in ovo*, in cell and e*x vivo* tests were fulfilled, an *in vivo* study was planned following the 3R's principles. The aims of the *in vivo* study were (i) to elucidate the advantages of using pravastatin-loaded CLs compared to eye drops in terms of drug permanence in the tear fluid and biodistribution in the eye tissues, and (ii) identify which *in vitro* release conditions may provide *in vitro-in vivo* correlations (IVIVC). *In vivo* experiments were performed in collaboration with Prof. Gonzalo Carracedo at Ocupharm, University Complutense of Madrid. The protocols were approved by the Committee for Animal Experimentation of the University Complutense of Madrid.

3. To predict the *in vivo* behaviour of medicated contact lenses using an *in vitro* drug release eye blink model

Most *in vitro* studies to measure drug release from CLs involve a fixed volume vial model with no standardized protocols. There is no standardized guideline for performing *in vitro* assays, nor is there information on the extent to which *in vitro* results can be used to predict *in vivo* results. This means that *in vivo* testing in animal models and preclinical studies in humans are still required, even to evaluate early-stage drug-contact lens combination products, making development very costly in terms of time and resources.

In recent years, researchers have explored *in vitro* devices that better simulate the ocular environment parameters such as tear flow rate, tear volume and thickness, air exposure, and eyelid blinking frequency.

The aim of this step of the Thesis was to analyze the release profiles of drug-loaded contact lenses in a 3D printed *in vitro* eye blink model

USC UNIVERSIDADE DE SANTIAGO DE COMPOSTELA

and compare the results obtained with the release in a vial and the drug levels in the tear fluid recorded *in vivo* in animal models. The 3D printed eye model used was developed by Professor Lyndon Jones and Dr. Chau Minh-Phan at CORE (Centre of Ocular Research and Education), University of Waterloo. The model consists of an eyeball made of resin that simulates the ocular surface of the eye and a polyvinyl alcohol eyelid that slides over the eyeball or over fitted contact lenses, spreading the tear solution (supplied through a tube that is attached to the eyelid support). The output solution is collected in the collection unit located below the eyeball.

To validate the 3D printed *in vitro* eye blink model, CLs were loaded with two drugs, pravastatin and resveratrol, with different physicochemical properties. *In vitro* release in the 3D eye blink model was tested at two different tears fluid flow rates (5 and 10 μL/min of fluid) and a blink speed of 1 blink/10 s. Correlations between release profiles in the *in vitro* 3D printed eye model and *in vivo* levels in tear fluid (IVIVC) were attempted. 3D printed eye model experiments were carried out in collaboration with Prof. Lyndon Jones and Dr. Chau Minh-Phan at CORE (Centre for Ocular Research & Education), University of Waterloo during a research secondment.

4. To use melanin to enhance the affinity of CLs for specific drugs and provide them with photothermal responsiveness

Melanin is a natural pigment present in microorganisms, animals, and plants and has a variety of functionalities, including pigmentation, scavenging radicals, protection against radiation, and thermal regulation. Melanin at the ocular level (eumelanin) acts as a chemical binding reservoir by retaining drugs within the pigmented cells and

USC UNIVERSIDADE DE SANTIAGO DE COMPOSTELA

influencing their biodistribution. In addition, melanin has an important characteristic of converting absorbed light into heat. The rapid and local increase in temperature through melanin has been shown to be a promising method to kill bacteria without the risk of bacterial resistance or side effects.

On the last chapter of the Thesis, melanin was incorporated into contact lenses with the double aim of (i) evaluating an alternative procedure of incorporating drugs into contact lenses through drug-melanin affinity, and (ii) endowing contact lenses with photothermal capacity to increase temperature in localized areas. The work was focused on the incorporation of ciprofloxacin and the possible use of antimicrobial therapy combined with photothermal therapy in the treatment of bacterial infections associated with the use of contact lenses in diabetic patients.

USC UNIVERSIDADE DE SANTIAGO DE COMPOSTELA

USC
UNIVERSIDADE
DE SANTIAGO
DE COMPOSTELA

Chapter 3

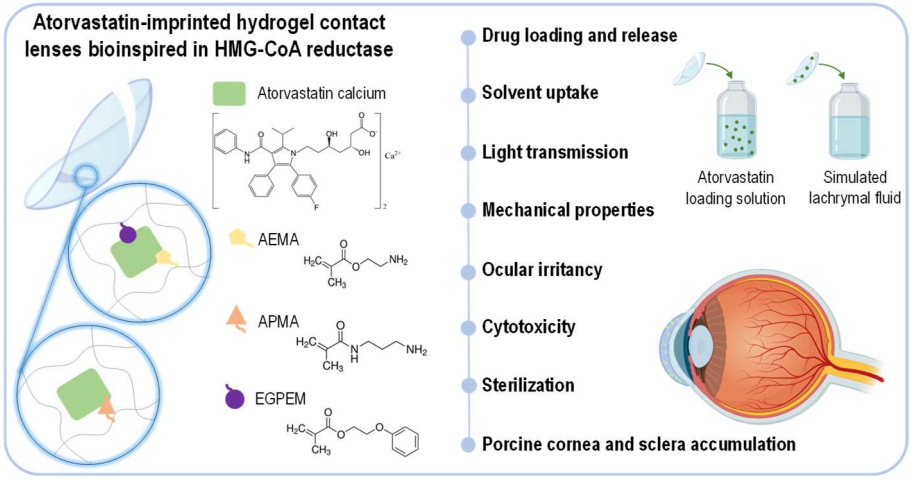

The work described in this chapter was published in **Atorvastatin-eluting contact lenses: effects of molecular imprinting and sterilization on drug loading and release**, *Pharmaceutics* 13, 606, 2021, authored by:

Ana F. Pereira-da-Mota[a], María Vivero-Lopez[a], Ana Topete[b], Ana Paula Serro[b], Angel Concheiro[a] and Carmen Alvarez-Lorenzo[a]

[a]Departamento de Farmacología, Farmacia y Tecnología Farmacéutica, I+D Farma (GI-1645), Facultad de Farmacia and Health Research Institute of Santiago de Compostela (IDIS), Universidade de Santiago de Compostela, 15782 Santiago de Compostela, Spain.

[b]Centro de Química Estrutural, Departamento de Engenharia Química, Instituto Superior Técnico, Universidade de Lisboa, Av. Rovisco Pais, 1049-001 Lisbon, Portugal

USC UNIVERSIDADE DE SANTIAGO DE COMPOSTELA

USC
UNIVERSIDADE
DE SANTIAGO
DE COMPOSTELA

3. ATORVASTATIN-ELUTING CONTACT LENSES: EFFECTS OF MOLECULAR IMPRINTING AND STERILIZATION ON DRUG LOADING AND RELEASE

3.1 INTRODUCTION

Statins, 3-hydroxy-3-methyl-glutaryl coenzyme A (HMG–CoA) reductase inhibitors, are a class of lipid-lowering drugs widely prescribed for regulation of cholesterol levels and notably contributing to the prevention of cardiovascular diseases [Bielecka-Dabrowa et al., 2019]. They act on a key step of the metabolic pathway for the biosynthesis of intracellular cholesterol, i.e., the mevalonate pathway [Sirtori, 2014]. In addition to lowering cholesterol, statins are recognized to have pleiotropic effects, which are shown as anti-inflammatory, antiproliferative, neuroprotective activities, etc. [Bedi et al., 2016].

Although there are not commercially available ophthalmic formulations of statins, oral administration has been associated with beneficial effects on eye conditions. With respect to ocular surface inflammation, preliminary data suggest that oral administration of statins may increase the regenerative quality of corneal repair promoting corneal wound healing [Gordon et al., 2016]. Nevertheless,

USC UNIVERSIDADE DE SANTIAGO DE COMPOSTELA

the effect of statins on dry eye symptoms and meibomian gland function is still unclear [Ooi et al., 2019a].

Statins cholesterol-lowering function may have a role in the prevention of cataracts since cholesterol synthesis is required to regulate the metabolism of the crystalline [Fong and Poon, 2012] and accumulation of cholesterol in human lens fibers facilitates cataractogenesis [Vejux et al., 2021]. In open-angle glaucoma, statins may increase retinal and choroidal blood flow maintaining the optic nerve and retinal nerve fiber layer health, reducing the severity of glaucoma [Nagaoka et al., 2006]. In age-related macular degeneration, statins may reduce drusen formation between the retinal pigment epithelium and Bruch membrane [Ma et al., 2015]. In diabetic retinopathy, statins appear to reduce hard exudates formation [Cusick et al., 2003] and macular edema [Gupta et al., 2004], improve the endothelial structure, function, blood flow velocity, and vascular resistance, reducing microaneurysm formation and leakage or hemorrhage from new vessels [Özkiris et al., 2007]. Overall, systemic delivery of statins is revealing beneficial to treat ophthalmic disorders affecting anterior and posterior segments. These therapeutic effects could be improved if efficient ocular formulations are developed.

Atorvastatin calcium is a synthetic statin with relatively moderate lipophilicity and low molecular weight, which may be able to penetrate the ocular structures if topically applied [Joshi et al., 1999; Ooi et al., 2019b]. Preclinical studies have demonstrated that atorvastatin (50 μM) ophthalmic solutions have a greater immunomodulatory effect on activated human T cells than lovastatin and simvastatin solutions [Jameel et al., 2013]. Moreover, atorvastatin drops can be safely administered for long-term treatment of dry eye and blepharitis,

USC UNIVERSIDADE DE SANTIAGO DE COMPOSTELA

showing tear film stabilization and anti-inflammatory effects [Ooi et al., 2015].

Diabetes mellitus is a metabolic disease defined by elevated blood glucose that leads to macrovascular (e.g., coronary heart disease, peripheral vascular disease, and stroke) and microvascular (e.g., retinopathy, nephropathy, and neuropathy) complications [Vieira-Potter et al., 2016; Wong et al., 2016]. Dysregulation of blood glucose can cause alterations in a multitude of anterior and posterior structures of the eye [Zhu et al., 2019]. The most well-studied manifestation is diabetic retinopathy, although it is estimated that diabetic keratopathy affects up to two-thirds of diabetic patients [Vieira-Potter et al., 2016; Han et al., 2019; Abdelkader et al., 2011]. Diabetic keratopathy complications could be superficial punctate keratitis, corneal erosions, and persistent epithelial defects and, in advanced stages, loss of the basement membrane and subsequent stromal ulceration [Zhu et al., 2019]. Corneal sensitivity is also impaired in diabetes and may predispose to bacterial corneal ulcers, compromising the healing mechanism [Negi and Vernon, 2003]. Furthermore, tear film secretion and stability could be altered in diabetic patients [Dogru et al., 2001; Misra et al., 2014]. Efficient wound healing mechanisms are important to maintain transparency and restore the barrier function of the cornea. The use of topical anti-inflammatory medications is useful for alleviating ocular surface inflammation and promoting re-epithelialization [Han et al., 2019].

Contact lenses (CLs) are being positioned as advantageous platforms for the sustained release of ophthalmic drugs [Phan et al., 2016; Phan et al., 2014; Varela-Garcia et al., 2020a]. Once applied to the eye, the CL may release the drug toward the post-lens tear film, which has slower turnover than the lachrymal fluid in the absence of

USC UNIVERSIDADE DE SANTIAGO DE COMPOSTELA

the lens. Prolonged permanence and higher drug levels on the ocular surface facilitate drug penetration into eye tissues [Alvarez-Lorenzo et al., 2019; Dixon et al., 2018; Tieppo et al., 2012]. Despite the therapeutic advantages of medicated CLs, their design is still a huge challenge because most available CLs lack affinity for ophthalmic drugs [Hui et al., 2017]. This problem can be overcome by means of bioinspired strategies that rely on mimicking the human pharmacological receptor of the drug into the CL structure [Alvarez-Lorenzo et al., 2019]. The incorporation of functional monomers bearing chemical groups similar to those present in the natural drug binding site, and their arrangement assisted by molecular imprinting has been shown useful to im-prove the performance of CLs as platforms for the sustained release of acetazolamide and ethoxzolamide [Ribeiro et al., 2011], ketotifen fumarate [Tieppo et al., 2012], olopatadine [González-Chomón et al., 2016], epalrestat [Alvarez-Rivera et al., 2018], naltrexone [Alvarez-Rivera et al., 2019], transferulic acid [Varela-Garcia et al., 2020b], etc. This bioinspired strategy does not compromise the performance of CLs as medical devices for vision correction.

The present work relies on the hypothesis that hydrogels that can mimic the components of the active site of HMG–CoA reductase might exhibit enhanced affinity for statins. Thus, the aim of the work was to design, for first time, atorvastatin-loaded CLs using functional monomers that bear chemical groups that resemble those present in HMG–CoA reductase and that can be successfully integrated with the CL network in order to optimize the loading and release of atorvastatin calcium while still preserving the properties required for CLs, mainly in terms of ocular tolerance, light transmission, and mechanical properties. Statins have a polar head group that mimics the natural substrate of HMG–CoA reductase and, thus, bind the active site,

USC UNIVERSIDADE DE SANTIAGO DE COMPOSTELA

blocking the access of the natural substrate. In the binding of type II statins (as atorvastatin), the isopropyl group participates in Van der Waals contacts with the enzyme involving residues Leu^{562}, Val^{683}, Leu^{853}, Ala^{856}, and Leu^{857}. Atorvastatin (**Figure 3.1A**) forms a hydrogen bond through its carbonyl oxygen atom with Ser^{565}, while the fluorophenyl group can coordinate to Arg^{590} through polar interactions [Istvan and Deisenhofer, 2001]. Taking into account the functionalities of the amino acids involved in the binding site of HMG–CoA reductase, ethylene glycol phenyl ether methacrylate (EGPEM), 2-aminoethyl methacrylate hydrochloride (AEMA), and N-(3-aminopropyl) methacrylamide hydrochloride (APMA) (**Figure 3.1**) were chosen as functional monomers after a first screening of the interaction with atorvastatin using computational modeling. Hydrogels were prepared from mixtures of 2-hydroxyethyl methacrylate (HEMA), EGPEM, AEMA, and APMA at various ratios (**Table 3.1**). Some hydrogels were synthesized in the presence of the drug (imprinted hydrogels) to verify whether the drug molecules could contribute to a better arrangement of the monomers for a more efficient formation of ad hoc artificial receptors.

USC UNIVERSIDADE DE SANTIAGO DE COMPOSTELA

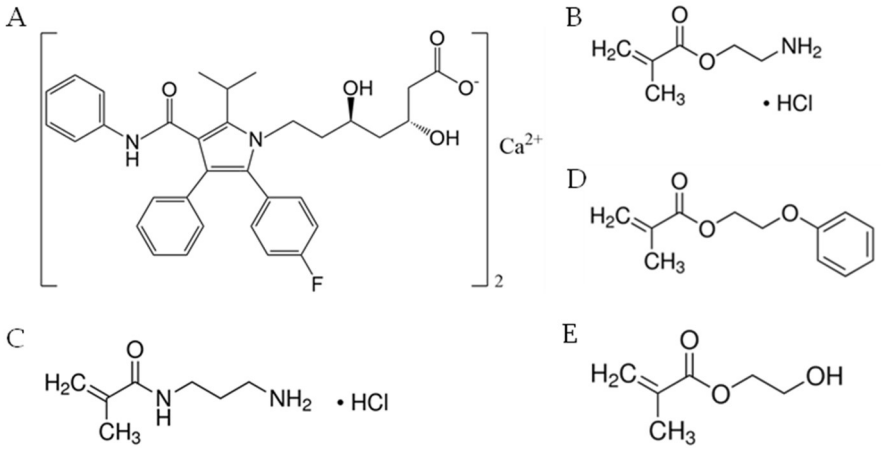

Figure 3.1. Structure of atorvastatin calcium (**A**) and the functional monomers used to synthesize the hydrogels: (**B**) 2-aminoethyl methacrylate hydrochloride (AEMA); (**C**) N-(3-aminopropyl) methacrylamide hydrochloride (APMA); (**D**) ethylene glycol phenyl ether methacrylate (EGPEM), and (**E**) 2-hydroxyethyl methacrylate (HEMA).

Since sterilization is a mandatory step in the conditioning of CLs and may affect the material properties, the drug stability, and the drug release pattern, a relevant second aim of the present work was to evaluate to what extent several sterilization techniques may alter the capability of the designed CLs to act as platforms for atorvastatin release. The stability of the hydrogels and the drug in separate and of the drug-loaded hydrogels against steam heat (autoclave), gamma radiation, and high hydrostatic pressure (HHP) techniques was evaluated. Steam heat and gamma radiation are the most used methods for sterilization of medical devices [Galante et al., 2018]. Steam heat is efficient, fast, and does not involve toxic agents, but it is not suitable for materials and drugs that are heat sensitive [Rogers, 2013]. Gamma radiation allows operating at low temperatures, but it is expensive,

USC UNIVERSIDADE DE SANTIAGO DE COMPOSTELA

complex, and may affect the polymer properties [Simmons, 2012]. HHP is increasingly used in the food industry to inactivate microorganisms without altering the food properties [Chawla, 2011]. Pressure-based methods are also used for the disinfection of biomaterials and for vaccine production [Follonier et al., 2012]. Furthermore, according to previous reports [Topete et al., 2020], HHP seems to be an alternative method for terminal sterilization of drug-loaded intraocular lenses.

Finally, the most promising CLs were evaluated regarding cytocompatibility with Balb/3T3 fibroblasts, ocular tolerance (HET–CAM), and *ex vivo* accumulation/permeability of atorvastatin into/through the porcine cornea and sclera tissues.

3.2 MATERIALS AND METHODS

3.2.1 Materials

Atorvastatin calcium was from Biosynth (Compton, UK). 2-Hydroxyethyl methacrylate (HEMA) was supplied by Merck (Darmstadt, Germany). Ethylene glycol di-methacrylate (EGDMA), ethylene glycol phenyl ether methacrylate (EGPEM), 2,2′-azo-bis(isobutyronitrile) (AIBN), 2-aminoethyl methacrylate hydrochloride (AE-MA), and dichlorodimethylsilane were from Sigma-Aldrich (Steinheim, Germany). N-(3-aminopropyl) methacrylamide hydrochloride (APMA) was from PolySciences Inc. (Warrington, PA, USA). Sodium chloride (NaCl) was from Scharlau (Barcelona, Spain), and ethanol absolute was from VWR Chemicals (Leuven, Belgium). Ultrapure water (resistivity > 18.2 MΩ cm; Milli-Q®, Millipore Ibérica, Madrid, Spain) was obtained by reverse osmosis. Simulated lachrymal fluid (SLF) was prepared with the following composition in

USC UNIVERSIDADE DE SANTIAGO DE COMPOSTELA

water: 6.78 g/L NaCl from Scharlau (Barcelona, Spain), 1.90 g/L $NaHCO_3$ from Probus (Barcelona, Spain), 1.38 g/L KCl, and 0.042 g/L $CaCl_2$ from Merck (Darmstadt, Germany) with pH 7.4 [Dogru et al., 2001]. Carbonate buffer pH 7.2 was prepared by mixing two buffer solutions: buffer solution A (100 mL: 1.24 g NaCl, 0.071 g KCl, 0.02 g NaH_2PO_4 from Merck (Darmstadt, Germany), 0.49 g $NaHCO_3$) and buffer solution B (100 mL: 0.023 g $CaCl_2$, 0.031 g $MgCl_2$ from Panreac (Barcelona, Spain)). Balb/3T3 fibroblasts were provided by American Type Culture Collection (Manassas, VA, USA).

3.2.2 Computational Modeling

The 3D structure of the functional monomers (EGPEM, AEMA, and APMA) and atorvastatin calcium was taken from the PubChem database [Kim et al., 2016]. The Autodock Tools version 4.2.6 software (Molecular Graphics Lab., La Jolla, CA, USA) was used to perform computational molecular docking in two steps, using a semiempirical free energy force field. The molecules under study, the ligand (in this case, the monomer) and the receptor (drug) started in an unbound conformation, and after that, the intramolecular energetics were estimated from these unbound states to the conformation in the bound state. Then, the intermolecular energetics of their bound conformation were analyzed using the Lamarckian genetic algorithm [Morris et al., 2009]. Finally, estimated free energy of binding (ΔGbinding) and dissociation constant (Ki) values were obtained [Morris et al., 2014]. In all cases, the grid was generated with default settings around the monomer and the drug.

USC UNIVERSIDADE DE SANTIAGO DE COMPOSTELA

3.2.3 Hydrogel Preparation

Compositions of the monomers' mixtures and the amounts of atorvastatin calcium added are shown in **Table 3.1**. The hydrogels were designed with AF codes, followed by a number referring to a specific combination of monomers and one/two letters, which indicate whether the networks were imprinted (letter i) or not (letters ni).

Table 3.1. Composition of the monomer mixtures used to synthesize the hydrogels. ni: non-imprinted; i: imprinted

Hydrogel Code	HEMA (mL)	EGDMA (µL)	EGPEM (µL)	AEMA (mg)	APMA (mg)	Atorvastatin (mg)	AIBN (mg)
AF1	3	12.10	-	-	-	-	4.93
AF1ni	3	12.10	-	-	-	-	4.93
AF1i	3	12.10	-	-	-	12.57	4.93
AF2	3	12.10	112.50	-	-	-	4.93
AF2ni	3	12.10	17.18	-	-	-	4.93
AF2i	3	12.10	17.18	-	-	12.57	4.93
AF3	3	12.10	112.50	19.90	-	-	4.93
AF3ni	3	12.10	17.18	14.91	-	-	4.93
AF3i	3	12.10	17.18	14.91	-	12.57	4.93
AF4	3	12.10	112.50	-	21.45	-	4.93
AF4ni	3	12.10	17.18	-	16.08	-	4.93
AF4i	3	12.10	17.18	-	16.08	12.57	4.93
AF5	3	12.10	-	19.90	-	-	4.93
AF5ni	3	12.10	-	14.91	-	-	4.93
AF5i	3	12.10	-	14.91	-	12.57	4.93
AF6	3	12.10	-	-	21.45	-	4.93
AF6ni	3	12.10	-	-	16.08	-	4.93
AF6i	3	12.10	-	-	16.08	12.57	4.93

USC UNIVERSIDADE DE SANTIAGO DE COMPOSTELA

The components were mixed under magnetic stirring (400 rpm) for 120 min and then 5 min in sonication. AIBN (initiator) was added, and the solutions were magnetically stirred again (100 rpm) for 10 min. Finally, the solutions were injected into molds made from two glass plates (10 × 10 cm) previously treated with dichlorodimethylsilane and separated by a silicone frame (0.3 mm thickness) [Alvarez-Lorenzo et al., 2002]. The polymerization was carried out by heating at 50 °C for 12 h, then the temperature was raised to 70 °C, and the polymerization was continued for a further 24 h. In such a way controlled thermal decomposition of the initiator AIBN prevented nitrogen bubbles formation [Su, 2013].

After polymerization, each hydrogel was immersed in boiling water (1000 mL) for 15 min to remove unreacted monomers and to facilitate the cut as 10 mm discs. The hydrogels were washed in ultrapure water for 24 h replacing the medium twice a day and then 0.9% NaCl and in water, every other day, replacing the medium twice a day for 10 days. During the cleaning process, the medium was kept under magnetic stirring (200 rpm) at room temperature and protected from the light. The cleaning process was monitored spectrophotometrically (Agilent 8453, Waldbronn, Germany) for both residual monomers leakage (only observed in the first washing solutions) and quantification of the amount of atorvastatin extracted. Atorvastatin was quantified from absorbance measurements at 242 nm using a validated calibration curve prepared for drug solutions in ethanol:water (20:80 *v/v*). Finally, the discs were dried at 70 °C for 24 h.

USC UNIVERSIDADE DE SANTIAGO DE COMPOSTELA

3.2.4 Hydrogel Characterization

Solvent uptake. Dried hydrogel discs were weighed (W_0) and immersed in SLF or atorvastatin calcium solution (0.04 mg/mL in ethanol:water 20:80 *v/v*) for 24 h at room temperature. Four replicates were tested for each hydrogel type. At a pre-established time (0.5, 1, 1.5, 2, 3, 4, 5, 6, and 24 h), the discs were removed, carefully wiped, and weighed (W_t). The solvent uptake was monitored as the increase in weight with respect to the dried disc as the following equation

$$Solvent\ uptake = \frac{W_0 - W_t}{W_0} \times 100 \qquad \text{(Eq. 3.1)}$$

Light transmission. The transmittance of discs hydrated in SLF and atorvastatin calcium solution (0.04 mg/mL in ethanol:water 20:80 *v/v*) was recorded, in quadruplicate, in 200–800 nm range (UV–Vis spectrophotometer, Agilent 8453, Boeblingen, Germany).

Mechanical properties. The mechanical properties of hydrated hydrogels (in 0.9% NaCl) were evaluated through tensile tests using a TA.XT Express Texture Analyser (Stable Micro Systems, Godalming, UK), with a 0.005 N trigger force, 50 N load cell, and test speed of 0.25 mm/s. Each hydrogel was cut with a dog bone-shaped mold (total 18 × 5 mm, in the center 6 × 2.5 mm). The samples were fixed to the upper and lower clamps. The Young's modulus was determined from the initial slope of the obtained stress–strain curves. Five independent experiments were conducted for each hydrogel formulation, before and after the different sterilization methods.

USC UNIVERSIDADE DE SANTIAGO DE COMPOSTELA

3.2.5 Atorvastatin Loading and Release

Nonimprinted and imprinted dried discs, in quadruplicate, were weighed (approx. 20 mg) and immersed in vials containing 10 mL of atorvastatin calcium solution (0.04 mg/mL in ethanol:water 20:80 *v/v*). The vials were kept under magnetic stirring (150 rpm) at room temperature and protected from the light for 48 h. At pre-established periods of time, the absorbance of the loading solution was measured by UV spectrophotometry (Agilent 8453, Boeblingen, Germany) at 242 nm and the amount of atorvastatin loaded was calculated as the difference between the initial and final amount of drug in the solution. The network/water partition coefficient of atorvastatin, $K_{N/W}$, was estimated for each hydrogel type from the total amount loaded as follows [Kim et al., 1992].

$$Amount\ loaded = \frac{V_s + K_{N/W} \times V_p}{W_p} \times C_0 \qquad \text{(Eq. 3.2)}$$

In this equation, V_s is the volume of solution absorbed by the hydrogel, V_p the dried polymer volume, W_p the dried hydrogel weight, and C_0 the drug concentration in the loading solution.

Atorvastatin-loaded discs were rinsed with SLF and the discs were placed in vials with 10 mL of SLF (pH = 7.4, similar to the precorneal film [Garcia-Valldecabres et al., 2004]) at 37 °C and magnetically stirred at 150 rpm. The vials were protected from the light. Samples of the medium (3 mL) were periodically withdrawn and returned to the vial immediately after absorbance measurement at 242 nm. After 8 h and until the end of the test, samples of the release medium (2 mL) were withdrawn and replaced with the same volume of fresh SLF to maintain sink conditions and avoid false plateaus.

USC UNIVERSIDADE DE SANTIAGO DE COMPOSTELA

3.2.6 HET-CAM Test

The hen's egg test chorioallantoic membrane (HET–CAM) assay was used for pre-liminary screening of ocular irritancy of the hydrogels according to the ICCVAM protocol [ICCVAM, 2010], as previously described [Alvarez-Rivera et al., 2018]. Briefly, fertilized hen's eggs (Coren, San Cibrao das Viñas, Spain) were incubated at 37 °C with 60% relative humidity for 7 days and were manually rotated 180° three times a day for the duration of the incubation. On the eighth day, the eggs were cut on the wider extreme to extract the eggshell, remove the inner membrane, and expose the chorioallantoic membrane (CAM). Atorvastatin-loaded hydrogel discs and 300 µL of atorvastatin calcium (0.04 mg/mL in ethanol:water 20:80 *v/v*) were carefully placed on the CAM and the possible hemorrhage, vascular lysis, or coagulation of the vessels were monitored for 5 min. Two independent experiments were carried out for each hydrogel and the drug solution. The discs were previously loaded with atorvastatin calcium for 48 h, as described above. NaCl (0.9%) and NaOH (0.1 N) solutions were used as negative and positive controls, respectively. Then, the irritation score (IS) was estimated, as previously reported [Alvarez-Rivera et al., 2019].

3.2.7 Sterilization

Three different sterilization protocols were tested for hydrogels previously swollen in NaCl 0.9% for at least 24 h or in drug solution (0.04 mg/mL) for 48 h and maintained in the same solutions: (i) steam heat (SH) sterilization for 1 h using an autoclave (Uniclave 88/75L; A.J. Costa, Cacém, Portugal) at 121 °C and 1 bar [Topete et al., 2020; Silva et al., 2020]; (ii) gamma-radiation (GI) sterilization with 25 kGy radiation dose [Martínez-Sancho et al., 2004] and a dose rate of ≈5

USC UNIVERSIDADE DE SANTIAGO DE COMPOSTELA

kGy/h at room temperature (only for the hydrogels without drug); and (iii) high hydrostatic pressure (HHP) at 70 °C and 600 MPa for 10 min [Topete et al., 2020]. Four independent experiments were carried out for each hydrogel and sterilization condition. For the HHP, each hydrogel disc was previously packed and sealed in polyamide/polyethylene vacuum bags filled with NaCl 0.9% or drug solution and preheated at 70 °C for 10 min. Then, the bags were placed inside a polytetrafluoroethylene insulation vessel prefilled with water at the same temperature and immediately pressurized in a Hiperbaric 55 equipment (Burgos, Spain) [Oliveira et al., 2020].

Aliquots of the drug solution (0.02 mg/mL in ethanol:water 20:80 *v/v*) were sterilized under the same conditions as the hydrogels and thereafter analyzed by UV–Vis spectrophotometry and HPLC (as described in Section 3.2.10).

After the sterilization processes, the mechanical properties of fully hydrated hydrogels (in NaCl 0.9%) previously equilibrated at room temperature were evaluated. Furthermore, the loading and release experiments were carried out again with the discs sterilized in NaCl 0.9% medium and that were washed in water for 24 h and dried at 70 °C for another 24 h under the same conditions as described above (Section 3.2.5).

3.2.8 FTIR-ATR Analysis

The FTIR-attenuated total reflectance (ATR) spectra of the nonsterilized and sterilized AF1, AF6, AF6ni, and AF6i hydrogels (after steam heat, gamma radiation, and high hydrostatic pressure) were recorded in an FTIR Varian 670-IR equipped with a PIKE GladiATR

USC UNIVERSIDADE DE SANTIAGO DE COMPOSTELA

Diamond Crystal Attenuated Total Reflectance accessory with a resolution of 4 cm^{-1} and 64 scans.

3.2.9 Cytocompatibility Studies

Nonloaded and loaded hydrogels (AF6, AF6ni, and AF6i) were evaluated against Balb/3T3 fibroblasts cells (ATCC CCL-163; Manassas, VA, USA). Hydrogels (10 mm in diameter; approx. 20 mg) were loaded for 48 h in an atorvastatin solution (0.04 mg/mL in ethanol:water 20:80 *v/v*) or immersed in 0.9% NaCl solution (nonloaded hydrogels), cut in four symmetric pieces, and sterilized by HHP at 70 °C and 600 MPa for 10 min.

Balb/3T3 cells were cultured in T75 flasks using Dulbecco's modified Eagle medium (DMEM; Fisher Scientific, Newington, NH, USA) supplemented with 10% fetal bovine serum and 1% antibiotics (10,000 U/mL penicillin and 10,000 µg/mL streptomycin) in an incubator at 37 °C and 5% CO_2. Then, cells were detached from the flasks at 80% confluence using TrypLE® (Sigma Aldrich, St. Louis, MO, USA). Suspended cells were counted, seeded in wells of 96-well plates (20,000 cells/well), and allowed to attach for 24 h. Pieces (five) of discs were then placed individually in contact with the cells incubated for 24 h. Cells incubated in culture medium (negative control) and cells incubated in medium containing atorvastatin (0.04 and 0.02 mg/mL) were also evaluated.

The viability of the cells was evaluated using a Cell Counting kit-8 (CCK-8; Dojindo Molecular Technologies, Rockville, MD, USA) following the instructions from the manufacturer. Briefly, samples and culture medium were removed from the wells and 200 µL of a CCK-8

USC UNIVERSIDADE DE SANTIAGO DE COMPOSTELA

working solution (10% *v/v* CCK-8 reagent in complete culture medium) were added to each well and incubated for 1 h at 37 °C. Finally, absorbance was measured at 450 nm (UV Bio-Rad Model 680 microplate reader, Hercules, CA, USA), and cell viability (%) was calculated as follows

$$Cell\ viability\ (\%) = \frac{Abs_{exp}}{Abs_{negative\ control}} \times 100 \qquad \text{(Eq. 3.3)}$$

3.2.10 Cornea and Sclera Permeability and Accumulation

Ex vivo permeability assays were carried out, in triplicate, with nonsterilized AF6, AF6ni, and AF6i loaded hydrogels following the BCOP test protocol, as previously described [Alvarez-Rivera et al., 2016; Varela-Garcia et al., 2018]. Porcine eyes were collected from a local slaughterhouse in the first hour after death and transported completely immersed in PBS solution in an ice bath. Corneas and scleras were isolated using a scalpel, washed with PBS, and mounted in vertical diffusion (Franz) cells. The donor and receptor chambers were filled with carbonate buffer pH 7.2 and maintained in a bath at 37 °C, gentle magnetic stirring. After 30 min, the solution in the donor chamber was completely removed using a Pasteur pipette and the corneas and scleras were exposed for 6 h to atorvastatin-loaded discs (AF6, AF6ni, and AF6i discs with 2 mL of SLF) or to control atorvastatin solution (60 µg/mL in ethanol:water 20:80 *v/v*, 1 mL). The donor chambers were covered with para-film to prevent evaporation. Samples (1 mL) were removed from the receptor chamber at 0.5, 1, 2, 3, 4, 5, and 6 h, replacing with the same volume of fresh carbonate buffer each time and taking care of removing air bubbles from the diffusion cell.

USC UNIVERSIDADE DE SANTIAGO DE COMPOSTELA

The amount of atorvastatin in the receptor medium samples was quantified by HPLC (AS-4140 Autosampler, PU-4180 Pump, LC-NetII/ADC Interface Box, CO-4060 Column Oven, MD-4010 Photodiode Array Detector, JASCO, Tokyo, Japan) fitted with a C18 column (Waters Symmetry C18, 5 µm, 4.6 × 250 mm) and operated with ChromNAV software v.2. Mobile phase consisted of methanol: 0.05 M sodium phosphate (NaH_2PO_4) buffer (70:30 *v/v*, pH adjusted to 4.1 with o-phosphoric acid) at 1.00 mL/min and 25 °C [Mustafa et al., 2016]. The injection volume was 50 µL, and the total run time of each sample was 10 min. Atorvastatin was quantified at 247 nm (retention time of 6.3 min). The HPLC method was validated using two different calibration curves of atorvastatin in carbonate buffer, one between 0.125–2 µg/mL and the other one 2–16 µg/mL. The limit of detection (LOD) and limit of quantification (LOQ) values were 0.05 and 0.125 µg/mL, respectively.

After 6 h of experiment, the discs and solutions were removed from the donor chambers. The corneas and scleras were also removed from the diffusion cells and rinsed with 0.9% NaCl and immersed in 3 mL of ethanol:water (50:50 *v/v*) overnight at 37 °C under magnetic stirring. Then, they were sonicated for 99 min at 37 °C, centrifuged (1000 rpm, 5 min, 25 °C), and the supernatant filtered (Scharlau® Syringe Filter, 0.22 µm 13 mm PTFE hydrophilic), centrifuged again (14,000 rpm, 20 min, 25 °C), and filtered to be measured by HPLC, as explained above.

3.2.11 Light Stability of Atorvastatin Calcium Solution

Solutions of atorvastatin calcium (0.02 mg/mL in ethanol:water 20:80 *v/v*) were placed in quartz cells (2 mL per cell) and exposed to fluorescent tube light (F8T5 Day-light, 6500 K, HITACHI) for 8 h at

USC UNIVERSIDADE DE SANTIAGO DE COMPOSTELA

room temperature. The experiments were carried out in duplicate. UV-Vis spectra and HPLC chromatograms were recorded before and after exposition.

3.2.12 Statistical Analysis

Statistical analysis was performed using SPSS v.26.0 (IBM Co., Armonk, NY, USA). The descriptive data are presented as mean ± standard deviation. The normality of all variables was evaluated using the Shapiro–Wilk test. If normality was respected, a paired-samples t-test was used to compare the means between the two groups. One-way analysis of variance was used to compare the means of more than two groups. If normality was not verified, nonparametric tests were performed using Kruskal−Wallis test with post hoc Games–Howell correction. The level of significance used was 0.05.

3.3 RESULTS AND DISCUSSION

3.3.1 Hydrogels Synthesis and Conditioning

The intensity of the interactions between atorvastatin calcium and the functional monomers was preliminary assessed using computer-assisted molecular modeling, which is considered as a green screening strategy for the rational selection of the composition [Yañez et al., 2010; Marć et al., 2018]. The estimated free energy of the binding, inhibition constant, and the most probable structure are shown in **Figure 3.2**. Atorvastatin interacted with the structural monomer (HEMA) through a hydrogen bond between the hydrogen atom of the hydroxyl group and the carbonyl group of atorvastatin. Atorvastatin interacted with

USC UNIVERSIDADE DE SANTIAGO DE COMPOSTELA

EGPEM through a hydrogen bond between the N atom of the amido group of atorvastatin and the oxygen ether group of EGPEM, stabilized through π–π stacking of the benzyl groups of both molecules. In the case of AEMA and APMA, the interaction occurred between the amino group of these monomers and the carboxylic acid group of atorvastatin. The interaction of the drug with APMA was remarkably more favorable both in terms of binding energy (ΔGbinding) and stability against dissociation (Ki). The interaction with the two other monomers, EGPEM and AEMA, was thermodynamically weaker but still favorable. Therefore, the three functional monomers were investigated regarding their capability to endow the hydrogels with an affinity for atorvastatin. It should be noted that the ΔGbinding values, although small, are in the same order of magnitude as those reported for other functional monomer:template 1:1 interactions using similar computational modeling software [Terracina et al., 2016; Chen et al., 2016]. The binding enthalpy reported for HMG–CoA reductase and atorvastatin calcium in microcalorimetry titration experiments was higher (–10.9 Kcal/mol) but still in a comparable range [Carbonell and Freire, 2005].

USC UNIVERSIDADE DE SANTIAGO DE COMPOSTELA

HEMA and atorvastatin	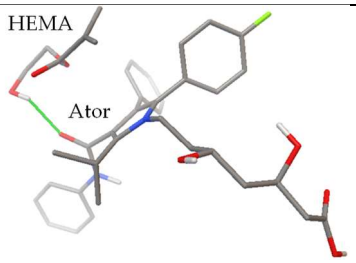	$\Delta G_{binding}$ = -2.17 Kcal/mol Ki = 25.49 mM
EGPEM and atorvastatin	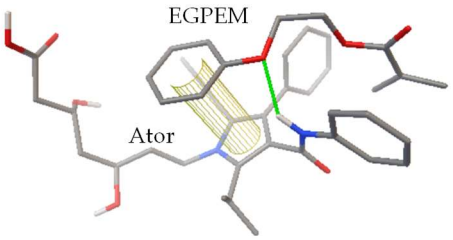	$\Delta G_{binding}$ = -3.44 Kcal/mol Ki = 3.00 mM
AEMA and atorvastatin	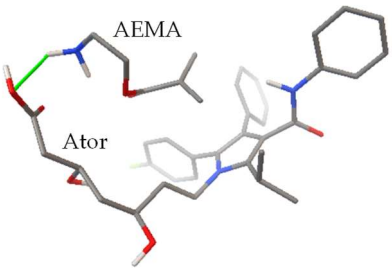	$\Delta G_{binding}$ = -3.43 Kcal/mol Ki = 3.05 mM
APMA and atorvastatin	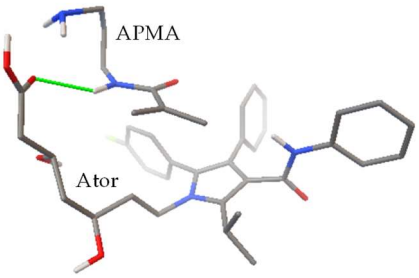	$\Delta G_{binding}$ = -4.24 Kcal/mol Ki = 0.784 mM

Figure 3.2. AutoDock modeling of structural and functional monomers–atorvastatin (Ator) interactions and the respective estimated free energy of the binding and inhibition constant. In the structures, N atoms are shown in blue, oxygen atoms in red, and the main bond interaction is shown in green.

USC UNIVERSIDADE DE SANTIAGO DE COMPOSTELA

Sets of hydrogels were prepared by combining AEMA, APMA, and EGPEM at various proportions as summarized in **Table 3.1**. AF1, AF1ni, and AF1i hydrogels were prepared without any functional monomer to be used as control. The first set of hydrogels AF2–AF6 was prepared with a concentration of APMA or AEMA of 40 mM and EGPEM of 200 mM. All monomers dissolved rapidly in HEMA medium with the exception of AEMA, and therefore AF3 and AF5 did not incorporate all feed AEMA content. Therefore, the second set of nonimprinted (AF1ni–AF6ni) and imprinted (AF1i–AF6i) hydrogels were prepared with lower concentrations of functional monomers (30 mM). Atorvastatin dissolved easily in the monomer solutions. Atorvastatin amount corresponded to drug:functional monomer 1:4 molar ratio. After polymerization, the hydrogel sheets were boiled in distilled water, which is the typical cleaning process of soft CLs after fabrication. Then, the hydrogels were successively immersed in water and NaCl 0.9% for the complete removal of atorvastatin before loading assay. Cleaning with NaCl 0.9% solution was needed to weaken the ionic interactions of atorvastatin with the hydrogels prepared with AEMA and APMA, as previously observed for other HEMA-based hydrogels [Andrade-Vivero et al., 2007]. The removal process was monitored spectrophotometrically at 242 nm until no leakage of drug or monomers was recorded. filtered to be measured by HPLC, as explained above.

3.3.2 Hydrogels Characterization

Dried discs rapidly sorbed SLF (**Figure 3.3**) and the equilibrium was reached in one hour. The hydrogels prepared with the highest amount of EGPEM (AF2, AF3, and AF4) presented the lowest solvent uptake either in SLF or atorvastatin calcium solution because of the

USC UNIVERSIDADE DE SANTIAGO DE COMPOSTELA

hydrophobicity of this monomer. Imprinted and nonimprinted hydrogels presented similar solvent uptake values. The solvent uptake in atorvastatin solution was significantly higher than that recorded in SLF, about 90% due to the addition of ethanol. Organic solvents as ethanol increase the solubility of the hydrophobic moieties of pHEMA in the aqueous medium, promoting hydrogel swelling [Refojo, 1997].

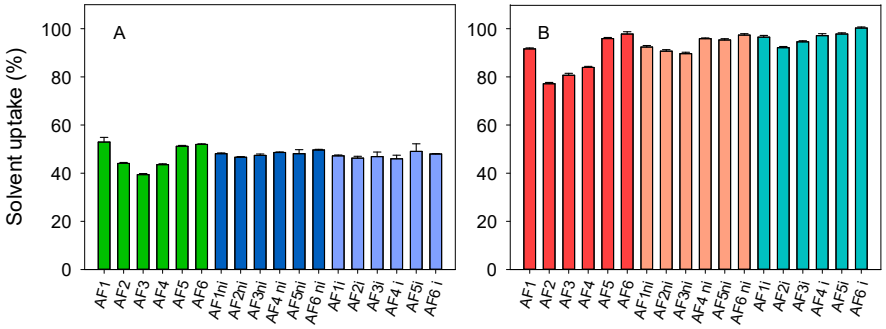

Figure 3.3. Solvent uptake (%) in (**A**) simulated lachrymal fluid and (**B**) atorvastatin calcium solution (0.04 mg/mL in ethanol:water 20:80 *v*/*v*) for all hydrogels before sterilization. Codes as in Table 3.1 (*n* = 4; mean values and standard deviations).

Regarding light transmission, all hydrated hydrogels were transparent in the visible range (400–700 nm), with transmittance values close to or above 90% (**Figure 3.4**) [Efron and Maldonado-Codina, 2011]. The presence of the drug did not alter the transmittance in the visible region.

USC UNIVERSIDADE DE SANTIAGO DE COMPOSTELA

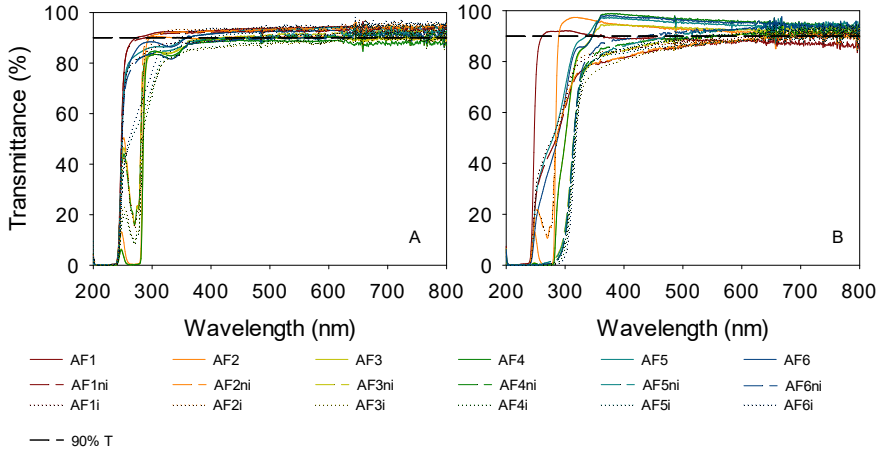

Figure 3.4. Light transmittance (%) of the hydrogels after being swollen in SLF (**A**) and in drug solution (**B**). Codes as in Table 3.1 (n = 4).

3.3.3 Atorvastatin Loading and Release

Hydrogel discs were dried and immersed in atorvastatin solution (0.04 mg/mL in ethanol:water 20:80 *v/v*) to quantify the drug loading ability (**Figure 3.5**). Nonfunctionalized hydrogels did not uptake any atorvastatin (AF1, AF1ni, and AF1i). Predictably, the amount of atorvastatin loaded increased with the content in APMA and AEMA functional monomers. The hydrogels with larger content in functional monomers required more than 24 h to complete the sorption, while the other nonimprinted and imprinted hydrogels completed the loading in the first 8 h. Addition of EGPEM did not further improve the loading (code AF2). The uptake was remarkably higher for hydrogels prepared with APMA (AF4, AF6, AF4ni, AF6ni, AF4i, and AF6i), which had the highest affinity for atorvastatin. Imprinted hydrogels showed minor increases in the amount of atorvastatin loaded compared to

USC UNIVERSIDADE DE SANTIAGO DE COMPOSTELA

nonimprinted ones, which is typical of drugs in which one-point interaction prevails over other feasible interactions [Ito et al., 2003].

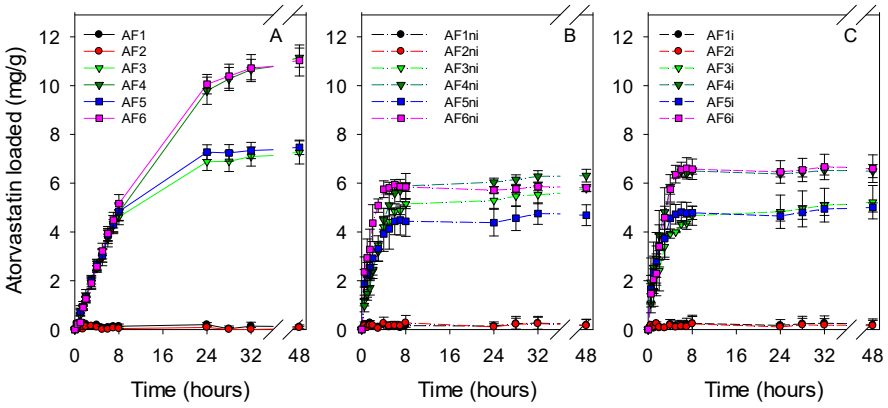

Figure 3.5. Atorvastatin loading profiles of all hydrogels ((**A**) first set of hydrogels; (**B**) nonimprinted hydrogels and (**C**) imprinted hydrogels) soaked in 10 mL of atorvastatin solution (0.04 mg/mL in ethanol:water 20:80 *v*/*v*) at room temperature under magnetic stirring (150 rpm) for 48 h. Codes as in Table 3.1 (*n* = 4; mean values and standard deviations).

Compared to nonfunctionalized hydrogel (AF1) and EGPEM hydrogels (AF2), hydrogels bearing AEMA or APMA hydrogels showed two orders of magnitude greater $K_{N/W}$ values (**Table 3.2**). The highest $K_{N/W}$ values were recorded for hydrogels with the largest content in functional monomers. APMA hydrogels (AF4 and AF6) had statically significant higher ($p < 0.05$) $K_{N/W}$ values than AEMA hydrogels (AF3 and AF5), in good agreement with the computational modeling analysis. Comparing the imprinted and nonimprinted hydrogels, no statistically significant differences in $K_{N/W}$ values were recorded, except for AF6ni and AF6i ($p < 0.05$). The $K_{N/W}$ values of atorvastatin recorded for hydrogels prepared with AEMA or APMA

USC UNIVERSIDADE DE SANTIAGO DE COMPOSTELA

were higher than those previously found for functionalized CLs designed to uptake other drugs such as naltrexone [Alvarez-Rivera et al., 2019], polymyxin B [Malakooti et al., 2015], acetazolamide, ethoxzolamide [Ribeiro et al., 2011], or ferulic acid [Varela-Garcia et al., 2020b]. High $K_{N/W}$ values can be typically found for drugs that can establish strong ionic interactions with the hydrogel moieties, as observed for epalrestat and APMA-functionalized networks [Alvarez-Rivera et al., 2018].

Table 3.2. Amounts of atorvastatin loaded by each hydrogel, and the $K_{N/W}$ values calculated (mean value and in parenthesis standard deviations).

Hydrogel Code	Amount of Atorvastatin Loaded (mg/g)	$K_{N/W}$
AF1	0.11 (0.08)	2.1 (2.3)
AF1ni	0.17 (0.20)	3.9 (6.2)
AF1i	0.18 (0.21)	4.1 (6.3)
AF2	0.09 (0.04)	1.7 (1.1)
AF2ni	0.16 (0.21)	3.4 (6.3)
AF2i	0.16 (0.21)	3.4 (5.6)
AF3	7.12 (0.38)	177.6 (11.6)
AF3ni	5.66 (0.12)	140.9 (3.0)
AF3i	5.22 (0.69)	130.1 (17.1)
AF4	11.32 (0.18)	282.6 (5.5)
AF4ni	6.31 (0.21)	157.2 (6.5)
AF4i	6.77 (0.27)	168.7 (6.6)
AF5	7.50 (0.28)	187.0 (8.6)
AF5ni	4.69 (0.35)	116.7 (10.7)
AF5i	5.00 (0.15)	124.6 (4.7)
AF6	11.08 (0.63)	276.4 (19.2)
AF6ni	5.81 (0.12)	144.7 (3.5)
AF6i	6.69 (0.23)	166.7 (7.0)

USC UNIVERSIDADE DE SANTIAGO DE COMPOSTELA

Atorvastatin-loaded discs were rinsed with water and immersed in 10 mL of SLF at 37 °C (sink conditions). The vials were maintained under oscillatory movement (150 rpm) to avoid the formation of a boundary layer around the discs, which could delay the release and lead to false sustained release [Tieppo et al., 2014]. The hydrogels prepared with the largest contents in functional monomers showed release patterns (**Figure 3.6**) similar to those recorded for less functionalized hydrogels when plotted as percentage released (**Figure 3.7**). Relevantly, all hydrogels provided sustained release almost for one week, covering extended wear of CL.

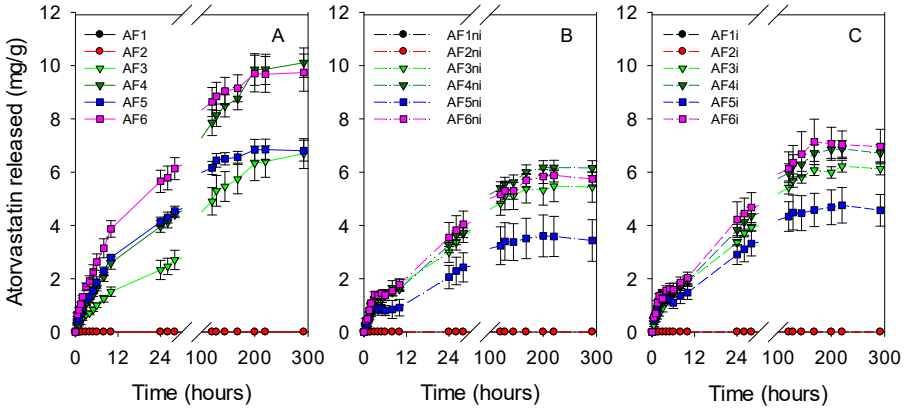

Figure 3.6. Atorvastatin release profiles from drug-loaded discs ((**A**) first set of hydrogels; (**B**) nonimprinted hydrogels and (**C**) imprinted hydrogels) in SLF at 37 °C under magnetic stirring (150 rpm). Codes as in Table 3.1 (*n* = 4; mean values and standard deviations).

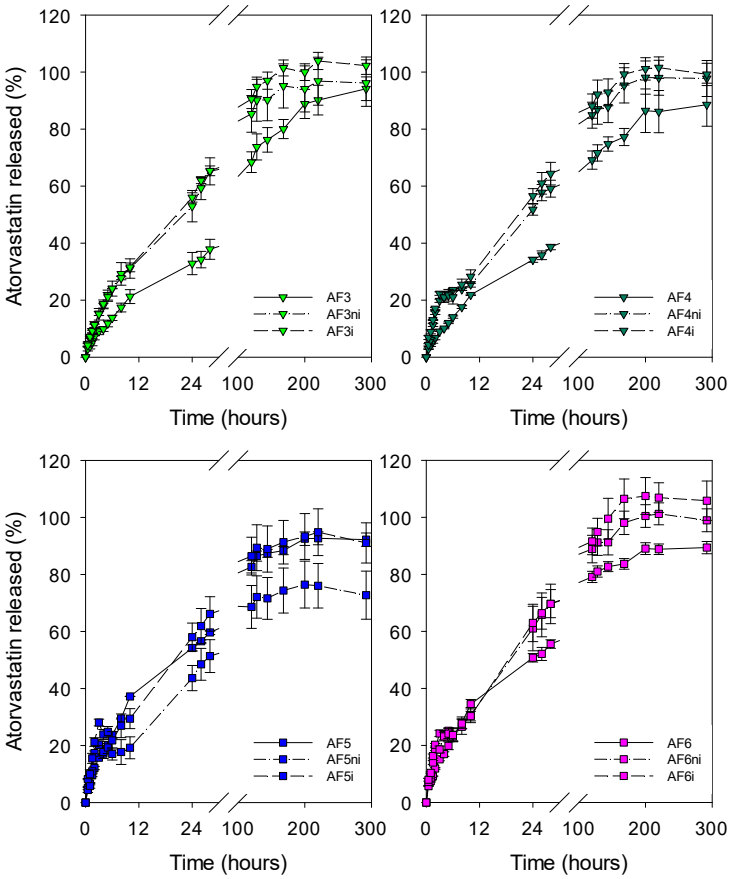

Figure 3.7. Atorvastatin release profiles (%) for AF3, AF4, AF5 and AF6 hydrogels in simulated lachrymal fluid at 37 ºC under magnetic stirring. Codes as in Table 3.1 (*n* = 4; mean values and standard deviations).

The Higuchi equation was fitted quite well to the release profiles, indicating that drug diffusion through the swollen network is the main mechanism regulating the release [Alvarez-Rivera et al., 2018] (**Table 3.3**).

USC UNIVERSIDADE DE SANTIAGO DE COMPOSTELA

Table 3.3. Fitting of Higuchi equation* Amounts of atorvastatin loaded by each hydrogel, and the $K_{N/W}$ values calculated (mean value and in parenthesis standard deviations).

Hydrogel Code	k_H (%·h$^{-0.5}$)	R^2
AF3ni	11.77 (1.08)	>0.98
AF4ni	10.94 (0.93)	>0.98
AF5ni	9.46 (1.29)	>0.95
AF6ni	12.21 (1.59)	>0.97
AF3i	12.43 (0.18)	>0.99
AF4i	11.80 (1.02)	>0.98
AF5i	11.24 (1.06)	>0.96
AF6i	12.40 (1.03)	>0.97

*Higuchi equation was fitted to the release profiles in the 10% to 60% amount released interval as follows: $(Q/Q_0)*100 = k_H \cdot t^{-0.5}$. In this Equation, Q represents the amount released at time t, Q_0 is the total amount loaded, k_H is the release rate constant, and the time t was expressed as hours.

3.3.4 HET-CAM Test and Cytocompatibility

The hen's egg test on the chorioallantoic membrane is a fast and sensitive procedure that provides useful preliminary information about ocular irritancy and may be a validated alternative to the low volume eye test scale developed for rabbits [Wilson et al., 2015]. The CAM tissue of fertilized hen eggs is non-innervated and contains arteries, veins, and capillaries that respond to injury in an analog way to ocular conjunctiva [McKenzie et al., 2015]. Images of CAM after 5 min exposure to atorvastatin calcium solution (300 µL, 0.04 mg/mL in ethanol:water 20:80 *v/v*) and atorvastatin-loaded discs showed no damages, as occurred for the negative control (NaCl 0.9%) (**Figure 3.8**). The presence of small contents of ethanol in the drug loading solution and in the atorvastatin-loaded hydrogels did not cause irritation, as previously reported for formulations containing up to 33% ethanol [Gettings et al., 1996]. Differently, the positive control (NaOH

USC UNIVERSIDADE DE SANTIAGO DE COMPOSTELA

0.1 N) caused an irritation score (IS) of 18.82. Therefore, all formulations can be considered as non-irritant for the ocular surface.

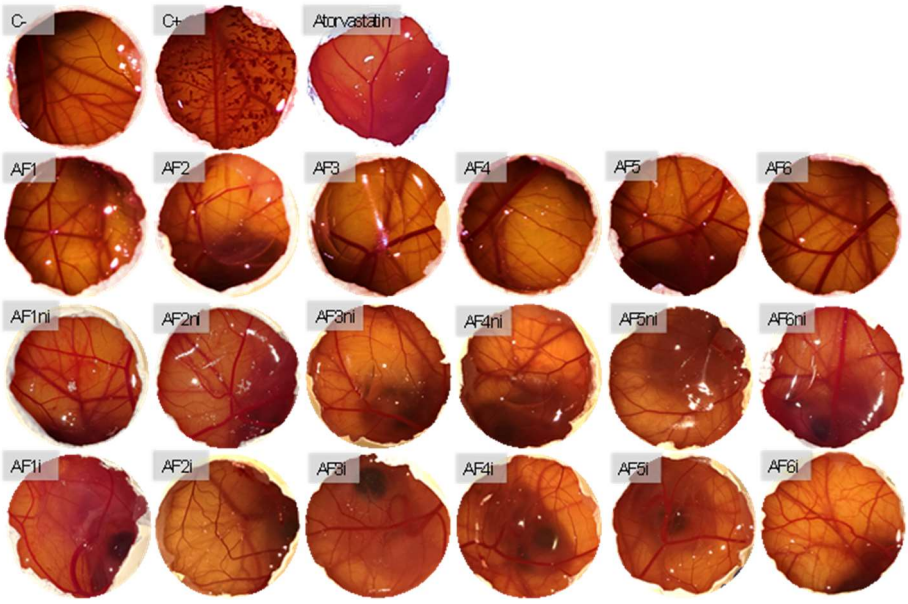

Figure 3.8. Pictures of HET-CAM test showing the CAM after 5 min in contact with atorvastatin-loaded discs and drug solution (0.04 mg/mL) in ethanol:water 20:80 *v/v*. Effects of negative (0.9% NaCl) and positive (0.1 N NaOH) controls are also shown. The diameter of the HET-CAM portion showed was 2 cm. Codes as in Table 3.1.

The cytotoxicity of the sterilized hydrogels (nonloaded and loaded with atorvastatin) was assessed through exposure to Balb/3T3 cells (**Figure 3.9**). The loading solution (0.04 mg/mL) and a solution containing the maximum amount of atorvastatin loaded by the hydrogels after 48 h (0.02 mg/mL) were also evaluated. In all cases, cell viability was above 90%. Overall, the designed hydrogels did not

USC UNIVERSIDADE DE SANTIAGO DE COMPOSTELA

produce cytotoxic effects and could be safely used as biomaterials suitable for contact lenses, according to ISO 10993-5:2009 [ISO, 2009].

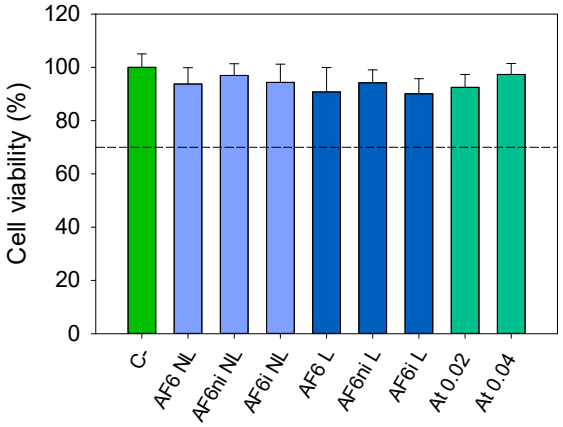

Figure 3.9. Viability of Balb/3T3 cells (%; mean and standard deviations) determined by CCK-8 assay, after 24 h exposure to nonloaded (NL), and atorvastatin loaded (L) hydrogels (AF6, AF6ni and AF6i) and two atorvastatin solutions (At; 0.04 and 0.02 mg/mL in ethanol:water 20:80 *v*/*v*). Negative control (C-) cells cultured in the absence of any treatment. Dashed line corresponds to 70% cell viability.

3.3.5 Effects of Sterilization

Sterilization of CLs is usually carried out by steam heat (autoclave) or gamma radiation [McEvoy and Rowan, 2019]. Sterilization becomes a big challenge for drug-loaded CLs because it may compromise the stability of the drug or impact negatively on the drug release profile [Topete et al., 2020]. In the present work, steam heat, gamma radiation, and HHP were tested in order to evaluate their effects on the material properties and on their subsequent capability to load atorvastatin and control drug release. First, hydrogels were sterilized while immersed in

USC UNIVERSIDADE DE SANTIAGO DE COMPOSTELA

a NaCl solution, and the elastic modulus was evaluated (**Figure 3.10**). Steam heat sterilization did not significantly affect the elastic modulus of any hydrogel (Kruskal–Wallis test, $p > 0.05$). Differently, gamma radiation significantly decreased the elastic modulus value of AF1ni, AF2ni, AF3ni, AF4ni, AF5ni, AF6ni, AF3i, and AF5i hydrogels (Kruskal–Wallis test, $p < 0.05$). HHP sterilization increased significantly the elastic modulus to 0.87 ± 0.02 MPa for AF4 and 0.79 ± 0.0 for AF6 (Kruskal–Wallis test, $p < 0.05$). Nevertheless, in all cases, the changes were small in magnitude and the elastic modulus obtained of the sterilized hydrogels (0.61–1.04 MPa) remained within the typical values for SCLs (0.38–1.44 MPa) [Kim et al., 2018].

To gain further insight into the effects of the sterilization technique on the hydrogel structure, the FTIR–ATR spectra of AF1, AF6, AF6ni, and AF6i dried discs before and after SH and HPP sterilization were compared (**Figure 3.11**). The spectra were normalized taking as a reference the main absorption peak of HEMA at 1704 cm^{-1}, corresponding to the C=O band [Perova et al., 1997]. AF1, which lacks functional monomers, showed the typical bands of pHEMA networks with strong intensities at 1483 (CH_2), 1367 (CH_2), 1153, and 1073 (C-O-C) cm^{-1}. Relevantly, none band of AF1 was altered after sterilization by either steam heat or HHP. The spectra of nonsterilized AF6, AF6ni, and AF6i evidenced a relative increase in the bands at 1367, 1153, 1073, and 965–938 cm^{-1}, which can be attributed to the copolymerization with APMA. Relevantly, the sterilization did not cause significant changes in the spectrum bands with respect to the nonsterilized discs. Unfortunately, FTIR spectra were not useful to analyze atorvastatin–hydrogel interactions probably because of the relatively low content in the drug.

USC UNIVERSIDADE DE SANTIAGO DE COMPOSTELA

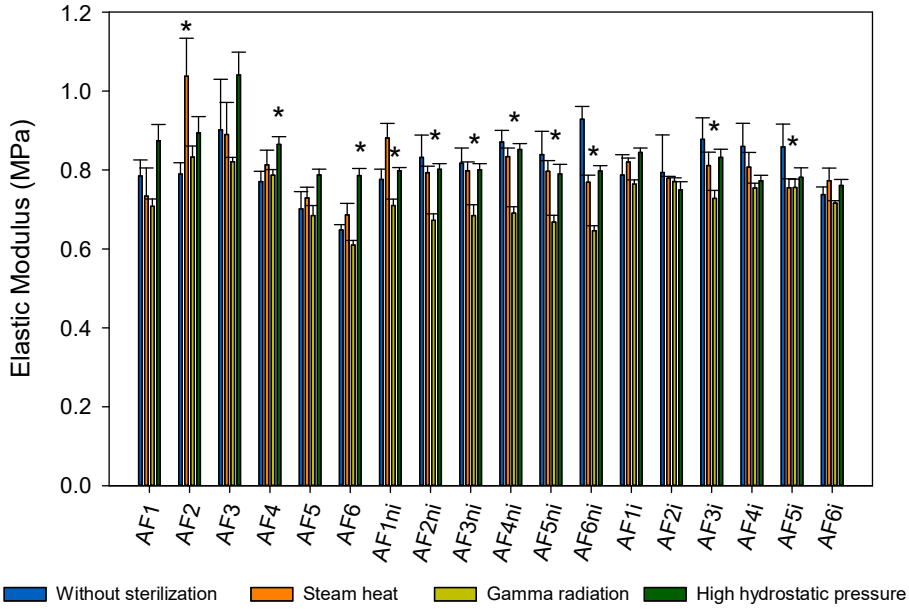

Figure 3.10. Elastic modulus (MPa) obtained for all hydrogels hydrated with 0.9% NaCl before and after each sterilization method. (*) Statistically different from the nonsterilized hydrogels (Kruskal–Wallis test and Games–Howell post hoc test, $p < 0.05$). Codes as in Table 3.1 ($n = 5$; mean values and standard deviations).

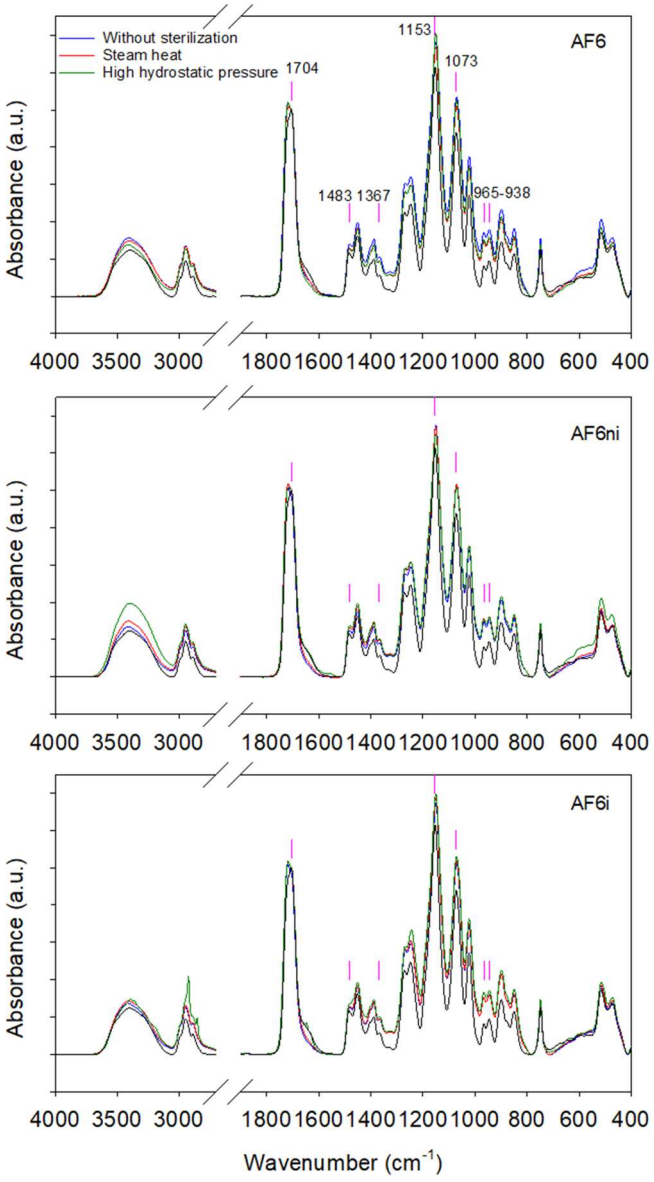

Figure 3.11. FTIR-ATR spectra obtained for AF6, AF6ni and AF6i hydrogels hydrated in NaCl 0.9% before and after being sterilized with steam heat and HHP. As a reference AF1 hydrogel spectrum is shown in black in the three plots.

USC UNIVERSIDADE DE SANTIAGO DE COMPOSTELA

Concerning the drug, as a first step, the effect of the different sterilization processes on the atorvastatin stability was evaluated. The UV–Vis spectra of the drug solutions acquired before and after steam heat (121 °C, 1 bar for 1 h) and HHP sterilization (600 MPa, 10 min, and 70 °C) (**Figure 3.12**) were quite similar to that of non-processed solution. A strong decrease in the absorbance was recorded after gamma-radiation (25 kGy), indicating that the drug suffered degradation. Previous studies have shown that many drugs (e.g., moxifloxacin, ketorolac, diclofenac) degrade when exposed to gamma radiation in solution [Topete et al., 2020] due to the presence of free radicals and ions formed during the radiolysis of water [Bojanowska-Czajka et al., 2015]. Atorvastatin stability during steam heat and HHP was further investigated by HPLC (**Figure 3.13**). The drug was found to be sensitive to 121 °C originating degradation products with retention times of 3.62, 5.98, and 6.85 min. Goel et al. also reported atorvastatin degradation when heating the solution at 80 °C for 4 h [Goel et al., 2013]. Contrarily, HHP, which involved heating at 70 °C for 10 min and pressurize with 600 MPa did not trigger degradation.

USC UNIVERSIDADE DE SANTIAGO DE COMPOSTELA

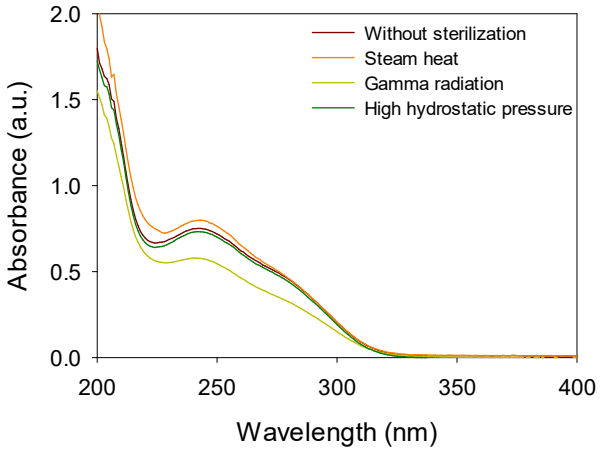

Figure 3.12. UV-Vis spectra of atorvastatin calcium (0.04 mg/mL) solution in ethanol:water 20:80 *v/v* before and after steam heat, gamma-radiation and high hydrostatic pressure sterilization.

USC UNIVERSIDADE DE SANTIAGO DE COMPOSTELA

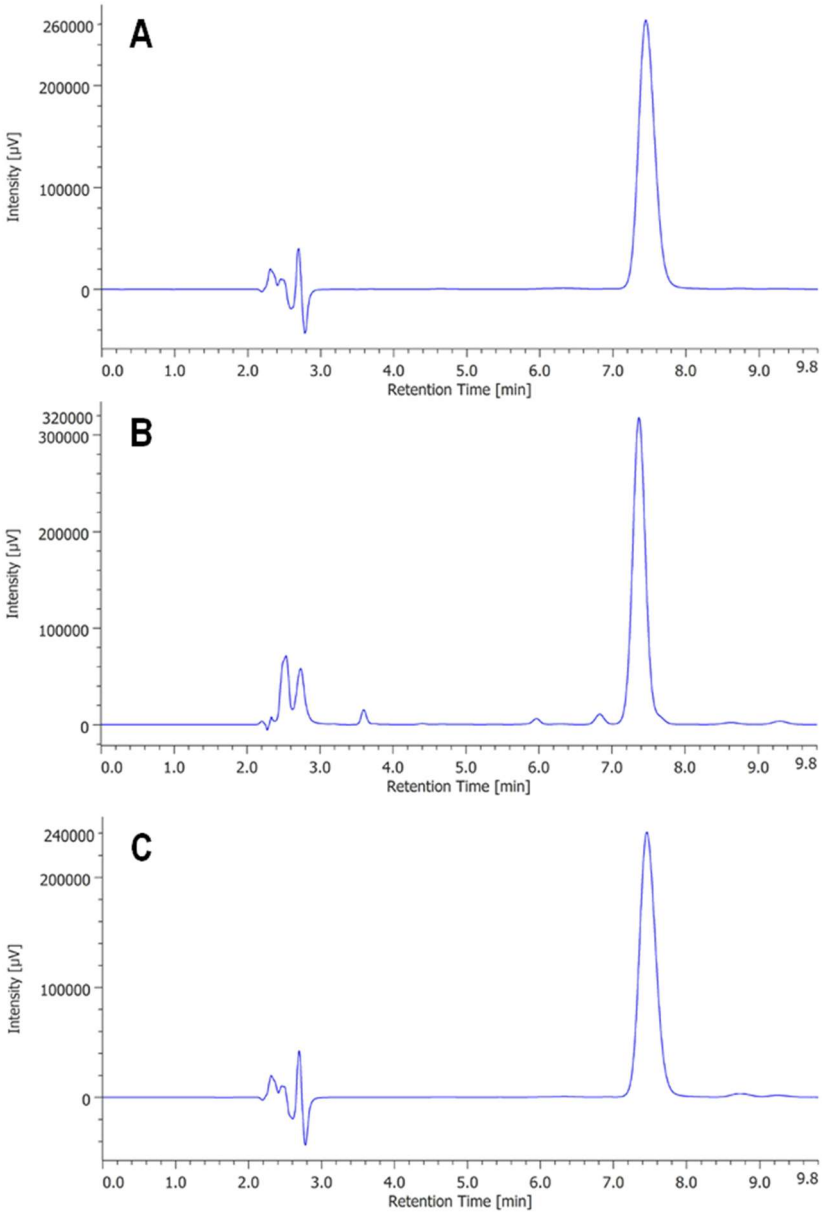

Figure 3.13. HPLC chromatograms of the atorvastatin loading solution before (**A**) and after sterilization pro-cessing applying steam heat (**B**) and high hydrostatic pressure (**C**).

USC UNIVERSIDADE DE SANTIAGO DE COMPOSTELA

Then, hydrogels sterilized applying gamma radiation, steam heat, or HHP were tested again in terms of atorvastatin loading and release under the same conditions as for the nonsterilized hydrogels. Steam heat and HHP sterilized hydrogels evidenced a small decrease in the capability to load atorvastatin (**Figure 3.14**). This finding was especially remarkable for non-imprinted and imprinted hydrogels prepared by combining the two functional monomers EGPEM and AEMA (AF3ni and AF3i). This effect may be attributed to the impact of the moist heat conditions on the amino and hydroxyl groups that interact with the drug by hydrogen bonds, although no changes were recorded in the FTIR spectra probably because of the relatively low molar content in functional monomers, compared to pHEMA. Similar results were observed in previous studies using acrylic hydrogels containing 80–90% of polymethyl methacrylate (PMMA) and 10–20% of HEMA [Topete et al., 2020; Topete et al., 2019], in which steam heat sterilization decreased the amount of ketorolac and diclofenac loaded after 14 days of loading. As expected, the amount of drug released by the sterilized discs was lower, compared to nonsterilized hydrogels (**Figure 3.15**).

After gamma-radiation sterilization, the amount of drug loaded by the hydrogels was remarkably low (below 1 mg/g of hydrogel, data not shown), and the amount of drug released was below the quantification limit. For this reason, and because gamma radiation triggered the degradation of the drug in an aqueous solution, this technique was discarded for further experiments.

USC UNIVERSIDADE DE SANTIAGO DE COMPOSTELA

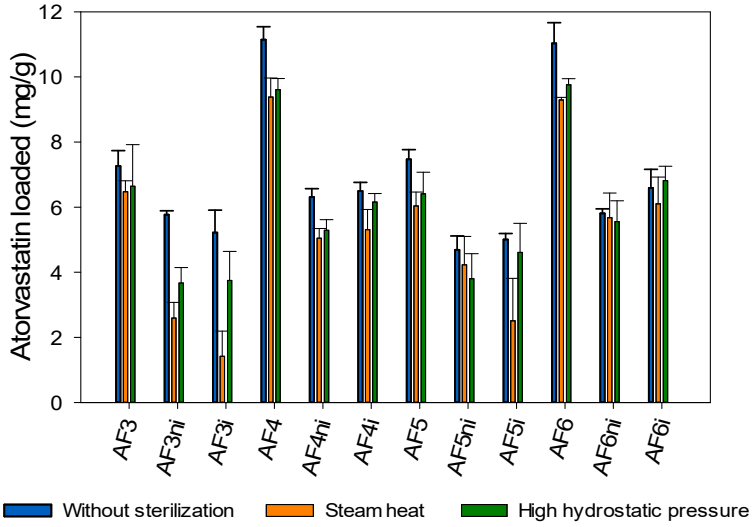

Figure 3.14. Atorvastatin loaded, after 48 h soaking, by hydrogels that had not been sterilized (blue bars) and hydrogels sterilized by steam heat (orange bars) or high hydrostatic pressure (green bars) before the loading. Codes as in Table 3.1 (*n* = 4; mean values and standard deviations).

USC UNIVERSIDADE DE SANTIAGO DE COMPOSTELA

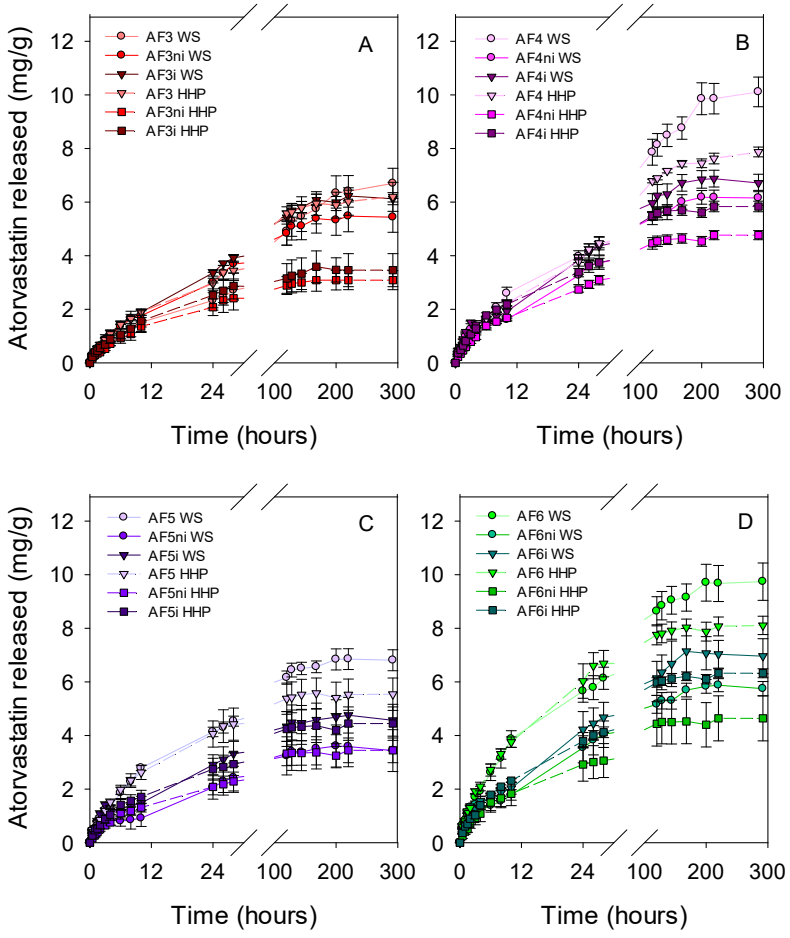

Figure 3.15. Comparison of atorvastatin release profiles from hydrogels that had not been sterilized (WS) and hydrogels that had been sterilized by high hydrostatic pressure (HHP) before loading. (**A**) F3 series, (**B**) F4 series, (**C**) F5 series, and (**D**) F6 series. Codes as in Table 3.1 (*n* = 4; mean values and standard deviations).

The next step was to elucidate the feasibility of performing the sterilization by steam heat or HHP while the hydrogels were already in

USC UNIVERSIDADE DE SANTIAGO DE COMPOSTELA

the atorvastatin loading solution (one-pot processing). This procedure could allow for loading and sterilization in one step, which may be advantageous in terms of time and processing steps. Only the most promising hydrogels in terms of atorvastatin affinity and network stability, i.e., those prepared with APMA as a functional monomer (AF6, AF6ni, AF6i) were tested. The hydrogels were immersed in atorvastatin solution (0.04 mg/mL ethanol:water 20:80 *v/v*) for 48 h under magnetic stirring (150 rpm) at room temperature before steam heat or HHP sterilization. The hydrogels sterilized with steam heat loaded less drug than the nonsterilized hydrogels (**Figure 3.16**), which could be due to a combination of changes in the functional groups that interact with atorvastatin and degradation of the drug. Differently, the hydrogels that underwent HHP loaded similar amounts of atorvastatin as the nonsterilized ones. Namely, HHP sterilization did not affect the loading of atorvastatin. As expected, the amount of atorvastatin released from hydrogels sterilized with steam heat decreased, compared with nonsterilized hydrogels, while sterilization by HHP did not modify the drug released pattern (**Figure 3.17**). These results agreed well with those recorded for hydrogels that were first sterilized and then loaded with atorvastatin, suggesting that degradation of both the hydrogels and the drug under steam heat conditions may compromise the performance of the hydrogels as drug-eluting contact lenses.

USC UNIVERSIDADE DE SANTIAGO DE COMPOSTELA

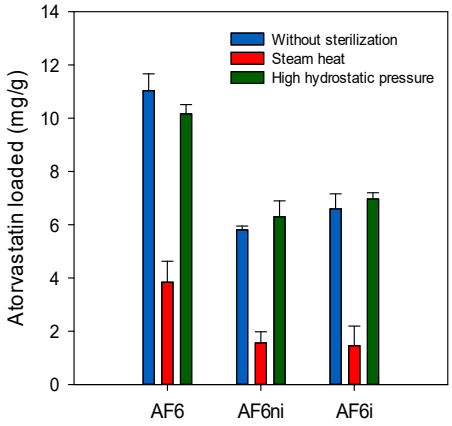

Figure 3.16. Atorvastatin loaded by AF6, AF6ni, and AF6i hydrogels when they were sterilized in drug solution by means of steam heat or high hydrostatic pressure, compared to nonsterilized hydrogels (*n* = 4; mean values and standard deviations).

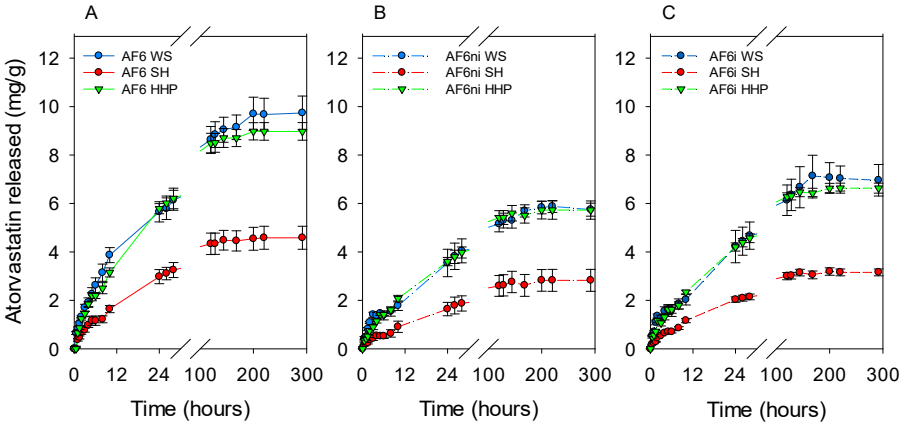

Figure 3.17. Comparison of atorvastatin release profiles in SLF from AF6 (**A**), AF6ni (**B**), and AF6i (**C**) hydrogels that had not been sterilized (WS) or that were sterilized during loading (immersed in drug solution) by means of steam heat (SH) or high hydrostatic pressure (HHP), (*n* = 4; mean values and standard deviations).

USC UNIVERSIDADE DE SANTIAGO DE COMPOSTELA

3.3.6 Cornea and Sclera Permeability and Accumulation

Ex vivo permeability tests were carried out with the most promising hydrogels (AF6, AF6ni, and AF6i) to evaluate their capability of providing therapeutic amounts of atorvastatin to the eye structures. The amount of atorvastatin released from the hydrogels towards the donor chamber (filled with simulated lachrymal fluid) and then diffused toward cornea and sclera tissues, and the receptor medium was monitored by HPLC. An atorvastatin solution (60 μg/mL in ethanol:water 20:80 *v/v*, 1 mL) was also used as a control. The tests were performed using cornea and sclera tissues from porcine cattle since the porcine eyes are reported to present the most similar anatomical properties to the human eyes [Loch et al., 2012].

Regarding the concentration of atorvastatin in the donor chamber after 6 h of experiment, these values were 28.43 ± 0.43 μg/mL for AF6, 19.67 ± 1.68 μg/mL for AF6ni and 22.00 ± 0.51 μg/mL for AF6i for cornea tissue (**Figure 3.18A**). For scleral tissue, the concentration of drug in the donor chamber was significantly lower for all hydrogels (21.32 ± 3.40 μg/mL for AF6; 13.17 ± 0.63 μg/mL for AF6ni; and 15.46 ± 1.81 μg/mL for AF6i; ANOVA, $p < 0.05$). In the case of the control solution, the concentration of atorvastatin remaining in the donor chamber was still significantly high in contact with cornea and sclera tissues (54.31 ± 2.98 and 52.11 ± 0.64 μg/mL, respectively) and, in all cases, greater than that recorded for the hydrogels (ANOVA, $p < 0.05$).

USC UNIVERSIDADE DE SANTIAGO DE COMPOSTELA

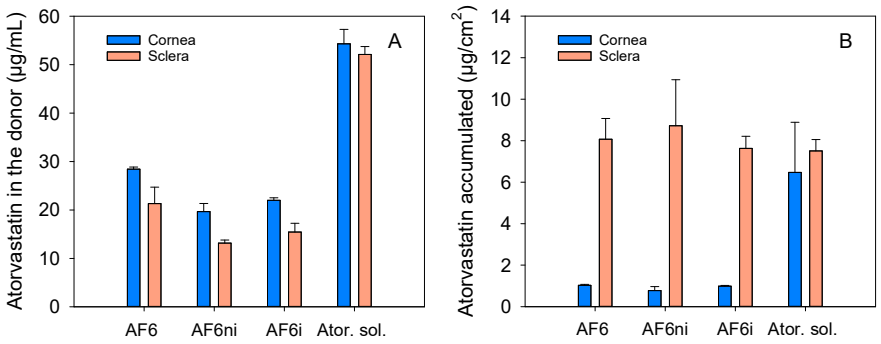

Figure 3.18. Amounts of atorvastatin in the donor chamber (**A**) and accumulated in cornea and sclera tissues (**B**) after 6 h of contact with drug-loaded hydrogels (AF6, AF6ni, and AF6i) and atorvastatin solution (60 µg/mL in ethanol:water 20:80 *v*/*v*, 1 mL), (*n* = 3; mean values and standard deviations).

Amounts accumulated in cornea were 1.03 ± 0.04 µg/cm^2 for AF6, 0.78 ± 0.19 µg/cm^2 for AF6ni and 0.99 ± 0.04 µg/cm^2 for AF6i (**Figure 3.18B**). These values were statistically different from those obtained for the atorvastatin solution (6.47 ± 0.41 µg/cm^2, ANOVA, $p < 0.05$). In sclera, atorvastatin accumulation was higher and no statistical differences were observed between the drug-loaded hydrogels and the control drug solution (ANOVA, $p = 0.78$).

The amount of atorvastatin in the receptor chambers was below the quantification limit in the time frame of the study. This means that atorvastatin mainly accumulated into the cornea and sclera tissues but did not progress further or the diffusion was too slow to be detected.

In a reported preclinical study, atorvastatin calcium formulated as eye drops (50 µM drug concentration) was instilled 1 drop 8 times a day for 4 weeks in patients with blepharitis and dry eye, showing tear film stabilization and anti-inflammatory effects [Ooi et al., 2015]. Therefore,

USC UNIVERSIDADE DE SANTIAGO DE COMPOSTELA

in each instillation, roughly 0.6 μg drug dose was applied onto the cornea, and this amount could rapidly vanish due to lachrymal fluid turnover. The hydrogels designed in the present work provided amounts of atorvastatin accumulated in the cornea and sclera that may be considered therapeutically effective.

3.3.7 Stability of Atorvastatin Calcium Solution

Finally, since during CL wearing the hydrogels are exposed to daylight, drug stability against UV–Vis radiation may be critical for the successful development of a drug-eluting CL. Atorvastatin in solution was exposed to white light (fluorescent lamp) mimicking the daylight conditions. After 8 h of exposure, UV–Vis spectrum recorded by spectrophotometry and HPLC runs (**Figure 3.19**) of atorvastatin solutions before and after white light exposition were identical, this means that atorvastatin calcium did not suffer any degradation. Therefore, atorvastatin loaded by the designed hydrogels is expected to remain stable under day-light conditions, as also found in previous studies [Yulianita et al., 2018].

USC UNIVERSIDADE DE SANTIAGO DE COMPOSTELA

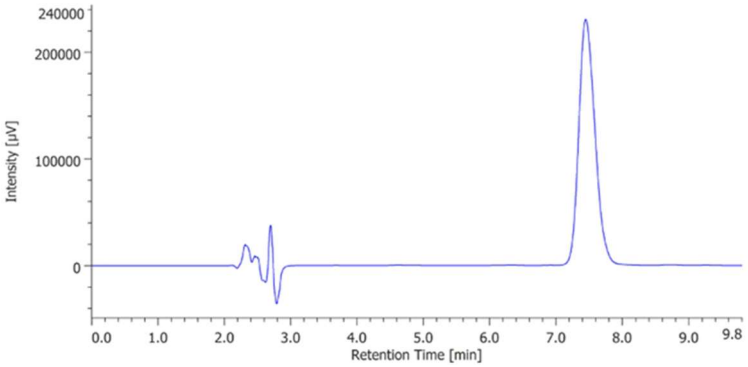

Figure 3.19. HPLC chromatogram of atorvastatin calcium solution (0.04 mg/mL in ethanol:water 20:80 *v*/*v*) after 8 h of exposure to white light.

3.4 CONCLUSIONS

In the present work, bioinspired contact lenses were designed, for the first time, to have an increased affinity for atorvastatin calcium by mimicking the active site of HMG–CoA reductase. The synthesized hydrogels presented solvent uptake, light transmission, and mechanical properties values in the common range for commercially available CLs. No potential eye (CAM) irritation was observed neither cytotoxicity effects in Balb/3T3 cells. The APMA hydrogels are the most promising candidates to be used as drug-eluting contact lenses in terms of the amount of drug loaded and released. From the fabrication point of view, loading and sterilization in the same container (one-pot processing) is a crucial step. The loading capacity of the hydrogels and stability of atorvastatin was not affected by HHP sterilization, which may advantageously substitute steam heat and gamma radiation in the sterilization of atorvastatin-loaded hydrogels, maintaining atorvastatin stability and hydrogels performance. Permeability studies through the porcine cornea and sclera tissues revealed that the amount of

USC UNIVERSIDADE DE SANTIAGO DE COMPOSTELA

atorvastatin accumulated in the cornea and sclera could be effective to treat ocular surface diseases. The success of this first attempt to design atorvastatin-loaded contact lenses must be contrasted with preclinical studies that confirm their efficacy in the treatment of ocular surface diseases.

3.5 REFERENCES

Abdelkader, H.; Patel, D.V.; Mcghee, C.N.; Alany, R.G. (**2011**). New therapeutic approaches in the treatment of diabetic keratopathy: A review. *Clin. Exp. Ophthalmol.* 39(3), 259–270.

Alvarez-Lorenzo, C.; Anguiano-Igea, S.; Varela-García, A.; Vivero-Lopez, M.; Concheiro, A. (**2019**). Bioinspired hydrogels for drug-eluting contact lenses. *Acta Biomater.* 84, 49–62.

Alvarez-Lorenzo, C.; Hiratani, H.; Gómez-Amoza, J.L.; Martínez-Pacheco, R.; Souto, C.; Concheiro, A. (**2002**). Soft contact lenses capable of sustained delivery of timolol. *J. Pharm. Sci.* 91(10), 2182-2192.

Alvarez-Rivera, F.; Concheiro, A.; Alvarez-Lorenzo, C. (**2018**). Epalrestat-loaded silicone hydrogels as contact lenses to address diabetic-eye complications. *Eur. J. Pharm. Biopharm*. 122, 126–136.

Alvarez-Rivera, F.; Fernández-Villanueva, D.; Concheiro, A.; Alvarez-Lorenzo, C. (**2016**). α-Lipoic acid in soluplus® polymeric nanomicelles for ocular treatment of diabetes-associated corneal diseases. *J. Pharm. Sci.* 105(9), 2855–2863.

USC UNIVERSIDADE DE SANTIAGO DE COMPOSTELA

Alvarez-Rivera, F.; Serro, A.P.; Silva, D.; Concheiro, A.; Alvarez-Lorenzo, C. (**2019**). Hydrogels for diabetic eyes: Naltrexone loading, release profiles and cornea penetration. *Mater. Sci. Eng. C* 105, 110092.

Andrade-Vivero, P.; Fernandez-Gabriel, E.; Alvarez-Lorenzo, C.; Concheiro, A. (**2007**). Improving the loading and release of NSAIDs from PHEMA hydrogels by copolymerization with functionalized monomers. *J. Pharm. Sci.* 96(4), 802–813.

Bedi, O.; Dhawan, V.; Sharma, P.L.; Kumar, P. (**2016**). Pleiotropic effects of statins: New therapeutic targets in drug design. *Naunyn Schmiedebergs Arch. Pharmacol*. 389(7), 695–712.

Bielecka-Dabrowa, A.; Bytyçi, I.; Von Haehling, S.; Anker, S.; Jozwiak, J.; Rysz, J.; Hernandez, A.V.; Bajraktari, G.; Mikhalidis, D.P.; Banach, M. (**2019**). Association of statin use and clinical outcomes in heart failure patients: A systematic review and meta-analysis. *Lipids Health Dis*. 18, 1–13.

Bojanowska-Czajka, A.; Kciuk, G.; Gumiela, M.; Borowiecka, S.; Nałęcz-Jawecki, G.; Koc, A.; Garcia-Reyes, J.F.; Ozbay, D.S.; Trojanowicz, M. (**2015**). Analytical, toxicological and kinetic investigation of decomposition of the drug diclofenac in waters and wastes using gamma radiation. *Environ. Sci. Pollut. Res.* 22(24), 20255–20270.

Carbonell, T.; Freire, E. (**2005**). Binding Thermodynamics of Statins to HMG-CoA Reductase. *Biochemistry.* 44(35), 11741–11748.

Chawla, R.; Patil, G.R.; Singh, A.K. (**2011**). High hydrostatic pressure technology in dairy processing: A review. *J. Food Sci. Technol.* 48(3), 260–268.

USC UNIVERSIDADE DE SANTIAGO DE COMPOSTELA

Chen, J.; Lewis, C.; Balamurugan, D.; Yang, Z.; Ai, L.; Cai, D. (**2016**). Theoretical analysis of a high performance protein imprint on a nanosensor. *Sens. Biosen. Res.* 7, 12–19.

Cusick, M.; Chew, E.Y.; Chan, C.C.; Kruth, H.S.; Murphy, R.P.; Ferris, F.L. (**2003**). Histopathology and regression of retinal hard exudates in diabetic retinopathy after reduction of elevated serum lipid levels. *Ophthalmology.* 110(11), 2126–2133.

Dixon, P.; Fentzke, R.C.; Bhattacharya, A.; Konar, A.; Hazra, S.; Chauhan, A. (**2018**). In vitro drug release and in vivo safety of vitamin E and cysteamine loaded contact lenses. *Int. J. Pharm.* 544(2), 380–391.

Dogru, M.; Katakami, C.; Inoue, M. (**2001**). Tear function and ocular surface changes in noninsulin-dependent diabetes mellitus. *Ophthalmology.* 108(3), 586–592.

Efron, N.; Maldonado-Codina, C. (**2011**). Development of contact lenses from a biomaterial point of view–materials, manufacture, and clinical application. In *Comprehensive Biomaterials*; Ducheyne, P., Healy, K., Hutmacher, D.W., Grainger, D.W., Kirkpatrick, C.J., Eds.; Elsevier: Amsterdam, The Netherlands, 517–541.

Follonier, S.; Panke, S.; Zinn, M. (**2012**). Pressure to kill or pressure to boost: A review on the various effects and applications of hydrostatic pressure in bacterial biotechnology. *Appl. Microbiol. Biotechnol.* 93(5), 1805–1815.

Fong, D.S.; Poon, K.Y.T. (**2012**). Recent statin use and cataract surgery. *Am. J. Ophthalmol.* 153(2), 222–228.

USC UNIVERSIDADE DE SANTIAGO DE COMPOSTELA

Galante, R.; Oliveira, A.S.; Topete, A.; Ghisleni, D.; Braga, M.; Pinto, T.J.A.; Colaço, R.; Serro, A.P. (**2018**). Drug-eluting silicone hydrogel for therapeutic contact lenses: Impact of sterilization methods on the system performance. *Colloids Surfaces B Biointerf.* 161, 537–546.

Garcia-Valldecabres, M.; López-Alemany, A.; Refojo, M.F. (**2004**). pH Stability of ophthalmic solutions. *Optometry.* 75(3), 161–168.

Gettings, S.D.; Lordo, R.A.; Demetrulias, J.; Feder, P.I.; Hintze, K.L. (**1996**). Comparison of low-volume, draize and in vitro eye irritation test data. I. Hydroalcoholic formulations. *Food Chem. Toxicol*. 34(8), 737–749.

Goel, A.; Baboota, S.; Sahni, J.K.; Srinivas, K.S.; Gupta, R.S.; Gupta, A.; Semwal, V.P.; Ali, J. (**2013**). Development and validation of stability-indicating assay method by UPLC for a fixed dose combination of atorvastatin and ezetimibe. *J. Chromatogr. Sci.* 51(3), 222–228.

González-Chomón, C.; Silva, M.; Concheiro, A.; Alvarez-Lorenzo, C. (**2016**). Biomimetic contact lenses eluting olopatadine for allergic conjunctivitis. *Acta Biomater.* 41, 302–311.

Gordon, G.M.; Lagier, A.J.; Ponchel, C.; Bauskar, A.; Itakura, T.; Jeong, S.; Patel, N.; Fini, M.E. (**2016**). A Cell-based screening assay to identify pharmaceutical compounds that enhance the regenerative quality of corneal Repair. *Wound Repair Regen*. 24(1), 89–99.

Gupta, A.; Gupta, V.; Thapar, S.; Bhansali, A. (**2004**). Lipid-lowering drug atorvastatin as an adjunct in the management of diabetic macular edema. *Am. J. Ophthalmol.* 137(4), 675–682.

USC UNIVERSIDADE DE SANTIAGO DE COMPOSTELA

Han, S.B.; Yang, H.K.; Hyon, J.Y. (**2019**). Influence of diabetes mellitus on anterior segment of the eye. *Clin. Interv. Aging.* 14, 53–63.

Hui, A.; Bajgrowicz-Cieslak, M.; Phan, C.M.; Jones, L. (**2017**). In vitro release of two anti-muscarinic drugs from soft contact lenses. *Clin. Ophthalmol.* 11, 1657–1665.

ICCVAM (**2010**). ICCVAM-Recommended test method protocol: Hen's egg test–chorioallantoic membrane (HET-CAM) test method; https://ntp.niehs.nih.gov/iccvam/docs/protocols/ivocular-hetcam.pdf (accessed on February 2021).

ISO 10993-5:2009(en). (**2009**). Biological evaluation of medical devices—Part 5: Tests for in vitro cytotoxicity; https://www.iso.org/obp/ui/#iso:std:iso:10993:-5:ed-3:v1:en (accessed on February 2021).

Istvan, E.S.; Deisenhofer, J. (**2001**). Structural mechanism for statin inhibition of HMG-CoA reductase. *Science.* 292(5519), 1160–1164.

Ito, K.; Chuang, J.; Alvarez-Lorenzo, C.; Watanabe, T.; Ando, N.; Grosberg, A.Y. (**2003**). Multiple point adsorption in a heteropolymer gel and the tanaka approach to imprinting: Experiment and theory. *Prog. Polym. Sci.* 28(10), 1489–1515.

Jameel, A.; Ooi, K.G.J.; Jeffs, N.R.; Galatowicz, G.; Lightman, S.L.; Calder, V.L. (**2013**). Statin modulation of human T-cell proliferation, IL-1 β and IL-17 production, and IFN- γ T cell expression: Synergy with conventional immunosuppressive agents. *Int. J. Inflam.* 2013, 43458.

USC UNIVERSIDADE DE SANTIAGO DE COMPOSTELA

Joshi, H.N.; Fakes, M.G.; Serajuddin, A.T.M. (**1999**). Differentiation of 3-Hydroxy-3-Methylglutaryl-Coenzyme A reductase inhibitors by their relative lipophilicity. *Pharm. Pharmacol. Commun.* 5, 269–271.

Kim, E.; Saha, M.; Ehrmann, K. (**2018**). Mechanical properties of contact lens materials. *Eye Contact Lens.* 44, S148–S156.

Kim, S.; Thiessen, P.A.; Bolton, E.E.; Chen, J.; Fu, G.; Gindulyte, A.; Han, L.; He, J.; He, S.; Shoemaker, B.A.; et al. (**2016**). PubChem substance and compound databases. *Nucl. Acids Res.* 44(D1), D1202–D1213.

Kim, S.W.; Bae, Y.H.; Okano, T. (**1992**). Hydrogels: Swelling, drug loading, and release. *Pharm. Res.* 9(3), 283–290.

Loch, C.; Zakelj, S.; Kristl, A.; Nagel, S.; Guthoff, R.; Weitschies, W.; Seidlitz, A. (**2012**). Determination of permeability coefficients of ophthalmic drugs through different layers of porcine, rabbit and bovine eyes. *Eur. J. Pharm. Sci*. 47(1), 131–138.

Marć, M.; Kupka, T.; Wieczorek, P.P.; Namieśnik, J. (**2018**). Computational modeling of molecularly imprinted polymers as a green approach to the development of novel analytical sorbents. *Trends Anal. Chem.* 98, 64–78.

Malakooti, N.; Alexander, C.; Alvarez-Lorenzo, C. (**2015**). Imprinted contact lenses for sustained release of polymyxin B and related antimicrobial peptides. *J. Pharm. Sci.* 104(10), 3386–3394.

Ma, L.; Wang, Y.; Du, J.; Wang, M.; Zhang, R.; Fu, Y. (**2015**). The association between statin use and risk of age-related macular degeneration. *Sci. Rep.* 5, 18280.

USC UNIVERSIDADE DE SANTIAGO DE COMPOSTELA

Martínez-Sancho, C.; Herrero-Vanrell, R.; Negro, S. (**2004**). Study of gamma-irradiation effects on aciclovir Poly(D,L-Lactic-Co-Glycolic) acid microspheres for intravitreal administration. *J. Control. Release.* 99(1), 41–52.

McEvoy, B.; Rowan, N.J. (**2019**). Terminal sterilization of medical devices using vaporized hydrogen peroxide: A review of current methods and emerging opportunities. *J. Appl. Microbiol.* 127(5), 1403–1420.

McKenzie, B.; Kay, G.; Matthews, K.H.; Knott, R.M.; Cairns, D. (**2015**). The hen's egg chorioallantoic membrane (HET-CAM) test to predict the ophthalmic irritation potential of a cysteamine-containing gel: Quantification using Photoshop® and ImageJ. *Int. J. Pharm.* 490(1-2), 1–8.

Misra, S.L.; Patel, D.V.; McGhee, C.N.J.; Pradhan, M.; Kilfoyle, D.; Braatvedt, G.D.; Craig, J.P. (**2014**). Peripheral neuropathy and tear film dysfunction in type 1 diabetes mellitus. *J. Diabetes Res.* 2014, 848659.

Morris, G.M.; Goodsell, D.S.; Pique, M.E.; Lindstrom, W.; Huey, R.; Forli, S.; Hart, W.E.; Halliday, S.; Belew, R.; Olson, A.J. (**2014**). User Guide-AutoDock Version 4.2; https://autodock.scripps.edu/downloads/faqs-help/manual/autodock-4-2-user-guide/AutoDock4.2.6_UserGuide.pdf (accessed on February 2021).

Morris, G.M.; Huey, R.; Lindstrom, W.; Sanner, M.F.; Belew, R.K.; Goodsell, D.S.; Olson, A.J. (**2009**). AutoDock4 and AutoDockTools4: Automated Docking with Selective Receptor Flexibility. *J. Comput. Chem.* 30(16), 2785–2791.

USC UNIVERSIDADE DE SANTIAGO DE COMPOSTELA

Mustafa, G.; Azeem, A.; Ahmad, F.J.; Khan, Z.I.; Shakeel, F.; Talegaonkar, S. (**2010**). Stability-indicating RP-HPLC method for analysis of atorvastatin in bulk drug, marketed tablet and nanoemulsion formulation. *J. Chil. Chem. Soc.* 55(2), 184–188.

Nagaoka, T.; Takahashi, A.; Sato, E.; Izumi, N.; Hein, T.W.; Kuo, L.; Yoshida, A. (**2006**). Effect of systemic administration of simvastatin on retinal circulation. *Arch. Ophthalmol.* 124(5), 665–670.

Negi, A.; Vernon, S.A. (**2003**). An overview of the eye in diabetes. *J. R. Soc. Med*. 96(6), 266–272.

Oliveira, A.S.; Schweizer, S.; Nolasco, P.; Barahona, I.; Saraiva, J.; Serro, A.P. (**2020**). Tough and low friction polyvinyl alcohol hydrogels loaded with anti-inflammatories for cartilage replacement. *Lubricants.* 8(3), 36.

Ooi, K.G.J.; Khoo, P.; Vaclavik, V.; Watson, S.L. (**2019b**). Statins in ophthalmology. *Surv. Ophthalmol.* 64(3), 401–432.

Ooi, K.G.J.; Lee, M.H.H.; Burlutsky, G.; Gopinath, B.; Mitchell, P.; Watson, S. (**2019a**). Association of dyslipidaemia and oral statin use, and dry eye disease symptoms in the blue mountains eye etudy. *Clin. Exp. Ophthalmol.* 47(2), 187–192.

Ooi, K.G.J.; Wakefield, D.; Billson, F.A.; Watson, S.L. (**2015**). Efficacy and safety of topical atorvastatin for the treatment of dry eye associated with blepharitis: A pilot study. *Ophthalmic Res.* 54(1), 26–33.

Özkiris, A.; Erkiliç, K.; Koç, A.; Mistik, S. (**2007**). Effect of atorvastatin on ocular blood flow velocities in patients with diabetic retinopathy. *Br. J. Ophthalmol.* 91(1), 69–73.

USC UNIVERSIDADE DE SANTIAGO DE COMPOSTELA

Phan, C.M.; Bajgrowicz, M.; Gao, H.; Subbaraman, L.N.; Jones, L.W. (**2016**). Release of fluconazole from contact lenses using a novel in vitro eye model. *Optom. Vis. Sci.* 93(4), 387–394.

Phan, C.M.; Subbaraman, L.; Jones, L. (**2014**). Contact lenses for antifungal ocular drug delivery: A review. *Expert Opin. Drug Deliv.* 11(4), 537–546.

Perova, T.S.; Vij, J.K.; Xu, H. (**1997**). Fourier transform infrared study of poly(2-hydroxyethyl methacrylate) PHEMA. *Colloid Polym. Sci.* 275, 323–332.

Refojo, M.F. (**1967**). Hydrophobic interaction in poly(2-Hydroxyethyl methacrylate) homogeneous hydrogel. *J. Polym. Sci.* 5(12), 3103–3113.

Ribeiro, A.; Veiga, F.; Santos, D.; Torres-Labandeira, J.J.; Concheiro, A.; Alvarez-Lorenzo, C. (**2011**). Receptor-based biomimetic NVP/DMA contact lenses for loading/eluting carbonic anhydrase inhibitors. *J. Memb. Sci.* 383(1), 60–69.

Rogers, W.J. (**2013**). The Effects of Sterilization on Medical Materials and Welded Devices. In *Joining and Assembly of Medical Materials and Devices*; Zhou, Y., Breyen, M.D., Eds.; Woodhead Publishing Limited: Cambridge, UK, 79.

Silva, D.; de Sousa, H.C.; Gil, M.H.; Santos, L.F.; Moutinho, G.M.; Salema-Oom, M.; Alvarez-Lorenzo, C.; Serro, A.P.; Saramago, B. (**2020**). Diclofenac sustained release from sterilised soft contact lens materials using an optimised layer-by-layer coating. *Int. J. Pharm.* 585, 119506.

Simmons, A. (**2012**). Future trends for the sterilisation of biomaterials and medical devices. In *Sterilisation of Biomaterials and Medical*

USC UNIVERSIDADE DE SANTIAGO DE COMPOSTELA

Devices; Lerouge, S., Simmons, A., Eds.; Woodhead Publishing Limited: Cambridge, UK; 310–320.

Sirtori, C.R. (**2014**). The pharmacology of statins. *Pharmacol. Res*. 88, 3–11.

Su, W.F. (**2013**). Radical chain polymerization. In *Principles of Polymer Design and Synthesis.* Lecture Notes in Chemistry; Su, W.F., Ed.; Springer: Berlin/Heidelberg, Germany, Volume 82, 137–183.

Terracina, J.J.; Bergkvist, M.; Sharfstein, S.T. (**2016**). Computational investigation of stoichiometric effects, binding site heterogeneities, and selectivities of molecularly imprinted polymers. *J. Mol. Model.* 22, 1-9.

Tieppo, A.; Boggs, A.C.; Pourjavad, P.; Byrne, M.E. (**2014**). Analysis of release kinetics of ocular therapeutics from drug releasing contact lenses: Best methods and practices to advance the field. *Contact Lens Ant. Eye.* 37(4), 305–313.

Tieppo, A.; White, C.J.; Paine, A.C.; Voyles, M.L.; McBride, M.K.; Byrne, M.E. (**2012**). Sustained in vivo release from imprinted therapeutic contact lenses. *J. Control. Release.* 157(3), 391–397.

Topete, A.; Pinto, C.A.; Barroso, H.; Saraiva, J.A.; Barahona, I.; Saramago, B.; Serro, A.P. (**2020**). High hydrostatic pressure as sterilization method for drug-loaded intraocular lenses. *ACS Biomater. Sci. Eng.* 6(7), 4051–4061.

Topete, A.; Serro, A.P.; Saramago, B. (**2019**). Dual drug delivery from intraocular lens material for prophylaxis of endophthalmitis in cataract surgery. *Int. J. Pharm.* 558, 43–52.

USC UNIVERSIDADE DE SANTIAGO DE COMPOSTELA

Varela-Garcia, A.; Concheiro, A.; Alvarez-Lorenzo, C. (**2020b**). Cytosine-functionalized bioinspired hydrogels for ocular delivery of antioxidant transferulic acid. *Biomater. Sci.* 8(4), 1171–1180.

Varela-Garcia, A.; Concheiro, A.; Alvarez-Lorenzo, C. (**2018**). Soluplus micelles for acyclovir ocular delivery: Formulation and cornea and sclera permeability. *Int. J. Pharm.* 552(1-2), 39–47.

Varela-Garcia, A.; Gomez-Amoza, J.L.; Concheiro, A.; Alvarez-Lorenzo, C. (**2020a**). Imprinted contact lenses for ocular administration of antiviral drugs. *Polymers.* 12(9), 2026.

Vejux, A.; Samadi, M.; Lizard, G. (**2011**). Contribution of cholesterol and oxysterols in the physiopathology of cataract: Implication for the development of pharmacological treatments. *J. Ophthalmol.* 2011, 471947.

Vieira-Potter, V.J.; Karamichos, D.; Lee, D.J. (**2016**). Ocular complications of diabetes and therapeutic approaches. *Biomed. Res. Int.* 2016, 3801570.

Wilson, S.L.; Ahearne, M.; Hopkinson, A. (**2015**). An overview of current techniques for ocular toxicity testing. *Toxicology.* 327, 32–46.

Wong, T.Y.; Ming, C.; Cheung, G.; Larsen, M.; Sharma, S. (**2016**). Diabetic retinopathy. *Nat. Rev. Disease Primers.* 2, 16012.

Yañez, F.; Chianella, I.; Piletsky, S.A.; Concheiro, A.; Alvarez-Lorenzo, C. (**2010**). Computational modeling and molecular imprinting for the development of acrylic polymers with high affinity for bile salts. *Anal. Chim. Acta.* 659(1-2), 178–185.

Yulianita, R.; Sopyan, I.; Muchtaridi, M. (**2018**). Forced degradation study of statins: A review. *Int. J. Appl. Pharm.* 10(6), 38–42.

USC UNIVERSIDADE DE SANTIAGO DE COMPOSTELA

Zhu, L.; Titone, R.; Robertson, D.M. (**2019**). The impact of hyperglycemia on the corneal epithelium: Molecular mechanisms and insight. *Ocul. Surf.* 17(4), 644–654.

USC UNIVERSIDADE DE SANTIAGO DE COMPOSTELA

USC
UNIVERSIDADE
DE SANTIAGO
DE COMPOSTELA

Chapter 4

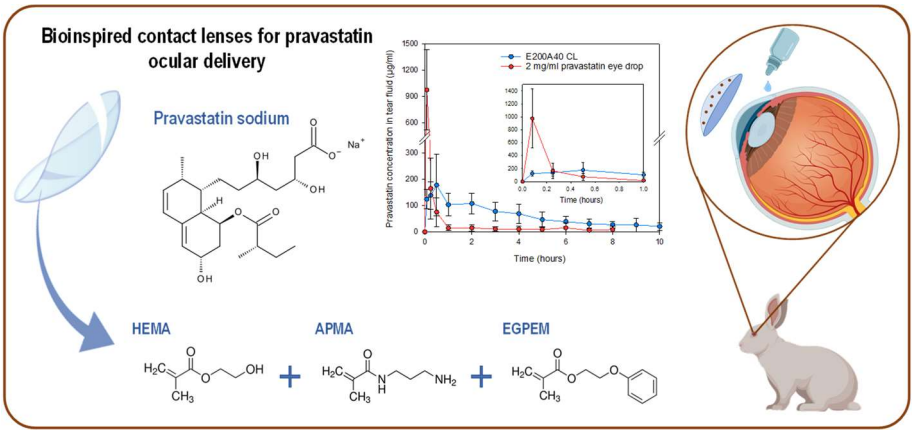

The work described in this chapter was published in **Contact lenses for pravastatin delivery to eye segments: Design and *in vitro-in vivo* correlations**, *Journal of Controlled Release* 348, 2022, 431-443, authored by

Ana F. Pereira-da-Mota[a], María Vivero-Lopez[a], Maria Serramito[b], Luis Diaz-Gomez[a], Ana Paula Serro[c], Gonzalo Carracedo[b], Fernando Huete-Toral[b], Angel Concheiro[a] and Carmen Alvarez-Lorenzo[a]

[a]Departamento de Farmacología, Farmacia y Tecnología Farmacéutica, I+D Farma Group (GI-1645), Facultad de Farmacia, Instituto de Materiales (iMATUS) and Health Research Institute of Santiago de Compostela (IDIS), Universidade de Santiago de Compostela, 15782 Santiago de Compostela, Spain.

[b]Ocupharm Research Group, Faculty of Optic and Optometry, University Complutense of Madrid, C/Arcos del Jalon 118, 28037 Madrid, Spain.

[c]Centro de Química Estrutural, Departamento de Engenharia Química, Instituto Superior Técnico, Universidade de Lisboa, Av. Rovisco Pais, 1049-001 Lisbon, Portugal.

USC UNIVERSIDADE DE SANTIAGO DE COMPOSTELA

USC
UNIVERSIDADE
DE SANTIAGO
DE COMPOSTELA

4. CONTACT LENSES FOR PRAVASTATIN DELIVERY TO EYE SEGMENTS: DESIGN AND IN VIVO-IN VITRO CORRELATIONS

4.1 INTRODUCTION

Statins are one of the most commonly prescribed drugs in the world. They are orally used for the first line treatment of hypercholesterolemia and reduction of cardiovascular disease risks by inhibiting 3-hydroxy-3-methyl-glutaryl coenzyme A (HMG-CoA) reductase, an important enzyme in the mevalonate pathway. Additionally, a better understanding of the mechanism of action of statins has revealed their pleiotropic capacity [Bedi et al., 2016]. Statins can inhibit the activity of Rho proteins and some of their targets, which provides anti-inflammatory, anti-proliferative, immunomodulatory, neuroprotective, and anti-diabetic effects, among others [Liao and Laufs, 2005]. Prolonged oral treatments with statins have revealed beneficial effects on ocular health [Ooi et al., 2019]. Statins may promote corneal healing, prevent cataract formation, and also reduce glaucoma severity [Ooi et al., 2019].

Regarding to the posterior segment, oral therapy of hypercholesterolemia with statins has been associated with reduction of hard exudates and microaneurysms in patients with diabetic macular edema, and lower incidence and slower progression of proliferative

USC UNIVERSIDADE DE SANTIAGO DE COMPOSTELA

diabetic retinopathy [Gupta et al., 2004; Ozkiris et al., 2007; Chung et al., 2017; Nielsen and Nordestgaard, 2014].

Diabetes mellitus is one of the world's greatest health challenges and is reaching epidemic proportions [International Diabetes Federation, 2021]. The lack of glycaemia control causes a variety of damages in multiple structures of the anterior and posterior segments of the eye, triggering the development of diabetic keratopathy, dry eye syndrome, cataracts, glaucoma, diabetic retinopathy and macular edema [Sayin, 2015; Misra et al., 2016]. Dysregulation of multiple molecular pathways contributes to upregulation of growth factors and inflammatory cytokines [Gologorsky et al., 2012; Wong et al. 2016]. Increased levels of plasma cytokines (tumor necrosis factor-α and interleukin-6) have been found in ocular fluid of diabetic patients [Esposito et al., 2002]. Other inflammatory mediators as prostaglandin E2 may also have a pathogenic role in diabetic retinopathy [Schoenberger et al., 2012]. Inhibition of mevalonate pathway by statins reduces oxidative stress, endothelial dysfunction, inflammation, and angiogenesis; thereby improving retina health [Zhang and McGwin, 2007]. Also, statins improve the integrity of endothelial cells, hence preserving the blood–retinal barrier [Ioannidou et al., 2017]. However, high oral doses may cause adverse systemic collateral effects, mainly on liver and muscle tissue [Murphy et al., 2020]. Therefore, the development of statin ophthalmic formulations that can provide sufficiently high levels of statins in the anterior and posterior segment of the eye, avoiding systemic absorption, may notably improve the ocular outcomes and the overall safety of the treatment. Statin ophthalmic formulations would also be useful for people who do not have hypercholesterolemia.

USC UNIVERSIDADE DE SANTIAGO DE COMPOSTELA

Pilot studies have shown that topical ocular administration of atorvastatin eye drops is well tolerated in prolonged treatments of dry eye and blepharitis, but frequent instillation is required due to low ocular bioavailability [Ooi et al., 2015]. Sustained drug release from contact lenses (CLs) may provide more prolonged levels in tear fluid and with fewer fluctuations compared to eye drops, which in turn favours drug penetration into anterior eye segment [Li and Chauhan, 2006; Dixon et al., 2018; Wu et al., 2021]. Indeed, the first medicated CL has been approved in 2021 for the management of allergic conjunctivitis [Johnson & Johnson News, 2021]. Moreover, it has been recently demonstrated in animal models that such an increase in the amount permeated may make even possible that some specific drugs may reach the posterior segment as recorded for, for example, epalrestat [Zhu and Sheng, 2020], ofloxacin [Shikamura et al., 2016] and timolol [Maulvi et al., 2019]. Nevertheless, the development of medicated CLs has to face up to the problem of that the affinity of commercially available CLs for most used ophthalmic drugs is low. Therefore, CLs have to be *ad hoc* designed for each target drug in order to uptake therapeutic doses and to provide sustained release on the eye surface [Alvarez-Lorenzo et al., 2019].

A variety of approaches, which include film coatings, molecular imprinting and drug nanoencapsulation, among others, are under investigation to overcome the loading and release limitations shown by CLs [Kakisu et al., 2013; Minami et al., 2019; Sekar and Chauhan, 2019; DiPasquale et al., 2021; Toffoletto et al., 2021]. Among these approaches, the recreation of biomimetic receptors that resemble the composition and spatial ordering of the physiological receptor of the drug without compromising relevant optical properties of CLs is pointed out as a successful strategy [Alvarez-Lorenzo et al., 2019]. Another barrier to be solved for the development and clinical translation

USC UNIVERSIDADE DE SANTIAGO DE COMPOSTELA

of drug-loaded CLs is that *in vitro* release methods that can predict *in vivo* release behaviour are still to be identified because there are too many variables involved [Tieppo et al., 2014; Mahomed et al., 2016; Paradiso et al., 2017; Phan et al., 2021]. In most reports on CLs the *in vitro* release tests are used for optimization of drug release kinetics although with limited basis of how the *in vitro* release profiles may correlate with the *in vivo* release kinetics [Hui and Wilcox, 2016; Pereira-da-Mota et al., 2022].

In a previous study, CLs soaked in atorvastatin calcium solution demonstrated improved drug accumulation *ex vivo* in cornea and sclera, but the drug did not penetrate further probably because its large molecular weight (1155.3 g/mol) and hydrophobicity (Log P = 6.36) caused the ocular permeability to be very low [Pereira-da-Mota et al., 2021]. Thus, the present work relied on the hypothesis of that a smaller and more hydrophilic statin, like pravastatin sodium (446.5 g/mol; Log P = - 0.23 [Murphy et al., 2020]; **Figure 4.1**) adequately formulated in a CL may get access to deeper eye tissues. Accordingly, the aim of this work was to design CLs bioinspired in the natural receptor of pravastatin, i.e., the HMG-CoA reductase. This natural receptor contains amino acids with a wide variety of hydroxyl groups, hydrophobic groups, and high density of protonated amino groups [Jain et al., 2007], which could be resembled using 2-hydroxyethyl methacrylate (HEMA), ethylene glycol phenyl ether methacrylate (EGPEM), and N-(3-aminopropyl) methacrylamide hydrochloride (APMA), respectively (**Figure 4.1**). All hydrogels were characterized in terms of solvent uptake, light transmission, mechanical properties and pravastatin loading and release capacity. The effects of high hydrostatic pressure (HHP) and autoclave sterilization on pravastatin solutions and pravastatin-loaded hydrogels were also evaluated. Preliminary screening of cytocompatibility and ocular tolerance was

USC UNIVERSIDADE DE SANTIAGO DE COMPOSTELA

carried out with Balb/3T3 fibroblasts and HET-CAM assay. Pravastatin permeability was assessed *ex vivo* using porcine cornea and sclera tissues. Anti-inflammatory activity of pravastatin-loaded hydrogels was also investigated. Finally, *in vivo* experiments with the most promising CLs were performed in New Zealand white rabbits to investigate the *in vivo* release profiles of pravastatin-loaded CLs and to quantify pravastatin levels in anterior and posterior segment ocular tissues. An additional aim of the work was to identify *in vitro* release conditions that may provide *in vitro-in vivo* correlations (IVIVC). To the best of our knowledge, this is the first time that the effect of the volume and protein composition of the release medium on Levy plots is evaluated.

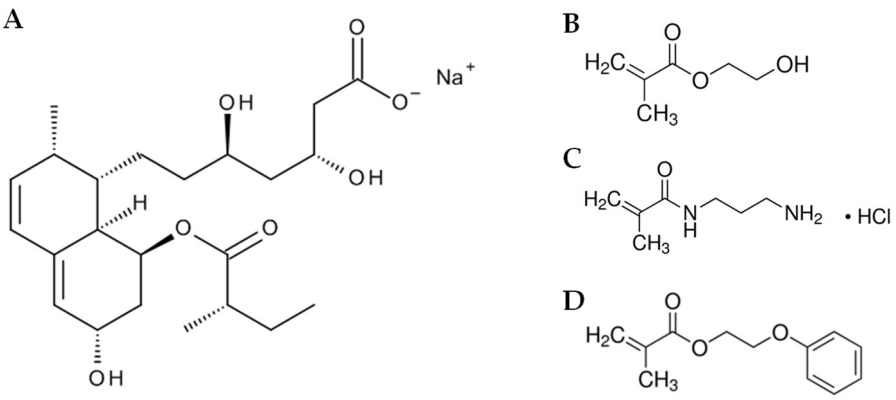

Figure 4.1. Molecular structure of pravastatin sodium (**A**) and monomers used to synthesize the hydrogels: (**B**) 2-hydroxyethyl methacrylate (HEMA); (**C**) N-(3-aminopropyl) methacrylamide hydrochloride (APMA), and (**D**) ethylene glycol phenyl ether methacrylate (EGPEM).

USC UNIVERSIDADE DE SANTIAGO DE COMPOSTELA

4.2 MATERIALS AND METHODS

4.2.1 Materials

Pravastatin sodium was supplied by Biocon Limited (Bengaluru, Karnataka, India). 2-Hydroxyethyl methacrylate (HEMA) was from Merck (Darmstadt, Germany), and N-(3-aminopropyl) ethacrylamide hydrochloride (APMA) from PolySciences Inc. (Warrington, PA, USA). Ethylene glycol dimethacrylate (EGDMA), ethylene glycol phenyl ether methacrylate (EGPEM), 2,2′ -azobis(isobutyronitrile) (AIBN), and dichlorodimethylsilane were from Sigma-Aldrich (Steinheim, Germany). Simulated lachrymal fluid (SLF), pH 7.4, was prepared in 1 liter of ultrapure water as follows: 2.18 g $NaHCO_3$ from Probus (Barcelona, Spain), 6.78 g NaCl from Scharlab (Barcelona, Spain), 1.38 g KCl, and 0.084 g $CaCl_2 \cdot 2H_2O$ from Merck (Darmstadt, Germany). Bicarbonate Ringer's solution, pH 7.2, was prepared by mixing 100 mL of buffer solution A (0.071 g KCl, 1.24 g NaCl, 0.49 g $NaHCO_3$, and 0.02 g NaH_2PO_4, from Merck (Darmstadt, Germany)) and buffer solution B (0.031 g $MgCl_2$, and 0.023 g $CaCl_2$ from Panreac (Barcelona, Spain)). Ultrapure water (resistivity >18.2 MΩ cm; Milli-Q®, Millipore Ibérica, Madrid, Spain) was obtained by reverse osmosis. Methanol 99.9% for LC-MS grade was from Fisher Scientific (Loughborough, UK). Acetonitrile for HPLC LC-MS grade and NaOH were from VWR Chemicals (Fontenary-Sous-Bois, France). Balb/3T3 fibroblasts (ATCC CCL-163™) and THP-1 cells (ATCC TIB-202™) were provided by American Type Culture Collection (ATCC, Manassas, VA, USA). Dulbecco's modified Eagle medium (DMEM), Dulbecco's phosphate buffered solution (DPBS), and RPMI 1640 was from Fisher Scientific (Newington, NH, USA). Fetal bovine serum, antibiotic solution (penicillin and streptomycin), lipopolysaccharides (LPS) from Escherichia coli O111:B4, phorbol 12-myristate 13-acetate

USC UNIVERSIDADE DE SANTIAGO DE COMPOSTELA

(PMA), and TrypLE® were acquired from Sigma-Aldrich (St. Louis, MO, USA). Cell counting kit-8 (CCK-8) was from Dojindo Molecular Technologies (Rockville, MD, USA). Schirmer test strips were from Contacare Ophthalmics and Diagnostics (Gujarat, India). Pentobarbital (400 mg/mL) was from Richter Pharma AG, Wels, Austria.

4.2.2 Synthesis of Hydrogel Discs and CLs

Four different hydrogels were synthesized combining HEMA, EGPEM, and APMA, as summarized in **Table 4.1**. Briefly, the monomers were mixed into glass vials and magnetically stirred (200 rpm) for 120 min at room temperature. Then, EGDMA (crosslinker) and AIBN (initiator) were added, and the solutions were magnetically stirred again (100 rpm) for 10 min. The resulting solutions were immediately injected into moulds composed of two glass plates (10 × 10 cm) separated by a silicone frame with 0.3 mm of thickness, and heated at 50 °C for 12 h, and then to 70 °C for further 24 h for thermal polymerization [Alvarez-Lorenzo et al., 2002].

After polymerization, each hydrogel sheet was boiled (1 L water) for 15 min to remove unreacted substances and facilitate cutting in the form of 10 mm discs. The discs were alternatively washed in water and 0.9% NaCl twice a day (200 rpm magnetic stirring, room temperature), until complete removal of the unreacted monomers as monitored spectrophotometrically (UV–Vis spectrophotometer, Agilent 8453, Waldbronn, Germany). Finally, the discs were dried at 70 °C for 24 h before being stored and used in further experiments.

CLs were prepared with the same composition as E200A40 hydrogel, but adding more AIBN (14.79 mg, initiator) for a complete

USC UNIVERSIDADE DE SANTIAGO DE COMPOSTELA

polymerization of the thinner hydrogels. The monomer solution was pipetted (60 µL) in curved polypropylene moulds (similar to those used for industrial production of CLs) to have final CL dimensions in the hydrated state (phosphate buffer pH 7.4) of approx. 12 mm diameter, 7.8 mm curvature, and 0.1 mm thickness. After polymerization at 50 °C for 12 h and then at 70 °C for 24 h, all CLs were washed as described above. Finally, the CLs were dried at 70 °C for 24 h.

Table 4.1. Composition of the monomer mixtures used to synthesize the hydrogels. To each mixture, 4.93 mg AIBN were added.

Hydrogel Code	HEMA (mL)	EGDMA (µL)	EGPEM (µL)	APMA (mg)
E0A0	3	12.10	-	-
E200A0	3	12.10	112.50	-
E200A40	3	12.10	112.50	21.45
E0A40	3	12.10	-	21.45

4.2.3 Hydrogel Characterization

Solvent uptake capacity was evaluated, in triplicate, from the mass increase of previously weighed dried discs (W_0) after being immersed in 10 mL of SLF at room temperature without agitation until equilibrium (W_t), as follows:

$$Solvent\ uptake = \frac{W_0 - W_t}{W_0} \times 100 \qquad \text{(Eq. 4.1)}$$

Water contact angles on dried and wet hydrogels (10 mm in diameter) were measured using the sessile drop method with a Phoenix-300 goniometer (Surface Electro Optics Co., Suwon, Korea). The measurements were performed over 2 discs of each formulation, at room temperature, and with distilled water. A total of 10 images were

USC UNIVERSIDADE DE SANTIAGO DE COMPOSTELA

captured in 10 s, and the best-adjusted pictures were selected to obtain the contact angle value.

Ion permeability was recorded in triplicate by fixing individual wet hydrogel discs between two flat Teflon washers (8 mm open diameter), which were fixed in a screw cap (open top) and screwed in a 5-mL HPLC vial. The bottom of the vials was previously removed. The vials were placed downward in beakers containing 15 mL distilled water at 35 °C and magnetically stirred (130 rpm) (**Figure 4.2**). The surface available for diffusion was 50.27 mm^2. Then 4 mL NaCl 0.1 M solution were added to the vial and the conductivity was recorded as a function of time using an InLab® 741 conductivity probe fitted to a Mettler Toledo T70 titrator (Greifensee, Switzerland).

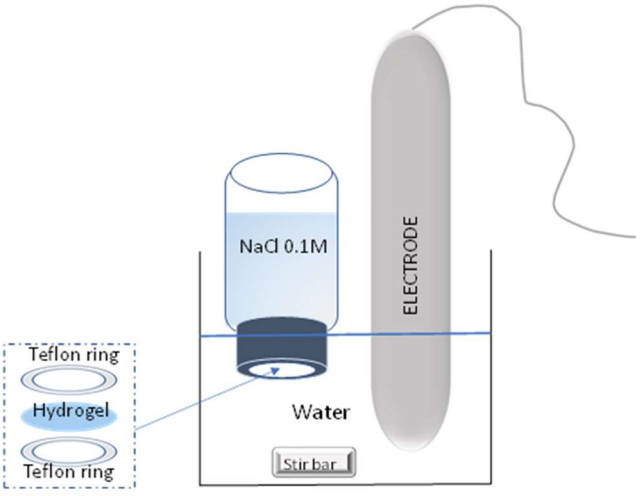

Figure 4.2. Setup used to measure the ion permeability of the hydrogels.

The transmittance of the hydrogels swollen in SLF was recorded in an UV–Vis spectrophotometer (Agilent 8453, Waldbronn, Germany), in the 200–800 nm range (n = 3).

Mechanical properties of dog bone-shaped hydrogels (18 × 5 mm, in the center 6 × 2.5 mm) were tested using a TA.XT Express Texture Analyzer (Stable Micro Systems, Godalming, UK) fitted with a 50 N load cell. The hydrogel probes (n = 5) were fixed to the upper and lower clamps, and the tensile test was carried out applying a test speed of 0.25 mm/s and 0.005 N trigger force. The elastic modulus was calculated from the initial slope of the engineered stress-strain curve [Kim et al., 2018].

4.2.4 Pravastatin Loading and Release

Pravastatin was loaded by soaking the dried discs in pravastatin sodium (0.1 mg/mL; 10 mL) solution. The experiment was repeated several times and in each run 4 discs of each composition were tested. The vials were kept under oscillatory movement (180 osc/min) at room temperature and protected from light. After 48 h, the absorbance of the loading solution was measured at 238 nm (UV–Vis spectrophotometer, Agilent 8453, Waldbronn, Germany). The amount loaded was calculated as the difference between the initial and final amount of pravastatin in the solutions using previously prepared calibration curves. The network/water partition coefficient was estimated as follows [Kim et al., 1992]:

$$K_{\frac{N}{W}} = \frac{Loading - \left(\frac{V_S}{W_p}\right) \times C_0}{C_0} \qquad \text{(Eq. 4.2)}$$

USC UNIVERSIDADE DE SANTIAGO DE COMPOSTELA

In this equation, V_s is the solvent volume sorbed by the hydrogel, W_p the dried hydrogel weight, and C_0 the initial concentration of the loading solution.

In vitro drug release patterns were recorded by immersing loaded discs ($n = 4$) in vials containing 10 mL of SLF (pH = 7.4) at 37 °C. The discs were previously rinsed with SLF to remove the excess of pravastatin from the hydrogel surface. The experiments were performed for 120 h under oscillatory movement (180 osc/min) and protected from light. At predetermined time points, 3 mL of the release medium were collected, absorbance measured at 238 nm and the sample returned to the vial immediately. After 8 h of experiment, 2 mL of the release medium were collected and replaced by the same volume of fresh SLF to avoid false plateaus. The test was carried out under sink conditions.

4.2.4.1 Pravastatin Release from Sterile CLs

The synthetized CLs (E200A40 composition) were immersed in a pravastatin solution (0.1 mg/mL) for 48 h and then sterilized in closed packages by high hydrostatic pressure (HHP) (Section 4.2.8). The CLs were stored at room temperature until release experiments were performed. The CLs were immersed in 2 or 10 mL of SLF without or with lysozyme or bovine serum albumin (2.68 mg/mL). The experiments were performed at 37 °C, under oscillatory movement (180 osc/min) and at predefined timepoints, 150 μL were removed and replaced by the same volume of fresh SLF, or SLF plus lysozyme or BSA. The amount of pravastatin released from the CLs was quantified by HPLC (as described in section 4.2.7) after denaturation of the proteins (section 4.2.9.2). The amount of protein deposited on blank (non-drug loaded) CLs was monitored at 280 nm (UV–Vis

USC UNIVERSIDADE DE SANTIAGO DE COMPOSTELA

spectrophotometer, Agilent 8453, Waldbronn, Germany) at the same time points as for the drug release test.

4.2.5 HET-CAM Test

The potential ocular irritation of pravastatin-loaded hydrogels was evaluated using the hen's egg test on the chorioallantoic membrane (HET–CAM) assay, as previously described [Alvarez-Rivera et al., 2019]. On the eighth day after egg fertilization, the eggshell at the wider extreme of the egg was removed and the CAM was exposed. Pravastatin-loaded hydrogels (n = 2, 10 mm discs) and 300 µL of pravastatin solution (0.1 mg/mL) were carefully placed on the CAM and the possible haemorrhage, vascular lysis, or coagulation of the vessels was monitored for 5 min. 0.9% NaCl and 0.1 N NaOH solutions were used as negative and positive controls, respectively. Finally, the irritation score (IS) was calculated as reported previously [Alvarez-Rivera et al., 2019].

4.2.6 Cytocompatibility and Anti-inflammatory Activity

Balb/3T3 fibroblasts (ATCC CCL-163™) were cultured in Dulbecco's modified Eagle medium (DMEM) with 10% fetal bovine serum and 1% antibiotics (10,000 U/mL penicillin and 10,000 µg/mL streptomycin) at 37 °C and 5% CO_2. Then, cells were detached from the culturing flasks using TrypLE® at 80% confluence. Suspended cells were counted, seeded in wells of 96-well plates (20,000 cells/well), and allowed to attach for 24 h.

USC UNIVERSIDADE DE SANTIAGO DE COMPOSTELA

Non-loaded and pravastatin-loaded hydrogels were evaluated. Dried hydrogels (10 mm discs) were immersed in pravastatin solution (0.1 mg/mL) for 48 h or in 0.9% NaCl (non-loaded hydrogels), cut in four symmetric pieces and sterilized using HHP method (as described in Section 4.2.8). One piece of each hydrogel was placed in contact with the cells and incubated for 24 or 48 h. Five replicates for each hydrogel were tested. Cells without treatment (negative control) and cells incubated with pravastatin solution (0.05 and 0.1 mg/mL) were also tested.

Cell viability was assessed using a Cell Counting kit-8 (CCK-8) following the manufacturer' instructions. Briefly, hydrogel pieces and culture medium were removed from the wells, and 200 µL of a CCK-8 working solution (10% *v/v* CCK-8 reagent in DMEM) were added to each well and incubated for 1 h at 37 °C. The absorbance was measured at 450 nm (UV Bio-Rad Model 680 microplate reader, Hercules, CA, USA), and cell viability (%) was normalized to the negative control as follows.

$$Cell\ viability\ (\%) = \frac{Abs_{exp}}{Abs_{negative\ control}} \times 100 \qquad \text{(Eq. 4.3)}$$

The anti-inflammatory effects of non-loaded and pravastatin-loaded E200A40 hydrogels were evaluated in THP-1 human monocytes (ATCC TIB-202™). The macrophage cell line was cultured in RPMI 1640 supplemented with 10% fetal bovine serum, 1% penicillin-streptomycin and maintained at 37 °C, 5% of CO_2 and 90% relative humidity. Phorbol 12- myristate 13-acetate (PMA; 200 nM) was added to promote the differentiation of THP-1 cells into macrophages incubating for 72 h at 37 °C [Chanput et al., 2014]. After macrophage differentiation, PMA solution was removed and cell monolayers were washed with DPBS, trypsinized and a specific cell scraper was used to

USC UNIVERSIDADE DE SANTIAGO DE COMPOSTELA

remove all adherent cells. Macrophages were seeded at a density of 50,000 cells/well into 24-well plates for 6 h. After this period, one piece of non-loaded and loaded E200A40 previously sterilized discs was added to each well. Also, three different concentrations of pravastatin sodium (0.1, 1, and 10 μM) were tested. After 12 h, cells were stimulated with LPS (100 ng/mL) and incubated for 24 h at 37 °C, 5% of CO_2 and 90% relative humidity. Cells treated with only LPS served as positive controls, while unstimulated cells (without LPS) were used as negative controls. After incubation, cell culture supernatants were collected, and the secretion of TNF-α and IL-6 was analyzed by specific ELISA kits (Sigma-Aldrich, St. Louis, MO, USA, and RayBiotech, Norcross, GA, USA, respectively) following the manufacturer's instructions incubated with pravastatin solution (0.05 and 0.1 mg/mL) were also tested.

4.2.7 *Ex vivo* Cornea and Sclera Permeability

Ex vivo cornea and sclera permeability assays were carried out with pravastatin-loaded E200A40 and E0A40 hydrogels according to previous described protocols [Alvarez-Rivera et al., 2019; Varela-Garcia et al., 2020]. Fresh porcine eyes were provided by a local slaughterhouse and transported completely immersed in PBS solution in an ice bath. Corneas and sclera tissues were isolated, washed with PBS, and mounted in vertical diffusion Franz cells. Both chambers were filled with bicarbonate Ringer's solution, pH 7.2, prepared with concentrations of bicarbonate and electrolyte ions similar to those in the extracellular fluid [Wang et al., 2021] and commonly used to preserve ocular tissues [Paliwal et al., 2009]. The receptor chamber was immersed in a water bath at 37 °C. After 30 min of tissues balance, the buffer solution in the donor chamber was removed and replaced with

USC UNIVERSIDADE DE SANTIAGO DE COMPOSTELA

pravastatin-loaded hydrogels (E200A40 and E0A40) or 1 mL of pravastatin solution (128 μg/mL). SLF (2 mL) was added onto the hydrogels, and the donor chambers were covered with parafilm to prevent evaporation. Samples (1 mL) from the receptor medium were taken at 30 min, 1, 2, 3, 4, 5 and 6 h and replaced with the same volume of fresh bicarbonate Ringer's solution. After 6 h of experiment, the corneal and scleral tissues were removed from the diffusion cells, and soaked in 3 mL of ethanol:water (50:50 *v/v*) mixture overnight at 37 °C under magnetic stirring. Then, they were sonicated for 99 min at 37 °C and centrifuged (1,000 rpm, 5 min, 25 °C), and the supernatants filtered and centrifuged again (14,000 rpm, 20 min, 25 °C) for HPLC analysis.

The amounts of pravastatin in the donor chamber, drug accumulated in the tissues and drug permeated were quantified by HPLC (AS-4140 autosampler, PU-4180 pump, LC-NetII/ADC interface box, CO-4060 column oven, MD-4010 photodiode array detector, JASCO, Tokyo, Japan) fitted with a Waters Symmetry C18 column (5 μm, 3.9 × 150 mm) and operated with ChromNAV software v.2. Mobile phase consisted of methanol:0.02 M sodium phosphate (NaH_2PO_4) buffer (50:50 *v/v*, pH adjusted to 7.0 with NaOH) at 1.00 mL/min and 25 °C [Onal and Sagirli, 2006]. The injection volume was 50 μL, and the total run time of each sample was 10 min. Pravastatin was quantified at 238 nm (retention time 5.15 min). The HPLC method was validated using pravastatin solutions in bicarbonate Ringer's buffer in the 0.05 to 16 μg/mL range. The flux, J, was obtained from the slope of the regression of the amount of drug in the receptor chamber (Q) per surface area available for diffusion versus time (t) [Al-Ghabeish et al., 2015; Varela-Garcia et al., 2018]. The apparent permeability coefficient, P*app*, was calculated as the ratio between the flux (J) and the drug concentration in the donor chamber measured at time point 6 h.

USC UNIVERSIDADE DE SANTIAGO DE COMPOSTELA

4.2.8 Sterilization and Stability of Pravastatin-Loaded Hydrogels

The stability of pravastatin-loaded E200A40 and E0A40 hydrogels after sterilization was evaluated using two different protocols: a) steam heat (SH; autoclave Uniclave 88/75 L; A. J. Costa, Cacém, Portugal) for 1 h at 1 bar and 121 °C sterilization; and b) high hydrostatic pressure (HHP; 70 °C, 600 MPa for 10 min) sterilization. Previously developed protocols were followed [Pereira-da-Mota et al., 2021]. After sterilization, the amount of pravastatin in the hydrogels and the release kinetics were monitored again as described above (Section 4.2.4).

Aliquots of pravastatin solution (0.1 mg/mL) were also sterilized by SH or HHP under the same conditions as the hydrogels and investigated regarding degradation products using HPLC (Section 4.2.7).

Additionally, stability of pravastatin during exposition to daylight conditions was evaluated by exposing aliquots of pravastatin aqueous solution (0.05 mg/mL) in quartz cells to fluorescent tube light (F8T5 Daylight, 6500 K, Hitachi, Japan) for 6 h at room temperature. HPLC chromatograms were recorded before and after the exposition to the light (Section 4.2.7).

4.2.9 *In vivo* Experiments: Drug Release and Tissue Accumulation

Dried CLs were individually packed in polyamide/polyethylene bags filled with 10 mL of pravastatin solution (0.1 mg/mL). The CLs were maintained for 48 h in pravastatin solution, sterilized by HHP and stored at room temperature until being placed on the rabbits ocular

USC UNIVERSIDADE DE SANTIAGO DE COMPOSTELA

surface. All experiments were performed according to the Association for Research in Vision and Ophthalmology Statement for the Use of Animals in Ophthalmic and Vision Research and to European Directive 2010/63/EU. The protocols were approved by the Committee for Animal Experimentation of the Universidad Complutense de Madrid [Registration number: O00023280e2100023620]. The study was supported by the European Union's Horizon 2020 research and innovation programme under the Marie Skłodowska-Curie Actions grant agreement N◦ 813440 (ORBITAL–Ocular Research by Integrated Training And Learning). The founder had no role in the study.

Ten healthy male New Zealand white rabbits (age approx. 3 months weighing 4.36 ± 0.23 Kg) were included in the *in vivo* experiments. The animals were in a light-controlled room (12 h light/ 12 h dark cycles) at 18 °C in individual cages with total access to food and water. Rabbits with low weight or corneal disruptions were not included in the study. During the experiments and sampling, the rabbits were placed in rabbit restrainers with continuously monitoring to not remove the CLs placed on the ocular surface.

To minimize the effects of subjective bias, the experiments were carried out in three days and the rabbits were randomly divided into two groups, CLs group (n = 6) and one-eye drop group (n = 4). In the eye drops group, one drop (50 µL; 2 mg/mL of pravastatin) was instilled and the rabbits were euthanized 8 h after. The CLs group was divided into other two subgroups, the subgroup of rabbits (n = 3) that wore the CLs for 8 h and were euthanized after this period, and the subgroup of rabbits (n = 3) that wore the CLs for 10 h and were euthanized after 24 h (summarized in **Figure 4.3**). No confounders were controlled as the presence of the CLs was evident on the ocular surface of the rabbits. All experiments started at 7:30 – 8:30 a.m. No animal or data was

USC UNIVERSIDADE DE SANTIAGO DE COMPOSTELA

discarded. No adverse events were detected. On the first day, two rabbits of 8 h wear CLs, and one rabbit of eye drop groups were assayed. On the second day, one rabbit of 8h wear CLs and three rabbits of the eye drop groups were assayed. On the third day, the three rabbits of 10 h wear CLs group were assayed.

For the sample size calculation the 3R's principles were followed minimizing the number of rabbits used and trying to obtain the most reliable results. A total of 10 animals were used in this two-treatment parallel-design study. This design allowed the study detected a treatment difference at 0.05 significance level with a probability of 80% if the difference between treatments was 2.03 times the standard deviation.

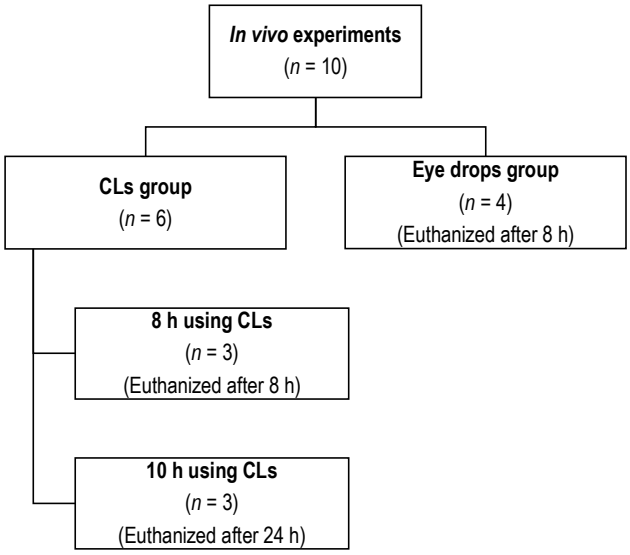

Figure 4.3. Animals distribution in *in vivo* experiments.

USC UNIVERSIDADE DE SANTIAGO DE COMPOSTELA

4.2.9.1 In vivo Release

The ocular surface of each rabbit was carefully inspected with a VX75 slit lamp (Luneau Technology, Chartres, France) before and after 8 h of the experiment. The CLs were removed from the sterilized bags, rinsed with sterile saline solution for CLs (to remove excess drug on the surface of the CL), and carefully placed on the rabbit right eye without local anaesthesia. The CLs were placed in the cornea and bulbar conjunctiva below the nictitating membrane. No nictitating membranectomy or tarsorrhaphy was needed. To prevent drying of CL on the surface of the eye, every 15 min the rabbits' eyes were closed for 1 min. The left eye was kept as control without treatment. In the eye drop group, a single drop (50 μL) of 2 mg/mL of pravastatin solution, which contained the same amount of pravastatin as that released from the CLs after 8–10 h, was gently instilled in the lower conjunctival sac of the right eye using a micropipette. Before and after administration (t = 5 min, 15 min, 30 min, and every hour until 8 or 10 h) tear fluid samples were collected using Schirmer test strips which were placed in the tarsal conjunctiva of the lower lid for 10 s with closed eyes [van Bijsterveld, 1969]. The volume of tears collected from the Schirmer strips was recorded as millimetres of moistened strip.

The mean residence time (MRT) was calculated as the area under the curve of concentration versus time (AUMC) referred to the area under the curve of concentration versus time (AUC). Both AUMC and AUC were calculated from the experimental data applying the trapezoidal rule [Hiratani et al., 2005]. After wearing, CLs were extracted with SLF (0.8 mL under stirring at 37 °C for 24 h) and the remnant pravastatin was quantified by HPLC.

USC UNIVERSIDADE DE SANTIAGO DE COMPOSTELA

4.2.9.2 Quantification of Pravastatin in Tear Fluid

The Schirmer test strips were placed in 2 mL Eppendorf tubes with 200 µL of SLF for 12 h at 4 °C. For protein denaturation, the samples were vortexed for 1 min, and the strips were removed from the tubes. Then, SLF solution was heated at 98 °C for 2 min, cooled in ice for 10 min, and centrifuged at 13,000 rpm for 10 min at 25 °C [Lazarowski et al., 2003]. Finally, the supernatants were collected and stored at − 20 °C until HPLC analysis (as described in Section 4.2.7). In preliminary tests, this protein denaturation method was shown to reproducibly recover >95% pravastatin present in the samples.

In vitro-in vivo correlations (IVIVC) were attempted through Levy plot analysis, where the X-axis was reported as the percentage of drug released *in vitro* at a certain time, and the Y-axis the percentage of drug released in the tear fluid at the same time estimated as follows [Xu et al., 2019].

$$Pravastatin\ released\ in\ vivo\ (\%) = \frac{AUC_{0-t}}{AUC_{0-tes}} \times 100 \qquad \text{(Eq. 4.4)}$$

Regression analysis was carried out using SigmaPlot for Windows v.14 software (Systat Sofware Inc., Germany).

4.2.9.3 Quantification of Pravastatin in Ocular Tissues

All the rabbits were euthanized by intravenous administration of 0.75 mL/Kg of propofol and 0.5 mL/Kg of pentobarbital sodium (approx. 2 mL, Exagon 400 mg/mL). Following euthanization, aqueous humour was directly extracted from the anterior chamber using a needle and stored at 4 °C until being processed for protein denaturation. Then, the eyes were enucleated and immediately stored at − 80 ◦C until tissue

USC UNIVERSIDADE DE SANTIAGO DE COMPOSTELA

dissection, when cornea, sclera, crystalline lens, vitreous humour, and retina were weighed and separately placed in Eppendorf tubes. SLF was added to cornea (500 µL), crystalline (500 µL), sclera (800 µL) and retina (200 µL). The tissues remained immersed in SLF for 12 h at 4 °C, and then the protein denaturation process was performed as previously described. The supernatant was collected and stored at − 20 °C until UPLC analysis. Before UPLC analysis all the samples were centrifuged at 5,000 rpm, 4 °C for 10 min. UPLC analysis was performed on a Waters Acquity UPLC H-Class coupled with a Xevo TQD MS System. The chromatographic separation was performed on a HypersilGOLD C18 (Thermo-Fisher, 1.9 µm, 2.1 × 50 mm) column with a column temperature of 35 °C, a flow rate of 0.6 mL/min, and a mobile phase containing 0.1% formic acid/water (A) and 0.1% formic acid/acetonitrile (B). The gradient was programmed as follows: 0–0.1 min 5% B, 0.1–1.0 min 5–100% B, 1.0–2.0 min 100% B, 2.0–2.1 min 100–95% B, and 2.1–2.5 min 5% B. Electrospray ionization (ESI) was run in positive mode with a source temperature of 150 °C and a desolvation temperature of 500 °C. Capillary voltage was set to 3 kV and the cone voltage was set to 45 V. Desolvation gas flow was 900 L/h and cone gas flow was set to 50 L/h. Pravastatin was monitored in selected ion recording (SIR) mode using the m/z of 447.101.

4.2.10 Statistical Analysis

Statistical analysis was performed using Statgraphics Centurion 18 v. 18.1.13 (Statgraphics Technologies, Inc., Warrenton, VA, USA). The descriptive data were presented as mean ± standard deviation. One-way analysis of variance (ANOVA) followed by Multiple Range Test was carried out. The level of significance was 0.05.

USC UNIVERSIDADE DE SANTIAGO DE COMPOSTELA

4.3 RESULTS AND DISCUSSION

4.3.1 Hydrogels Synthesis and Characterization

Hydrogels were synthesized combining HEMA with EGPEM and APMA searching for a good balance between solvent uptake, light transmission and mechanical properties, and binding affinity for statins. APMA was chosen as functional monomer able to mimic cationic amino acids involved in the binding site of HMG-CoA reductase [Istvan and Deisenhofer, 2001]. Incorporation of EGPEM was proposed for hydrophobic interactions with the benzyl group of pravastatin sodium enhancing drug binding through π–π stacking [Pereira-da-Mota et al., 2021]. EGPEM and APMA dissolved quickly in HEMA solution at concentrations of 200 and 40 mM, respectively. The hydrogels were coded as ExAy, where x referred to the concentration of EGPEM in mM, and y referred to APMA concentration in mM in the monomers mixture.

Dried hydrogels swelled quite fast after being immersed in SLF, achieving the solvent uptake plateau in 1 h (**Figure 4.4A**). Hydrogels prepared with the hydrophobic monomer EGPEM showed lower water uptake (44.05 ± 0.40% for E200A0) compared to those bearing only APMA (52.91 ± 1.97% for E0A0) ($p < 0.05$). APMA did not alter the swelling of HEMA hydrogels. EGPEM-bearing hydrogels also showed greater water contact angles when tested both in the dried and wet states (**Table 4.2**); nevertheless, in all cases the contact angles were below 90° and the hydrogels can be considered to have hydrophilic surface. NaCl permeability, calculated as recorded in **Figure 4.4B** ranked in the order E0A40 ($8.3 \cdot 10^{-6}$ cm/s) > E0A0 ($7.8 \cdot 10^{-6}$ cm/s) > E200A0 ($5.7 \cdot 10^{-6}$ cm/s) > E200A40 ($3.5 \cdot 10^{-6}$ cm/s). The higher values corresponded to the most hydrophilic hydrogels in good agreement with previous reports

USC UNIVERSIDADE DE SANTIAGO DE COMPOSTELA

and in the range typical of CLs [Peng and Chauhan, 2012; Pozuelo et al., 2014].

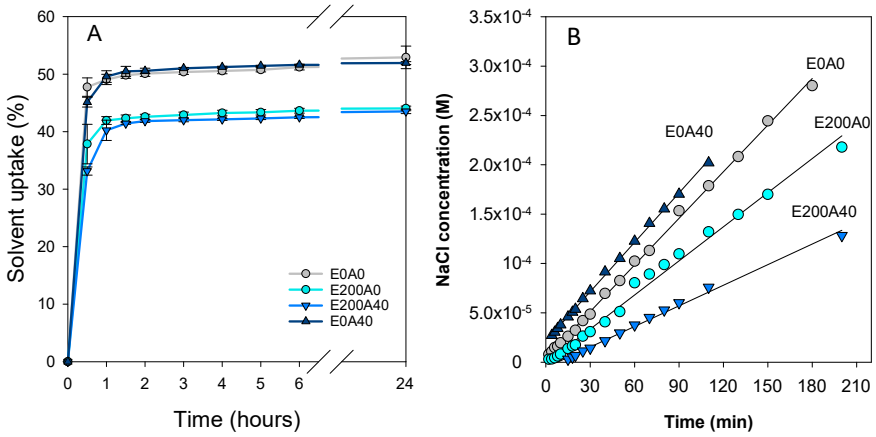

Figure 4.4. (**A**) Solvent uptake profiles in SLF at room temperature and (**B**) data recorded as increase in NaCl concentration in the receptor as a function of time. Codes as in Table 4.1.

Table 4.2. Water contact angles of the hydrogels before and after being swollen in water using the sessile drop method. Hydrogel codes as in Table 1 (*n* = 4; mean value ± standard deviations).

Hydrogel Code	Dry hydrogels	Hydrated hydrogels
E0A0	56.39 ± 4.40	61.68 ± 1.89
E200A0	72.48 ± 0.11	64.78 ± 1.60
E200A40	72.57 ± 2.46	71.05 ± 2.34
E0A40	49.50 ± 1.99	58.08 ± 0.41

For all compositions, light transmission of wet hydrogels was close to 90% in the visible range (**Figure 4.5A**) fulfilling the requirements for CLs. Representative optical images of discs and CLs are shown in

USC UNIVERSIDADE DE SANTIAGO DE COMPOSTELA

Figure 4.6. The elastic modulus of the hydrogels ranged between 0.65 and 0.79 MPa (**Figure 4.5B**); E0A40 hydrogel presented a significantly lower value compared to the other hydrogels ($p < 0.05$). Nevertheless, the obtained values were for all hydrogels in the range of those typical for HEMA-based CLs (0.2–2.0 MPa) [Musgrave and Fangg, 2019].

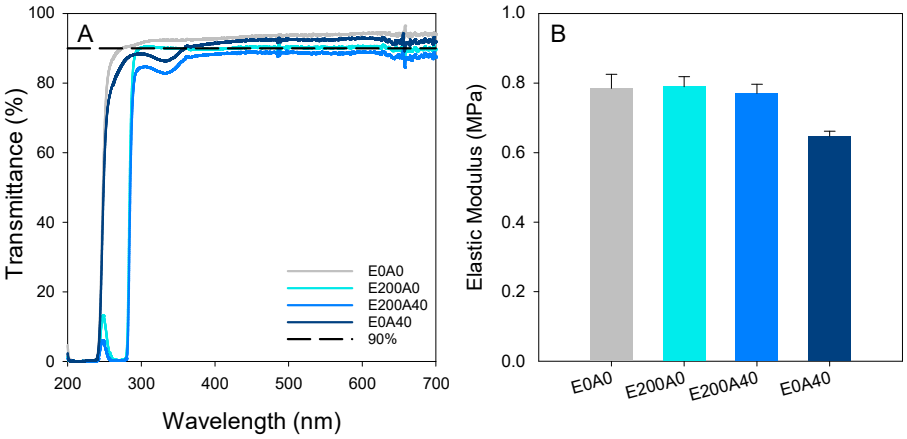

Figure 4.5. (**A**) Light transmittance (%) of the hydrogels after being swollen in SLF. Dashed line indicates 90% transmittance; (**B**) elastic modulus (MPa) obtained for hydrogels hydrated in 0.9% NaCl. Codes as in Table 4.1

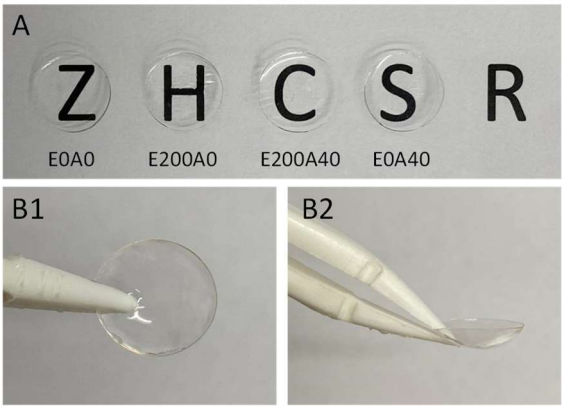

Figure 4.6. Pictures of (**A**) hydrated hydrogel discs and (**B1 and B2**) E200A40 CLs. Codes as in Table 4.1.

4.3.2 Pravastatin Loading and *In vitro* Release

Pravastatin loading was carried out by immersing the dried discs in pravastatin solution (0.1 mg/mL in water) for 48 h at room temperature. Loading of pravastatin during CL synthesis was discarded due to the poor solubility of the drug in the monomers mixture and the potential loss of a fraction of the incorporated drug during the required washing. Control E0A0 hydrogel loaded a small amount of pravastatin (0.42 ± 0.22 mg/g, **Figure 4.7A**). Incorporation of EGPEM monomer (E200A0 hydrogel) did not significantly improve the affinity for pravastatin (0.32 ± 0.17 mg/g; $p > 0.05$). Differently, the copolymerization of HEMA with APMA monomer (E200A40 and E0A40 hydrogels) remarkably increased the amount of pravastatin loaded (7.26 ± 0.59 and 6.70 ± 0.20 mg/g, respectively; $p < 0.05$). The $K_{N/W}$ values recorded for APMA-containing hydrogels (66.44 ± 2.30 for E0A40 and 72.17 ± 6.78 for E200A40) were about twenty-fold higher than those recorded for control hydrogels (3.70 ± 2.58 for E0A0) and hydrogels prepared with

USC UNIVERSIDADE DE SANTIAGO DE COMPOSTELA

EGPEM solely (2.75 ± 1.99 for E200A0) ($p < 0.05$). Compared to previous reports on atorvastatin [Pereira-da-Mota et al., 2021], $K_{N/W}$ values were lower for pravastatin, which may be related to the higher hydrophilicity of the latter.

When transferred to SLF, APMA hydrogels released higher amounts of pravastatin than non-functionalized (E0A0) and EGPEM (E200A0) hydrogels (**Figure 4.7B**). Comparing both APMA hydrogels, E200A40 presented slower release rate in the first hours, but the total amount of pravastatin released after 120 h was higher (7.84 ± 0.66 mg/g) compared to E0A40 hydrogel (7.07 ± 0.45 mg/g). The slower release rate recorded for E200A40 in the first hours may be related to the higher $K_{N/W}$ and pointed out to the role of the drug-EGPEM hydrophobic interactions in sustaining the release of the drug. These findings also suggest that both APMA and EGPEM are needed for resembling the multiple-point redundant interactions of the physiological receptor [Ribeiro et al., 2011; Tieppo et al., 2012]. Subsequent studies were carried out with both types of hydrogels containing APMA (E0A40 and E200A40).

USC UNIVERSIDADE DE SANTIAGO DE COMPOSTELA

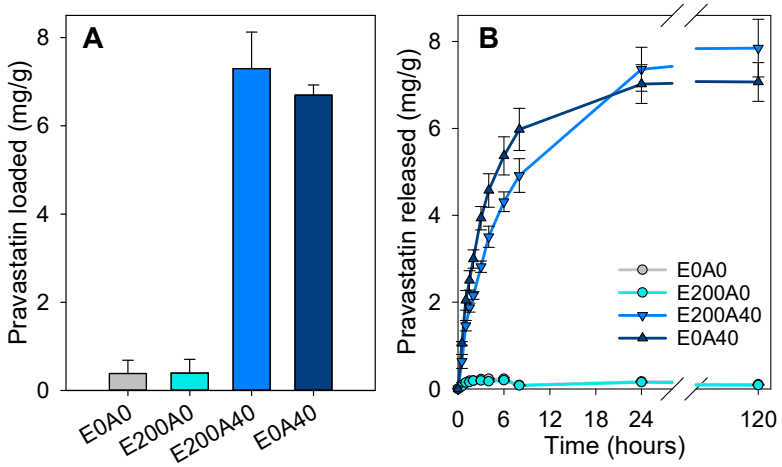

Figure 4.7. (**A**) Pravastatin loaded by the hydrogel discs (0.3 mm thickness) after 48 h of soaking in the drug solution (0.1 mg/mL in water) at room temperature under oscillatory movement (180 osc/min); (**B**) release profiles from pravastatin-loaded discs in SLF at 37 ◦C under oscillatory movement (180 osc/min). Codes as in Table 4.1. (*n* = 4; mean values and standard deviations).

4.3.3 Cytocompatibility and HET-CAM

Cell viability tests were performed using sterilized non-loaded and pravastatin-loaded hydrogels against Balb/3T3 fibroblasts, which is one of the most sensitive cell lines for biomaterials testing [Wataha et al., 1994]. Two solutions with different concentration in pravastatin were also evaluated. After 24 h of incubation, cell viability was 88.5 ± 8.2% and 89.6 ± 6.0% for non-loaded E200A40 and E0A40 hydrogels, and 80.2 ± 10.6% and 76.1 ± 4.4% for pravastatin-loaded hydrogels, respectively (**Figure 4.8**). After 48 h of incubation cell viability increased for non-loaded hydrogels and slightly decreased for pravastatin-loaded ones (72.5 ± 8.4% and 71.3 ± 7.7% for E200A40

USC UNIVERSIDADE DE SANTIAGO DE COMPOSTELA

and E0A40, respectively); statistically significant differences compared to control hydrogels ($p < 0.05$). Pravastatin solution of the highest concentration tested (0.1 mg/mL) caused similar decrease in cell viability. Differently and in good agreement with previous reports, pravastatin 0.05 mg/mL was highly cytocompatible as also observed for L6 fibroblasts [Itagaki et al., 2009]. In addition, it should be noted that *in vitro* cell studies do not reflect tear fluid renovation and drainage, which would reduce the contact time between pravastatin released from the hydrogels and ocular surface. Overall, all hydrogels could be considered as non-cytotoxic [ISO, 2009].

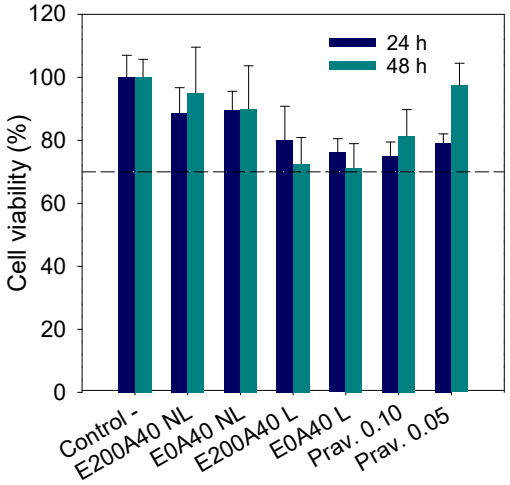

Figure 4.8. Balb/3T3 cells viability determined by CCK-8 assay after 24 and 48 h direct exposure to non-loaded (NL) and pravastatin-loaded (L) hydrogels (E200A40 and E0A40) and two pravastatin solutions (Prav. 0.10 and 0.05 mg/mL in water). Negative control (C-): cells cultured in the absence of any treatment. Dashed line corresponds to 70% cell viability. Codes as in Table 4.1. (n = 5; mean values and standard deviations).

USC UNIVERSIDADE DE SANTIAGO DE COMPOSTELA

The Hen's Egg Test on the Chorioallantoic Membrane (HET-CAM) assay was used as a preliminary test to evaluate the compatibility of the synthetized hydrogels with the ocular surface. The vascularized CAM tissue of an embryonated hen's eggs can provide information similar to the vascularized mucosal tissues of the eye, such as the conjunctiva [Kishore et al., 2008]. After 5 min in contact with the CAM, pravastatin-loaded hydrogels and pravastatin solution (300 µL, 0.1 mg/mL in water) did not trigger haemorrhage, vascular lysis or coagulation of CAM vessels, and could be considered as non-irritating for the ocular surface (**Figure 4.9**). As expected, the positive control (NaOH 0.1 N) registered an IS of 19.24.

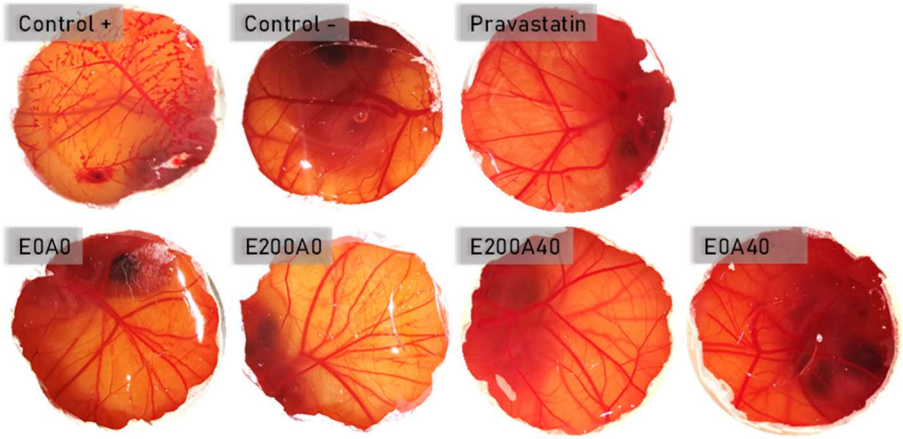

Figure 4.9. CAM images after 5 min in contact with pravastatin-loaded discs and pravastatin solution (0.1 mg/mL) in water. Effects of negative (0.9% NaCl) and positive (0.1 N NaOH) controls are also shown.

USC UNIVERSIDADE DE SANTIAGO DE COMPOSTELA

4.3.4 Effects of Sterilization and Light Exposition on Drug Stability and Release

Feasibility of sterilization and loading of the hydrogels in one single step was also evaluated. Firstly, the effect of SH and HHP sterilization on pravastatin solutions was tested. Pravastatin stability was compromised after exposition to 121 °C for 1 h and 1 bar originating degradation products at 3.9 min and 6.8 min (**Figure 4.10**). Contrarily, HHP sterilization (70 °C for 10 min and 600 MPa) did not trigger degradation, and the peak area at 5.15 min presented a variation lower than 5.5% compared to that of freshly prepared drug solution. As previously verified, degradation of pravastatin may be dramatically accelerated as temperature increases [Brain-Isasi et al., 2008]. Thus, heating up to 70 °C could be pointed out as safe for pravastatin.

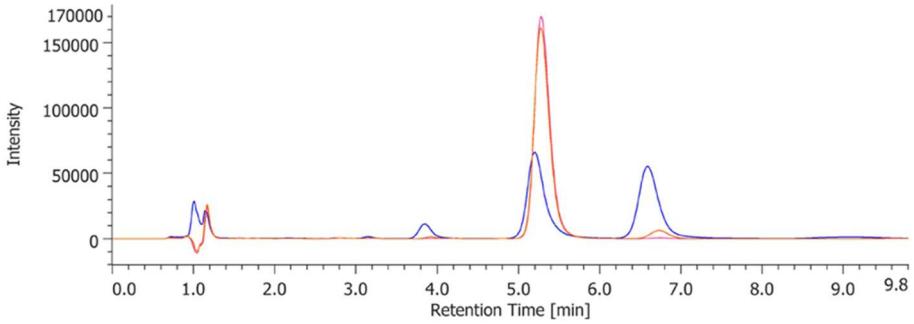

Figure 4.10. HPLC chromatograms of the pravastatin loading solution before (pink line) and after sterilization processing applying either steam heat (blue line) or high hydrostatic pressure (orange line).

Sterilization tests were also carried out with hydrogel discs previously soaked in 10 mL of pravastatin solution (0.1 mg/mL) for 48

USC UNIVERSIDADE DE SANTIAGO DE COMPOSTELA

h. The hydrogels sterilized applying SH contained lower amount of drug than the non-sterilized counterparts, especially E0A40 hydrogel ($p < 0.05$) (**Figure 4.11A**). Importantly, the hydrogels sterilized by HHP loaded amounts of pravastatin similar to those loaded by non-sterilized hydrogels. In good agreement, the amount of pravastatin released significantly decreased for hydrogels sterilized by SH ($p < 0.05$) (**Figure 4.11B**). Consequently, HHP was chosen for subsequent one-pot loading and sterilization of CLs.

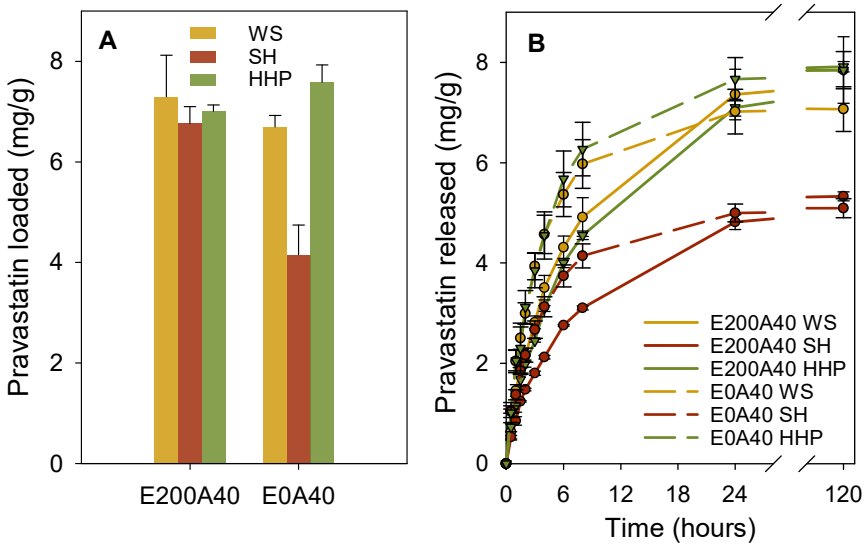

Figure 4.11. (**A**) Pravastatin loaded by E200A40 and E0A40 hydrogels when they were sterilized in drug solution by means of steam heat (SH) or high hydrostatic pressure (HHP), compared to non-sterilized hydrogels (WS); (**B**) pravastatin release profiles in 10 mL of SLF from E200A40 and E0A40 hydrogels that had not been sterilized (WS) or that were sterilized during loading (immersed in drug solution). Codes as in Table 4.1. (n = 4; mean values and standard deviations).

USC UNIVERSIDADE DE SANTIAGO DE COMPOSTELA

To gain further inside into drug stability, pravastatin solutions were exposed to white light mimicking the daylight conditions in the time frame of the 6–8 h of use of daily disposable CLs, and possible light induced degradation was evaluated. HPLC chromatograms recorded before and after 6 h of exposure were similar (**Figure 4.12**) with changes in peak area below 2% for replicated tests (n = 3), which indicated that pravastatin did not suffer degradation under light exposition. As previously observed, pravastatin is quite stable under sunlight conditions [Ahmad et al., 2011], which is an advantage for incorporation into CLs.

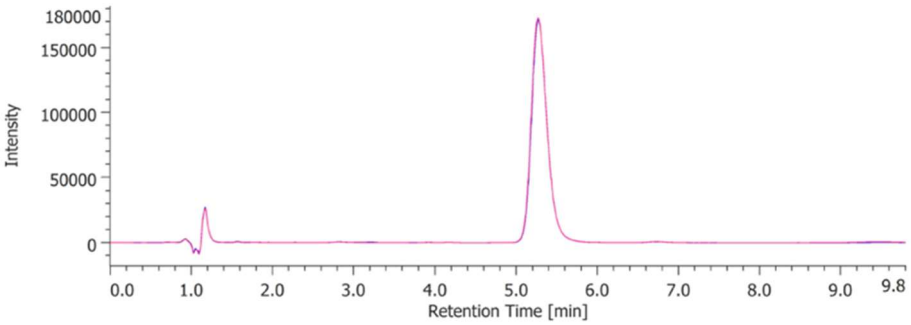

Figure 4.12. HPLC chromatograms of pravastatin sodium solution (0.05 mg/mL in water) before (pink line) and after 6 h of exposure to white light (blue line) were superimposable.

4.3.5 Effects of SLF Volume and Proteins on *In vitro* Drug Release Profiles

The *in vitro* release profiles of sterilized curved E200A40 CLs (0.1 mm of thickness) were investigated under six different conditions: two volume levels (2 and 10 mL) and three protein conditions (no protein, lysozyme, or albumin). In this work, the main tear fluid proteins

USC UNIVERSIDADE DE SANTIAGO DE COMPOSTELA

albumin and lysozyme were tested at a fix concentration of 2.68 mg/mL, which was considered as biorelevant [Marques et al., 2011].

Dried CLs (E200A40 formulation) were immersed in pravastatin solution (0.1 mg/mL) and sterilized by HHP. Then, the pravastatin-loaded CLs were rinsed with SLF and immersed in the release medium (**Figure 4.13**). The amounts of drug released in 10 mL of SLF from 0.3 mm thickness E200A40 hydrogels and from 0.1 mm thickness curved CLs of the same composition after HHP sterilization were similar ($p > 0.05$). This finding revealed that the hydrogel format (in the disc-CL range evaluated) did not impact on drug release.

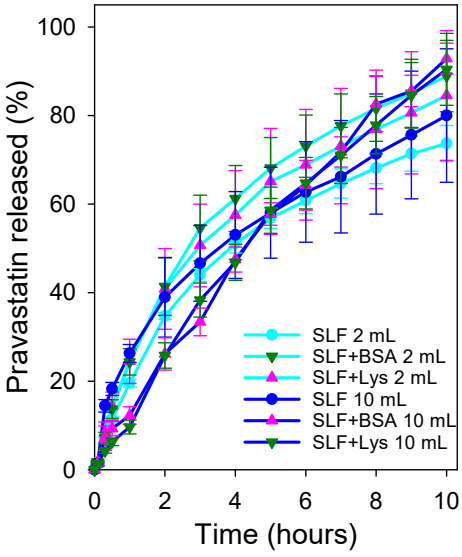

Figure 4.13. Pravastatin release profiles from E200A40 CLs (previously sterilized by HHP) in 2 or 10 mL of SLF without and with incorporation of lysozyme (Lys) and bovine serum albumin (BSA). (n = 4; mean values and standard deviations).

USC UNIVERSIDADE DE SANTIAGO DE COMPOSTELA

Pravastatin release in 2 mL of SLF was slightly slower than in 10 mL SLF, but the profiles run in parallel and no statistical differences could be detected due to the data variability. For 2 mL experiment, the incorporation of lysozyme and BSA proteins accelerated drug release, and the percentage released in the 8 to 10 h was statistically higher than in the absence of proteins ($p < 0.05$). Differently, lysozyme and BSA decreased release rate in 10 mL volume in the first 4 h but once again the percentage released in the 8 to 10 h was statistically higher than in the absence of proteins ($p < 0.05$).

As evidenced in a previous comprehensive report, the volume of the *in vitro* release medium may significantly affect drug release from CLs [Tieppo et al., 2014]. Since the CL is not inert against the drug, i.e., there exists an affinity, the volume of the release medium determines the concentration of drug outside the hydrogel, which affects to the release-rebinding equilibrium. When the loaded hydrogel is exposed to the release medium, the release is trigged by the drug concentration gradient between inside and outside the hydrogel. As more drug molecules accumulate in the release medium, hydrogels with high affinity for the drug, i.e., high $K_{N/W}$, may stop the release [Ribeiro et al., 2011; Blanco-Fernández et al., 2011]. The drug binding interactions counteract the release, and an equilibrium is observed when the number of drug molecules that abandon the network is similar to the number that is rebound by the hydrogel. Only under infinite dilution rebinding does not occur. Therefore, in any finite volume the equilibrium may be reached, and false plateaus or delays in the release may be observed. Nevertheless, this affinity-driven controlled release phenomenon gains more relevance as the volume of the release medium decreases and the $K_{N/W}$ increases. The high solubility of pravastatin and intermediate values of $K_{N/W}$ indicated that pravastatin affinity for water

USC UNIVERSIDADE DE SANTIAGO DE COMPOSTELA

is still quite high, which may explain the small effect of the volume on the percentage of pravastatin release.

Also, drug release from CLs could be affected by the presence of proteins, lipids, and mucin present in the tear film [Mahomed et al., 2016]. Interestingly, in this study, the incorporation of lysozyme and BSA in 2 mL volume slightly increased pravastatin release at all time points, while for 10 mL volume a change in the release profile, first slower and then faster, was observed (**Figure 4.13**). Lysozyme (pI 11.0) and BSA (pI 4.7) are positively and negatively charged, respectively, in SLF. Therefore, the likelihood of that their effect is related to ionic interactions with the drug or the hydrogel is low. In previous studies with a hydrophobic drug model (Rose Bengal dye), these same proteins were shown to accelerate the release, which could be related to hydrophobic interactions between the drug and the protein, promoting the extraction from the hydrogel [Phan et al., 2021]. Pravastatin sodium is a hydrophilic drug and the fraction unbound in plasma has been reported to be 0.485, which means that pravastatin is not a highly bound protein drug [Mao et al., 2018]. Also, the experimental protocol applied to denature the protein before drug quantification in the HPLC was demonstrated to recover >95% drug from the samples, which ensured that the decrease in the release was not due to losses of drug due to protein binding.

Slower release rate in artificial tear solution containing proteins and lipids was observed for moxifloxacin from a variety of CLs, compared to simple PBS [Phan et al., 2016]. As previously reported for other HEMA hydrogels [Moradi et al., 2004], deposition of albumin and lysozyme on the tested CLs was very low and not measurable. Thus, although the formation of a thin layer of proteins on the CL surface that may act as an additional barrier for drug diffusion could not be

USC UNIVERSIDADE DE SANTIAGO DE COMPOSTELA

discarded, its effect might be more relevant in the first hours after immersion of the discs in 10 mL medium (more total amount of proteins) due to the Voomer effect [Vilaseca et al., 2013]. This might explain the initial slower release and also the subsequent faster release as the adsorbed proteins detach and may drag some drug molecules with them.

4.3.6 *Ex vivo* Corneal and Scleral Permeability

Pravastatin diffusion tests from E200A40 and E0A40 hydrogels through cornea and sclera were evaluated *ex vivo* using porcine tissues. The vertical Franz cell may simulate the drug flux from the exterior of the eye to the aqueous or vitreous humour. As a control, the donor chamber was filled with a pravastatin solution (128 μg/mL) that provided an amount of pravastatin similar to the maximum amount of drug released from the hydrogels in 6 h.

After 6 h of experiment the concentration of pravastatin in the donor chamber in contact with cornea and sclera was significantly lower for both hydrogels compared to the drug solution (**Figure 4.14A**; $p < 0.05$). No differences were found between the hydrogels. The amount of pravastatin accumulated in cornea was significantly lower than in sclera (**Figure 4.14B**; $p < 0.05$), but for a given tissue no differences were found among the hydrogels and the solution. This means that pravastatin released from the hydrogels during 6 h could diffuse into the tissues in a similar amount than when supplied as a solution, in spite of that in the case of the solution the entire dose was placed into contact with the cornea or sclera tissue since the very beginning of the experiment.

USC UNIVERSIDADE DE SANTIAGO DE COMPOSTELA

Pravastatin permeated through sclera was detected in the receptor chamber after two hours of contact with pravastatin solution and after three hours for E200A40 and E0A40 hydrogels (**Figure 4.14C**). For porcine cornea tissue, the amount of pravastatin in the receptor chamber was below the HPLC quantification limit. This means that pravastatin mainly accumulated into the cornea in the time frame of the experiment. Generally, a poor penetration across the cornea was observed for more hydrophilic and larger molecules [Subrizi et al., 2019]. Pravastatin presents greater hydrophilicity than other statins (log P = − 0.23) which could explain the higher sclera permeability observed. Very recently, *ex vivo* cornea and sclera permeability studies revealed that atorvastatin mainly accumulated into cornea and sclera tissues but did not progress further [Pereira-da-Mota et al., 2021]. Due to its lipophilicity (log P = 5.39), atorvastatin could present higher cornea permeability, but this effect may have been thwarted by the higher molecular weight (558.64 g/mol). In the case of sclera, flux (J) and apparent permeability coefficient (P_{app}) of pravastatin ranked in the order: E200A40 < E0A40 < pravastatin solution (**Table 4.3**). These values agreed with those previously reported for other drugs such as transferulic acid (0.035 to 0.115 μg/ cm^2·h; 5.4 to $11.5 \cdot 10^{-6}$ cm/s) and valaciclovir (0.42 to 4.23 μg/cm^2·h; 9.75 to $11.37 \cdot 10^{-6}$ cm/s) when delivered from drug-eluting CLs [Varela-Garcia et al., 2020; Varela-Garcia et al., 2018].

USC UNIVERSIDADE DE SANTIAGO DE COMPOSTELA

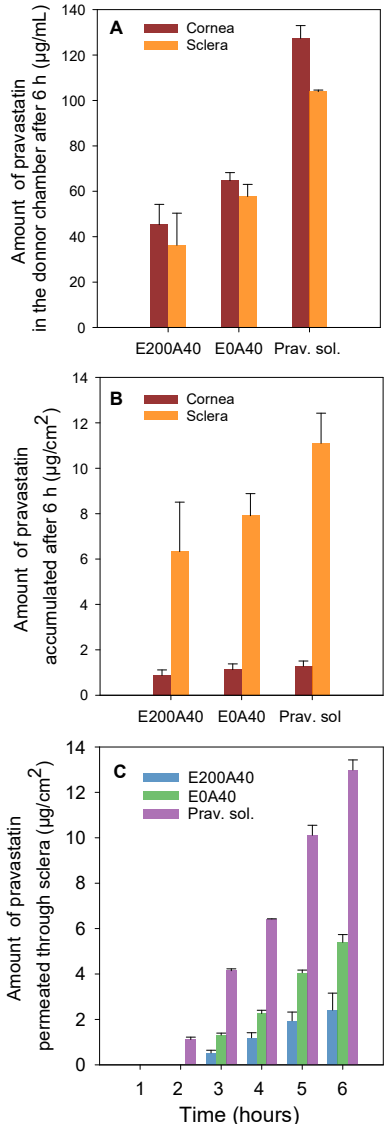

Figure 4.14. (**A**) Amounts of pravastatin in the donor chamber, (**B**) amounts accumulated in cornea and sclera tissues, and (**C**) amounts permeated through porcine sclera after 6 h of contact with drug-loaded hydrogels (E200A40 and E0A40) and pravastatin solution (128 µg/mL, 1 mL). Codes as in Table 4.1. (*n* = 3; mean values and standard deviations).

USC UNIVERSIDADE DE SANTIAGO DE COMPOSTELA

Table 4.3. Flux (J) and apparent permeability coefficient (P_{app}) of pravastatin applied as a solution or as pravastatin-loaded E200A40 and E0A40 hydrogels onto to sclera tissue (n = 3; mean values and standard deviations).

Hydrogel Code	J (μg/(cm²·h))	P_{app} (×10⁶) (cm/s)
E200A40	0.47 ± 0.11	3.16 ± 1.85
E0A40	1.02 ± 0.05	4.92 ± 2.93
Prav. Sol.	2.46 ± 0.09	6.57 ± 2.72

4.3.7 Anti-inflammatory Activity

Once pravastatin was demonstrated to be able to penetrate in the eye structures *ex vivo*, the next sept was to elucidate the anti-inflammatory activity of drug itself and of the drug-CL combination product. Cytokines and other mediators, such as prostaglandins, play important roles in eye inflammation. Some previous studies have been focused on the anti-inflammatory effects of statins, but results were not homogeneous [Bessler et al., 2005; Loppnow et al., 2011; McFarland et al., 2017]. McFarland et al. [McFarland et al., 2017] compared the effects of the six statins (including pravastatin) on PMA differentiated THP-1 cells and using LPS to induce inflammatory conditions. All statins significantly reduced LPS induced IL-1β and TNF-α release and also decreased prostaglandin E2 (PGE2) levels. Loppnow et al. [Loppnow et al., 2011] showed that pravastatin reduced the IL-6 production by 60% in human vascular smooth muscle cells (SMC) and human mononuclear cells (MNC). Conversely, Bessler et al. [Bessler et al., 2005] found that the IL-6 production in human peripheral blood mononuclear cells was not affected by pravastatin.

In the present study, the secretion of tumor necrosis factor alpha (TNF-α) and interleukin-6 (IL-6), two pro-inflammatory cytokines, was examined by stimulation of macrophages with LPS. The macrophages

USC UNIVERSIDADE DE SANTIAGO DE COMPOSTELA

were previously treated with non-loaded and pravastatin-loaded E200A40 hydrogels or pravastatin solutions (**Figure 4.15**). A statistically significant reduction in TNF-α secretion ($p < 0.05$) was observed for hydrogels (**Figure 4.15B**). Overall, the obtained results point out the effectiveness of pravastatin-loaded hydrogels to decrease the secretion of TNF-α showing promising anti-inflammatory activity.

USC UNIVERSIDADE DE SANTIAGO DE COMPOSTELA

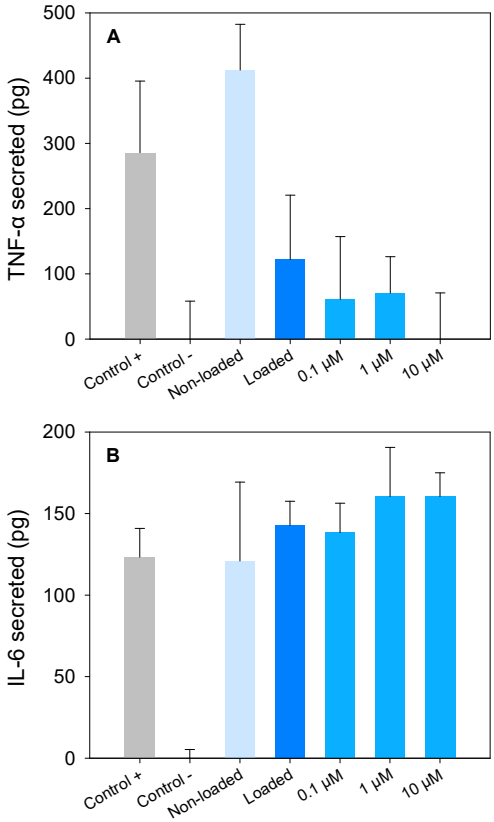

Figure 4.15. Effect of non-loaded and pravastatin-loaded E200A40 discs and pravastatin sodium solutions (0.1, 1, 10 μM) on the secretion levels of (**A**) TNF-α and (**B**) IL-6 from macrophages that were previous treated with the hydrogels or pravastatin solutions followed by addition of LPS. Positive control refers to cells only stimulated with LPS; negative control refers to unstimulated cells (without LPS); (*n* = 4; mean values and standard deviations).

USC UNIVERSIDADE DE SANTIAGO DE COMPOSTELA

4.3.8 *In vivo* Studies

After *in vitro*, *in ovo*, in cell and *ex vivo* tests were fulfilled, an *in vivo* study was planned with the double aim of (i) assess the advantages of using pravastatin-eluting CLs compared to eye drops in terms of drug levels in tear fluid and biodistribution to eye tissues (for a same drug dose), and (ii) elucidate whether *in vitro-in vivo* correlations (IVIVC) could be obtained and which *in vitro* release conditions may provide better correlations. New Zealand rabbit eyes have been extensively used in ophthalmology research due to their similarity with human eyes [Vézina, 2012; Zernii et al., 2016].

The *in vivo* release profiles of pravastatin in tear fluid (concentration versus time) after application of E200A40 CLs and eye drops (2 mg/mL of pravastatin) are shown in **Figure 4.16**. In the eye drops group, the maximum pravastatin concentration (C_{max}) in the rabbit tear fluid was recorded in the first 5 min (975.21 ± 456.40 μg/mL), followed by an exponential decrease, with a low drug concentration being detected after 1 h (14.88 ± 10.99 μg/mL to 9.30 ± 13.13 μg/mL at 8 h), which was found to be consistent with previous studies that demonstrated a rapid decline [van Bijsterveld, 1969; Xu et al., 2019; Maulvi et al., 2016].

Pravastatin-loaded CLs led to a smoother concentration curve and a sustained release over a period of 10 h, which demonstrated much less variability in the concentration of pravastatin in tear fluid and a significant improvement in mean residence time of pravastatin (**Table 4.4**). The C_{max} was found to be 177.5 ± 116.8 μg/mL after 30 min of CL wearing. No burst release was observed. Only in the first 5 min, pravastatin concentration in tear fluid was higher for the eye drop group than for the CL group ($p < 0.05$). No statistically significant differences were recorded at 15 and 30 min. After that, the concentrations recorded

USC UNIVERSIDADE DE SANTIAGO DE COMPOSTELA

in the CL group were higher than those provided by the eye drops in the first 7 h of wearing (with the exception of time point 6 h, which were not significantly different). When wearing drug-loaded CLs, pravastatin diffused through the CL matrix and gradually entered the post-lens tear film prolonging the retention in the precorneal area. Previous studies also evidenced that drug-eluting CLs can improve drug retention in comparison with eye drops. For example, in New Zealand white rabbits, the MRT of ketotifen delivered from non-imprinted CLs wore for an entire day was found to be 3.4 h compared to 0.25 h for eye drops [Tieppo et al., 2012]. Also, CLs loaded with timolol during synthesis increased the mean residence time from 0.33 h for eye drops to 26.27 h for CLs wore for 5 days [Xu et al., 2019]. In our case, pravastatin-loaded CLs were intended to be daily disposable and, therefore, the release was aimed to be completed in the common half a day time frame of CL wearing. Indeed, the amounts of pravastatin remnant inside the CLs after 8 h and 10 h wearing were 7.5 ± 4.2 μg and 2.8 ± 1.6 μg, respectively, which indicated that >90% drug was released in the first 8 h of wearing. Thus, when the CLs were taken out, environmental impact due to waste of drug was not expected. Pravastatin-loaded CLs provided >2-fold increase in $AUC_{0\text{-}8h}$ and almost triplicate the MRT compared to the eye drops, for the same dose administered of 100 μg. MRT values of 2.82 h recorded for pravastatin loaded CLs were significantly larger than those recorded for timolol (~0.3 h) [Hiratani et al., 2005] and puerarin (1.3 h) [Xu et al., 2010] using HEMA-based CLs.

The left eye of the rabbits served as a control, and no pravastatin was detected in tear fluid of left eye during treatment of the right eye either with CLs or eye drops. Also, no traces of pravastatin were detected in the tissues of the left eye. Therefore, systemic absorption could be considered as unlikely.

USC UNIVERSIDADE DE SANTIAGO DE COMPOSTELA

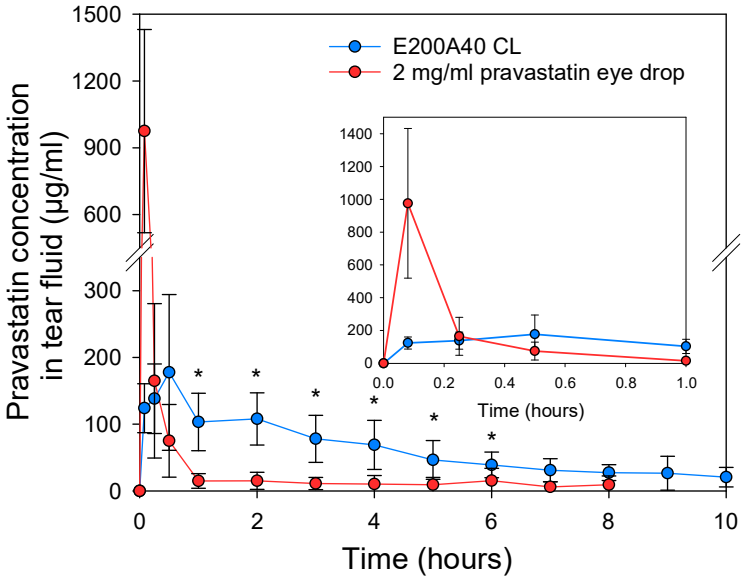

Figure 4.16. Pravastatin concentration in the tear fluid during E200A40 CL wearing (n = 6 for 8 h and n = 3 for 9 and 10 h) and after a single instillation of pravastatin eye drops (50 µL, 2 mg/mL, n = 4) (mean values and standard deviations; *CLs provided statistically significant higher concentrations than eye drops; $p < 0.05$).

Table 4.4. Pharmacokinetic parameters obtained from the pravastatin concentration-time profiles in tear fluid for an equivalent dose of 100 µg administered as CL (n = 6) or eye drop (n = 4) (mean values and standard deviations).

Formulation	C_{max} (µg/mL)	t_{max} (h)	$AUC_{0\text{-}8h}$ (µg/mL·h)	$AUMC_{0\text{-}8h}$ (µg·h /mL·h)	MRT (h)
E200A40 CLs	177.5 ± 116.8	0.50	573.5 ± 193.1	1637.3 ± 637.6	2.82 ± 0.24
Eye drops	975.2 ± 456.4	0.08	267.6 ± 94.3	365.9 ± 319.2	1.17 ± 0.89

USC UNIVERSIDADE DE SANTIAGO DE COMPOSTELA

Biodistribution of pravastatin in the anterior and posterior segments of the eye was investigated after 8 h of CL wearing and eye drop instillation. The amount of pravastatin in eye tissues was also quantified 14 h later of removing the CLs that were wore for 10 h in order to mimic the rest period without CL, which may provide information about risk of drug accumulation. Among the ocular tissues evaluated (cornea, crystalline lens, sclera, retina, aqueous humour and vitreous humour), pravastatin was detected in cornea, sclera, aqueous humour and vitreous humour after 8 h of CL wearing (**Figure 4.17**). Pravastatin was not detected in rabbits' left eye (control) neither in the eye drops group. A preferential biodistribution of pravastatin was observed in the anterior segment, which provided the highest accumulation in the cornea (158.46 ± 31.8 ng/g) and aqueous humour (108.73 ± 47.48 ng/g). CLs also facilitated pravastatin biodistribution and accumulation in the posterior segment, including sclera (1.53 ± 0.59 ng/g) and vitreous humour (2.00 ± 0.59 ng/g). It should be noted that no pravastatin was detected in eye tissues of rabbits that wore CLs for 10 h and remained 14 h more without CLs, which avoids risks of drug accumulation after successive applications. The rabbit model, although widely used, may have the limitation of lower blinking rate, and thus the release might be somehow faster when CL are applied to human eyes [Maurice, 1995; Galante et al., 2015].

USC UNIVERSIDADE DE SANTIAGO DE COMPOSTELA

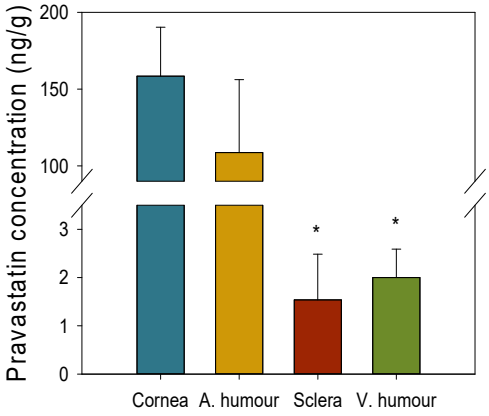

Figure 4.17. Pravastatin accumulated in various ocular tissues after 8 h of CL wear (n = 3; *statistically different from the amount of pravastatin accumulated in the cornea; $p < 0.05$).

Slit-lamp images were collected to evaluate a possible ocular irritation after 8 h of wearing pravastatin-loaded CLs or eye drops administration (**Figure 4.18**). No signs of ocular irritation were observed in any rabbit. Hence, pravastatin-loaded CLs showed good compatibility and safety to the rabbits' eyes as revealed in previous designed and optimized HEMA-based CLs.

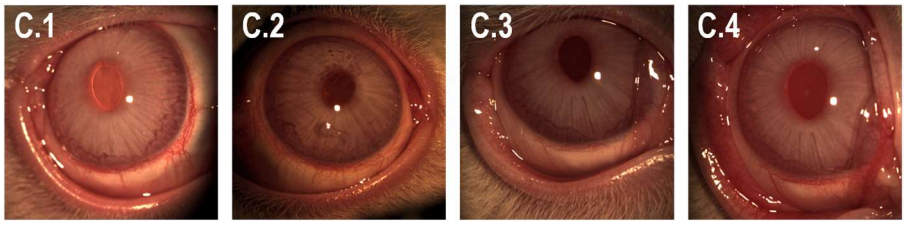

Figure 4.18. Slit-lamp images of rabbits' eyes without CLs (C.1) before and (C.2) after 8 h of wearing E200A40 CLs and (C.3) before and (C.4) after administration of a single eye drop (2 mg/mL).

USC UNIVERSIDADE DE SANTIAGO DE COMPOSTELA

4.3.9 *In vitro-in vivo* Correlations

Comparison between *in vivo* and *in vitro* release profiles in 2 and 10 mL of SLF are shown in **Figure 4.19**. The *in vivo* data showed similar percentages of drug released in the first hours but then accelerated compared to the *in vitro* release. Levy plots (**Figure 4.20**) were used to investigate *in vitro-in vivo* correlations (IVIVC). The regression was not forced to pass through the origin in order to see better the deviations at short times. *In vitro* release tests carried out in 2 mL led to Levy plots with correlation coefficient (r^2) values closer to 1 compared to the Levy plots obtained for 10 mL.

For 2 mL SLF (**Figure 4.20A**), the intercepts at the origin were in the −5 to −6 range disregarding the presence or absence of proteins and the slopes were 1.476 (s.e. 0.030), 1.321 (s.e. 0.036) and 1.224 (s.e. 0.028) for medium without proteins, with BSA and with lysozyme, respectively. Thus, strong correlations but with positive deviations were observed, and the slope shifted towards 1 in the presence of proteins.

For 10 mL SLF (**Figure 4.20B**), in the absence of proteins the intercept at the origin was −12.8, which evidenced that the percentage released *in vitro* was remarkably higher at the very beginning, and the slope was 1.536 (s.e. 0.072). In the presence of BSA and lysozyme the intercepts at the origin were in the +4 to +5 range and the slopes were 1.245 (s.e. 0.078) and 1.251 (s.e. 0.053), respectively. Thus, the presence of proteins in the *in vitro* release medium favored the goodness of the IVIVC.

USC UNIVERSIDADE DE SANTIAGO DE COMPOSTELA

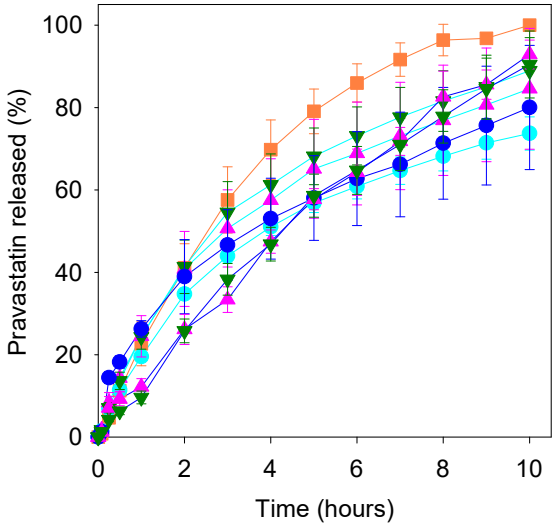

Figure 4.19. Pravastatin release profile from E200A40 CLs as estimated *in vivo* and as experimentally recorded in 2 or 10 mL of SLF without and with incorporation of lysozyme (Lys; 2.68 mg/mL) and bovine serum albumin (BSA; 2.68 mg/mL), (n = 4; mean values and standard deviations).

USC UNIVERSIDADE DE SANTIAGO DE COMPOSTELA

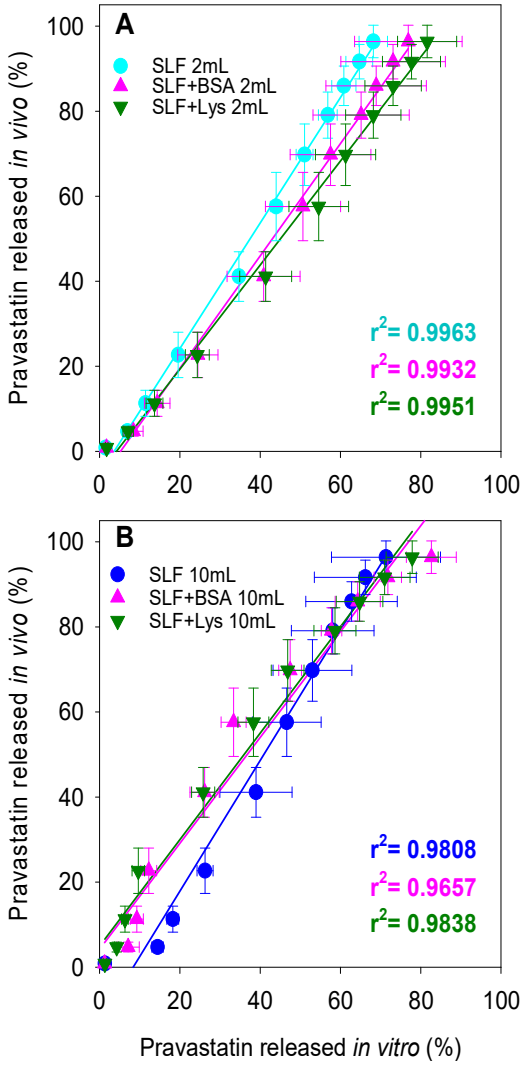

Figure 4.20. Levy plots for in vivo vs. *in vitro* percentage of drug released. The *in vitro* tests were carried out in (**A**) 2 mL of SLF solely or with BSA or lysozyme, and (**B**) 10 mL of SLF solely or with BSA or lysozyme.

USC UNIVERSIDADE DE SANTIAGO DE COMPOSTELA

4.4 CONCLUSIONS

CLs prepared with EGPEM and APMA as monomers that can resemble the hydrophobic and amine-based binding points of the natural receptor have been shown able to load remarkably high pravastatin amounts. Pravastatin-loaded CLs exhibited swelling capacity, light transmission and mechanical properties typical of soft CLs (thus, they may be suitable for refractive errors correction) and also sustained *in vitro* release for 10 h. Preliminary biocompatibility tests in cell cultures, HET-CAM and then *in vivo* confirmed the safety of this combination product. Regarding efficacy, pravastatin released from the CLs exhibited anti-inflammatory properties and capability to penetrate and accumulate in anterior and posterior eye segments. *In vivo* tests evidenced the suitability of the developed CLs to control pravastatin release on the ocular surface, notably prolonging the permanence time in the tear fluid compared to eye drops and also facilitating drug access to aqueous humour and vitreous humour. Preliminary assessment of IVIVC revealed that, despite pravastatin is not a highly bound protein drug and the CLs have low affinity for proteins, addition of BSA or lysozyme to the release medium may affect to the *in vitro* release profiles. Indeed, more linear Levy plots and with slopes closer to 1 were recorded for *in vitro* release media containing proteins. The information gathered in the present chapter may serve as a first step towards the search of how a change in the performance of the CLs to regulate drug release *in vitro* may be translated to a change in the *in vivo* drug profiles.

4.5 REFERENCES

Al-Ghabeish, M.; Xu, X.; Krishnaiah, Y.S.; Rahman, Z.; Yang, Y.; Khan, M.A. (**2015**). Influence of drug loading and type of ointment base

USC UNIVERSIDADE DE SANTIAGO DE COMPOSTELA

on the in vitro performance of acyclovir ophthalmic ointment. *Int. J. Pharm.* 495(2), 783-791.

Ahmad, A.; Panda, B. P.; Mujeeb, M. (**2011**). A validated stability-indicating method for simultaneous analysis of mevastatin and pravastatin in fermentation broth during bioconversion by Actinomadura macra. *Acta Chromatogr.* 23(1), 121-131.

Alvarez-Lorenzo, C.; Hiratani, H.; Gómez-Amoza, J.L.; Martínez-Pacheco, R.; Souto, C.; Concheiro, A. (**2002**). Soft contact lenses capable of sustained delivery of timolol. *J. Pharm. Sci.* 91(10), 2182-2192.

Alvarez-Rivera, F.; Serro, A.P.; Silva, D.; Concheiro, A.; Alvarez-Lorenzo, C. (**2019**). Hydrogels for diabetic eyes: Naltrexone loading, release profiles and cornea penetration. *Mater. Sci. Eng. C* 105, 110092.

Bedi, O.; Dhawan, V.; Sharma, P.L.; Kumar, P. (**2016**). Pleiotropic effects of statins: new therapeutic targets in drug design. *Naunyn Schmiedebergs Arch. Pharmacol.* 389(7), 695-712.

Bessler, H.; Salman, H.; Bergman, M.; Straussberg, R.; Djaldetti M. (**2005**). In vitro effect of statins on cytokine production and mitogen response of human peripheral blood mononuclear cells. *Clin. Immunol.* 117(1), 73-77.

Blanco-Fernández, B.; López-Viota, M.; Concheiro, A.; Alvarez-Lorenzo, C. (**2011**). Synergistic performance of cyclodextrin-agar hydrogels for ciprofloxacin delivery and antimicrobial effect. *Carbohydr. Polym.* 85(4), 765–774.

USC UNIVERSIDADE DE SANTIAGO DE COMPOSTELA

Brain-Isasi, S.; Requena, C.; Álvarez-Lueje, A. (**2008**). Stability study of pravastatin under hydrolytic conditions assessed by HPLC. *J. Chil. Chem. Soc.* 53(4), 1684-1688.

Chanput, W.; Mes, J.J.; Wichers, H.J. (**2014**). THP-1 cell line: an in vitro cell model for immune modulation approach. *Int. Immunopharmacol.* 23(1), 37-45.

Chung, Y.R.; Park, S.W.; Choi, S.Y.; Kim, S.W.; Moon, K.Y.; Kim, J.H.; Lee, K. (**2017**). Association of statin use and hypertriglyceridemia with diabetic macular edema in patients with type 2 diabetes and diabetic retinopathy. *Cardiovasc. Diabetol.* 16(4).

DiPasquale, S.A.; Uricoli, B.; DiCerbo, M.C.; Brown, T.L.; Byrne, ME. (**2021**). Controlled release of multiple therapeutics from silicone hydrogel contact lenses for post-cataract/post-refractive surgery and uveitis treatment. *Transl. Vis. Sci. Technol.* 10(14), 5.

DiPasquale, S. A.; Wuchte, L. D.; Mosley, R. J.; Demarest, R. M.; Voyles, M. L.; Byrne, M. E. (**2022**). One week sustained in vivo therapeutic release and safety of novel extended-wear silicone hydrogel contact lenses. *Adv. Healthcare Mater.* 11, 2101263.

Dixon, P.; Ghosh, T.; Mondal, K.; Konar, A.; Chauhan, A.; Hazra, S. (**2018**). Controlled delivery of pirfenidone through vitamin E-loaded contact lens ameliorates corneal inflammation. *Drug Deliv. Transl. Res.* 8(5), 1114-1126.

Esposito, K.; Nappo, F.; Marfella, R.; Giugliano, G.; Giugliano, F.; Ciotola, M.; Quagliaro, L.; Ceriello, A.; Giugliano, D. (**2002**). Inflammatory cytokine concentrations are acutely increased by hyperglycemia in humans: role of oxidative stress. *Circulation.* 106(16), 2067-2072.

USC UNIVERSIDADE DE SANTIAGO DE COMPOSTELA

Galante, R.; Paradiso, P.; Moutinho, M.G.; Fernandes, A.I.; Mata, J.L.; Matos, A.P.; Colaço, R.; Saramago, B.; Serro, A.P. (**2015**). About the effect of eye blinking on drug release from pHEMA-based hydrogels: an in vitro study. *J. Biomater. Sci. Polym. Ed.* 26(4), 235-251.

Gologorsky, D.; Thanos, A.; Vavvas, D. (**2012**). Therapeutic interventions against inflammatory and angiogenic mediators in proliferative diabetic retinopathy. *Mediators Inflamm.* 2012, 629452.

Gupta, A.; Gupta, V.; Thapar, S.; Bhansali, A. (**2004**). Lipid-lowering drug atorvastatin as an adjunct in the management of diabetic macular edema. *Am. J. Ophthalmol.* 137(4), 675-82.

Hiratani, H.; Fujiwara, A.; Tamiya, Y.; Mizutani, Y.; Alvarez-Lorenzo, C. (**2005**). Ocular release of timolol from molecularly imprinted soft contact lenses. *Biomaterials.* 26(11), 1293-1298.

Hui, A.; Willcox, M. (**2016**). In vivo studies evaluating the use of contact lenses for drug delivery. *Optom. Vis. Sci.* 93(4), 367-376.

International Diabetes Federation (**2021**). IDF Diabetes Atlas; https://www.diabetesatlas.org/> (accessed on February 2022).

Ioannidou, E.; Tseriotis, V.S.; Tziomalos, K. (**2017**). Role of lipid-lowering agents in the management of diabetic retinopathy. *World J. Diabetes.* 8(1), 1-6.

ISO 10993-5:2009(en). (**2009**). Biological evaluation of medical devices—Part 5: Tests for in vitro cytotoxicity; https://www.iso.org/obp/ui/#iso:std:iso:10993:-5:ed-3:v1:en (accessed on February 2022).

Istvan, E.S.; Deisenhofer, J. (**2001**). Structural mechanism for statin inhibition of HMG-CoA reductase. *Science.* 292(5519), 1160–1164.

USC UNIVERSIDADE DE SANTIAGO DE COMPOSTELA

Itagaki, M.; Takaguri, A.; Kano, S.; Kaneta, S.; Ichihara, K.; Satoh, K. (**2009**). Possible mechanisms underlying statin-induced skeletal muscle toxicity in L6 fibroblasts and in rats. *J. Pharmacol. Sci.* 109(1), 94-101.

Jain, K.S.; Kathiravan, M.K.; Somania, R.S.; Shishoo, C.J. (**2007**). The biology and chemistry of hyperlipidemia. *Bioorg. Med. Chem.* 15, 4674–4699.

Johnson & Johnson News (**2021**). Johnson & Johnson Vision Receives Approval in Canada for World's First and Only Drug-Releasing Contact Lens for Vision Correction and Allergic Eye Itch: ACUVUE® Theravision™ with Ketotifen; https://www.jjvision.com/press-release/johnson-johnson-vision-receives-approval-canada-worlds-first-and-only-drug-releasing (accessed February 2021).

Kakisu, K.; Matsunaga, T.; Kobayakawa, S.; Sato, T.; Tochikubo, T. (**2013**). Development and efficacy of a drug-releasing soft contact lens. *Invest. Ophthalmol. Vis. Sci.* 54(4), 2551-2561.

Kim, E.; Saha, M.; Ehrmann, K. (**2018**). Mechanical properties of contact lens materials. *Eye Contact Lens.* 44, S148–S156.

Kim, S.W.; Bae, Y.H.; Okano, T. (**1992**). Hydrogels: Swelling, drug loading, and release. *Pharm. Res.* 9(3), 283–290.

Kishore, A.S.; Surekha, P.A.; Sekhar, P.V.; Srinivas, A.; Murthy, P.B. (**2008**). Hen egg chorioallantoic membrane bioassay: an in vitro alternative to draize eye irritation test for pesticide screening. *Int. J. Toxicol.* 27(6), 449-453.

Lazarowski, E.R.; Boucher, R.C.; Harden, T.K. (**2003**). Mechanisms of release of nucleotides and integration of their action as P2X- and P2Y-receptor activating molecules. *Mol. Pharmacol.* 64(4), 785-795.

USC UNIVERSIDADE DE SANTIAGO DE COMPOSTELA

Liao, J.K.; Laufs, U. (**2005**). Pleiotropic effects of statins. *Annu. Rev. Pharmacol. Toxicol.* 45, 89-118.

Li, C.C.; Chauhan, A. (**2006**). Modeling ophthalmic drug delivery by soaked contact lenses. *Ind. Eng. Chem. Res.* 45, 3718–3734.

Loppnow, H.; Zhang, L.; Buerke, M.; Lautenschläger, M.; Chen, L.; Frister, A.; Schlitt, A.; Luther, T.; Song, N.; Hofmann, B.; Rose-John, S.; Silber, R.E.; Müller-Werdan, U.; Werdan, K. (**2011**). Statins potently reduce the cytokine-mediated IL-6 release in SMC/MNC cocultures. *J. Cell. Mol. Med.* 15(4), 994-1004.

Mahomed, A.; Wolffsohn, J.S.; Tighe, B.J. (**2016**). Structural design of contact lens-based drug delivery systems; in vitro and in vivo studies of ocular triggering mechanisms. *Cont. Lens Anterior Eye.* 39(2), 97-105.

Mao, J.; Doshi, U.; Wright, M.; Hop, C.E.C.A.; Li, A.P.; Chen, Y. (**2018**). Prediction of the Pharmacokinetics of Pravastatin as an OATP Substrate Using Plateable Human Hepatocytes With Human Plasma Data and PBPK Modeling. *CPT Pharmacometrics Syst Pharmacol.* 7(4), 251-258.

Marques, R.C.; Loebenberg, M.; Almukainzi, M. (**2011**). Simulated biological fluids with possible application in dissolution testing. *Dissol. Technol*. 18, 15–28.

Maulvi, F.A.; Lakdawala, D.H.; Shaikh, A.A.; Desai, A.R.; Choksi, H.H.; Vaidya, R.J.; Ranch, K.M.; Koli, A.R.; Vyas, B.A.; Shah, D.O. (**2016**). In vitro and in vivo evaluation of novel implantation technology in hydrogel contact lenses for controlled drug delivery. *J. Control. Release*. 226, 47-56.

USC UNIVERSIDADE DE SANTIAGO DE COMPOSTELA

Maulvi, F.A.; Patil, R.J.; Desai, A.R.; Shukla, M.R.; Vaidya, R.J.; Ranch, K.M.; Vyas, B.A.; Shah, S.A.; Shah, D.O. (**2019**). Effect of gold nanoparticles on timolol uptake and its release kinetics from contact lenses: In vitro and in vivo evaluation. *Acta Biomater.* 86, 350-362.

Maurice, D. (**1995**). The effect of the low blink rate in rabbits on topical drug penetration. *J. Ocul. Pharmacol. Ther.* 11(3), 297-304.

McFarland, A.J.; Davey, A.K.; Anoopkumar-Dukie, S. (**2017**). Statins reduce lipopolysaccharide-induced cytokine and inflammatory mediator release in an in vitro model of microglial-like cells. *Mediat. Inflamm.* 2017, 2582745.

Minami, T.; Ishida, W.; Kishimoto, T.; Nakajima, I.; Hino, S.; Arai, R.; Matsunaga, T.; Fukushima, A.; Yamagami, S. (**2019**). In vitro and in vivo performance of epinastine hydrochloride-releasing contact lenses. *PLoS One.* 14(1), e0210362.

Misra, S.L.; Braatvedt, G.D.; Patel, D.V. (**2016**). Impact of diabetes mellitus on the ocular surface: a review. *Clin. Exp. Ophthalmol.* 44(4), 278-288.

Moradi, O.; Modarress, H.; Noroozi, M. (**2004**). Experimental study of albumin and lysozyme adsorption onto acrylic acid (AA) and 2-hydroxyethyl methacrylate (HEMA) surfaces. *J. Colloid Interface Sci.* 271(1), 16-19.

Murphy, C.; Deplazes, E.; Cranfield, C.G.; Garcia, A. (**2020**). The role of structure and biophysical properties in the pleiotropic effects of statins. *Int. J. Mol. Sci.* 21(22), 8745.

Musgrave, C.S.A.; Fang, F. (**2019**). Contact lens materials: A materials science perspective. *Materials.* 12, 261.

USC UNIVERSIDADE DE SANTIAGO DE COMPOSTELA

Nielsen, S.F.; Nordestgaard, B.G. (**2014**). Statin use before diabetes diagnosis and risk of microvascular disease: a nationwide nested matched study. *Lancet Diabetes Endocrinol.* 2(11), 894-900.

Onal, A.; Sagirli, O. (**2006**). Development of a selective LC method for the determination of pravastatin sodium. *Chromatogr.* 64, 157–162.

Ooi, K.G.; Khoo, P.; Vaclavik, V.; Watson, S.L. (**2019**). Statins in ophthalmology. *Surv. Ophthalmol.* 64(3), 401-432.

Ooi, K.G.; Wakefield, D.; Billson, F.A.; Watson, S.L. (**2015**). Efficacy and safety of topical atorvastatin for the treatment of dry eye associated with blepharitis: A pilot study. *Ophthalmic Res.* 54(1), 26-33.

Ozkiris, A.; Erkiliç, K.; Koç, A.; Mistik, S. (**2007**). Effect of atorvastatin on ocular blood flow velocities in patients with diabetic retinopathy. *Br. J. Ophthalmol.* 91(1), 69-73.

Paliwal, S.K.; Chauhan, R.; Sharma, V.; Majumdar, D.K.; Paliwal, S. (**2009**). Entrapment of ketorolac tromethamine in polymeric vehicle for controlled drug delivery. *Indian J. Pharm. Sci.* 71(6), 687-691.

Paradiso, P.; Colaço, R.; Mata, J.L.G.; Krastev, R.; Saramago, B.; Serro, A.P. (**2017**). Drug release from liposome coated hydrogels for soft contact lenses: the blinking and temperature effect. *J. Biomed. Mater. Res. B Appl. Biomater*. 105(7), 1799-1807.

Peng, C.C.; Chauhan, A. (**2012**). Ion transport in silicone hydrogel contact lenses, *J. Membr. Sci.* 399-400, 95–105.

Pereira-da-Mota, A.F.; Phan, C.M.; Concheiro, A.; Jones, L.; Alvarez-Lorenzo, C. (**2022**). Testing drug release from medicated contact lenses: The missing link to predict in vivo performance. *J. Control. Release.* 343, 672-702.

USC UNIVERSIDADE DE SANTIAGO DE COMPOSTELA

Pereira-da-Mota, A.F.; Vivero-Lopez, M.; Topete, A.; Serro, A.P.; Concheiro, A.; Alvarez-Lorenzo, C. (**2021**). Atorvastatin-eluting contact lenses: Effects of molecular imprinting and sterilization on drug loading and release. *Pharmaceutics.* 13(5), 606.

Phan, C.M.; Bajgrowicz-Cieslak, M.; Subbaraman, L.N.; Jones, L. (**2016**). Release of moxifloxacin from contact lenses using an in vitro eye model: Impact of artificial tear fluid composition and mechanical rubbing. *Transl. Vis. Sci. Technol.* 5(6), 3.

Phan, C.M.; Shukla, M.; Walther, H.; Heynen, M.; Suh, D.; Jones, L. (**2021**). Development of an in vitro blink model for ophthalmic drug delivery. *Pharmaceutics.* 13(3), 300.

Pozuelo, J.; Compañ, V.; González-Méijome, J.M.; González, M.; Mollá, S. (**2014**). Oxygen and ionic transport in hydrogel and silicone-hydrogel contact lens materials: An experimental and theoretical study. *J. Membr. Sci.* 452, 62-72.

Ribeiro, A.; Veiga, F.; Santos, D.; Torres-Labandeira, J.J.; Concheiro, A.; Alvarez-Lorenzo, C. (**2011**). Bioinspired imprinted PHEMA-hydrogels for ocular delivery of carbonic anhydrase inhibitor drugs. *Biomacromolecules*. 12(3), 701-709.

Sayin, N.; Kara, N.; Pekel, G. (**2015**). Ocular complications of diabetes mellitus. *World J. Diabetes*. 6(1), 92-108.

Schoenberger, S.D.; Kim, S.J.; Sheng, J.; Rezaei, K.A.; Lalezary, M.; Cherney, E. (**2012**). Increased prostaglandin E2 (PGE2) levels in proliferative diabetic retinopathy, and correlation with VEGF and inflammatory cytokines. *Invest. Ophthalmol. Vis. Sci.* 53(9), 5906-5911.

USC UNIVERSIDADE DE SANTIAGO DE COMPOSTELA

Sekar, P.; Chauhan, A. (**2019**). Effect of vitamin-E integration on delivery of prostaglandin analogs from therapeutic lenses. *J. Colloid Interface Sci.* 539, 457-467.

Shikamura, Y.; Yamazaki, Y.; Matsunaga, T.; Sato, T.; Ohtori, A.; Tojo, K. (**2016**). Hydrogel ring for topical drug delivery to the ocular posterior segment. *Curr. Eye Res.* 41(5), 653-661.

Subrizi, A.; Del Amo, E.M.; Korzhikov-Vlakh, V.; Tennikova, T.; Ruponen, M.; Urtti, A. (**2019**). Design principles of ocular drug delivery systems: importance of drug payload, release rate, and material properties. *Drug Discov. Today.* 24(8), 1446-1457.

Tieppo, A.; Boggs, A.C.; Pourjavad, P.; Byrne, M.E. (**2014**). Analysis of release kinetics of ocular therapeutics from drug releasing contact lenses: Best methods and practices to advance the field. *Contact Lens Ant. Eye.* 37(4), 305–313.

Tieppo, A.; White, C.J.; Paine, A.C.; Voyles, M.L.; McBride, M.K.; Byrne, M.E. (**2012**). Sustained in vivo release from imprinted therapeutic contact lenses. *J. Control. Release.* 157(3), 391-397.

Toffoletto, N.; Saramago, B.; Serro, A.P. (**2020**). Therapeutic ophthalmic lenses: A review. *Pharmaceutics.* 13(1), 36.

van Bijsterveld, O.P. (**1969**). Diagnostic tests in the Sicca syndrome. *Arch. Ophthalmol.* 82(1), 10-14.

Varela-Garcia, A.; Concheiro, A.; Alvarez-Lorenzo, C. (**2020**). Cytosine-functionalized bioinspired hydrogels for ocular delivery of antioxidant transferulic acid. *Biomater. Sci.* 8(4), 1171–1180.

USC UNIVERSIDADE DE SANTIAGO DE COMPOSTELA

Varela-Garcia, A.; Concheiro, A.; Alvarez-Lorenzo, C. (**2018**). Soluplus micelles for acyclovir ocular delivery: Formulation and cornea and sclera permeability. *Int. J. Pharm.* 552(1-2), 39–47.

Vézina, M. (**2012**). Comparative ocular anatomy in commonly used laboratory animals. In Assessing ocular toxicology in laboratory animals (Weirm A.B., Collins, M., Eds.). Humana Press, Totowa, NJ., 1-21.

Vilaseca, P.; Dawson, K.A.; Franzese, G. (**2013**). Understanding and modulating the competitive surface-adsorption of proteins through coarse-grained molecular dynamics simulations. *Soft Matter.* 9, 6978–6985.

Wang, L.; Lou, J.; Cao, J.; Wang, T.; Liu, J.; Mi, W. (**2021**). Bicarbonate Ringer's solution for early resuscitation in hemorrhagic shock rabbits. *Ann. Transl. Med*. 9(6), 462.

Wataha, J.C.; Hanks, C.T.; Sun, Z. (**1994**). Effect of cell line on in vitro metal ion cytotoxicity. *Dent Mater.* 10(3), 156-161.

Wong, T.Y.; Cheung, C.M.; Larsen, M.; Sharma, S.; Simó, R. (**2016**). Diabetic retinopathy. *Nat. Rev. Dis. Primers.* 2, 16012.

Wu, C.; Or, P.W.; Chong, J.I.T.; Don, I.K.K.; Lee, C.H.C.; Wu, K.; Yu, M.; Lam, D.C.C.; Yang, Y. (**2021**). Extended delivery of pirfenidone with novel, soft contact lenses in vitro and in vivo. *J. Ocul. Pharmacol Ther*. 37(2), 75-83.

Xu, J.; Ge, Y.; Bu, R.; Zhang, A.; Feng, S.; Wang, J.; Gou, J.; Yin, T.; He, H.; Zhang, Y.; Tang, X. (**2019**). Co-delivery of latanoprost and timolol from micelles-laden contact lenses for the treatment of glaucoma. *J. Control. Release.* 305, 18-28.

USC UNIVERSIDADE DE SANTIAGO DE COMPOSTELA

Xu, J.; Li, X.; Sun, F. (**2010**). Preparation and evaluation of a contact lens vehicle for puerarin delivery. *J. Biomater. Sci. Polym. Ed.* 21(3), 271–288.

Zernii, E.Y.; Baksheeva, V.E.; Iomdina, E.N.; Averina, O.A.; Permyakov, S.E.; Philippov, P.P., et al. (**2016**). Rabbit models of ocular diseases: new relevance for classical approaches. *CNS & Neurological Disorders-Drug Targets.* 15(3), 267-291.

Zhang, J.; McGwin, G. Jr. (**2007**). Association of statin use with the risk of developing diabetic retinopathy. *Arch. Ophthalmol.* 125(8), 1096-1099.

Zhu, Y.; Sheng, Y. (**2020**). Sustained delivery of epalrestat to the retina using PEGylated solid lipid nanoparticles laden contact lens. *Int. J. Pharm.* 587, 119688.

USC UNIVERSIDADE DE SANTIAGO DE COMPOSTELA

USC
UNIVERSIDADE
DE SANTIAGO
DE COMPOSTELA

Chapter 5

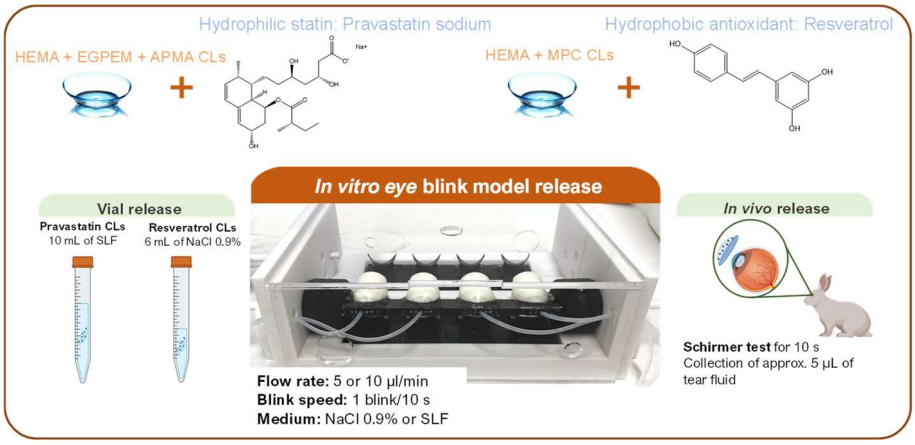

The work described in this chapter was published in ***In vitro* – *in vivo* correlation of drug release profiles from medicated contact lenses using an *in vitro* eye blink model,** *Drug Delivery and Translational Research* (DOI: 10.1007/s13346-022-01276-6), 2022, *authored by*

Ana F. Pereira-da-Mota[a], María Vivero-Lopez[a], Piyush Garg[b], Chau-Minh Phan[b,c], Angel Concheiro[a], Lyndon Jones[b,c] and Carmen Alvarez-Lorenzo[a]

[a]Departamento de Farmacología, Farmacia y Tecnología Farmacéutica, I+D Farma Group (GI-1645), Facultad de Farmacia, Instituto de Materiales (iMATUS) and Health Research Institute of Santiago de Compostela (IDIS), Universidade de Santiago de Compostela, 15782 Santiago de Compostela, Spain.

[b]Centre for Ocular Research & Education (CORE), School of Optometry and Vision Science, University of Waterloo, Waterloo, ON, Canada.

[c]Centre for Eye and Vision Research (CEVR), 17W, Hong Kong, Science Park, Hong Kong.

USC UNIVERSIDADE DE SANTIAGO DE COMPOSTELA

USC
UNIVERSIDADE
DE SANTIAGO
DE COMPOSTELA

5. IN VITRO – IN VIVO CORRELATION OF DRUG RELEASE PROFILES FROM MEDICATED CONTACT LENSES USING AN IN VITRO EYE BLINK MODEL

5.1 INTRODUCTION

The use of contact lenses (CLs) as platforms for controlled delivery of ophthalmic drugs was envisioned in 1961 by Otto Wichterle and co-workers [Wichterle, 1961]. After 60 years, the first commercial drug-delivering CL has become available in Japan, Canada and the USA [Johnson & Johnson Vision Care, 2022]. Compared to eye drops, CLs may significantly extend drug residence time and increase ocular bioavailability, while unproductive drug absorption is minimized [Lanier et al., 2020].

CLs are one of the most successfully commercialised biomedical devices, with nearly 150 million users worldwide [Review of Cornea & Contact Lenses, 2021]. However, several obstacles oppose their use as platforms for ocular drug delivery [Jones et al., 2021]. Most polymers used to prepare CLs, e.g. 2-hydroxyethyl methacrylate (HEMA) and 3-(methacryloyloxy)propyl tris(trimethylsiloxy)silane (TRIS), lack affinity for drugs, and thus typically, CLs do not uptake the required dose or release it too rapidly. A wide variety of strategies to overcome

USC UNIVERSIDADE DE SANTIAGO DE COMPOSTELA

this issue are under development [Minami et al., 2019; Sekar and Chauhan, 2019; Alvarez-Lorenzo et al., 2019; DiPasquale et al., 2022]. Additionally, there are no standardized methods for testing *in vitro* the drug release profiles from CLs. *In vitro* methods for mimicking the composition and dynamics of tear fluid, the frequency and pressure of blinking are still a challenge. Thus, in most reports focused on CLs, the *in vitro* drug release profiles are recorded in small beakers, using a variety of medium composition, volume, stirring, and replacement conditions [Hui and Wilcox, 2016; Pereira-da-Mota et al., 2022a]. As a consequence, most *in vitro* results are not predictive of *in vivo* performance [Minami et al. 2019]. This means that *in vivo* testing in animal models and human preclinical studies are still needed, even to evaluate early-stage drug-CL combination products, which makes the development very costly in time and resources.

In vitro models that mimic the *in vivo* scenario and key ocular parameters are highly explored. Microfluidic devices have been designed to regulate the flow and volume where CLs are immersed, but other physiological conditions were not reproduced by these devices, including factors such as corneal and eyelid shape and format, tear film thickness, or blinking [Tieppo et al., 2012; Pimenta et al., 2016]. 3D printed *in vitro* eye models to evaluate the *in vitro* performance of CLs have recently been undertaken to overcome some challenges faced by using microfluidic devices and more appropriately simulate the effects of tear flow rate, tear volume, air exposure, and eyelid blinking frequency [Phan et al., 2019; Phan et al., 2021]. Not surprisingly, under dynamic conditions of low tear fluid flow, CLs showed slower drug release profiles compared to static release in a beaker, prolonging the release for days or weeks for some specific compounds and drugs such as a red food dye [Phan et al., 2021], polyethylene glycol, hydroxypropyl methylcellulose [Phan et al., 2018], moxifloxacin [Phan

USC UNIVERSIDADE DE SANTIAGO DE COMPOSTELA

et al., 2016a] and fluconazole [Phan et al., 2016b]. Moreover, *in vitro* models can provide relevant insights in the development process of drug-loaded CLs and prioritize successful materials that may go forward to *in vivo* testing in animal preclinical models or human clinical studies.

There is still a paucity of information on how the *in vitro* release profiles recorded in the 3D printed eye models correlate with *in vivo* profiles. Comparison of the behaviour of the same drug-loaded CLs in both the *in vitro* model and the common rabbit eye model is, therefore, required for the validation of the information gathered *in vitro*. To gain an insight into the *in vitro-in vivo* correlations, the aim of this work was to analyze the release profiles of drug-loaded CLs recorded in a 3D printed *in vitro* eye blink model and compare the obtained results with the release in a small beaker and the tear levels previously obtained *in vivo*. For the sake of robustness, CLs loaded with drugs differing in physicochemical properties were tested; namely, CLs designed to uptake pravastatin (a hydrophilic statin, Log P = -0.23 [Murphy et al., 2020]) and resveratrol (a highly hydrophobic antioxidant, Log P = 3.09 [Yang et al., 2017]) were prepared and evaluated [Pereira-da-Mota et al., 2022b; Vivero-Lopez et al., 2021].

Pravastatin sodium and resveratrol may be useful for the treatment of a wide range of anterior and posterior ocular diseases. Prolonged oral therapy for hypercholesterolemia with statins has been shown to promote corneal healing, prevent cataract formation, reduce glaucoma severity, and reduce the appearance of hard exudates and microaneurysms in patients diagnosed with diabetic macular edema; ; topical ocular treatment has the advantage of avoiding systemic adverse reactions [Ooi et al., 2019; Gupta et al., 2004; Ozkiris et al., 2007; Nielsen and Nordestgaard, 2014]. Resveratrol is an antioxidant agent

USC UNIVERSIDADE DE SANTIAGO DE COMPOSTELA

that aids the management of oxidative-stress-related eye diseases and improves the healing of corneal epithelial cells [Tsai et al., 2015]. In previous studies, both drugs were incorporated in model CLs, and the *in vivo* performance evaluated in New Zealand white rabbits [Pereira-da-Mota et al., 2022b; Vivero-Lopez et al., 2022]. Both drug loaded-CLs provided significantly higher, and more prolonged drug levels in the rabbits' tear fluid compared to eye drops with the same dose, which favoured ocular biodistribution in the anterior and posterior structures of the eye, including cornea, sclera, lens, aqueous and vitreous humour, and retina. To carry out the present work, HEMA-based CLs were copolymerized with specific functional monomers that enhance drug affinity. In the case of pravastatin, HEMA was copolymerized with ethylene glycol phenyl ether methacrylate (EGPEM) and N-(3-aminopropyl) methacrylamide hydrochloride (APMA) (**Figure 5.1**). For resveratrol, methacryloyloxyethyl phosphorylcholine (MPC) was added as an antifouling comonomer. The developed CLs, coded as AECLs and MCLs, respectively, demonstrated adequate solvent uptake, light transmission, mechanical properties, and ocular safety. *In vitro* release experiments were carried out with sterile CLs loaded under specific conditions for each drug, depending on their physicochemical properties. *In vitro* release in the 3D eye blink model was tested at two different tears fluid flow rates (5 and 10 μL/min of fluid) and a blink speed of 1 blink/10 s. The amount of drug released from the CLs was collected and quantified by high-performance liquid chromatography (HPLC). To the best of our knowledge, this is the first time that drug-loaded CLs release profiles have been evaluated in an *in vitro* 3D eye model and *in vitro-in vivo* correlations (IVIVC) are attempted.

USC UNIVERSIDADE DE SANTIAGO DE COMPOSTELA

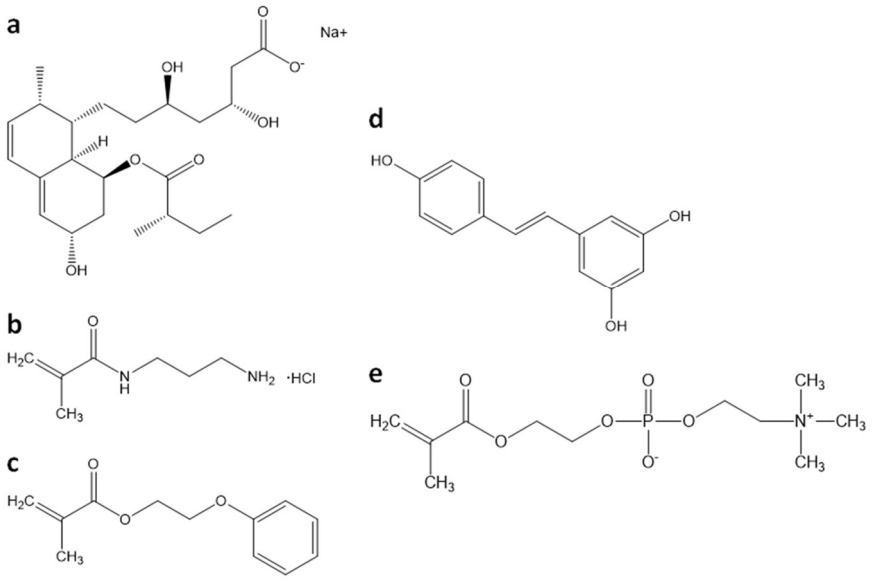

Figure 5.1. Chemical structures of the drugs and monomers. (**A**) Pravastatin sodium; (**B**) N-(3-aminopropyl) methacrylamide hydrochloride (APMA); (**C**) ethylene glycol phenyl ether methacrylate (EGPEM); (**D**) trans-resveratrol, and (**E**) 2-methacryloyloxyethyl phosphorylcholine (MPC).

5.2 MATERIALS AND METHODS

5.2.1 Materials

Pravastatin sodium was supplied by Biocon Limited (Bengaluru, Karnataka, India). Resveratrol was from ChemCruz, Santa Cruz Biotechnology Inc. (Dallas, TX, USA). 2-Hydroxyethyl methacrylate (HEMA) and di-sodium hydrogen phosphate anhydrous (NaH_2PO_4) were from Merck (Darmstadt, Germany). N-(3-aminopropyl) methacrylamide hydrochloride (APMA) was from PolySciences Inc. (Warrington, PA, USA). Ethylene glycol dimethacrylate (EGDMA), ethylene glycol phenyl ether methacrylate (EGPEM), 2,2′ -

USC UNIVERSIDADE DE SANTIAGO DE COMPOSTELA

azobis(isobutyronitrile) (AIBN), 2-methacryloyloxyethyl phosphorylcholine (MPC), polyvinyl alcohol (PVA, 89-98 kDa, 99% hydrolyzed), and dimethyl sulfoxide (DMSO) were from Sigma-Aldrich (Steinheim, Germany). Sodium chloride (NaCl) was from Labkem (Barcelona, Spain), and sodium hydroxide (NaOH) was from VWR Chemicals (Leuven, Belgium). 3D printing UV-sensitive resin was from Anycubic Technology Co. (Shenzhen, Guangdong, China). Methanol 99.9% for LC-MS grade was from Fisher Scientific (Loughborough, UK). Simulated lachrymal fluid (SLF) was prepared as previously reported [Pereira-da-Mota et al., 2022b]. Ultrapure water (resistivity >18.2 MΩ cm; Milli-Q®, Millipore Ibérica, Madrid, Spain) was obtained by reverse osmosis.

5.2.2 Contact Lens Preparation

Two different types of HEMA-based CLs were prepared, as previously described [Pereira-da-Mota et al., 2022b; Vivero-Lopez et al., 2022]. Briefly, AECLs for pravastatin were prepared by mixing HEMA (3 mL) with APMA (21.45 mg), EGPEM (112.50 µL) and EGDMA (12.10 µL). The monomer solutions were magnetically stirred (200 rpm, at room temperature) for 120 min, and the initiator (AIBN; 14.79 mg) was then added and solubilized by magnetic stirring for a further 30 min.

To prepare MCLs for resveratrol, HEMA (3 mL) was mixed with MPC (337.5 mg) and EGDMA (12.10 µL) under magnetic stirring (150 rpm, at room temperature) for 60 min. The mixture was kept under magnetic stirring for 30 min more to ensure the complete dissolution of the AIBN (32.85 mg).

USC UNIVERSIDADE DE SANTIAGO DE COMPOSTELA

Both AECLs and MCLs were synthesized by adding 60 µL of monomers solution into curved polypropylene moulds typically used for daily disposable CLs preparation. The moulds were kept at 50 °C for 12 h and then at 70 °C for 24 h to complete thermal polymerization. Then, the moulds were immersed in MilliQ® water to facilitate CL separation. The obtained CLs were washed under magnetic stirring (200 rpm) in 1 L of MilliQ® water and NaCl 0.9% until complete removal of the unreacted monomers occurred; the solvent was replaced at least 3 times per day. The absence of unreacted monomers was monitored by UV-Vis spectrophotometry (Agilent 8453, Waldbronn, Germany).

The final dimensions of hydrated CLs (immersed in phosphate buffer pH 7.4) were approx. 12 mm diameter, 7.8 mm curvature, and 0.1 mm thickness for AECLs and approx. 14 mm diameter, 8.8 mm curvature, and 0.1 mm thickness for MCLs.

5.2.3 Drug Loading

5.2.3.1 Pravastatin Sodium

Dried AECLs (average mass 16.91 ± 1.28 mg) were packaged and sealed in polyamide/polyethylene vacuum bags filled with 10 mL of an aqueous pravastatin solution (0.1 mg/mL) for at least 48 h and sterilized by high hydrostatic pressure (HHP, 70 °C and 600 MPa for 10 min) [Pereira-da-Mota et al., 2021]. The CLs were stored in sealed bags at room temperature and protected from the light until release experiments were performed. All experiments were carried out in quadruplicate. The amount of pravastatin loaded was quantified by HPLC, as explained in Section 5.2.6.

USC UNIVERSIDADE DE SANTIAGO DE COMPOSTELA

5.2.3.2 Resveratrol

Sterile MCLs (average mass 16.8 ± 1.86 mg, sterilized by steam heat at 121 °C, 20 min) were placed in tubes containing 7 mL of a resveratrol solution (0.1 mg/mL in ethanol:water 10:90 *v/v*) previously filtered (Filter-Lab® Polyethersulphone (PES) syringe filter 0.22 µm; Barcelona, Spain). The loading solution was added to the tubes under sterile conditions in a biological safety cabinet. The tubes were maintained protected from light to avoid resveratrol degradation at 37 °C, 180 rpm for 72 h, after which the release tests were performed (n = 4). The amount of resveratrol loaded was quantified by HPLC, as described in Section 5.2.6.

5.2.4 Eye Blink Model

The fabrication and assembly of the 3D eye model were similar to previous publications by some authors of this paper [Phan et al., 2019; Phan et al., 2021], with some minor changes (**Figure 5.2**).

USC UNIVERSIDADE DE SANTIAGO DE COMPOSTELA

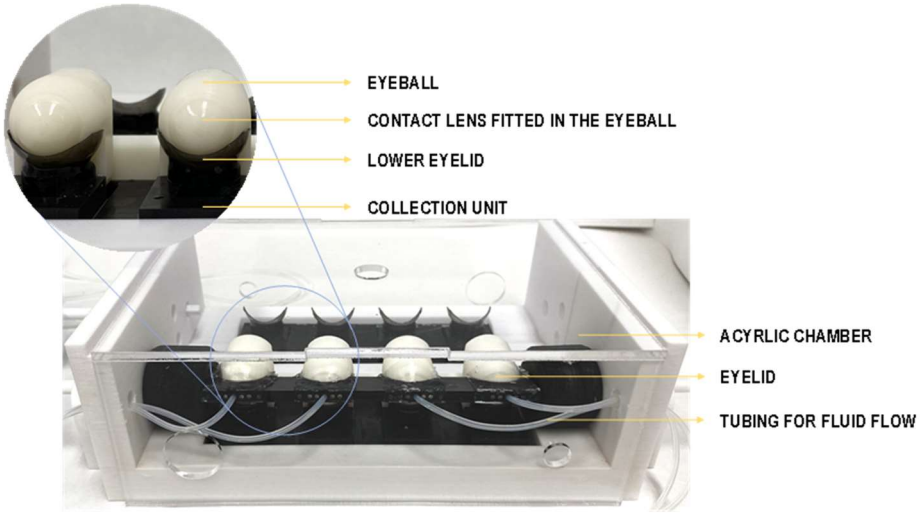

Figure 5.2. *In vitro* eye blink model (Ocublink) setup. The eyelid movement spreads the tear solution, which is supplied through the tubing that is attached to the eyelid support, over the eyeball, and the contact lens (fitted on the eyeball, shown in the close-up image). The out-flow solution is collected in the collection unit located below the eyeball.

5.2.4.1 Eyeball and Collection Unit

The eyeball, lower eyelid and collection unit were fabricated using a combination of 3D printing and moulding techniques [Phan et al., 2016c]. The components were printed using a hydrophobic UV-polymerizable resin on an SLA (stereolithography) 3D printer (Photon S, Anycubic, Shenzhen, China) and an FDM (fused deposition modelling) 3D printer (Prusa i3 MK3S+, Prusa Prague, Czech Republic) to ensure water-sealed parts. All printing parameters were set to the manufacturer's default settings. The eyeball was composed of two curvatures - 11.25 mm for the larger globe and 8.6 mm for the smaller globe containing the cornea. The 8.6 mm was chosen to match the most common base curve of CLs. Compared to previous models

USC UNIVERSIDADE DE SANTIAGO DE COMPOSTELA

[Phan et al., 2021], the model used in the current study did not have any coatings for the front corneal surface but instead had a 300 μm groove at the centre to allow for a CL to be mounted. In preliminary tests, it was found that the resin materials for the eyeball did not absorb pravastatin and resveratrol. The collection unit of the model was designed to allow the tear film to flow from the eyeball into the wells via gravity.

5.2.4.2 Eyelid

The eyelids were designed to have a curvature of 8.8 mm, which leaves a gap of approximately 200 μm between the eyeball and eyelid. Once a contact lens was applied on the eyeball, this gap was reduced by the thickness of the lens (75-150 μm). The eyelid was designed to rotate around the smaller globe, and flexes over the larger globe.

PVA eyelids were prepared by dissolving PVA (89-98 kDa, 20% w/v) in dimethyl sulfoxide: ultrapure water 80:20 *v/v* mixtures, following a previously described protocol [Phan et al., 2021]. Briefly, the mixture was gently stirred for 5 min and heated at 120 °C for 2 h. After heating, the mixture was stirred again to ensure proper mixing of PVA. The obtained viscous solution was cast in 3D printed moulds (allowing the preparation of 4 eyelids in the same mould) and then frozen at -30 °C for 12 h. The resulting gels were thawed at room temperature for 1 h, removed from the moulds and immersed in ultrapure water for 3 days, replacing the medium daily to remove the dimethyl sulfoxide used to prepare the PVA solution. After the washing process, the eyelids were immersed in ultrapure water to maintain the hydration of the eyelid until being used in the release experiments.

USC UNIVERSIDADE DE SANTIAGO DE COMPOSTELA

5.2.4.3 Flow Rate and Blinking

A commercial syringe pump (PHD ULTRA, Harvard Apparatus, Holliston, MA) was used to simulate the dynamic tear flow in the eye blink model. Simulated lachrymal fluid (SLF) or NaCl 0.9% was delivered through a hole at the top of the eyelid and spread over the eyeball surface/CL through blinking. In this study, the blink speed was set to 1 blink/10 s, and the flow rate was adjusted to 5 and 10 µL/min to ensure enough volume for sample collection at the predetermined time points. The blink velocity used in this model was 50 rpm or 45 mm/s for both closing and opening speeds; the average physiological speeds for closing and opening of the eyelid has been reported to be approximately 134 ± 4 mm/s and 26 ± 2 mm/s, respectively [Kwon et al., 2013].

5.2.4.4 Temperature and Humidity

The entire system was covered with an acrylic chamber to maintain a stable humidity and temperature (20 ± 1.5 °C) during the experiment. Humidity levels were maintained close to approximately 80% using a humidifier and controlled through a hygrometer.

5.2.4.5 Release Sampling

At predetermined time points (5, 15, 30 min and every hour until 10 h), the out-flow solution was pipetted from the collection unit, stored in 300 or 600 µL Eppendorf® tubes and frozen at -30 °C until HPLC analysis. The amount of resveratrol and pravastatin released from the CLs was quantified by HPLC previous dilution of the samples in ethanol:water 50:50 *v/v* and SLF, respectively. All the experiments were carried out in quadruplicate.

USC UNIVERSIDADE DE SANTIAGO DE COMPOSTELA

5.2.4.6 Drug Extraction from the Eyelid and CLs

After 10 h of experimentation, each PVA eyelid was removed from the system, cut into small pieces and immersed in 1 mL of SLF or 3 mL of ethanol:water 50:50 *v/v*, for AECLs and MCLs respectively. The eyelids were maintained at 37 °C, 180 rpm for at least 12 h to extract the amount of drug absorbed. The same procedure was applied for the CLs after 10 h on the eye model (without cutting) to determine the remaining amount of drug in the CLs at the end of the test.

5.2.5 Release in a Vial

Sterilized pravastatin-loaded AECLs (n = 4) were rinsed with SLF to remove the excess drug from the CLs surface and immersed in 2 or 10 mL of SLF (pH = 7.4) to evaluate if the release volume could have an impact on the drug release profile. The *in vitro* release experiments were performed at 37 °C, under oscillatory movement (180 rpm) and at predefined time points, 150 µL were removed and replaced by the same volume of fresh medium. The amount of pravastatin released from CLs was quantified by HPLC, as described in Section 5.2.6.

Resveratrol-loaded MCLs (n = 4) were rinsed with NaCl 0.9% and placed into 15 mL Falcon® tubes filled with 6 mL of NaCl 0.9%. At each predetermined timepoint, aliquots of 200 µL were removed and replaced with the same volume of fresh medium. After 8 h of release, 6 mL of fresh NaCl 0.9% were added, increasing the total volume of release medium to 12 mL to avoid medium saturation. The amount of resveratrol released from the CLs was quantified by HPLC, as described in Section 5.2.6.

USC UNIVERSIDADE DE SANTIAGO DE COMPOSTELA

5.2.6 Drug Quantification Methods

The amount of pravastatin and resveratrol loaded and released from the CLs was quantified by HPLC using previously developed methods [Pereira-da-Mota et al., 2022b; Vivero-Lopez et al., 2021]. *In vitro* release studies in vials were quantified by HPLC (AS-4140 autosampler, PU-4180 pump, LC-NetII/ADC interface box, CO-4060 column oven, MD-4010 photodiode array detector, JASCO, Tokyo, Japan) and operated with ChromNAV software v.2. *In vitro* release experiments using eye blink model were quantified by HPLC (Autosampler Waters 2690, Photodiode Detector 2996, Milford, MA, USA), operated with the Empower2 software.

In case of pravastatin, the mobile phase consisted of methanol:0.02 M sodium phosphate (NaH_2PO_4) buffer (50:50 *v/v*, pH adjusted to 7.0 with NaOH) at 1.00 mL/min and 25 °C. For pravastatin analysis, both HPLC equipment were fitted with a Waters Symmetry C18 column (5 µm, 3.9 × 150 mm). The injection volume was 80 µL, and the total run time of each sample was 10 min. Pravastatin was quantified at 238 nm (retention time 5.15 min). The HPLC method was validated using pravastatin solutions in simulated lachrymal fluid between 1 to 40 µg/mL. For resveratrol, the analysis was carried out under isocratic elution using a mobile phase of methanol: water 50:50 *v/v* at a flow rate of 1 mL/min, 35 °C and with 8 min of run time. The injection volume was 80 µL, and the UV detector was set at 305 nm. The retention time was 4.6 min. Both HPLC equipments were fitted with a Water Symmetry C18 column (5 µm, 4.6 × 250 mm). Validation of the method was performed using a calibration curve of resveratrol in ethanol:water 50:50 *v/v* in the 0.05 – 6 µg/mL range.

USC UNIVERSIDADE DE SANTIAGO DE COMPOSTELA

5.2.7 Statistical Analysis

Statistical analysis was performed using Statgraphics Centurion 18 v. 18.1.13 (Statgraphics Technologies, Inc., Warrenton, VA, USA). One-way analysis of variance (ANOVA) followed by Multiple Range Test was carried out. The descriptive data were presented as mean ± standard deviation. In all cases, statistical significance was considered significant for a value of $p < 0.05$.

5.3 RESULTS AND DISCUSSION

5.3.1 3D Eye Blink Model

In this work, a 3D printed eye blink model was used to mimic some physiological ocular parameters, and *in vivo* comparisons were carried out. To mimic the tear fluid flow in the eye, fluid flow rates of 5 and 10 µL/min were chosen to ensure there was enough volume for sample collection at every predetermined time point. Preliminary trials carried out with flow rates closer to those reported for physiological tear flow values in humans (1.4–4.3 µL/min, [Glasson et al., 2006] or in rabbits(0.47-0.66 µL/min [Chrai et al., 1973]) demonstrated that these rates were insufficient to maintain a reliable, constant flow rate of fluid on the eye model required for subsequent sample collections. It should be noted that the experiments with the eye blink model were carried out at room temperature as the system still lacks internal heating.

5.3.1.1 Pravastatin

The amount of pravastatin loaded by AECLs was approximately 3.50 ± 0.84 mg/g of dried hydrogel. Pravastatin stability against HHP sterilization was previously verified, and the chosen conditions did not

USC UNIVERSIDADE DE SANTIAGO DE COMPOSTELA

trigger degradation compared to non-sterilized pravastatin CLs, which showed that this method is compatible with the sterilization of pravastatin-loaded CLs [Pereira-da-Mota et al., 2021].

Pravastatin release was investigated *in vitro* by recording in parallel the amount of pravastatin released when the AECLs were placed in the eye blink model and in test tubes (**Figure 5.3A**). In the *in vitro* eye blink model, the pravastatin release profiles were more sustained, and the percentage of drug released after 10 h of the experiment was lower compared to *in vitro* vial release. Statistically significant differences were detected between the percentage of drug released in a vial filled with 2 and 10 mL and the eye blink model (flow rate of 5 and 10 µL/min) in the first 3 h of the experiment (ANOVA, $p < 0.007$). The influence of the flow rate in the eye blink model on the drug released was tested with two different flow rates (5 and 10 µL/min) and a slight decrease in the percentage of pravastatin released was observed with the flow rate of 5 µL/min compared to a flow rate of 10 µL/min, but no statistical differences were detected (ANOVA, $p > 0.05$).

After 10 h of experimentation in the eye blink model, the CLs and eyelids were immersed in SLF in order to measure the amount of pravastatin retained in the materials (**Figure 5.3B**). A significantly higher amount of pravastatin was detected in the PVA eyelid at 5 µL/min compared to the flow rate of 10 µL/min (ANOVA, $p < 0.001$). However, no significant differences were detected in the amount of drug that remained in the CLs for the different flow rates (ANOVA, $p = 0.72$).

USC UNIVERSIDADE DE SANTIAGO DE COMPOSTELA

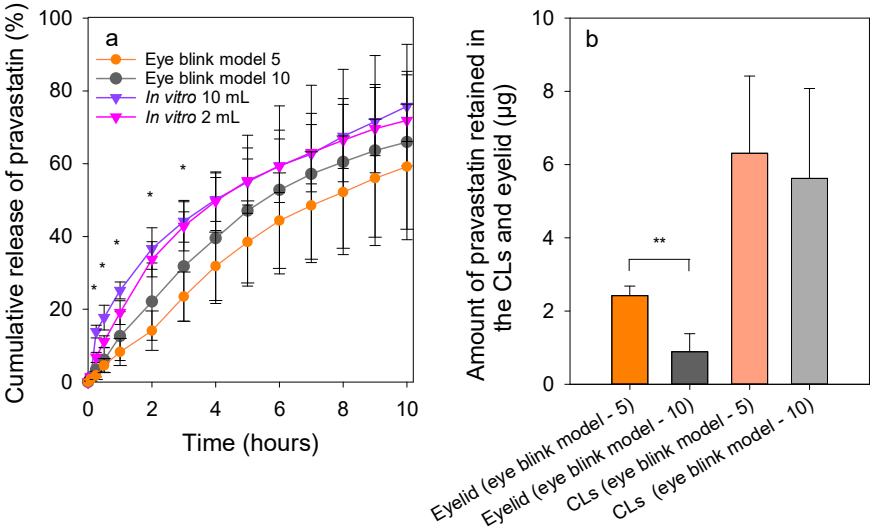

Figure 5.3. (**A**) Pravastatin release profiles from AECLs experimentally recorded in a vial filled with 2 or 10 mL of SLF over 10 h and using the eye blink model (flow rate of 5 and 10 µL/min); (**B**) amount of pravastatin retained in the PVA eyelid and CLs after 10 h on the eye blink model (n = 4; mean values and standard deviations); * Statistically significant differences from the amount of pravastatin released *in vitro* in 2 and 10 mL and in the eye blink model (flow rate of 5 and 10 µL/min); **Statistically different between the amount of pravastatin retained in the model eyelid with the flow rate of 5 and 10 µL/min, $p < 0.05$.

For the *in vitro* vial release, two different volumes were evaluated, 10 and 2 mL of SLF. No statistically significant differences were detected between pravastatin release profiles in 2 and 10 mL of SLF (ANOVA, $p > 0.05$). This minor effect of the volume on the percentage of pravastatin released may be explained by the free-water solubility of pravastatin (40 mg/mL, [European Directorate for the Quality of Medicines & HealthCare, 2008]), therefore, the volume decrease did not induce a false plateau or delayed the release.

USC UNIVERSIDADE DE SANTIAGO DE COMPOSTELA

The differences between the percentages of pravastatin released in the vial and in the eye blink model could be attributed to several reasons, such as the release volume and the absorption of the drug by the eye model materials, among others. Firstly, in the *in vitro* vial system, the CLs were immediately immersed into vials containing a volume 33 times higher than the volume delivered in the eye model (300 and 600 µL/h). This increase in fluid volume could influence the concentration gradient between the inside of the CL and the release medium, promoting a faster release in the first hours of the release. Secondly, in theory, the CLs in the eye blink model were exposed to a total fluid of 3.0 and 6.0 mL of SLF after 10 h. However, the amounts of fluid collected were 2.23 ± 0.21 mL and 5.47 ± 0.65 mL (for a flow rate of 5 and 10 µL/min, respectively), corresponding to a fluid loss of 25% and 9%. This nonspecific fluid loss due to evaporation, absorption by the eyelid or dead volume could also contribute to a decrease of the fluid that reached the CL and consequently a decrease in the volume available for drug release. Thirdly, a portion of pravastatin was absorbed by the PVA-eyelid over 10 h of experiment, 2.42 ± 0.26 µg at 5 µL/min and 0.88 ± 0.49 µg at 10 µL/min. As a result, the drug release was slower in the eye blink model, especially in the first few hours.

5.3.1.2 Resveratrol

For resveratrol release experiments, a two-step sterilization protocol was implemented as resveratrol may degrade at high temperature [Zupančič et al., 2015; Silva et al., 2017]. The MCLs were sterilized by steam heat (121 °C, 20 min) in empty Falcon® tubes and then the tubes were filled with a previous filtered resveratrol solution (0.1 mg/mL in ethanol:water 10:90 *v/v*). MCLs loaded, on average

USC UNIVERSIDADE DE SANTIAGO DE COMPOSTELA

approximately 13.20 ± 0.90 mg of resveratrol per g of dried hydrogel, after being immersed in drug solution for 72 h.

In the *in vitro* vial conditions, the MCLs released 54.43 ± 7.29% resveratrol in the first 10 h (**Figure 5.4A**). As happened with pravastatin, the amount of resveratrol released in the eye blink model was significantly lower: 0.37 ± 0.22% at 5 µL/min and 0.47 ± 0.26% at 10 µL/min (ANOVA, $p < 0.001$) than the amount released in the vial. The difference between the vial results and eye blink model might be related to the diffusion resistance associated with the hydrophobic nature of resveratrol [Salehi et al., 2018] since resveratrol solubility in NaCl 0.9% was quantified to be approx. 27.4 µg/mL [Vivero-Lopez et al., 2021]. In the case of the vial tests, the volume of the release medium was increased up to 12 mL to avoid medium saturation and false plateaus.

The amount of resveratrol absorbed by the PVA eyelid was about 10-fold higher compared to pravastatin, showing a higher affinity between resveratrol and the PVA eyelid (**Figure 5.4B**). This higher affinity could also contribute to the decrease of resveratrol detected in the fluid collected from the eye blink model. A higher fluid flow rate (10 µL/min) induced a higher amount of resveratrol absorbed by the eyelid (ANOVA, $p < 0.001$). As a consequence of the slow release from the MCLs, the amount of resveratrol remaining in the CLs after 10 h of the release tests was approx. 40% of the drug loaded (91.29 ± 13.85 µg for 5 µL/min and 71.37 ± 8.77 µg for 10 µL/min). No statistical differences were detected between both flow rates (ANOVA, $p = 0.10$).

USC UNIVERSIDADE DE SANTIAGO DE COMPOSTELA

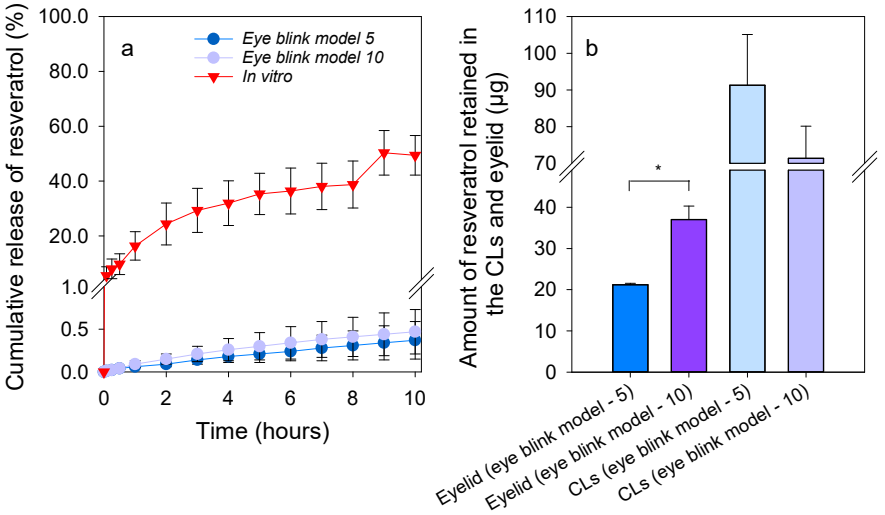

Figure 5.4. (**A**) Resveratrol release profiles from MCLs experimentally recorded in a vial filled with 6 mL of NaCl 0.9% over 10 h and on the eye blink model (flow rate of 5 and 10 µL/min); (**B**) amount of resveratrol retained in the PVA eyelid and CLs after 10 h on the eye blink model (n = 4; mean values and standard deviations; * Statistically different between the amount of resveratrol retained in the model eyelid with the flow rate of 5 and 10 µL/min, $p < 0.05$.

5.3.2 *In vivo* Release – Eye Blink Model Comparisons

The release profiles from the eye blink models for both pravastatin and resveratrol (concentration versus time) obtained were also compared to the *in vivo* rabbit data already reported for these same CLs [Pereira-da-Mota et al., 2022b; Vivero-Lopez et al., 2022]. Briefly, six healthy male New Zealand white rabbits were selected for the *in vivo* release studies wearing drug-loaded CLs. Drug-loaded CLs were removed from the loading solutions, rinsed with sterile saline solution for CLs, and carefully placed on the rabbits' right eye below the nictitating membrane and without local anesthesia. Samples of the tear

USC UNIVERSIDADE DE SANTIAGO DE COMPOSTELA

fluid were collected using Schirmer test strips before and after CLs wearing (t = 5 min, 15 min, 30 min, and every hour until 8 or 10 h). The drug concentration in tear fluid was quantified by immersing the Schirmer strips in SLF or ethanol: water (50:50 *v/v*), and the resulting solutions were quantified by HPLC [Pereira-da-Mota et al., 2022b; Vivero-Lopez et al., 2022].

5.3.2.1 Pravastatin

Pravastatin release profiles from AECLs during the *in vivo* experiment and in the eye blink model for both flow rates are compared in **Figure 5.5**. The maximum concentration for both experiments was obtained after 30 min of CL application. Pravastatin maximum levels were 177.5 ± 116.8 µg/mL for *in vivo*, and 28.39 ± 3.00 µg/mL and 39.13 ± 20.48 µg/mL for the eye blink model with a flow rate of 5 µL/min and 10 µL/min, respectively. The peak of maximum concentration was followed by a smooth decrease of drug concentration in the tear fluid and in the fluid collected from the eye blink model. No burst release was observed.

USC UNIVERSIDADE DE SANTIAGO DE COMPOSTELA

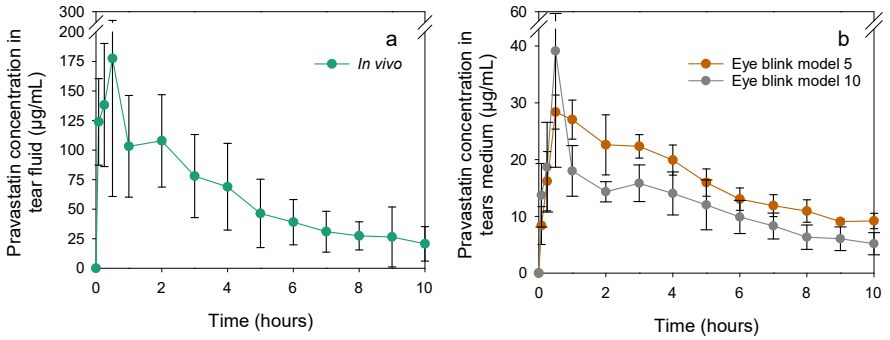

Figure 5.5. (**A**) *In vivo* tear fluid levels of pravastatin were recorded during wear of pravastatin-loaded AECLs for 8 and 10 h (n = 6 for 8 h and n = 3 for 9 and 10 h), data taken from Pereira-da-Mota et al. [Pereira-da-Mota et al., 2022b]; (**B**) Normalized pravastatin released concentration in SLF from pravastatin-loaded AECLs over 10 h on the eye model (flow rate of 5 and 10 µL/min) (*n* = 4; mean values and standard deviations).

Despite the similar release patterns, the amount of pravastatin released from the CLs in the eye blink model was about 5-fold lower than that recorded in the *in vivo* studies (ANOVA, $p < 0.05$). This finding might be related to several factors: (i) the drug absorption into the PVA eyelid in the model, (ii) the composition of the release medium, (iii) the temperature, and (iv) complexity of the eyeball piece. Firstly, the PVA eyelid absorbed approximately 2.42 ± 0.26 µg pravastatin when tested under 5 µL/min and 0.89 ± 0.49 µg for 10 µL/min. Secondly, the physiological tear fluid contains proteins, lipids and mucin that can promote drug release from the CLs [Mahomed et al., 2016]. In previous studies, the influence of BSA and lysozyme on pravastatin release rate from CLs was evaluated, and an increase in the amount of pravastatin released was observed with the incorporation of both proteins in the 2 mL of SLF [Pereira-da-Mota et al., 2022b]. The effect of proteins, lipids, and other components of the tear fluid on the

USC UNIVERSIDADE DE SANTIAGO DE COMPOSTELA

release kinetics from CLs is an important aspect to take into account in further studies. Thirdly, in this work, a stable room temperature of 20 ± 1.5 °C was maintained during the release experiments in the eye model, but an increase in temperature from 20°C to 34 °C was previously shown to enhance 20% of the fractional mass released from pHEMA hydrogels after 48 h *in vitro* in vials [Tieppo et al., 2014; Miyazaki et al., 2001]. This phenomenon could be related to higher kinetic energy of the drug molecules when the temperature increases, leading to a faster diffusional transport [Ferreira et al., 2020]. The effect of temperature on pravastatin solubility could also contribute to a higher amount of drug released from the CLs *in vivo* [Jia et al., 2008]. Fourthly, another limitation that could compromise the release from CLs in the eye blink model pertains to the composition of the eyeball piece. In the present study, the eyeball piece was printed with a hydrophobic UV-polymerizable resin which does not represent corneal surface properties. 90 per cent of the cornea consists of the stroma, which contains a high percentage of water and consists of collagen fibril lamellae oriented parallel to each other, which is more comparable to a hydrophilic hydrogel. In *in vivo* conditions, corneal osmosis adds water to the post-lens tear film (the tear film between the back surface of the CL and the corneal epithelium), diluting the concentration of the drug in the post-lens tear film, which could increase the drug release from the drug-loaded CL.

Comparing the release profiles from the different flow rates in the eye blink model, a slightly faster release was observed for a flow rate of 10 µL/min, achieving a higher maximum concentration at 30 min, followed by a decrease in the concentration of drug present in fluid collected (ANOVA, $p > 0.05$).

USC UNIVERSIDADE DE SANTIAGO DE COMPOSTELA

Correlations for *in vivo-in vitro* in the eye blink model or *in vitro-in vitro* (in a vial versus eye blink model) were investigated using Levy Plots (**Figure 5.6**). Release tests in the eye blink model with a flow rate of 10 µL/min led to a correlation coefficient (r^2) closer to 1 (0.993) compared to the Levy plot obtained for 5 µL/min (**Figure 5.6A**). The intercepts at the origin were +6.25 and +1.93; the slopes were 1.83 and 1.62 for a flow rate of 5 and 10 µL/min, respectively. Thus, a stronger correlation was observed with 10 µL/min flow rate that favoured the *in vivo-in vitro* correlations. Also, a higher correlation coefficient was obtained for the Levy plot comparing the *in vitro* tests in a vial (2 and 10 mL) and eye blink model with a flow rate of 10 µL/min (**Figure 5.6B**).

USC UNIVERSIDADE DE SANTIAGO DE COMPOSTELA

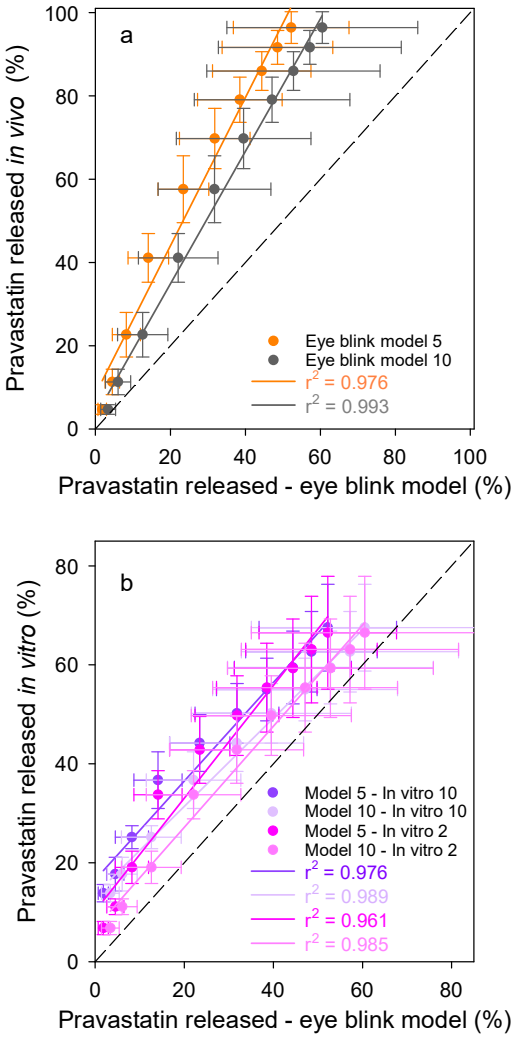

Figure 5.6. Levy plots for *in vivo* (**A**) or *in vitro* (**B**) *vs*. eye blink model percentage of pravastatin released. The eye blink model experiments were carried out with 5 and 10 µL/min of flow rate (eye blink model 5/Model 5 and eye blink model 10/Model 10, respectively). The *in vitro* tests in a vial were carried out in 2 and 10 mL of SLF.

5.3.2.2 Resveratrol

Resveratrol-loaded CLs presented a sustained release in the eye blink model as occurred *in vivo* (**Figure 5.7**). However, the concentration of resveratrol detected in the fluid collected in the eye blink model was approximately 150-fold lower than *in vivo* (ANOVA, $p < 0.001$), likely associated with several factors that also conditioned the release of the hydrophilic statin in the eye blink model, plus the low solubility of resveratrol in an aqueous medium, as previously mentioned. No statistical differences were detected between the two different flow rates (ANOVA, $p > 0.05$).

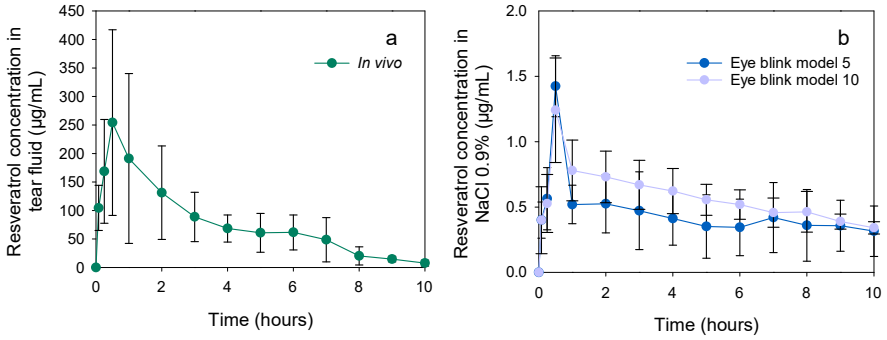

Figure 5.7. (**A**) *In vivo* tear fluid levels of resveratrol were recorded during wear of resveratrol-loaded MCLs for 8 and 10 h (n = 6 for 8 h and n = 3 for 9 and 10 h), data taken from Vivero-Lopez et al. [Vivero-Lopez et al., 2022]; (**B**) Normalized resveratrol released concentration in NaCl 0.9% from resveratrol-loaded MCLs over 10 h on the eye model (flow rate of 5 and 10 µL/min) (n = 4; mean values and standard deviations).

For resveratrol experiments, plots of *in vivo* release *versus in vitro* release in the eye blink model presented slopes that were remarkably high: 333.96 and 245.16 for a flow rate of 5 and 10 µL/min, respectively (**Figure 5.8**), which supported that the percentage of resveratrol

USC UNIVERSIDADE DE SANTIAGO DE COMPOSTELA

released *in vivo* was significantly higher than that recorded in the eye blink model. In comparison, no differences were obtained for *in vitro* vial release and the eye blink model. This finding highlights the difficulties in developing *in vitro* release models that can predict the *in vivo* performance of CLs loaded with hydrophobic drugs, which represent about 40% of current pharmaceutical treatments [Torres-Luna et al., 2020].

USC UNIVERSIDADE DE SANTIAGO DE COMPOSTELA

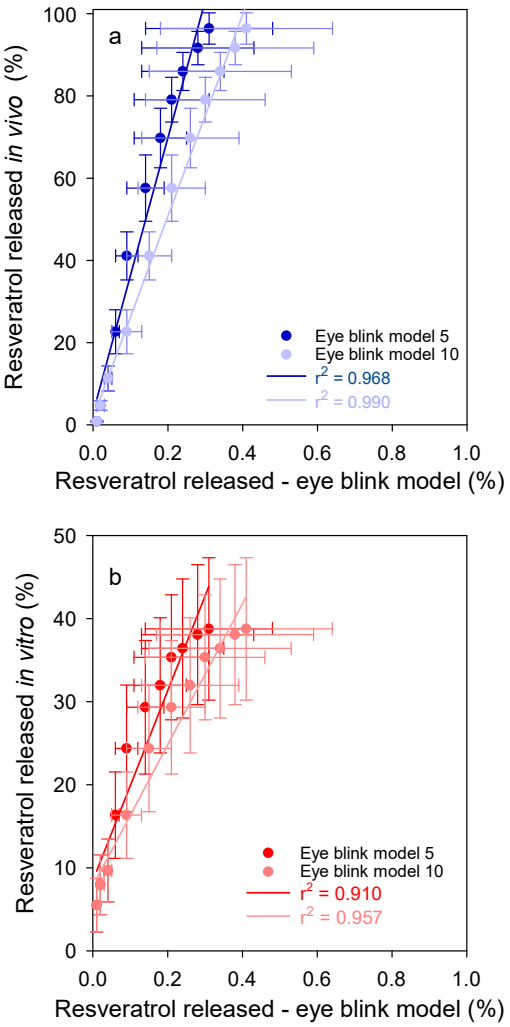

Figure 5.8. Correlations for *in vivo* (**A**) or *in vitro* (**B**) *vs.* eye blink model percentage of resveratrol released. The eye blink model experiments were carried out with 5 and 10 µL/min of flow rate (eye blink model 5; eye blink model 10, respectively).

USC UNIVERSIDADE DE SANTIAGO DE COMPOSTELA

5.4 CONCLUSIONS

In the current study, the usefulness of the developed 3D printed eye blink model for the evaluation of drug release profiles of medicated CLs has been explored in detail. To our knowledge, this was one of the first studies that have attempted to correlate the release of drugs from lenses from an in vivo rabbit study with a blink model. It may serve as an important starting point to understand the areas that need to be further developed and investigated to create better simulations. There are numerous factors in the eye that can affect drug release kinetics and understanding the contribution/effect of each factor individually to drug release kinetics is not obvious. For instance, in this study, increasing the flow rate by 2X was expected to increase the drug release rate by 2X. However, this was not the case – increasing the flow by 2X only resulted in a marginal increase in the amounts of drugs released, which was not obvious. The release profile of both drugs was more sustained and lower in the *in vitro* eye blink model compared to the *in vitro* release in vials, especially for the hydrophobic drug resveratrol. Both drug-loaded CLs showed similar release patterns in the eye blink model as in *in vivo* studies. However, the amount of drug released in the eye blink model was significantly lower compared to previously obtained *in vivo* data. More linear Levy plots were recorded for pravastatin release in the eye model (flow rate of 10 µL/min) and *in vivo* data. The information gathered in the present study may serve to gain an insight into relevant physiological parameters that influence the *in vivo* release from CLs, such as the composition of the tear fluid, tear flow rates, temperature of the system, and composition of the eyeball surface. The obtained results may serve as a guide for further improvements of the 3D printed eye blink model.

USC UNIVERSIDADE DE SANTIAGO DE COMPOSTELA

5.5 REFERENCES

Alvarez-Lorenzo, C.; Anguiano-Igea, S.; Varela-Garcia, A.; Vivero-Lopez, M.; Concheiro, A. (**2019**). Bioinspired hydrogels for drug-eluting contact lenses. *Acta Biomater.* 84, 49-62.

Chrai, S.S.; Patton, T.F.; Mehta, A.; Robinson, J.R. (**1973**). Lacrimal and instilled fluid dynamics in rabbit eyes. *J. Pharm. Sci*. 62(7), 1112-1121.

DiPasquale, S.A.; Wuchte, L.D.; Mosley, R.J.; Demarest, R.M.; Voyles, M.L.; Byrne, M.E. (**2022**). One week sustained in vivo therapeutic release and safety of novel extended-wear silicone hydrogel contact lenses. *Adv. Healthc. Mater.* 11(7), e2101263.

European Directorate for the Quality of Medicines & HealthCare. (**2008**). In European Pharmacopeia. 6th ed. Council of Europe.

Ferreira, J.A.; Oliveira, P.; Silveira, E. (**2020**). Drug release enhanced by temperature: An accurate discrete model for solutions in H3. *Comput. Math. Appl.* 79(3), 852-875.

Glasson, M.J.; Stapleton, F.; Keay, L.; Willcox, M.D. (**2006**). The effect of short term contact lens wear on the tear film and ocular surface characteristics of tolerant and intolerant wearers. *Cont. Lens Anterior Eye.* 29(1), 41-47.

Gupta, A.; Gupta, V.; Thapar, S.; Bhansali, A. (**2004**). Lipid-lowering drug atorvastatin as an adjunct in the management of diabetic macular edema. *Am. J. Ophthalmol.* 137(4), 675-682.

Hui, A.; Willcox, M. (**2016**). In vivo studies evaluating the use of contact lenses for drug delivery. *Optom. Vis. Sci.* 93(4), 367-376.

USC UNIVERSIDADE DE SANTIAGO DE COMPOSTELA

Jia, C.; Yin, Q.; Song, J.; Hou, G.; Zhang, M. (**2008**). Solubility of pravastatin sodium in water, methanol, ethanol, 2-propanol, 1-propanol, and 1-butanol from (278 to 333) K. *J. Chem. Eng. Data.* 53(10), 2466–2468.

Jones, L.; Hui, A.; Phan, C.M.; Read, M.L.; Azar, D.; Buch, J.; Ciolino, J.B.; Naroo, S.A.; Pall, B.; Romond, K.; Sankaridurg, P.; Schnider, C.M.; Terry, L.; Willcox, M. (**2021**). CLEAR - Contact lens technologies of the future. *Cont. Lens Anterior Eye*. 44, 398-430.

Johnson & Johnson Vision Care. (**2022**). Johnson & Johnson Vision Care Receives FDA Approval for ACUVUE® Theravision™ with Ketotifen – World's First and Only Drug-Eluting Contact Lens; https://www.jjvision.com/press-release/johnson-johnson-vision-care-receives-fda-approval-acuvuer-theravisiontm-ketotifen (accessed October 2022).

Kwon, K.A.; Shipley, R.J.; Edirisinghe, M.; Ezra, D.G.; Rose, G.; Best, S.M.; Cameron, R.E. (**2013**). High-speed camera characterization of voluntary eye blinking kinematics. *J. R. Soc. Interface.* 10(85), 20130227.

Lanier, O.L.; Christopher, K.G.; Macoon, R.M.; Yu, Y.; Sekar, P.; Chauhan, A. (**2020**). Commercialization challenges for drug eluting contact lenses. *Expert Opin. Drug Deliv.* 17, 1133-1149.

Mahomed, A.; Wolffsohn, J.S.; Tighe, B.J. (**2016**). Structural design of contact lens-based drug delivery systems; in vitro and in vivo studies of ocular triggering mechanisms. *Cont. Lens Anterior Eye.* 39(2), 97-105.

Minami, T.; Ishida, W.; Kishimoto, T.; Nakajima, I.; Hino, S.; Arai, R.; Matsunaga, T.; Fukushima, A.; Yamagami, S. (**2019**). In vitro and in

USC UNIVERSIDADE DE SANTIAGO DE COMPOSTELA

vivo performance of epinastine hydrochloride-releasing contact lenses. *PLoS One*. 14(1), e0210362.

Miyazaki, S.; Suzuki, S.; Kawasaki, N.; Endo, K.; Takahashi, A.; Attwood, D. (**2001**). In situ gelling xyloglucan formulations for sustained release ocular delivery of pilocarpine hydrochloride. *Int. J. Pharm.* 229(1-2), 29-36.

Murphy, C.; Deplazes, E.; Cranfield, C.G.; Garcia, A. (**2020**). The role of structure and biophysical properties in the pleiotropic effects of statins. *Int. J. Mol. Sci.* 21(22), 8745.

Nielsen, S.F.; Nordestgaard, B.G. (**2014**). Statin use before diabetes diagnosis and risk of microvascular disease: a nationwide nested matched study. *Lancet Diabetes Endocrinol*. 2(11), 894-900.

Ooi, K.G.; Khoo, P.; Vaclavik, V.; Watson, S.L. (**2019**). Statins in ophthalmology. *Surv. Ophthalmol*. 64(3), 401-432.

Ozkiris, A.; Erkiliç, K.; Koç, A.; Mistik, S. (**2007**). Effect of atorvastatin on ocular blood flow velocities in patients with diabetic retinopathy. *Br. J. Ophthalmol*. 91(1), 69-73.

Pereira-da-Mota, A.F.; Phan, C.M.; Concheiro, A.; Jones, L.; Alvarez-Lorenzo, C. (**2022a**). Testing drug release from medicated contact lenses: The missing link to predict in vivo performance. *J. Control Release.* 343, 672-702.

Pereira-da-Mota, A.F.; Vivero-Lopez, M.; Serramito, M.; Diaz-Gomez, L.; Serro, A.P.; Carracedo, G.; Huete-Toral, F.; Concheiro. A.; Alvarez-Lorenzo, C. (**2022b**). Contact lenses for pravastatin delivery to eye segments: Design and in vitro-in vivo correlations. *J. Control. Release.* 348, 431-443.

USC UNIVERSIDADE DE SANTIAGO DE COMPOSTELA

Pereira-da-Mota, A.F.; Vivero-Lopez, M.; Topete, A.; Serro, A.P.; Concheiro, A.; Alvarez-Lorenzo, C. (**2021**). Atorvastatin-eluting contact lenses: Effects of molecular imprinting and sterilization on drug loading and release. *Pharmaceutics.* 13(5), 606.

Phan, C.M.; Bajgrowicz, M.; Gao, H.; Subbaraman, L.N.; Jones, L.W. (**2016b**). Release of fluconazole from contact lenses using a novel in vitro eye model. *Optom. Vis. Sci.* 93(4), 387-394.

Phan, C.M.; Bajgrowicz-Cieslak, M.; Subbaraman, L.N.; Jones, L. (**2016a**). Release of moxifloxacin from contact lenses using an in vitro eye model: Impact of artificial tear fluid composition and mechanical rubbing. *Transl. Vis. Sci. Technol*. 5(6), 3.

Phan, C.M.; Shukla, M.; Walther, H.; Heynen, M.; Suh, D.; Jones, L. (**2021**). Development of an in vitro blink model for ophthalmic drug delivery. *Pharmaceutics.* 13(3), 300.

Phan, C.M.; Walther, H.; Gao, H.; Rossy, J.; Subbaraman, L.N.; Jones, L. (**2016c**). Development of an in vitro ocular platform to test contact lenses. *J. Vis. Exp*. 6(110), e53907.

Phan, C.M.; Walther, H.; Qiao, H.; Shinde, R.; Jones, L. (**2019**). Development of an eye model with a physiological blink mechanism. *Trans. Vis. Sci. Tech*. 8(5), 1.

Phan, C.M.; Walther, H.; Smith, R.W.; Riederer, D.; Lau, C.; Osborn-Lorenz, K.; Subbaraman, L.N.; Jones, L. (**2018**). Determination of the release of PEG and HPMC from nelfilcon A daily disposable contact lenses using a novel in vitro eye model. *J. Biomater. Sci. Polym. Ed.* 29(17), 2124-2136.

USC UNIVERSIDADE DE SANTIAGO DE COMPOSTELA

Pimenta, A.F.; Valente, A.; Pereira, J.M.; Pereira, J.C.; Filipe, H.P.; Mata, J.L.; Colaço, R.; Saramago, B.; Serro, A.P. (**2016**). Simulation of the hydrodynamic conditions of the eye to better reproduce the drug release from hydrogel contact lenses: experiments and modeling. *Drug Deliv. Transl. Res.* 6(6), 755-762.

Review of Cornea & Contact Lenses. (**2021**). Material Gains: 50 Years of the Soft Contact Lens; Material Gains: 50 Years of the Soft Contact Lens; https://www.reviewofcontactlenses.com/article/material-gains-50-years-of-the-soft-contact-lens (accessed October 2022).

Salehi, B.; Mishra, A.P.; Nigam, M.; Sener, B.; Kilic, M.; Sharifi-Rad, M.; Fokou, P.V.T.; Martins, N.; Sharifi-Rad, J. (**2018**). Resveratrol: A Double-edged sword in health benefits. *Biomedicines*. 6(3), 91.

Sekar, P.; Chauhan, A. (**2019**). Effect of vitamin-E integration on delivery of prostaglandin analogs from therapeutic lenses. *J. Colloid. Interface Sci.* 539, 457-467.

Silva, R.C.D.; Teixeira, J.A.; Nunes, W.D.G.; Zangaro, G.A.C.; Pivatto, M.; Caires, F.J.; Ionashiro, M. (**2017**). Resveratrol: A thermoanalytical study. *Food Chem*. 237, 561-565.

Tieppo, A.; Boggs, A.C.; Pourjavad, P.; Byrne, M.E. (**2014**). Analysis of release kinetics of ocular therapeutics from drug releasing contact lenses: Best methods and practices to advance the field. *Cont. Lens Anterior Eye.* 37(4), 305-313.

Tieppo, A.; Pate, K.M.; Byrne, M.E. (**2012**). In vitro controlled release of an anti-inflammatory from daily disposable therapeutic contact lenses under physiological ocular tear flow. *Eur. J. Pharm. Biopharm.* 81(1), 170-177.

USC UNIVERSIDADE DE SANTIAGO DE COMPOSTELA

Torres-Luna, C.; Fan, X.; Domszy, R.; Hu, N.; Wang, N.S.; Yang, A. (**2020**). Hydrogel-based ocular drug delivery systems for hydrophobic drugs. *Eur. J. Pharm. Sci.* 154, 105503.

Tsai, T.Y.; Chen, T.C.; Wang, I.J.; Yeh, C.Y.; Su, M.J.; Chen, R.H.; Tsai, T.H.; Hu, F.R. (**2015**). The effect of resveratrol on protecting corneal epithelial cells from cytotoxicity caused by moxifloxacin and benzalkonium chloride. *Invest. Ophthalmol. Vis Sci.* 56(3), 1575-1584.

Vivero-Lopez, M.; Muras, A.; Silva, D.; Serro, A.P.; Otero, A.; Concheiro, A.; Alvarez-Lorenzo, C. (**2021**). Resveratrol-loaded hydrogel contact lenses with antioxidant and antibiofilm performance. *Pharmaceutics*. 13(4), 532.

Vivero-Lopez, M.; Pereira-da-Mota, A.F.; Carracedo, G.; Huete-Toral, F.; Parga, A.; Otero, A.; Concheiro, A.; Alvarez-Lorenzo, C. (**2022**). Phosphorylcholine-based contact lenses for sustained release of resveratrol: design, antioxidant and antimicrobial performances, and in vivo behavior. *ACS Appl. Mater. Interf.*; in press (DOI: 10.1021/acsami.2c18217) .

Wichterle O. (**1961**). U.S. Patents. 3,660,545; 3,408,429; 3,496,254; 3,499,862.

Yang, S.C.; Tseng, C.H.; Wang, P.W.; Lu, P.L.; Weng, Y.H.; Yen, F.L.; Fang, J.Y. (**2017**). Pterostilbene, a methoxylated resveratrol derivative, efficiently eradicates planktonic, biofilm, and intracellular MRSA by topical application. *Front. Microbiol.* 8, 1103.

Zupančič, Š.; Lavrič, Z.; Kristl, J. (**2015**). Stability and solubility of trans-resveratrol are strongly influenced by pH and temperature. *Eur. J. Pharm. Biopharm.* 93, 196-204.

USC UNIVERSIDADE DE SANTIAGO DE COMPOSTELA

Chapter 6

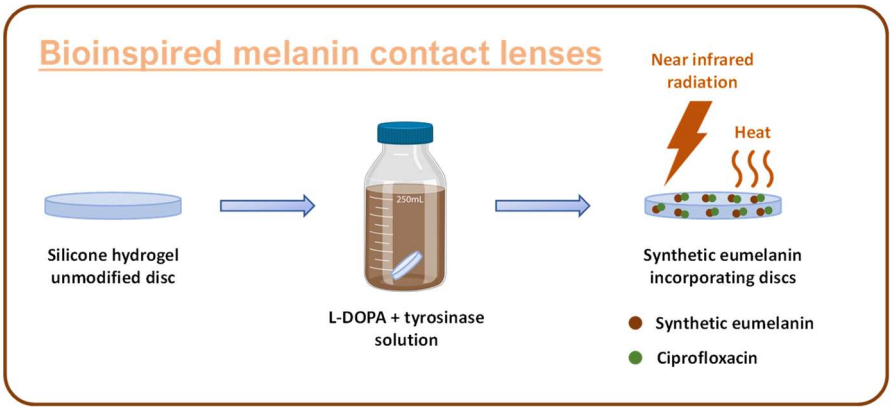

The work described in this chapter has not been published yet.

USC UNIVERSIDADE DE SANTIAGO DE COMPOSTELA

USC
UNIVERSIDADE
DE SANTIAGO
DE COMPOSTELA

6. BIOINSPIRED MELANIN CONTACT LENSES WITH ANTIBACTERIAL PROPERTIES

6.1 INTRODUCTION

The natural pigment melanin is one of the most enigmatic compounds found in living organisms from different species. Its presence in microorganisms, animals and plants leads to a variety of functionalities, including pigmentation, radical scavenging, radiation protection, and thermal regulation [Simon et al., 2010]. The exact physical and chemical properties of melanin are still unclear and has captured the attention of several scientists in the last century. Generally, melanin is classified into five groups: eumelanin, pheomelanin, neuromelanin, allomelanin and pyomelanin, based on its specific origin and location [Cao et al., 2021]. Allomelanin and pyomelanin are mostly found in microorganisms (fungi and bacteria) and plants, respectively [d'Ischia et al., 2015]. In human beings, melanin is synthesized in melanocytes and exists in three main forms, eumelanin, pheomelanin and neuromelanin (the last one mainly associated with the nervous system) [Xie et al., 2019]. Eumelanin and pheomelanin present different molecular structures and color, eumelanin is a black-to-brown insoluble polymer existing in human skin and eyes and pheomelanin is a yellow-to-reddish, alkali-soluble pigment of red-haired individuals

USC UNIVERSIDADE DE SANTIAGO DE COMPOSTELA

with high propensity to sunburn and skin cancer [d'Ischia et al., 2009; Napolitano et al., 2013].

Natural eumelanin biosynthesis is initiated involving the tyrosinase-catalyzed oxidation of tyrosine to the common precursors L-dihydroxyphenylalanine (L-DOPA) and DOPAquinone (**Figure 6.1**). Then, DOPAquinone forms the 5,6-dihydroxylindole (DHI) and 5,6-dihydroxyindole-2-carboxylic (DHICA) through the intermediate molecule DOPAchrome [d'Ischia et al., 2014]. DOPAchrome is decomposed into DHI and DHICA depending on the presence of tyrosinase-related protein 2 (Tyrp-2). In the presence of the protein (*in vivo*), the reaction induces isomerization to DHICA, whereas *in vitro* the reaction is spontaneously induced with decarboxylation to DHI [Xie et al., 2019]. Numerous methods have been proposed to initiate the formation of synthetic eumelanin from L-DOPA, through autoxidation, chemical oxidants and tyrosinase assisted oxidation [d'Ischia et al., 2015]. *In vitro*, under ambient oxygen conditions, conversion of L-DOPA to DHI/DHICA monomers is thermodynamically spontaneous and kinetically facile from the dopaquinone oxidation state. In the current work, we are investigating the pathway of synthetic DOPA-melanin preparation from L-DOPA via tyrosinase-assisted oxidation under oxygen conditions.

USC UNIVERSIDADE DE SANTIAGO DE COMPOSTELA

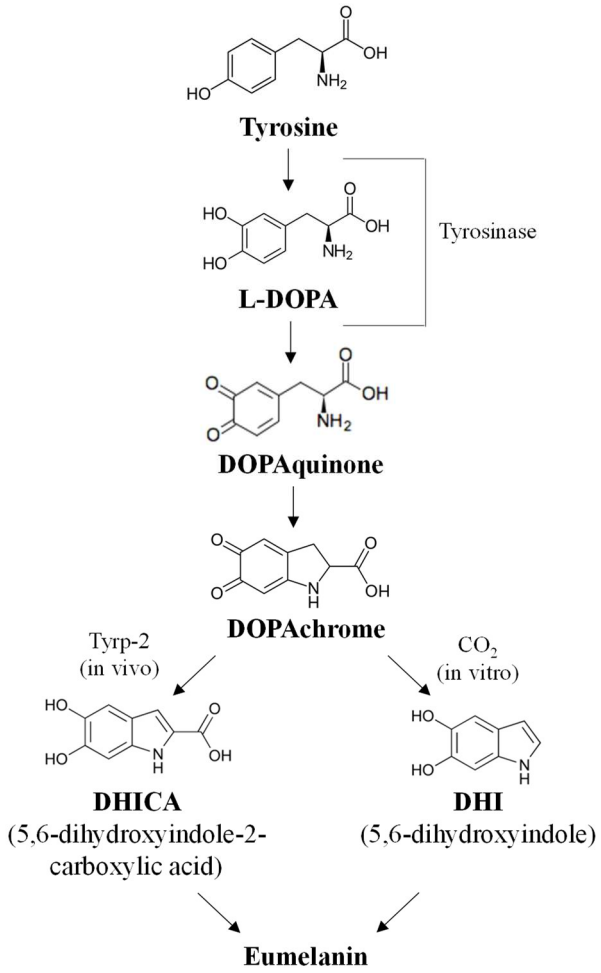

Figure 6.1. Biosynthesis of natural eumelanin. Adapted from [Hida et al., 2020] (Open access Creative Common CC BY license).

In the eye, melanin is primarily present in the iris, ciliary body, choroid and retinal pigment epithelium (RPE) [Rimpelä, et al., 2017]. In general, eumelanin presents a much larger amount in pigmented ocular tissues acting as an antioxidant and protecting the eye against

USC UNIVERSIDADE DE SANTIAGO DE COMPOSTELA

oxidative stress caused by reactive oxygen species (ROS) through its metal ion chelation capacity [Hu et al., 2008; Bustamante et al., 1993]. Ocular melanin function is mainly focused on light absorption including near-infrared, visible light and ultraviolet (UV) radiation [Sarna, 1992]. In the anterior segment of the eye, the melanin present in iris melanocytes reduces the amount of visible light and UV radiation entering in the eye. However, even a high amount of light escapes to the posterior segment being absorbed by the RPE protecting the neural retina and minimizing light reflection and scattering [Sarna, 1992]. In addition to these functionalities, melanin has been proposed to act as a chemical binding reservoir by retaining drugs inside the pigmented cells and influencing drug biodistribution [Larsson, 1993]. Comparative studies performed in albino and pigmented animals revealed that the accumulation of a variety of compounds in melanin containing tissues causes a slow-release kinetics and increases the ocular residence time [Salazar et al., 1993]. Indeed, melanin binding has been suggested as a strategy for reaching a sustained release of therapeutic drugs to eye tissues.

Diabetes mellitus is reaching pandemic proportions and is the leading cause of blindness in adults. It has been reported that diabetic patients have an increased risk of developing conjunctival bacterial infections and corneal infections (such as fungal keratitis) due to weakened corneal epithelial barrier function [Skarbez et al., 2010]. Ciprofloxacin (**Figure 6.2**) is a fluoroquinolone antibiotic frequently used in ophthalmology as eyedrops or ointments to treat bacterial infections/blepharitis or ulcers of the eye [Smith et al., 2001]. The recommended dosage regimen for the treatment of bacterial infections/blepharitis is: one drop every two hours while awake for two days and one drop every four hours while awake for the next five days. For the treatment of corneal ulcers, the recommended dosage regimen

USC UNIVERSIDADE DE SANTIAGO DE COMPOSTELA

is: two drops in the affected eye every 15 minutes for the first 6 h, then two drops every 30 min for the remainder of the first day. Melanin has high binding affinity for a wide range of drugs from different therapeutic classes. Pelkonen et al. classified drugs as low (e.g. diclofenac and prednisolone), intermediate (e.g. atropine and betaxolol) and high binders to melanin (e.g. ciprofloxacin and propranolol) [Pelkonen et al., 2017]. Among others, ciprofloxacin demonstrated a high binding percentage to melanin (about 95%).

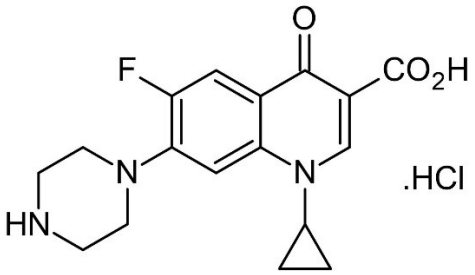

Figure 6.2. Molecular structure of ciprofloxacin hydrochloride.

Melanin-like nanoparticles, and in particular polydopamine (PDA), have been investigated for photothermal therapy due to its capability to convert absorbed light into heat [Xiao, 2021]. Fast and local increase in temperature has been shown to be a promising method to kill bacteria without risk of bacterial resistance or side effects. Near-infrared (NIR) light irradiation of materials that can absorb light energy and transfer into heat could lead to irreparable damage of bacterial cells and appears as a suitable tool for prophylaxis and treatment of medical device-related infections [Cabana et al., 2017]. To effectively kill bacteria through temperature increase, high temperature of 70 °C is generally

USC UNIVERSIDADE DE SANTIAGO DE COMPOSTELA

necessary. However, such high temperature could cause inevitable damage to nearby host cells or tissues. Combination of photothermal therapy and chemotherapy with antimicrobial agents has been demonstrated to provide synergic effects on bacteria eradication with lower temperature [Fan et al, 2019]. Polydopamine nanoparticles modified with magainin I, an antimicrobial peptide, were shown to effectively kill *Escherichia coli* reaching 45 °C under NIR light irradiation [Fan et al, 2019].

In this part of the Thesis, melanin was incorporated into contact lenses with the double aim of (i) evaluating an alternative procedure of incorporating drugs into contact lenses through drug-melanin affinity, and (ii) endowing contact lenses with photothermal capacity to increase temperature in localized areas. The work was focused on the incorporation of ciprofloxacin and the possible use of antimicrobial therapy combined with photothermal therapy in the treatment of bacterial infections associated with the use of contact lenses in diabetic patients.

6.2 MATERIALS AND METHODS

6.2.1 Materials

Ciprofloxacin hydrochloride, L-dihydroxyphenylalanine (L-DOPA), tyrosinase from mushroom, ethylene glycol dimethacrylate (EGDMA), 2,2′-azobis(isobutyronitrile) (AIBN), and N-vinylpyrrolidone (NVP) were supplied by Sigma-Aldrich (Steinheim, Germany). 2-Hydroxyethyl methacrylate (HEMA) and di-sodium hydrogen phosphate anhydrous (NaH_2PO_4) were from Merck (Darmstadt, Germany). 3-(Methacryloyloxy)propyl

USC UNIVERSIDADE DE SANTIAGO DE COMPOSTELA

tris(trimethylsiloxy)silane (TRIS) was from Alfa Aesar (Thermo Fisher, Kandel, Germany). Sodium chloride (NaCl) was from Labkem (Barcelona, Spain). Tryptic Soy Broth (TSB-1) was from Oxoid (Hampshire, UK). Simulated lachrymal fluid (SLF) was prepared as previously reported [Pereira-da-Mota et al., 2022]. Ultrapure water (resistivity >18.2 MΩ cm; Milli-Q®, Millipore Ibérica, Madrid, Spain) was obtained by reverse osmosis. Clarity® 1-day CLs (Somofilcon A, CooperVision®, Lake Forest, CA, USA), power - 3.50 D, water content 56%, Dk/t 86; and Air Optix® Aqua (Lotrafilcon B, Alcon®, Geneve, Switzerland), power –3.50 D, water content 33%, Dk/t 138, were gently offered by a local optical store.

6.2.2 Silicone Hydrogel Discs Preparation

Silicone hydrogel (SiHy) discs were prepared by mixing 0.92 mL of HEMA, 1.58 mL of TRIS, 2.50 mL of NVP and 32 µL of EGDMA. The monomers mixture was magnetically stirred (180 rpm) for 120 min at room temperature. AIBN (12.50 mg) was added, and the mixture was kept under magnetic stirring for 30 min more to ensure the complete dissolution of the initiator. The resulting solution was injected into moulds made of two glass plates (10 x 10 cm) separated by Teflon frame (0.2 mm of thickness) and pre-treated with dichlorodimethylsilane. The hydrogels were polymerized at 50 °C for 12 h and then at 70 °C for 24 h.

Following the polymerization procedure, the hydrogel sheets were boiled in 1 L of distilled water to remove the unreacted monomers and facilitate cutting in 10-mm discs. The discs were washed in water and 0.9% NaCl replacing the medium twice a day, until complete removal

USC UNIVERSIDADE DE SANTIAGO DE COMPOSTELA

of the unreacted monomers. Finally, the discs were dried at 70 °C for 24 h and stored in plastic bags for further experiments.

6.2.3 Melanin Synthesis and Incorporation on the Hydrogels

DOPA-melanin was synthetized following oxidative polymerization of L-DOPA solution with tyrosinase, according to the method described earlier [Sono et al., 2012]. L-DOPA solution was prepared by dissolving 100 mg of L-DOPA in 100 mL of sodium phosphate buffer (NaH_2PO_4, 50 mM, pH 7.0 adjusted with NaOH) to obtain a concentration of 1 mg/mL.

A mushroom tyrosinase stock solution of 1000 units/mL was also prepared in the same buffer pH 7.0. Tyrosinase stock solution (850 µL) was added to the freshly prepared L-DOPA solution (84 mL) in a glass bottle. Twelve discs or commercially CLs (previously washed in water for 24 h and dried at 40 °C for 2 h and then at 70 °C for 2 h more) were added to this solution (in separated flasks for discs and CLs). The bottle was oscillatory shaken at 250 rpm for 5, 8 or 16 h at room temperature and protected from the light.

After shaking, the discs and CLs were washed twice in water, 15 min each cycle. Then, the discs were maintained in water for 12 h and finally dried at 70 ˚C for 24 h and stored in plastic bags at room temperature and protected from the light. The CLs were dried as previously explained.

USC UNIVERSIDADE DE SANTIAGO DE COMPOSTELA

6.2.4 Characterization of Melanin Discs and CLs

6.2.4.1 Raman Spectroscopy

Melanin incorporated, and blank discs and CLs were analyzed by Raman spectroscopy to qualitatively identify the presence of DOPA-melanin on the discs and CLs surface. Samples were recorded using a confocal Ramman microscope (alpha 300R, WITec, Ulm, Germany), with a 532 nm laser, x50 objective, 2mW laser power and 1 s of accumulation time. The analysis was processed using WITec Control FIVE software.

6.2.5 Ciprofloxacin Loading and Release

Dried blank and melanin-incorporated discs and CLs were placed in a ciprofloxacin hydrochloride loading solution (2 and 3 mg/mL prepared in water) for 48 h. The vials were maintained under oscillatory movement (180 rpm) at room temperature and protected from the light. All experiments were carried out in triplicate.

After 48 h, loaded discs and CLs were removed from the loading solution, rinsed with simulated lachrymal fluid (SLF), and placed in vials containing 10 mL of SLF. The vials were then incubated in a shaker at 37 ˚C, 180 rpm for 24 h. At various time points, the absorbance of the release solution was measured by spectrophotometry at 275 nm (UV–Vis spectrophotometer, Agilent 8453, Waldbronn, Germany). The amount of ciprofloxacin released was calculated using previously prepared and validated calibration curves (1 - 10 µg/mL).

USC UNIVERSIDADE DE SANTIAGO DE COMPOSTELA

6.2.6 Light Transmittance and Photothermal Activity

Light transmission of water-swollen discs and CLs with an without melanin was recorded in the 200-800 nm range in an UV–Vis spectrophotometer (Agilent 8453, Waldbronn, Germany).

SiHy discs and CLs were irradiated using a NIR laser (808 nm, 1284 lux; beam diameter 3.0 mm; Biglasers.com, Monroe, NY, USA) for 10 s and the initial and final temperatures of the hydrogels were recorded using a FLIR model E75 thermographic camera (Teledyne FLIR LLC, Oregon). At the same time, the intensity of the NIR light that passed through the hydrogels was registered with a lux light meter sensor (model SBS-LM-400C; Steinberg Systems, Zielona Gora, Poland).

6.2.7 Antibacterial Performance by Isothermal Microcalorimetry

The antibacterial capacity of blank SiHy discs and melanin-incorporated discs against the most common bacteria that cause ocular infections, *Staphylococcus aureus* (*S. aureus*), was evaluated. The metabolic heat of bacteria was determined in an I-Cal Flex Isothermal calorimeter system (Calmetrix, Needham, MA, USA) equipped with 8 calorimeters (20 mL capacity) and previously stabilized and calibrated at 35 ºC.

Among the developed conditions, SiHy discs after 8 h of melanin incubation were selected to the antibacterial assays. Blank and melanin-incorporated discs were sterilized with ethanol and loaded in 3 mg/mL of ciprofloxacin solution for 48 h. Then, the discs were incubated in 3 mL of *S. aureus* inoculum (adjusted optical density to 0.1) in

USC UNIVERSIDADE DE SANTIAGO DE COMPOSTELA

calorimeter vials for 24 h at 37 °C. Changes in energy as a function of time were recorded as power (mW) for 24 h; data were gathered every 10 s for the first hour and every 1 min for the next 23 h using the I-Cal Logger software. Two calorimeter vials were incubated with bacteria in culture medium without any disc for monitoring. After incubation, bacteria growth in the vials was also determined by measuring the optical density of the culture medium at 600 nm (UV-Vis spectrophotometer Thermo Scientific Helios Omega).

6.3 RESULTS AND DISCUSSION

6.3.1 Melanin Incorporation

Natural and synthetic melanins share the abundance of functional groups in their molecular backbone as, carboxyl (-COOH), aromatic amine (-NH), hydroxyl (OH), as well as catechol groups which provide reactive sites for functionalization and interaction with potential drugs [Cavallini et al., 2020].

Preliminary experiments were assessed to evaluate whether HEMA or SiHy discs might have a higher affinity with the synthetized melanin. HEMA hydrogel discs were incubated for different periods of time in melanin solution and the amount of melanin incorporated in the discs was similar, showing a limited affinity with melanin. On other hand, SiHy discs showed a more accentuated brown colour with longer incubation times, which seems that melanin has a higher affinity for hydrophobic monomers as silicone.

Two commercially available contact lenses with silicone monomers were selected. Clarity® 1 Day (somofilcon A) CL is composed by tetraethyleneglycol dimethacrylate and di-functional

USC UNIVERSIDADE DE SANTIAGO DE COMPOSTELA

methacryloxypropyl-terminated poly(dimethylsiloxane). Air Optix® (Lotrafilcon B) is made of N,N-dimethylaminoethyl methacrylate, 3-[tris(trimethylsiloxy)silyl]propyl methacrylate and siloxane.

SiHy discs and commercially available CLs successfully incorporated melanin in their structure as was observed in **Figure 6.3**. A rapid oxidation of L-DOPA was observed once tyrosinase was added to L-DOPA solution. The solution acquired a brown colour which became darker over time. The brown colour of the solution is the result of because of the formation of dopachrome [Saghaie et al., 2013].

Notably, there were differences among the melanin-incorporated SiHy hydrogels or CLs. SiHy discs incubated in a melanin solution showed a darker colour in comparison to CLs, and this brown colour was more accentuated with longer incubation times. However, no evident differences were detected between 5 and 8 h of incubation. A less accentuated brown colour was observed after incubation of both commercially CLs, especially for Air Optix®.

USC UNIVERSIDADE DE SANTIAGO DE COMPOSTELA

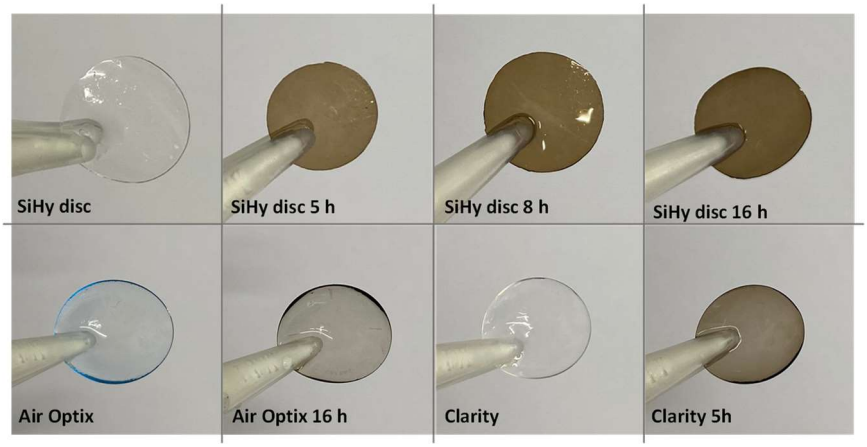

Figure 6.3. Photos of SiHy discs before (transparent) and after 5, 8 and 16 h of melanin incubation, and Air Optix® and Clarity® CLs before and after 16 and 5 h of incubation, respectively.

The presence of DOPA-melanin in the SiHy discs and contact lenses was confirmed by Raman analysis (**Figure 6.4 and 6.5**). Strong peaks at 2909-2968 cm^{-1}, and 1409-1459 cm^{-1} (C-H groups) were observed in SiHy discs and CLs samples. These results were also found in literature for hydrogel contact lenses [Tran and Yang, 2020]. Silicone bonds presented in the discs and CLs were also evidenced in the Raman spectrum; -Si-$(CH_3)_x$ presented a two weak band at 683 and 735 cm^{-1}, and -Si-O_3 at 636 cm^{-1} as evidenced for silicone hydrogel contact lenes [Chien and Kuo, 2019]. Isolated DOPA-melanin synthetized presented two bands at 1370 cm^{-1} and 1580 cm^{-1} as verified on bibliography for synthetic melanin [Huang et al., 2004]. Melanin -discs and CLs showed peaks at 1370 cm^{-1}, and 1580 cm^{-1}, which evidences the presence of melanin in their surface. Raman analysis was considered a qualitative, analysis to verify the presence of melanin on the discs or CLs surface.

USC UNIVERSIDADE DE SANTIAGO DE COMPOSTELA

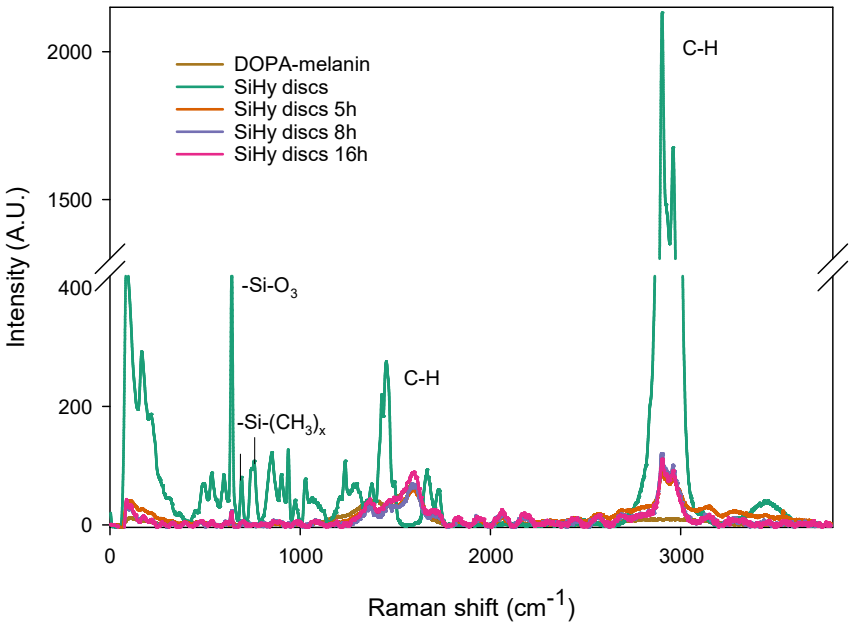

Figure 6.4. Raman results for DOPA-melanin, SiHy discs, and melanin-incorporated SiHy discs (5, 8 and 16h).

USC UNIVERSIDADE DE SANTIAGO DE COMPOSTELA

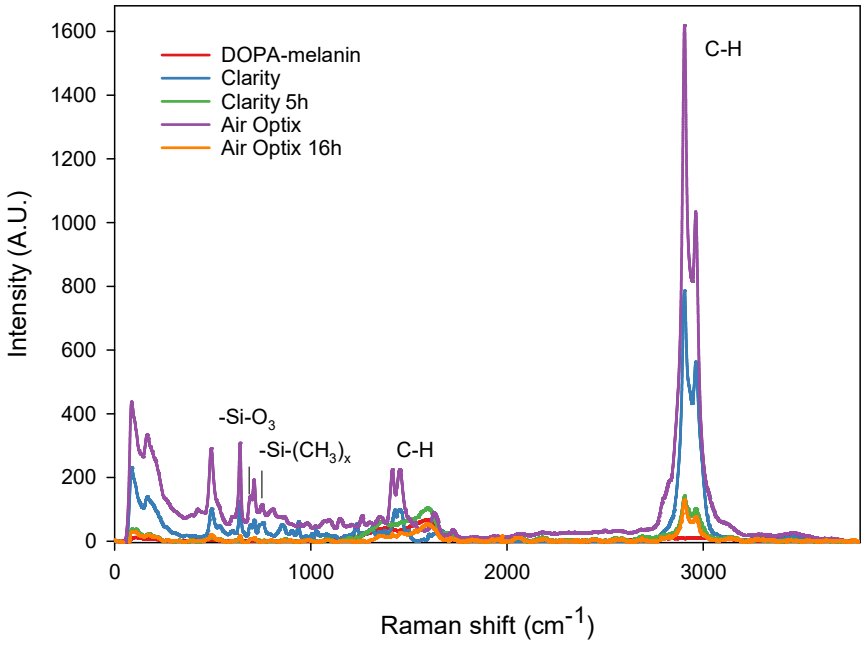

Figure 6.5. Raman results for DOPA-melanin, commercially available CLs (Clarity® and Air Optix®), and melanin-incorporated CLs.

6.3.2 Light Transmittance and Photothermal Activity

Due to the relevant photo-protectant properties of melanin (absorbs harmful ultraviolet and visible radiation) [Madkhali et al., 2019], the light transmittance of blank and melanin-incorporated discs and CLs was evaluated (**Figure 6.6**). Blank SiHy discs and CLs showed transmittance values close to 80% and 90% in the visible range (600 nm), respectively. As expected, a transmittance decrease was verified in the UV and visible region after melanin incubation for all hydrogels. Air Optix® CLs exhibited the slightest decrease at 600 nm, 86% to 72%

USC UNIVERSIDADE DE SANTIAGO DE COMPOSTELA

(after 16 h of incubation) and melanin incorporation gave a significant UV protection to the lens, especially in the UV-B and UV-A regions (280-400 nm). Clarity® CL already presented a UV protection filter and a decrease in the visible range was verified, 90% to 60%. Regarding to the SiHy discs, the light transmittance decrease was more accentuated with longer incubation times.

UV-visible light transmittance results were in agreement with the measured light intensity that passed through the discs and CLs when irradiated with NIR laser (**Table 6.1**).

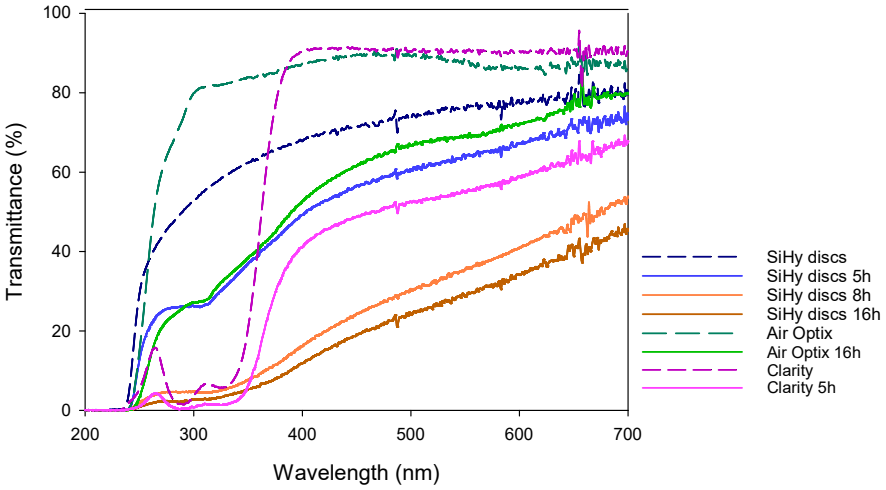

Figure 6.6. Light transmittance of the silicone hydrogel discs (SiHy discs) and commercially available contact lenses (Air Optix® and Clarity®) without and with DOPA-melanin incorporation (*n* = 3).

Table 6.1. Light intensity that passed through the discs or CLs without and with melanin incorporation when irradiated with an 808 nm laser. Reference NIR laser intensity: 1284 lux (without any lens).

	Without melanin (lux)	With melanin (lux)		
	-	5h	8h	16h
SiHy discs	1288	958.3	830.4	820.0
Air Optix®	1250	-	-	1090
Clarity®	1267	880.1	-	-

Photothermal activity of melanin-incorporated discs and CLs was evaluated. The blank and melanin-incorporated materials were irradiated with a NIR laser (808 nm) for 10 s and the temperature change of the materials was monitored (**Figure 6.7 and 6.8**). Minimal temperature changes were verified on the blank SiHy discs and CLs. On the other hand, a notably and very fast (in 10 s) temperature increase was recorded on discs incorporating melanin, this temperature change was more accentuated for discs that were incubated in melanin solution for longer incubation times.

Similar results were obtained for commercially available contact lenses, melanin-incorporated Air Optix® CLs revealed a lower temperature increase as the amount of pigment incorporated was lower than Clarity® CLs, as verified with the light transmittance values.

Other authors observed a significantly improved antibacterial activity of melanin-modified hydrogels following NIR radiation. Recently, NIR-responsive chitosan/silk fibroin cryogels incorporating polydopamine have been developed and when irradiated with NIR radiation for 10 min an increase from 25 to 35 °C was verified showing a significant antibacterial efficacy [Han et al., 2019]. The combination of PDA-mediated photothermal treatments with antibiotic drugs has

USC UNIVERSIDADE DE SANTIAGO DE COMPOSTELA

also been explored. PDA hydrogels incorporated with doxycycline have demonstrated a photothermal-mediated antimicrobial activity and sustained antibiotic release capacity [Liang et al., 2022].

USC UNIVERSIDADE DE SANTIAGO DE COMPOSTELA

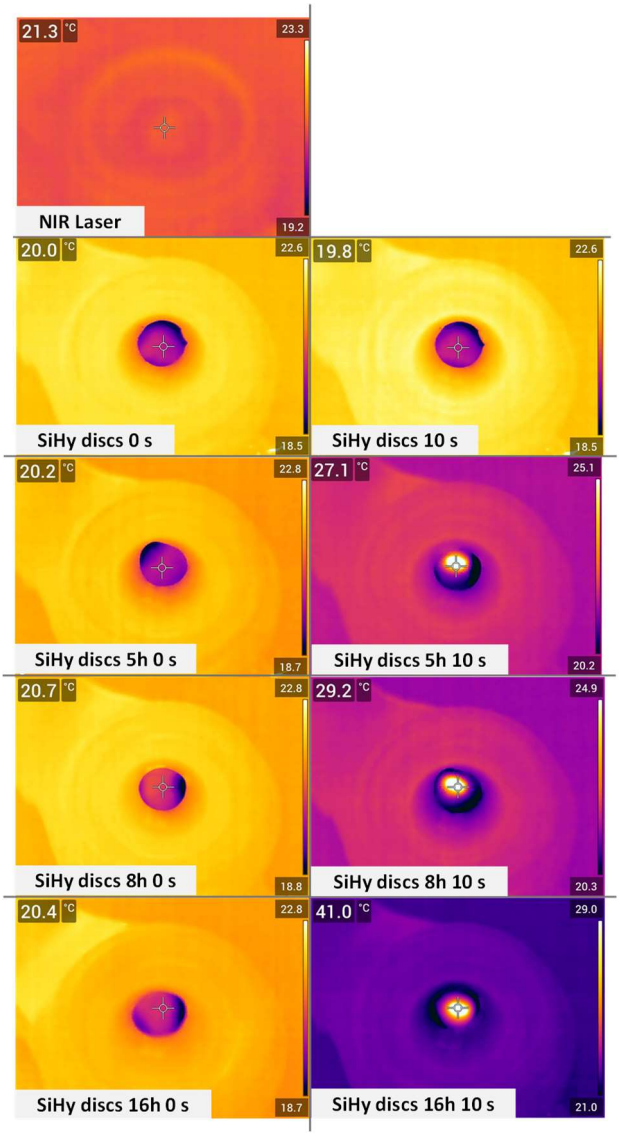

Figure 6.7. Infrared thermal camera images of temperature changes in the irradiated area of the SiHy discs after 10 s of laser radiation.

USC UNIVERSIDADE DE SANTIAGO DE COMPOSTELA

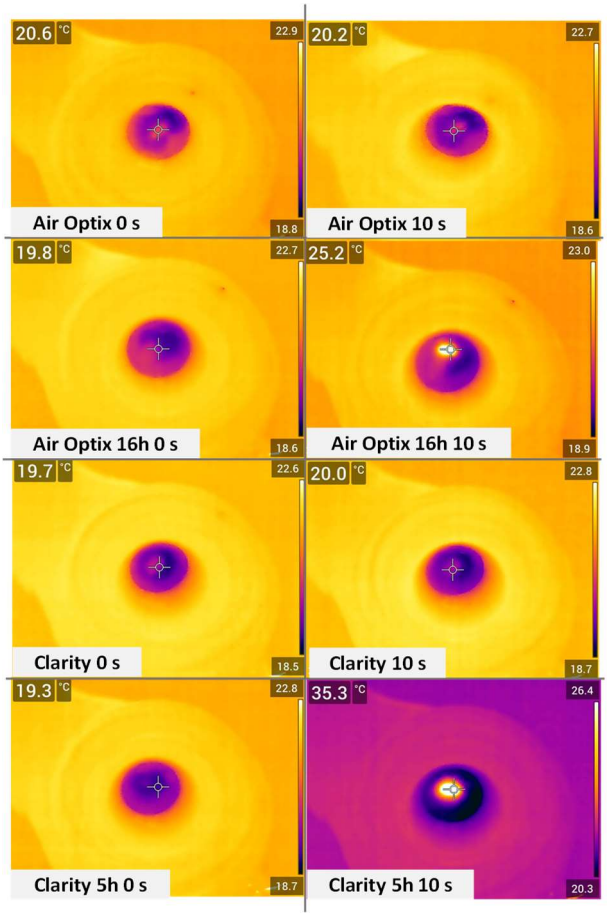

Figure 6.8. Infrared thermal camera images of temperature changes in the irradiated area of the commercial CLs after 10 s of laser radiation.

6.3.3 Ciprofloxacin Loading and Release

SiHy discs and commercial CLs without and with melanin incorporation were immersed in a prepared ciprofloxacin solution (2 or 3 mg/mL in ultrapure water) and incubated for 48 h under mild agitation (180 rpm) and protected from the light. The amount of drug loaded was

USC UNIVERSIDADE DE SANTIAGO DE COMPOSTELA

not possible to quantify due to the high absorbance of the loading solution, the difference between the initial and final absorbance was not quantifiable. Thus, it was assumed that the amount of ciprofloxacin loaded was totally released. After this time, ciprofloxacin-loaded discs and CLs were incubated in 10 mL of SLF at 37 °C for 24 h. At predetermined timepoints, the absorbance of the release medium was measured at 275 nm and the results are showed in Figures 6.9 and 6.10.

For all discs and CLs, the majority of ciprofloxacin loaded was released on the first 1-2 h of release experiment. However, a slightly increase in the amount of ciprofloxacin released was verified for the melanin-incorporated discs (continuous lines, **Figure 6.9**). An increase of drug released was demonstrated when the discs were immersed in 3 mg/mL of ciprofloxacin, which reveal an improvement of drug loaded from the discs. The amount of drug release was higher for discs with longer melanin incubation times, evidencing the affinity of ciprofloxacin and melanin.

For commercialised CLs, the scenario is different, Clarity® CLs released a significant higher amount of ciprofloxacin over 24 h compared to Air Optix® CLs. However, the amount of drug released was lower for melanin-incorporated Clarity® CLs than blank CLs. In the case of Air Optix® CLs, the lenses that were incubated in 3 mg/mL showed a higher amount of drug released.

Ciprofloxacin is a bactericidal antibiotic that inhibits DNA replication by inhibiting bacterial DNA topoisomerase and DNA-gyrase. The minimum inhibitory concentration (MIC_{90}) of ciprofloxacin for Gram-positive *S. aureus* was reported to be 0.5 μg/mL [Liu et al., 2020]. The amount of ciprofloxacin released over 24 h from discs and CLs is above the minimum inhibitory concentration (between 5 – 11 μg/mL in 10 mL of simulated lachrymal fluid).

USC UNIVERSIDADE DE SANTIAGO DE COMPOSTELA

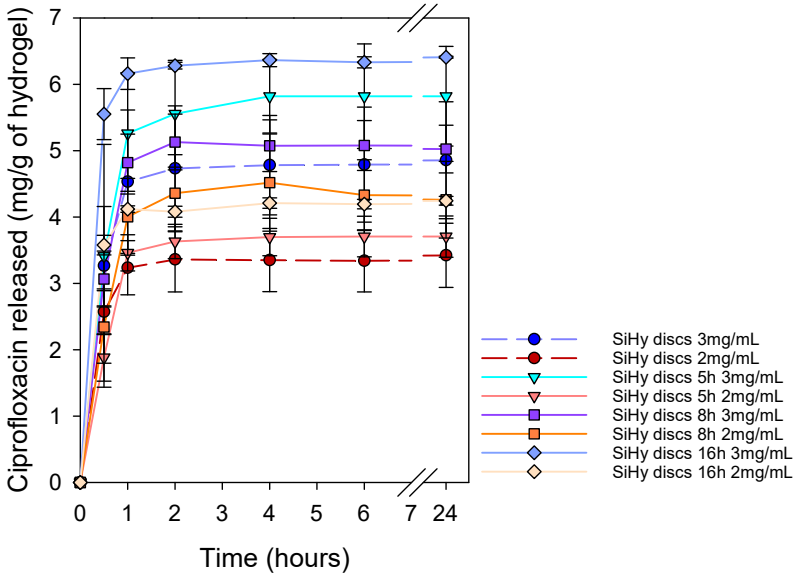

Figure 6.9. Ciprofloxacin release profiles from blank SiHy discs and melanin-incorporated discs (5, 8 or 16 h) after being incubated for 48 h in a 3 or 2 mg/mL ciprofloxacin loading solution (n = 3; mean values and standard deviations).

USC UNIVERSIDADE DE SANTIAGO DE COMPOSTELA

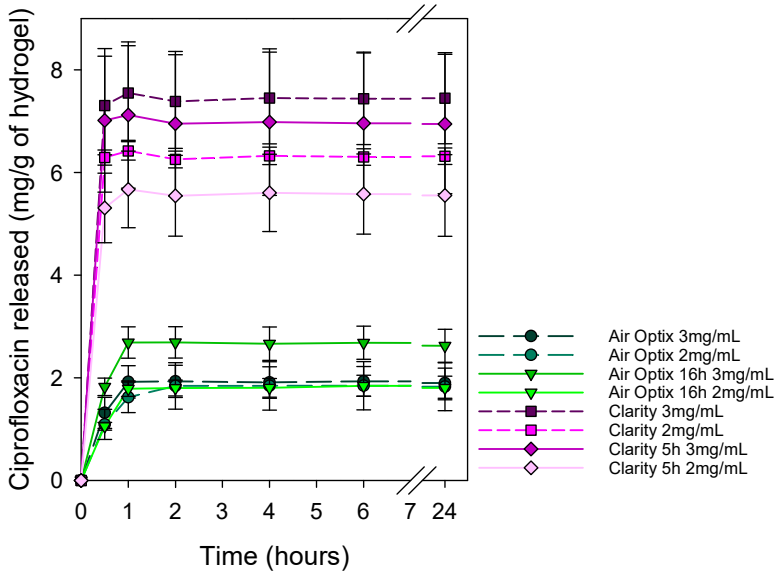

Figure 6.10. Ciprofloxacin release profiles from blank Air Optix® and Clarity® CLs and melanin-incorporated CLs (16 or 5 h) after being incubated for 48 h in a 3 or 2 mg/mL ciprofloxacin loading solution (n = 3; mean values and standard deviations).

6.3.4 Antibacterial Performance

Isothermal microcalorimetric analyses were performed as a proof of concept to gain further insight into the effects that the SiHy discs with melanin incorporation and the amount of ciprofloxacin released from the discs may have on the metabolic activity of the bacteria. This method is a highly sensitive technique that enables a real-time monitoring of bacterial viability in terms of metabolism-related heat production and detect any change in bacterial metabolic rate due to the administration of drugs or compounds [Braissant et al., 2010].

USC UNIVERSIDADE DE SANTIAGO DE COMPOSTELA

According to the thermokinetic models of bacteria growth previously reported [Fricke et al., 2019], the shape of the heat flow signals revealed an initial exponential bacteria growth phase until 300 min and after reaching a maximum heat flow, the signal returned to the baseline (the stationary phase, plateau in number of living bacterial cells). The incubation of *S. aureus* inoculum solely (without discs) caused an increase in the power recorded as observed for the SiHy discs without the presence of ciprofloxacin (**Figure 6.11**). No differences were observed in the release of energy for blank SiHy discs and after 8 h of melanin incubation. On other hand, melanin-incorporated SiHy discs with ciprofloxacin caused relevant changes in the heat flow signals (no peak detected). These changes clearly indicated that the metabolic activity of the bacteria was significantly altered by the ciprofloxacin released from the SiHy discs.

The optical density values at 600 nm were in agreement with the microcalorimetric analysis (**Figure 6.12**). The positive control, where *S. aureus* grew freely, showed an optical density of 0.30 (diluted 1:10), while melanin-incorporated SiHy discs with ciprofloxacin showed a minimal bacterial growth with an optical density of 0.13 (non-diluted), similar to the initial optical density (0.1).

USC UNIVERSIDADE DE SANTIAGO DE COMPOSTELA

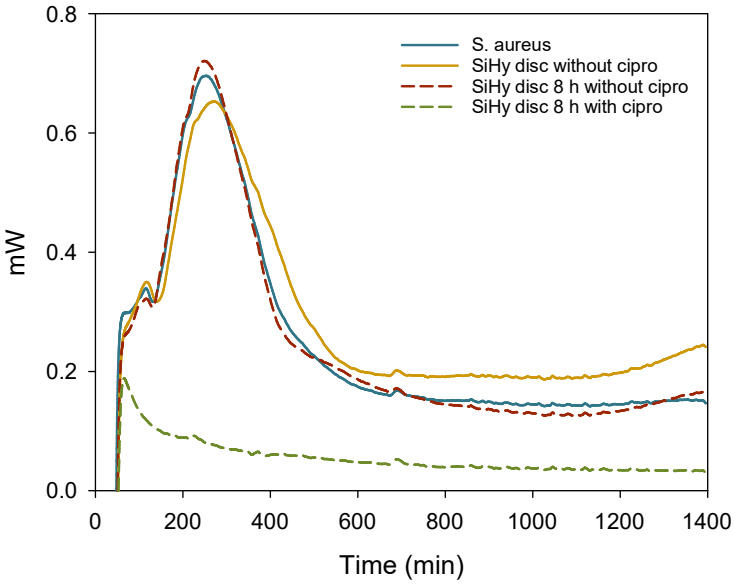

Figure 6.11. Isothermal microcalorimetry runs carried out at 37 ºC for 24 h incubated with *S. aureus* (OD 0.1). SiHy discs were incubated with the bacteria inoculum directly in the calorimeter vials and the power was monitored. Non-loaded blank SiHy discs and melanin-incorporated non-loaded and ciprofloxacin-loaded SiHy discs were tested. Mean of two replicates is represented.

USC UNIVERSIDADE DE SANTIAGO DE COMPOSTELA

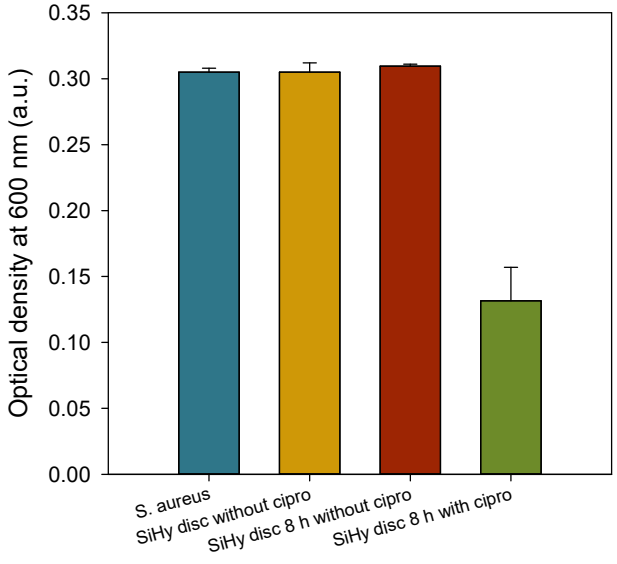

Figure 6.12. Optical density values recorded after incubation of SiHy discs with *S. aureus* in calorimeter vials for 24 h (n = 2; mean values and standard deviations). Bacteria media from positive control of *S. aureus*, SiHy discs without ciprofloxacin and SiHy discs incubated 8 h in melanin without ciprofloxacin samples were diluted 1:10 with TSB-1 medium. Initial optical density of *S. aureus* inoculum = 0.1.

6.4 CONCLUSIONS

Taking advantage of photothermal conversion of melanin, a multifunctional incorporation of melanin in SiHy discs was developed. SiHy discs and commercially available CLs successfully incorporated different degrees of melanin in their structure. Raman spectroscopy evidenced the presence of melanin in the discs and CLs Surface. SiHy discs and CLs light transmittance values noticeably differed, showing a darker colour and a decrease of light transmission when incubated in melanin solution for longer periods of time. A good balance between

USC UNIVERSIDADE DE SANTIAGO DE COMPOSTELA

relevant CLs properties and necessary temperature to produce an antimicrobial effect needs to be optimized.

When incubated in ciprofloxacin hydrochloride solution, the amount of drug released from melanin-incorporated SiHy discs and Air Optix® CLs was higher for these hydrogels than without the presence of melanin. Furthermore, the amount of ciprofloxacin released from the melanin-incorporated SiHy discs promoted a significant inhibition of *S. aureus* growth recorded using isothermal microcalorimetry. The information gathered in the present chapter may serve as a first step towards the development of strategies that combine hydrogels modification and incorporation of active substances for stimuli-responsiveness.

6.5 REFERENCES

Braissant, O.; Wirz, D.; Göpfert, B.; Daniels, A.U. (**2010**). Use of isothermal microcalorimetry to monitor microbial activities. *FEMS Microbiol. Lett.* 303(1), 1-8.

Bustamante, J.; Bredeston, L.; Malanga, G.; Mordoh, J. (**1993**). Role of melanin as a scavenger of active oxygen species. *Pigment Cell Res.* 6(5), 348-353.

Cabana, S.; Lecona-Vargas, C.S.; Meléndez-Ortiz, H.I; Contreras-García, A.; Barbosa, S.; Taboada, P.; Magariños, B.; Bucio, E.; Concheiro, A.; Alvarez-Lorenzo, C. (**2017**). Silicone rubber films functionalized with poly(acrylic acid) nanobrushes for immobilization of gold nanoparticles and photothermal therapy. *J. Drug Deliv. Sci. Technol*. 42, 245-254.

USC UNIVERSIDADE DE SANTIAGO DE COMPOSTELA

Cao,W.; Zhou, X.; McCallum, N.C.; Hu, Z.; Ni, Q.Z.; Kapoor, U.; Heil, C.M.; Cay, K.S.; Zand, T.; Mantanona, A.J.; et al. (**2021**). Unraveling the structure and function of melanin through synthesis. *J. Am. Chem. Soc.* 143(7), 2622–2637.

Cavallini, C.; Vitiello, G.; Adinolfi, B.; Silvestri, B.; Armanetti, P.; Manini, P.; Pezzella, A.; d'Ischia, M.; Luciani, G.; Menichetti, L. (**2020**). Melanin and Melanin-Like Hybrid Materials in Regenerative Medicine. *Nanomaterials.* 10(8), 1518.

Chien, H.W.; Kuo, C.J. (**2019**). Preparation, material properties and antimicrobial efficacy of silicone hydrogel by modulating silicone and hydrophilic monomer. *J. Biomater. Sci. Polym. Ed.* 30(12), 1050-1067.

d'Ischia, M.; Napolitano, A.; Ball, V.; Chen, C. T.; Buehler, M. J. (**2014**). Polydopamine and eumelanin: from structure-property relationships to a unified tailoring strategy. *Acc. Chem. Res.* 47(12), 3541−3550.

d'Ischia, M.; Napolitano, A.; Pezzella, A.; Meredith, P.; Sarna, T. (**2009**). Chemical and structural diversity in eumelanins: unexplored bioOptoelectronic materials. *Angew. Chem. Int. Ed.* 48(22), 3914-3921.

d'Ischia, M.; Wakamatsu, K.; Cicoira, F.; Di Mauro, E.; GarciaBorron, J. C.; Commo, S.; Galvan, I.; Ghanem, G.; Kenzo, K.; Meredith, P.; Pezzella, A.; Santato, C.; Sarna, T.; Simon, J. D.; Zecca, L.; Zucca, F. A.; Napolitano, A.; Ito, S. (**2015**). Melanins and melanogenesis: from pigment cells to human health and technological applications. *Pigm. Cell Melanoma Res.* 28(5), 520−544.

Fan, X.L.; Li, H.Y.; Ye, W.Y.; Zhao, M.Q.; Huang, D.N.; Fang, Y.; Zhou, B.Q.; Ren, K.F.; Ji, J.; Fu, G.S. (**2019**). Magainin-modified polydopamine nanoparticles for photothermal killing of bacteria at low temperature. *Colloids Surf. B Biointerfaces.* 183, 110423.

USC UNIVERSIDADE DE SANTIAGO DE COMPOSTELA

Fricke, C.; Harms, H.; Maskow, T. (**2019**). Rapid calorimetric detection of bacterial contamination: Influence of the cultivation technique. *Front. Microbiol.* 10, 2530.

Han, L.; Li, P.; Tang, P.; Wang, X.; Zhou, T.; Wang, K.; Ren, F.; Guo, T.; Lu, X. (**2019**). Mussel-inspired cryogels for promoting wound regeneration through photobiostimulation, modulating inflammatory response and suppressing bacterial invasion. *Nanoscale.* 11, 15846-15861.

Hida, T.; Kamiya, T.; Kawakami, A.; Ogino, J.; Sohma, H.; Uhara, H.; Jimbow, K. (**2020**). Elucidation of melanogenesis cascade for identifying pathophysiology and therapeutic approach of pigmentary disorders and melanoma. *Int. J. Mol. Sci.* 21(17), 6129.

Huang, Z.; Lui, H.; Chen, X.K.; Alajlan, A.; McLean, D.I.; Zeng, H. (**2004**). Raman spectroscopy of in vivo cutaneous melanin. *J. Biomed. Opt.* 9(6), 1198-205.

Hu, D.N.; Simon, J.D.; Sarna, T. (**2008**). Role of ocular melanin in ophthalmic physiology and pathology. *Photochem. Photobiol.* 84(3), 639-644.

Liang,Y.; Liang, Y.; Zhang, H.; Guo, B. (**2022**). Antibacterial biomaterials for skin wound dressing. *Asian J. Pharm. Sci.* 17(3), 353-384.

Larsson, B.S. (**1993**). Interaction between chemicals and melanin. *Pigment Cell Res.* 6, 127–133.

Liu, Y.; Moore, J.H.; Kolling, G.L.; McGrath, J.S.; Papin, J.A.; Swami, N.S. (**2020**). Minimum bactericidal concentration of ciprofloxacin to pseudomonas aeruginosa determined rapidly based on pyocyanin secretion. *Sens. Actuators B Chem.* 312, 127936.

USC UNIVERSIDADE DE SANTIAGO DE COMPOSTELA

Madkhali, N.; Alqahtani, H.; Al-Terary, S. et al. (**2019**). Control of optical absorption and fluorescence spectroscopies of natural melanin at different solution concentrations. *Opt. Quant. Electron.* 51, 227.

Napolitano, A.; Panzella, L.; Leone, L.; d'Ischia, M. (**2013**). Red hair benzothiazines and benzothiazoles: Mutation-inspired chemistry in the quest for functionality. *Acc. Chem. Res.* 46(2), 519−528.

Pelkonen, L.; Tengvall-Unadike, U.; Ruponen, M.; Kidron, H.; Del Amo, E.M.; Reinisalo, M.; Urtti, A. (**2017**). Melanin binding study of clinical drugs with cassette dosing and rapid equilibrium dialysis inserts. *Eur. J. Pharm. Sci.* 109, 162-168.

Pereira-da-Mota, A.F.; Vivero-Lopez, M.; Serramito, M.; Diaz-Gomez, L.; Serro, A.P.; Carracedo, G.; Huete-Toral, F.; Concheiro, A.; Alvarez-Lorenzo, C. (**2022**). Contact lenses for pravastatin delivery to eye segments: Design and in vitro-in vivo correlations. *J. Control. Release.* 348, 431-443.

Saghaie, L.; Pourfarzam, M.; Fassihi, A.; Sartippour, B. (**2013**). Synthesis and tyrosinase inhibitory properties of some novel derivatives of kojic acid. *Res. Pharm. Sci.* 8(4), 233-242.

Salazar, M.; Shimada, K.; Patil, P. N. Iris pigmentation and atropine mydriasis. J. Pharmacol. Exp. Ther. 1976, 197, 79−88; Nagata, A.; Mishima, H. K.; Kiuchi, Y.; Hirota, A.; Kurokawa, T.; Ishibashi, S. (**1993**). Binding of antiglaucomatous drugs to synthetic melanin and their hypotensive effects on pigmented and nonpigmented rabbit eyes. *Jpn. J. Ophthalmol.* 37, 32−38.

Sarna, T. (**1992**). Properties and function of the ocular melanin-a photobiophysical view. *J. Photochem. Photobiol. B.* 12, 215–258.

USC UNIVERSIDADE DE SANTIAGO DE COMPOSTELA

Skarbez, K.; Priestley, Y.; Hoepf, M.; Koevary, S.B. (**2010**). Comprehensive review of the effects of diabetes on ocular health. *Expert Rev. Ophthalmol.* 5(4), 557-577.

Simon, J. D.; Peles, D. N. (**2010**). The red and the black. *Acc. Chem. Res.* 43(11), 1452−1460.

Smith, A.; Pennefather, P.M.; Kaye, S.B.; Hart, C.A. (**2001**). Fluoroquinolones: place in ocular therapy. *Drugs*. 61(6), 747-761.

Sono, K.; Lye, D.; Moore, C.A.; Boyd, W.C.; Gorlin, T.A.; Belitsky, J.M. (**2012**). Melanin-based coatings as lead-binding agents. *Bioinorg. Chem. Appl.* 2012, 361803.

Rimpelä, A.K.; Reinisalo, M.; Hellinen, L.; Grazhdankin, E.; Kidron, H.; Urtti, A.; Del Amo, E.M. (**2018**). Implications of melanin binding in ocular drug delivery. *Adv. Drug Deliv. Rev.* 126, 23-43.

Tran, N.P.; Yang, M.C. (**2020**). The ophthalmic performance of hydrogel contact lenses loaded with silicone nanoparticles. *Polymers.* 12(5), 1128.

Xiao, Z. (**2021**). Photothermal Therapy Mediated by Nanomaterial; https://encyclopedia.pub/entry/6885 (accessed on November 2022).

Xie, W.; Pakdel, E.; Liang, Y.; Kim, Y. J.; Liu, D.; Sun, L.; Wang, X. (**2019**). Natural eumelanin and its derivatives as multifunctional materials for bioinspired applications: A Review. *Biomacromolecules.* 20(12), 4312−433

USC UNIVERSIDADE DE SANTIAGO DE COMPOSTELA

USC
UNIVERSIDADE
DE SANTIAGO
DE COMPOSTELA

CONCLUSIONS

USC
UNIVERSIDADE
DE SANTIAGO
DE COMPOSTELA

USC
UNIVERSIDADE
DE SANTIAGO
DE COMPOSTELA

7. CONCLUSIONS

According to the aims of the present Thesis, the development of drug-CL combinations products was carried out, and the possibility of loading drugs useful for ophthalmic administration was evaluated. Several bioinspired approaches were explored, and the obtained combination products were characterized in detail.

The work was carried out in four steps and the specific conclusions of each chapter are summarized in the following paragraphs.

1. Bioinspired contact lenses mimicking the active site of HMG–CoA reductase were successfully designed for the first time with an enhanced affinity for atorvastatin calcium. The hydrogels presented solvent uptake, light transmission, and mechanical properties values in the common range for commercially available CLs. No potential eye (CAM) irritation was observed neither cytotoxicity effects. The APMA hydrogels notably increased the amount of atorvastatin loaded and released. Hydrostatic pressure sterilization was found to be an advantageous substitute of steam heat and gamma radiation in the sterilization of atorvastatin-loaded hydrogels, maintaining atorvastatin stability and hydrogels performance. Permeability studies suggest that

USC UNIVERSIDADE DE SANTIAGO DE COMPOSTELA

the amount of atorvastatin accumulated in the cornea and sclera could be effective to treat ocular surface diseases.

2. Pravastatin was successfully loaded in bioinspired contact lenses mimicking the active site of HMG–CoA reductase prepared with EGPEM and APMA as monomers that can resemble the hydrophobic and amine-based binding points of the natural receptor. Pravastatin-loaded CLs sustained *in vitro* the release for 10 h, exhibited anti-inflammatory properties, and the drug released could penetrate and accumulate in anterior and posterior eye segments. The safety of this combination product was confirmed in cell studies, HET-CAM and *in vivo* studies. *In vivo* tests in a rabbit model demonstrated the suitability of the developed CLs to control pravastatin release on the ocular surface, notably prolonging the permanence time in the tear fluid compared to eye drops as well as facilitating drug access to aqueous humour and vitreous humour. Preliminary assessment of IVIVC revealed that addition of BSA or lysozyme to the release medium may affect to the *in vitro* release profiles demonstrating stronger IVIVC for *in vitro* release media containing proteins.

3. The usefulness of a 3D printed eye blink model for the evaluation of drug release profiles of medicated CLs was explored in detail in this part of the Thesis. Two drugs of different physicochemical properties, pravastatin sodium and resveratrol, were used to load the CLs in order to validate the robustness of this approach. The release profile of both drugs was more sustained and lower in the *in vitro* eye blink model compared to the *in vitro* release in vials, especially for the hydrophobic drug resveratrol. Interestingly, both drug-loaded CLs showed similar

USC UNIVERSIDADE DE SANTIAGO DE COMPOSTELA

release patterns in the eye blink model as in *in vivo* studies. However, the amount of drug released in the eye blink model was significantly lower compared to previously obtained *in vivo* data. Levy plots presented stronger correlations for pravastatin release in the eye model (flow rate of 10 µL/min) and *in vivo* data. The obtained results may serve as a guide for further improvements of the 3D printed eye blink model.

4. Melanin was successfully incorporated to SiHy discs and commercially available CLs to communicate multifunctional performances. Namely, melanin was shown to act as a light filter that can efficiently convert patient-friendly near-infrared light into moderate increases in temperature. A very fast (in 10 s) and localized increase in temperature conveyed through the contact lenses may be useful to treat a variety of surface eye diseases including tumors and infections. Moreover, melanin may endow CLs with affinity for a variety of drugs, allowing for the combination of photothermal therapy and chemotherapy. The information gathered in the present chapter may serve as a first step towards the development of strategies that combine hydrogels modification and incorporation of active substances for stimuli-responsiveness.

Taken together, the bioinspired strategies developed in this PhD Thesis render drug-CL combination products for topical ocular drug delivery that provide sustained drug levels in the ocular surface and also allow for feasible photothermal therapy of surface eye diseases. Moreover, *in vitro* test methods that mimic drug release on the ocular

USC UNIVERSIDADE DE SANTIAGO DE COMPOSTELA

surface have been identified, which may pave the way towards the setup of methodologies that can provide strong *in vitro-in vivo* correlations.

USC UNIVERSIDADE DE SANTIAGO DE COMPOSTELA

ANNEXES

USC
UNIVERSIDADE DE SANTIAGO DE COMPOSTELA

USC
UNIVERSIDADE
DE SANTIAGO
DE COMPOSTELA

ANNEXES

DECLARACIÓNS, CONFLITO DE INTERESES E RELACIÓN DE PUBLICACIÓNS QUE ACHEGAN CONTIDOS

CONFLITO DE INTERESE

A doutoranda declara non ter ningún conflito de interese en relación coa Tese de Doutoramento.

RELACIÓN DE PUBLICACIÓNS QUE ACHEGAN CONTIDOS

Capítulo 1:

Autores (p.o. de firma): A. F. Pereira-da-Mota, C. Minh-Phan, A. Concheiro, L. Jones, Carmen Alvarez-Lorenzo.

Título: Testing drug release from medicated contact lenses: The missing link to predict in vivo performance.

Revista: *Journal of Controlled Release* 343, 672-702, 2022.

Factor de impacto: 11.467 (2021); Q1 (D1) en Pharmaceutical Science. ISSN: 0168-3659

Contribución da doutoranda: Pesquisa bibliográfica e participación na redacción do texto da revisión.

USC UNIVERSIDADE DE SANTIAGO DE COMPOSTELA

Capítulo 3:

Autores (p.o. de firma): A. F. Pereira-da-Mota, M. Vivero-Lopez, A. Topete, A. P. Serro, A. Concheiro, Carmen Alvarez-Lorenzo.

Título: Atorvastatin-eluting contact lenses: effects of molecular imprinting and sterilization on drug loading and release.

Revista: *Pharmaceutics* 13, 606, 2021.

Factor de impacto: 6.525 (2021). JCR (Q1, Pharmacology & Pharmacy); CiteScore (Q2, Pharmaceutical Science). ISSN: 1999-4923.

Contribución da doutoranda: Pesquisa bibliográfica, colaboración no deseño dos experimentos, realización da experimentación, análise dos resultados, redacción do borrador do traballo e participación na preparación do texto definitivo.

Capítulo 4:

Autores (p.o. de firma): A. F. Pereira-da-Mota, M. Vivero-Lopez, M. Serramito, L. Diaz-Gomez, A. P. Serro, G. Carracedo, F. Huete-Torral, A. Concheiro, C. Alvarez-Lorenzo

Título: Contact lenses for pravastatin delivery to eye segments: Design and in vitro-in vivo correlations.

Revista: *Journal of Controlled Release* 348, 431-443, 2022.

Factor de impacto: 11.467 (2021); Q1 (D1) en Pharmaceutical Science. ISSN: 0168-3659

Contribución da doutoranda: Pesquisa bibliográfica, colaboración no deseño dos experimentos, realización da experimentación, análise dos resultados, redacción do borrador do traballo e participación na preparación do texto definitivo.

USC UNIVERSIDADE DE SANTIAGO DE COMPOSTELA

Capítulo 5:

Autores (p.o. de firma): A. F. Pereira-da-Mota, M. Vivero-Lopez, P. Garg, C. Minh-Phan, A. Concheiro, L. Jones, C. Alvarez-Lorenzo

Título: *In vitro – in vivo* correlation of drug release profiles from medicated contact lenses using an in vitro eye blink model.

Revista: *Drug Delivery and Translational Research* (DOI: 10.1007/s13346-022-01276-6).

Factor de impacto: 5.671 (2021); Q1 en Pharmaceutical Science. ISSN: 2190-3948.

Contribución da doutoranda: Pesquisa bibliográfica, colaboración no deseño dos experimentos, realización da experimentación, análise dos resultados, redacción do borrador do traballo e participación na preparación do texto definitivo.

USC UNIVERSIDADE DE SANTIAGO DE COMPOSTELA

PERMISOS DE REPRODUCIÓN TOTAL OU PARCIAL DE TRABALLOS PUBLICADOS POLO DOUTORANDO

Chapter 1. Testing drug release from medicated contact lenses: The missing link to predict in vivo performance,

The work described in this chapter was published in **Testing drug release from medicated contact lenses: The missing link to predict *in vivo* performance**, *Journal of Controlled Release* 343, 2022, 672-702, authored by

Ana F. Pereira-da-Mota[a], Chau Minh-Phan[b,c], Angel Concheiro[a], Lyndon Jones[b,c], and Carmen Alvarez-Lorenzo[a]

[a]Departamento de Farmacología, Farmacia y Tecnología Farmacéutica, I+D Farma Group (GI-1645), Facultad de Farmacia, Instituto de Materiales (iMATUS) and Health Research Institute of Santiago de Compostela (IDIS), Universidade de Santiago de Compostela, 15782 Santiago de Compostela, Spain.

[b]Centre for Ocular Research & Education (CORE), School of Optometry and Vision Science, University of Waterloo, Waterloo, ON, Canada.

[c]Centre for Eye and Vision Research (CEVR), 17W, Hong Kong, Science Park, Hong Kong.

Author contribution: Bibliographic research and participation in the writing of the review text.

Journal of Controlled Release

ISSN: 0168-3659

Journal Impact Factor: 11.467 (2021)

JCR Category: Pharmaceutical Science

Category Quartile: Q1

USC UNIVERSIDADE DE SANTIAGO DE COMPOSTELA

Reproduction permission:

Chapter 3. Atorvastatin-eluting contact lenses: effects of molecular imprinting and sterilization on drug loading and release

The work described in this chapter was published in **Atorvastatin-eluting contact lenses: effects of molecular imprinting and sterilization on drug loading and release**, *Pharmaceutics* 13, 606, 2021, authored by:

Ana F. Pereira-da-Mota[a], María Vivero-Lopez[a], Ana Topete[b], Ana Paula Serro[b], Angel Concheiro[a] and Carmen Alvarez-Lorenzo[a]

[a]Departamento de Farmacología, Farmacia y Tecnología Farmacéutica, I+D Farma (GI-1645), Facultad de Farmacia and Health Research Institute of Santiago de Compostela (IDIS), Universidade de Santiago de Compostela, 15782 Santiago de Compostela, Spain.

[b]Centro de Química Estrutural, Departamento de Engenharia Química, Instituto Superior Técnico, Universidade de Lisboa, Av. Rovisco Pais, 1049-001 Lisbon, Portugal.

Author contribution: Bibliographic research, collaboration in the design of the experiments, data collection and processing, participation in the elaboration of the final text.

USC UNIVERSIDADE DE SANTIAGO DE COMPOSTELA

Pharmaceutics

ISSN: 1999-4923

Journal Impact Factor: 6.525 (2021)

JCR Category: Pharmacology & Pharmacy

Category Quartile: (Q1, Pharmacology & Pharmacy); **CiteScore** (Q2, Pharmaceutical Science).

Reproduction permission: The article was published in Open Access.

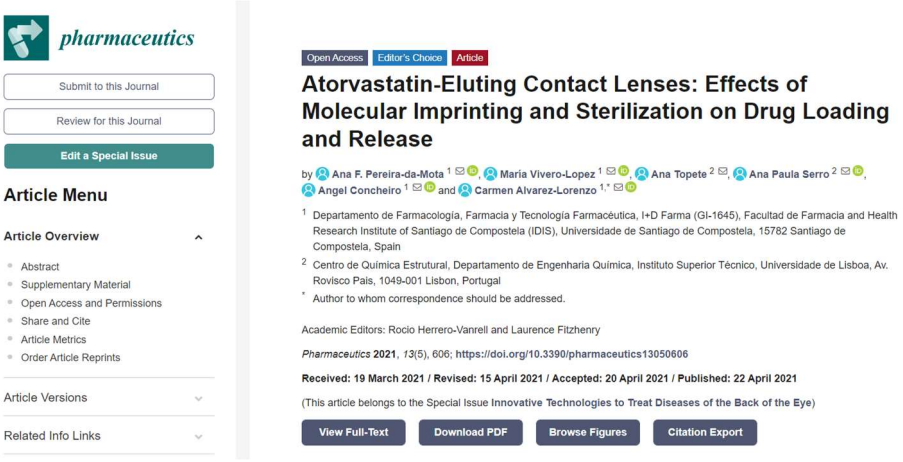

Chapter 4. Contact lenses for pravastatin delivery to eye segments: Design and in vitro-in vivo correlations

The work described in this chapter was published in **Contact lenses for pravastatin delivery to eye segments: Design and *in vitro-in vivo* correlations**, *Journal of Controlled Release* 348, 2022, 431-443, authored by

Ana F. Pereira-da-Mota[a], María Vivero-Lopez[a], Maria Serramito[b], Luis Diaz-Gomez[a], Ana Paula Serro[c], Gonzalo Carracedo[b], Fernando Huete-Toral[b], Angel Concheiro[a] and Carmen Alvarez-Lorenzo[a]

USC UNIVERSIDADE DE SANTIAGO DE COMPOSTELA

[a]Departamento de Farmacología, Farmacia y Tecnología Farmacéutica, I+D Farma Group (GI-1645), Facultad de Farmacia, Instituto de Materiales (iMATUS) and Health Research Institute of Santiago de Compostela (IDIS), Universidade de Santiago de Compostela, 15782 Santiago de Compostela, Spain.

[b]Ocupharm Research Group, Faculty of Optic and Optometry, University Complutense of Madrid, C/Arcos del Jalon 118, 28037 Madrid, Spain.

[c]Centro de Química Estrutural, Departamento de Engenharia Química, Instituto Superior Técnico, Universidade de Lisboa, Av. Rovisco Pais, 1049-001 Lisbon, Portugal.

Author contribution: Bibliographic research, collaboration in the design of the experiments, data collection and processing, participation in the elaboration of the final text.

Journal of Controlled Release

ISSN: 0168-3659

Journal Impact Factor: 11.467 (2021)

JCR Category: Pharmaceutical Science

Category Quartile: Q1 (D1)

USC UNIVERSIDADE DE SANTIAGO DE COMPOSTELA

Reproduction permission:

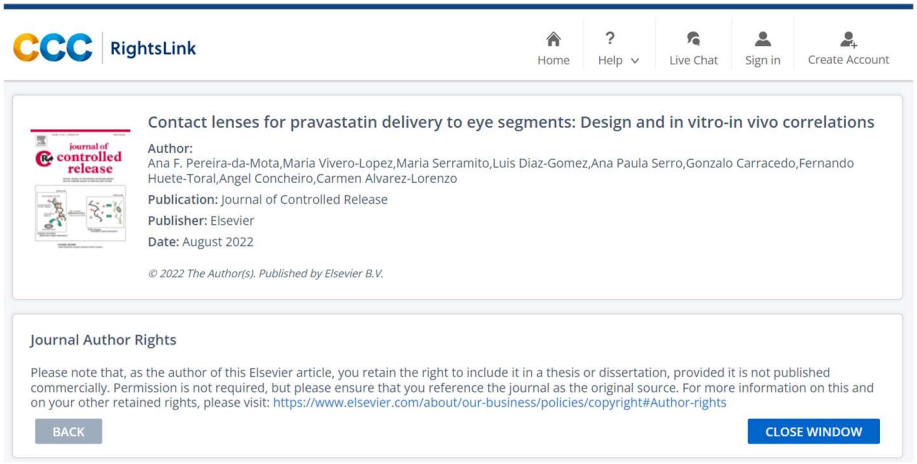

Chapter 5. In vitro-in vivo correlation of drug release profiles from medicated contact lenses using an in vitro eye blink model

The work described in this chapter was accepted for publication in **In vitro-in vivo correlation of drug release profiles from medicated contact lenses using an in vitro eye blink model**, *Drug Delivery and Translation Research*, 2022, authored by

Ana F. Pereira-da-Mota[a], María Vivero-Lopez[a], Piyush Garg[b], Chau Minh-Phan[b,c], Angel Concheiro[a], Lyndon Jones[b,c], and Carmen Alvarez-Lorenzo[a]

[a]Departamento de Farmacología, Farmacia y Tecnología Farmacéutica, I+D Farma Group (GI-1645), Facultad de Farmacia, Instituto de Materiales (iMATUS) and Health Research Institute of Santiago de Compostela (IDIS), Universidade de Santiago de Compostela, 15782 Santiago de Compostela, Spain.

[b]Centre for Ocular Research & Education (CORE), School of Optometry and Vision Science, University of Waterloo, Waterloo, ON, Canada.

[c]Centre for Eye and Vision Research (CEVR), 17W, Hong Kong, Science Park, Hong Kong.

Author contribution: Bibliographic research, collaboration in the design of the experiments, data collection and processing, participation in the elaboration of the final text.

Drug Delivery and Translation Research

ISSN: 2190-3948

Journal Impact Factor: 5.671 (2021)

JCR Category: Pharmaceutical Science

Category Quartile: Q1

Reproduction permission:

USC UNIVERSIDADE DE SANTIAGO DE COMPOSTELA

CHECKLIST FOR THESIS THAT INCLUDE EXPERIMENTAL ANIMALS. EXPERIMENTAL ANIMALS ARRIVE

Yes/No/NA		page
	Title	
Yes	Provide as accurate and concise a description of the content of the article as possible.	235
	Abstract	
Yes	Provide an accurate summary of the background, research objectives, including details of the species or strain of animal used, key methods, principal findings and conclusions of the study.	11-13
	Background	
Yes	Provide an accurate summary of the background, research objectives, including details of the species or strain of animal used, key methods, principal findings and conclusions of the study.	235-295
Yes	Explain how and why the animal species and model being used can address the scientific objectives and, where appropriate, the study's relevance to human biology.	276-280
	Objectives	
Yes	Clearly describe the primary and any secondary objectives of the study, or specific hypotheses being tested.	238-239
	Methods	
	Ethical statement	
Yes	Indicate the nature of the ethical review permissions, relevant licenses, and national or institutional guidelines for the care and use of animals, that cover the research.	251
	Study design	

USC UNIVERSIDADE DE SANTIAGO DE COMPOSTELA

Yes	Number of experimental and control groups	251-252
Yes	Steps taken to minimize the effects of subjective bias when allocating animals to treatment (e.g. randomization procedure) and when assessing results (e.g. if done, describe who was blinded and when).	251-252
Yes	The experimental unit (e.g. a single animal, group or cage of animals). A time-line diagram or flow chart can be useful to illustrate how complex study designs were carried out.	251-252
	Experimental procedures	
Yes	How (e.g. drug formulation and dose, site and route of administration, anesthesia and analgesia used [including monitoring], surgical procedure, method of euthanasia). Provide details of any specialist equipment used, including supplier(s).	250-255
Yes	When (e.g. time of day).	251
Yes	Where (e.g. home cage, laboratory, water maze).	251
Yes	Why (e.g. rationale for choice of specific anesthetic, route of administration, drug dose used).	250-255
	Experimental animals	
Yes	Provide details of the animals used, including species, strain, sex, developmental stage (e.g. mean or median age plus age range) and weight (e.g. mean or median weight plus weight range).	251
Yes	Provide further relevant information such as the source of animals, international strain nomenclature, genetic modification status (e.g. knock-out or transgenic), genotype, health/immune status, drug or test naïve, previous procedures, etc.	251
	Housing and husbandry	
Yes	Housing (type of facility e.g. specific pathogen free [SPF]; type of cage or housing; bedding	251

USC UNIVERSIDADE DE SANTIAGO DE COMPOSTELA

	material; number of cage companions; tank shape and material etc. for fish).	
Yes	Husbandry conditions (e.g. breeding program, light/dark cycle, temperature, quality of water etc for fish, type of food, access to food and water, environmental enrichment).	251
Yes	Welfare-related assessments and interventions that were carried out prior to, during, or after the experiment.	250-255
	Sample size	
Yes	Specify the total number of animals used in each experiment, and the number of animals in each experimental group.	251-252
Yes	Explain how the number of animals was arrived at. Provide details of any sample size calculation used.	251-252
Yes	Indicate the number of independent replications of each experiment, if relevant.	251-252
	Allocating animals to experimental groups	
Yes	Indicate the number of independent replications of each experiment, if relevant.	251-252
Yes	Describe the order in which the animals in the different experimental groups were treated and assessed.	251-252
	Experimental outcomes	
Yes	Clearly define the primary and secondary experimental outcomes assessed (e.g. cell death, molecular markers, behavioral changes).	253-255
	Statistical methods	
Yes	Provide details of the statistical methods used for each analysis.	255
Yes	Specify the unit of analysis for each dataset (e.g. single animal, group of animals, single neuron).	255, 278, 280

USC UNIVERSIDADE DE SANTIAGO DE COMPOSTELA

Yes	Describe any methods used to assess whether the data met the assumptions of the statistical approach.	255, 278, 280
	Results and discussion	
	Basal data	
Yes	For each experimental group, report relevant characteristics and health status of animals (e.g. weight, microbiological status, and drug or test naïve) prior to treatment or testing (this information can often be tabulated).	251-252
	Numbers analyzed	
Yes	Report the number of animals in each group included in each analysis. Report absolute numbers (e.g. 10/20, not 50%).	251-252
Yes	If any animals or data were not included in the analysis, explain why.	251-252
	Outcomes and estimation	
Yes	Report the results for each analysis carried out, with a measure of precision (e.g. standard error or confidence interval).	276-280
	Adverse events	
NA	Give details of all important adverse events in each experimental group.	
Yes	Describe any modifications to the experimental protocols made to reduce adverse events.	251-253
	Interpretation/scientific implications	
Yes	Interpret the results, taking into account the study objectives and hypotheses, current theory and other relevant studies in the literature.	276-280
Yes	Comment on the study limitations including any potential sources of bias, any limitations of the animal model, and the imprecision associated with the results.	251
NA	Describe any implications of your experimental methods or findings for the replacement,	

USC UNIVERSIDADE DE SANTIAGO DE COMPOSTELA

	refinement or reduction (the 3Rs) of the use of animals in research.	
	Generalizability/translation	
Yes	Comment on whether, and how, the findings of this study are likely to translate to other species or systems, including any relevance to human biology.	276-280
	Funding	
Yes	List all funding sources (including grant number) and the role of the funder(s) in the study.	251

Based on The ARRIVE guidelines: Animal Research: Reporting of In Vivo Experiments.

PhD Student signature

USC UNIVERSIDADE DE SANTIAGO DE COMPOSTELA

Código seguro de Verificación : GEISER-5740-83a2-42e5-469d-a558-3855-bbfc-93ed | Puede verificar la integridad de este documento en la siguiente dirección : https://sede.administracionespublicas.gob.es/valida

Investigador Principal Proyecto	Nombre: Juan Gonzalo Carracedo Rodríguez DNI: 07505953H	
	Centro: Facultad de Óptica y Optometría	Departamento/ Sección: Departamento de Optometría y Visión
	Teléfono: 616513539	Correo electrónico: jgcarrac@ucm.es
Investigador Responsable Procedimientos	Nombre: Juan Gonzalo Carracedo Rodríguez (IP) DNI:	
	Centro:	Departamento/ Sección:
	Teléfono:	Correo electrónico:
Título del Proyecto	Título: Efecto de la luz azul y las lentes de contacto de ortoqueratología para el control de la progresión de la miopía sobre la morfología, la fisiología y la bioquímica ocular	
	Fecha de inicio: 01/01/2022	Fecha de finalización: 03/03/2022
Finalidad del Informe	☒ Científica	☐ Docente ☐ Imposición legal
	Presentación de proyecto para ser financiado Organismo: Ministerio de Ciencia e Innovación	Convocatoria: 2021
	Proyecto financiado en ejecución Organismo:	Referencia:
	Autorización de experimentación o actividad	
	Otros (especificar):	

Fecha y Firma 06/05/2021

Vº.Bº. Vicerrectora de Investigación y Transferencia y Responsable administrativo de usuario	Investigador/a Principal
Dña. Margarita San Andrés Moya	D./Dña. Juan Gonzalo Carracedo Rodríguez (Al firmar declaro haber leído y aceptado la cláusula de protección de datos al pie indicada)

Información básica de protección de datos del tratamiento: Investigación
Responsable Vicerrectorado de Investigación y Transferencia
Finalidad Ayudas y acciones para desarrollo de la investigación Científica
Legitimación Cumplimiento de una obligación legal; Misión en interés público
Destinatarios Se prevén cesiones
Derechos Acceder y rectificar los datos, así como otros derechos, explicados en la información adicional
Infor. adicional Puede consultarla con detalle en: https://www.ucm.es/data/cont/docs/3-2018-05-23-Info-Adic-Tratamiento-Investigación.pdf

ÁMBITO- PREFIJO
CSV
GEISER-5740-83a2-42e5-469d-a558-3855-bbfc-93ed
DIRECCIÓN DE VALIDACIÓN
https://sede.administracionespublicas.gob.es/valida
FECHA Y HORA DEL DOCUMENTO
14/05/2021 12:30:31 Horario peninsular
Validez del documento
Copia
GEISER-5740-83a2-42e5-469d-a558-3855-bbfc-93ed

Documento firmado electrónicamente por:
Margarita San Andres Moya
Fecha: 17/05/2021
CSV: 4175-4475-6C36P6263-4C34
Puede comprobar la validez de la firma en:
https://sede.ucm.es/verificacion

Código seguro de Verificación : GEISER-5740-83a2-42e5-469d-a558-3855-bbfc-93ed | Puede verificar la integridad de este documento en la siguiente dirección : https://sede.administracionespublicas.gob.es/valida

1. DATOS DEL PROYECTO DE INVESTIGACIÓN O PROCEDIMIENTO (se ruega que estos apartados sean lo más breves y concisos posibles)	
Título	Efecto de la luz azul y las lentes de contacto de ortoqueratología para el control de la progresión de la miopía sobre la morfología, la fisiología y la bioquímica ocular
Resumen*	Se realizará un estudio prospectivo a 3 meses en el que se evaluará el efecto de la luz azul y las lentes de contacto de ortoqueratología sobre la morfología, la fisiología y la bioquímica ocular para entender los mecanismos implicados en el crecimiento ocular y cómo estos tratamientos actúan para frenar dicho crecimiento y, por tanto, controlar la progresión de la miopía. Se utilizarán cobayas para estudiar el efecto de la luz azul y conejos para estudiar el efecto de las lentes de contacto de ortoqueratología. Las medidas de las variables estadísticas se harán antes y tras 1, 15, 30 y 90 d.
Objetivos	Evaluar el efecto de dos tratamientos para el control de la progresión de la miopía, la luz azul y las lentes de contacto de ortoqueratología, sobre la morfología, la fisiología y la bioquímica ocular.
Importancia de la Investigación	Explicar los beneficios científicos de este trabajo en el avance del conocimiento, o en el bien para la sociedad: La miopía es un defecto refractivo que afecta al 22% de la población mundial. Para el año 2050, se estima que este número alcance un 50% debido a los cambios en los hábitos de vida como una mayor demanda visual de cerca y un menor tiempo al aire libre. La miopía no está exenta de riesgo para la salud ocular, ya que cuanto mayor es su magnitud, mayor es el riesgo de sufrir patologías oculares asociadas como cataratas (hasta 5x), glaucoma (14x), desprendimiento de retina (22x) o maculopatía miópica (41x). En la actualidad, se conocen tratamientos para frenar el crecimiento del ojo, y por tanto la miopía, como son el uso de luz azul de alta intesidad y lentes de contacto de ortoqueratología. Sin embargo, no se conocen los mecanismos fisiológicos y bioquímicos por los que se produce este control de la progresión de la miopía. Por tanto, este estudio pretende investigar tanto los eventos fisiológicos como la cascada bioquímica implicada en el crecimiento del ojo con el fin de desarrollar y optimizar nuevos tratamientos que permitan un control más eficaz de la progresión de la miopía y poder reducir así su impacto negativo en la salud ocular de las personas, la sociedad y la economía.
Análisis previsto de los resultados	Variable(s) que se va(n) a medir y unidad(es) de medida: Longitud del ojo (mm), refracción (dioptrías), espesor de las estructuras oculares (µm), densidad celular en las estructuras oculares (células/mm2) y tanto la concentración de dopamina como de otras moleculas asociadas al crecimiento del ojo (moles). Factor(es) que se va(n) a estudiar y niveles (tratamientos) de cada factor: luz (luz blanca ambiental, oscuridad, luz azul ambiental y luz azul focalizada en el nervio óptico -4 niveles-), lentes de contacto de ortoqueratología (sin lente y con lente -2 niveles-) y tiempo (medida basal y tras 1, 15, 30 y 90 días -5 niveles-). Modelo(s) estadístico(s) o metodología(s): Se estimará la normalidad de las variables estadísticas mediante el test de Shapiro-Wilk. Una vez estimada la normalidad, se hará un contraste de hipótesis entre los grupos de un mismo factor, utilizando la T de Student para muestras independientes, en caso de muestras normales, o el test de la U de Mann-Whitney, en caso de muestras no normales. Además, se hará un análisis de la varianza (ANOVA) de un factor (tiempo de tratamiento) en cada uno de los grupos.

ÁMBITO- PREFIJO | CSV | FECHA Y HORA DEL DOCUMENTO
GEISER | **GEISER-5740-83a2-42e5-469d-a558-3855-bbfc-93ed** | **14/05/2021 12:30:31 Horario peninsular**
Nº registro | DIRECCIÓN DE VALIDACIÓN | Validez del documento
O00023280e2100023620 | **https://sede.administracionespublicas.gob.es/valida** | **Copia**

GEISER-5740-83a2-42e5-469d-a558-3855-bbfc-93ed

	(Ejemplo: modelo unifactorial, bifactorial, con bloques, regresión, etc. o comparaciones entre grupos indicando el tipo de test que se realizará, análisis de la varianza de una vía, de dos vías, etc.)

Tipo de proyecto (Ver art.31 RD 53/2013)

Tipo I ☐	**Tipo II** ☒	**Tipo III** ☐

***Resumen máximo 300 caracteres**

2. DATOS DE LOS PARTICIPANTES

Si necesita más líneas, puede añadirlas pulsando + a la derecha de la última línea activa

Cargo o Puesto	Capacitación categorías/funciones según RD 53/2013 y Órden ECC/566/2015 / en trámite*	Nombre	Centro
Investigador principal del proyecto	C y B	Juan Gonzalo Carracedo Rodríguez	Facultad de Óptica y Optometría
Investigador responsable del diseño de los proyectos y procedimientos	C y B	Juan Gonzalo Carracedo Rodríguez (IP)	Facultad de Óptica y Optometría
Miembro del equipo investigador	B	Beatriz Ornés Poleo	Otras entidades de investigación
Miembro del equipo investigador	B	María Luisa González Rubio	Otras entidades de investigación
Miembro del equipo investigador	B	Basilio Colligris	Facultad de Óptica y Optometría
Miembro del equipo investigador			
Miembro del equipo investigador			
Miembro del equipo investigador			

* Grupo de Categoría según RD 53/2013. (E.t.): Si está en trámite (e.t.), indíquese la persona que supervisa la realización del procedimiento. Cumplimentación obligatoria en todos los miembros.

Observaciones punto 2.

Las capacitaciones de los investigadores son:

- Según Real Decreto 1201/2005, de 10 de octubre:

  Categoría A: personal para el cuidado de los animales.
  Categoría B: personal que lleva a cabo los procedimientos.
  Categoría C: personal responsable para dirigir o diseñar los procedimientos.
  Categoría D. personal especialista en ciencias del animal de experimentación con funciones de asesoramiento sobre el bienestar de los animales:
  Categoría D1. Personal especialista en bienestar animal: persona con titulación universitaria superior en el área de Ciencias de la Salud, encargada de supervisar y asesorar todos los aspectos relacionados con el bienestar de los animales.
  Categoría D2. Personal especialista en salud animal: persona licenciada en Veterinaria con formación complementaria especializada en animales de experimentación, encargada de supervisar y asesorar todos los aspectos relacionados con la salud de los animales.

- Según la Orden ECC 566/2015, de 20 de marzo:

  Función a: Cuidado de los animales.
  Función b: Eutanasia de los animales.
  Función c: Realización de los procedimientos.
  Función d: Diseño de los proyectos y procedimientos.
  Función e: Asunción de la responsabilidad de la supervisión «in situ» del bienestar y cuidado de los animales.
  Función f: Asunción de las funciones de veterinario designado.

Código seguro de Verificación : GEISER-5740-83a2-42e5-469d-a558-3855-bbfc-93ed | Puede verificar la integridad de este documento en la siguiente dirección : https://sede.administracionespublicas.gob.es/valida

ÁMBITO- PREFIJO	CSV	FECHA Y HORA DEL DOCUMENTO
GEISER	**GEISER-5740-83a2-42e5-469d-a558-3855-bbfc-93ed**	**14/05/2021 12:30:31 Horario peninsular**
Nº registro	DIRECCIÓN DE VALIDACIÓN	Validez del documento
O00023280e2100023620	**https://sede.administracionespublicas.gob.es/valida**	**Copia**

GEISER-5740-83a2-42e5-469d-a558-3855-bbfc-93ed

- Equivalencias:

  Categoría A: función a y b / Categoría B: función b y c / Categoría C: función c y d/ Categoría D1: función e /Categoría D2: función f y b

3. DATOS DE LOS ANIMALES (incluidos los modificados genéticamente)

Si necesita más líneas, puede añadirlas pulsando + a la derecha de la última línea activa

Descripción y número de animales por cada grupo (incluido/s el/los grupo/s de control)

Experimento	Especie	Raza/estirpe/línea	Sexo	Edad (d,m,a)	Peso	Procedencia	Nº por Grupo	Nº Grupos	Nº Total
1	Cobaya (Cavia porcellus)	Americana tricolor	M	14 d	0.5 kg	Granja Cunícola SAN BERNARDO SL	10	4	40
2	Conejo (Oryctolagus cuniculus	de Nueva Zelanda	M	14 d	2 kg	Granja Cunícola SAN BERNARDO SL	6	2	12
3									
4									
5									
6									
7									
8									
9									
10									

Si la procedencia de los animales es de origen externo, indicar el medio de transporte (Laboratorio de procedencia, empresa suministradora/empresa trasporte/traslado por parte del investigador)	Tanto las cobayas como los conejos se transportarán desde la granja externa hasta la Facultad de Óptica y Optometría en un camión acondicionado para dicho fin.

Centro de estabulación Nombre y código de registro:	☒ Instalaciones reglamentadas que el CAI (Animalario de la Universidad Complutense) tiene en las Facultades de Biología, Psicología y Medicina (Nº de Registro: ES-28079-0000086) ☐ Instalaciones de animalarios oficialmente autorizados y registrados en la UCM Nombre y Centro : Nº de Registro: ☐ Otras instalaciones expresamente diseñadas para la estabulación de animales de experimentación. - Departamento o Laboratorio responsable: - Condiciones y mecanismos de control ambiental de los que dispone temperatura, fotoperiodo, humedad, renovación aire, filtros, limpieza): - Motivos que justifiquen la necesidad de manipular los animales en estas instalaciones: ☐ Condiciones y cuidado de los animales no estabulados (animales con propietario):

Código seguro de Verificación : GEISER-5740-83a2-42e5-469d-a558-3855-bbfc-93ed | Puede verificar la integridad de este documento en la siguiente dirección : https://sede.administracionespublicas.gob.es/valida

ÁMBITO- PREFIJO: GEISER
CSV: GEISER-5740-83a2-42e5-469d-a558-3855-bbfc-93ed
FECHA Y HORA DEL DOCUMENTO: 14/05/2021 12:30:31 Horario peninsular
Nº registro: O00023280e2100023620
DIRECCIÓN DE VALIDACIÓN: https://sede.administracionespublicas.gob.es/valida
Validez del documento: Copia

GEISER-5740-83a2-42e5-469d-a558-3855-bbfc-93ed

Observaciones punto 3.

Descripción y número de animales por grupo:
Edad (d, m, a): Escribir d por "días", m por "meses" y a por "años".
Nº por grupos.: Es el número de animales (de cada grupo) por cada experimento.
Nº grupos. Número de grupos en cada experimento.
Nº Total. Número total de animales en cada experimento.

4. DATOS DEL PROCEDIMIENTO ANIMAL*

Si necesita más líneas, puede añadirlas pulsando + a la derecha de la última línea activa

Título del proyecto: Efecto de la luz azul y las lentes de contacto de ortoqueratología para el control de la miopía sobre la morfología, la fisiología y la bioquímica ocular	**Duración/ Frecuencia** 3 meses
☐ Adscripción a un Procedimiento autorizado Referencia, PROEX: (Adjuntar copia)	
☒ Breve descripción de cada procedimiento (P) que se realiza en el Proyecto, indicando brevemente, **en orden cronológico,** la cadena de actuaciones con el animal, así como la duración y frecuencia de cada uno**:**	Duración (tiempo que se estima para realizar el procedimiento) / Frecuencia (número de veces que se realiza dicho procedimiento).
P1 Exposición a la luz y oscuridad: Las cobayas se expondrán a ciclos de 12 h de luz blanca/oscuridad, 12 h de luz azul/oscuridad o 24 h de oscuridad en función del grupo de tratamiento. Este procedimiento se realizará diariamente durante los 90 días de experimentación.	Duración/frecuencia P1: 3 meses
P2 Colocación de lentes de contacto: En los conejos se colocarán lentes de contacto de ortoqueratología 8 horas al día durante los 90 días de experimentación, asegurándose de que generan el efecto deseado. Una vez se cumplan las 8 horas de porte, las lentes de contacto se quitarán durante las 16 horas restantes del día.	Duración/frecuencia P2: 3 meses
P3 Aislamiento y contención: Este procedimiento se hará acorde a la Directiva 2010/63/UE del Parlamento Europeo y del Consejo. En el caso de los cobayas, 3 o 4 de ellas se agruparán en jaulas de un mínimo de 5000 cm^2 y 23 cm de altura, perteneciendo las cobayas de cada jaula a un mismo grupo de estudio. En el caso del grupo de cobayas que se someterá a la cirugía de vitrectomía, las cobayas se aislarán en jaulas individuales para evitar que la interacción de unas con otras aumente el riesgo de efectos secundarios. En el caso de los conejos, cada uno de ellos se estabulará en jaulas individuales, independientemente del grupo al que pertenezcan, de 3500 cm^2 y 45 cm de altura.	Duración/frecuencia P3: 3 meses
P4 Vitrectomía: Se realizará una perforación ocular para acceder al humor vítreo. En este estudio se requiere introducir una fibra óptica de luz azul a través de dicha perforación para iluminar selectivamente el nervio óptico 2 minutos al día (procedimiento en cobayas). El procedimiento se hará una sola vez en un único día y en un único grupo de cobayas, a las que se le estimulará el nervio óptico con luz azul focalizada mediante el posicionamiento dentro del ojo de una fibra óptica.	Duración/frecuencia P4: 1 día
P5 Biomicroscopía: Es un método óptico no invasivo de observación la superficie ocular mediante una lámpara de hendidura. Se utilizará tanto para la vitrectomía como para evaluar la seguridad de los tratamientos (procedimiento en cobayas y conejos). El procedimiento se hará una sola vez en 5 días diferentes.	Duración/frecuencia P5: 5 días
P6 Biometría óptica: Es un método óptico no invasivo para medir la longitud del ojo. Permite medir el efecto de cada uno de los tratamientos sobre el crecimiento ocular (procedimiento en cobayas y conejos). El procedimiento se hará una sola vez en 5 días diferentes.	Duración/frecuencia P6: 5 días

Código seguro de Verificación : GEISER-5740-83a2-42e5-469d-a558-3855-bbfc-93ed | Puede verificar la integridad de este documento en la siguiente dirección : https://sede.administracionespublicas.gob.es/valida

ÁMBITO- PREFIJO	CSV	FECHA Y HORA DEL DOCUMENTO
GEISER	**GEISER-5740-83a2-42e5-469d-a558-3855-bbfc-93ed**	**14/05/2021 12:30:31 Horario peninsular**
Nº registro	DIRECCIÓN DE VALIDACIÓN	Validez del documento
O00023280e2100023620	**https://sede.administracionespublicas.gob.es/valida**	**Copia**

GEISER-5740-83a2-42e5-469d-a558-3855-bbfc-93ed

P7 Retinoscopía: Es un método óptico no invasivo para medir la refracción del ojo. Permite estudiar si los cambios en el grado de miopía están asociados a los cambios en la longitud del ojo (procedimiento en cobayas y conejos). El procedimiento se hará una sola vez en 5 días diferentes.	Duración/frecuencia P7: 5 días
P8 Topografía corneal: Es un sistema de imagen no invasivo para medir la morfología de la córnea. Este sistema permite obtener medidas in vivo de la curvatura de la córnea, su poder refractivo y/o su espesor (procedimiento en cobayas y conejos). El procedimiento se hará una sola vez en 5 días diferentes.	Duración/frecuencia P8: 5 días
P9	Duración/frecuencia P9:
P10	Duración/frecuencia P10:
P :	Duración/frecuencia :

Severidad esperada del procedimiento (ver anexo I)
Si necesita más líneas, puede añadirlas pulsando + a la derecha de la última línea activa

Procedimiento	Leve	Moderado	Severo	Sin recuperación
P1	☒	☐	☐	☐
P2	☒	☐	☐	☐
P3	☒	☐	☐	☐
P4	☐	☒	☐	☐
P5	☒	☐	☐	☐
P6	☒	☐	☐	☐
P7	☒	☐	☐	☐
P8	☒	☐	☐	☐
P9	☐	☐	☐	☐
P10	☐	☐	☐	☐
P	☐	☐	☐	☐

Severidad global esperada de los procedimientos

Severidad global	Leve	Moderado	Severo	Sin recuperación
Según el investigador responsable de los procedimientos	☐	☒	☐	☐

METODOLOGÍA
Si necesita más líneas, puede añadirlas pulsando + a la derecha de la última línea activa

Administración/Inoculación

Producto (indicar principio activo cuando sea posible) / Concentración / Vehículo	**Vía**	**CANTIDAD (volumen, peso, etc)**	**Frecuencia**		**Intervalo**
			Dosis	**Nº de veces**	

Código seguro de Verificación : GEISER-5740-83a2-42e5-469d-a558-3855-bbfc-93ed | Puede verificar la integridad de este documento en la siguiente dirección : https://sede.administracionespublicas.gob.es/valida

ÁMBITO- PREFIJO: **GEISER**
Nº registro: **O00023280e2100023620**
CSV: **GEISER-5740-83a2-42e5-469d-a558-3855-bbfc-93ed**
DIRECCIÓN DE VALIDACIÓN: **https://sede.administracionespublicas.gob.es/valida**
FECHA Y HORA DEL DOCUMENTO: **14/05/2021 12:30:31 Horario peninsular**
Validez del documento: **Copia**

GEISER-5740-83a2-42e5-469d-a558-3855-bbfc-93ed

Código seguro de Verificación : GEISER-5740-83a2-42e5-469d-a558-3855-bbfc-93ed | Puede verificar la integridad de este documento en la siguiente dirección : https://sede.administracionespublicas.gob.es/valida

Toma de muestras				
Muestra (in vivo)	**Vía**	**CANTIDAD (Volumen, peso, etc.)**	**Frecuencia (nº de veces e intervalo)**	**Nº veces Total**

Procedimientos conductuales
Si necesita más líneas, puede añadirlas pulsando + a la derecha de la última línea activa

Procedimiento conductual / Test	**Breve descripción**	**Duración**	**Nº de veces que se realiza / intervalo**

Ayunos

Ayunos	**Breve descripción (indicar si es parcial o total)**	**Duración**	**Nº de veces que se realiza / intervalo**
☒ **Agua**	Parcial (previa a la anestesia)	2 horas	6 veces / durante cirugía, medida basal y tras 1, 15, 30 y 90 días.
☒ **Comida**	Parcial (previa a la anestesia)		

Procedimientos quirúrgicos

Cirugía: breve descripción de la cirugía a realizar	**Anestesia**		**Analgesia**		**Duración estimada**
La vitrectomía consistirá en una perforación del ojo mediante una cánula de 0.4 mm (27 G) para poder acceder al humor vítreo. El objetivo es introducir una fibra óptica de menor diámetro (0.1 mm) para iluminar el nervio óptico de forma selectiva con un LED azul. Esta cirugía sólo se hará en un grupo de cobayas para comprobar si dicha estimulación del nervio óptico produce el mismo efecto que la estimulación completa de la retina con luz azul sobre los parámetros a estudiar en relación con el crecimiento del ojo y la miopía. El procedimiento se llevará a cabo bajo anestesía general inducida por inhalación de	☐ SI ☐ Inyectable ☒ Inhalatoria	☐ NO	☐ SI ☐ Previa ☐ Solo posterior	☒ NO	1 hora

ÁMBITO- PREFIJO
GEISER
Nº registro
O00023280e2100023620

CSV
GEISER-5740-83a2-42e5-469d-a558-3855-bbfc-93ed
DIRECCIÓN DE VALIDACIÓN
https://sede.administracionespublicas.gob.es/valida

FECHA Y HORA DEL DOCUMENTO
14/05/2021 12:30:31 Horario peninsular
Validez del documento
Copia

GEISER-5740-83a2-42e5-469d-a558-3855-bbfc-93ed

isoflurano al 4-5%. Previamente a la anestesia general, las cobayas se someterán a un ayuno de 2 horas.					

5. APLICACIÓN DE MÉTODOS PARA REEMPLAZAR, REDUCIR Y REFINAR (3R) EL USO DE ANIMALES EN PROCEDIMIENTOS

Justificación de la necesidad de utilización de animales

¿Existe un método alternativo?[1]	Si se cree que no existen métodos alternativos, explicar cómo ha llegado a esa conclusión. Citar las fuentes consultadas: Debido a la naturaleza de ambos tratamientos, tanto la luz azul como las lentes de contacto de ortoqueratología, y de las variables que se quieren analizar, no existen métodos alternativos para llevar a cabo la experimentación. Se requiere de animales para estudiar la influencia de ambos tratamientos en la progresión del crecimiento del ojo y el resto de parámetros morfológicos, fisiológicos y bioquímicos, por lo que no existe un método alternativo de experimentación in vivo o ex vivo. Tras hacer una búsqueda sistemática en los recursos web de métodos alternativos facilitada por el comité de experimentación animal de la Universidad Complutense de Madrid, no se han encontrado otros métodos alternativos de experimentación in vivo o ex vivo. Algunos de las principales fuentes de búsqueda pertenecen a los siguientes organismos: Alternatives Research & Development Foundation, Guidelines for Ethical Conduct in the Care and Use of Animals, CMR, In Vitro Testing Platform (IVTIP). Todos los recursos web utilizados se pueden consultar en el siguiente enlace: https://www.ucm.es/data/cont/docs/3-2019-02-08-paginas%20web%20relativas%20a%20metodos%20alternativos.pdf

Justificar el tamaño de la muestra (animales/grupo) **y método estadístico utilizado para ello**

Describa brevemente cada uno de los experimentos que vaya a realizar y el método estadístico propuesto para el análisis (ver NOTAS). Si necesita más líneas, puede añadirlas pulsando + a la derecha de la última línea activa

Experimento 1:	En el caso de los cobayas, se estudiará el efecto que tiene la estimulación de la retina con luz blanca ambiental, oscuridad, luz azul ambiental y luz azul focalizada en el nervio óptico (4 grupos) sobre diferentes variables en relación a la morfología, la fisiología y la bioquímica ocular. Por lo tanto, para el análisis estadístico se requerirá un contraste de hipótesis para comparar simultáneamente los resultados de cada variable entre los 4 grupos independientes. Estas comparaciones se harán para las medidas basales, y tras 1, 15, 30 y 90 días.
Experimento 2:	En el caso de los conejos, se estudiará el efecto que tienen las lentes de contacto de ortoqueratología sobre diferentes variables en relación a la morfología, la fisiología y la bioquímica ocular. Se establecerán dos grupos

Código seguro de Verificación : GEISER-5740-83a2-42e5-469d-a558-3855-bbfc-93ed | Puede verificar la integridad de este documento en la siguiente dirección : https://sede.administracionespublicas.gob.es/valida

ÁMBITO- PREFIJO **GEISER** | CSV **GEISER-5740-83a2-42e5-469d-a558-3855-bbfc-93ed** | FECHA Y HORA DEL DOCUMENTO **14/05/2021 12:30:31 Horario peninsular**
Nº registro **O00023280e2100023620** | DIRECCIÓN DE VALIDACIÓN **https://sede.administracionespublicas.gob.es/valida** | Validez del documento **Copia**

GEISER-5740-83a2-42e5-469d-a558-3855-bbfc-93ed

	(conejos sin lentes de contacto como control y con lentes), por lo que se realizará también un contraste de hipótesis para comparar los resultados de cada variable entre los 2 grupos independientes. Estas comparaciones se harán para las medidas basales, y tras 1, 15, 30 y 90 días.
Experimento 3:	
Experimento :	

NOTAS:

- Si el análisis estadístico a realizar en el/los experimento/s propuesto/s es descriptivo o requiere comparaciones o contrastes de hipótesis, ya sea entre dos o más grupos en comparación simultánea, indicar en la Tabla 1 los parámetros a fijar para justificar el tamaño muestral de cada experimento.
- Si se emplea otra metodología de análisis estadístico (modelos de regresión, análisis factorial, modelos de supervivencia, etc.), justificar, en cada caso y brevemente, el tamaño muestral estimado

Estimación del número total de animales del proyecto (incluida la cría de líneas)	El número total de animales es el que se deriva del cálculo del tamaño de la muestra que se especifica en esta misma sección. No se requerirá de la cría de líneas, por lo que el número de animales utilizados se limitará al calculado.
Justificar la necesidad ausencia de enriquecimiento ambiental	Durante los experimentos, los animales se mantendrán en las mismas condiciones ambientales de estabulación a las que estaban sometidos previamente en la granja donde se crían (18ºC, humedad relativa ambiental de aproximadamente el 40% y libre acceso a comida y agua). No obstante, los conejos se aislarán en jaulas individuales, al igual que las cobayas pertenecientes al grupo al que se le realiza la vitrectomía para estimular el nervio óptico con luz azul.
Métodos de Refinamiento para mejorar el bienestar animal[2]	Justificar las decisiones tomadas: Los animales tendrán libre acceso a comida y agua, condiciones ambientales controladas, un estabulario acorde a la Directiva 2010/63/EU del Parlamento Europeo y del Consejo y tanto un control como un mantenimiento diario. En caso de dolor, sufrimiento o angustia animal que no sea lo esperando en cada uno de los procedimientos, se tomarán las medidas necesarias para cada caso concreto, pudiendo practicarse la eutanasia en caso de que dichos efectos sean irreversibles. En el caso de los conejos, no se espera que el tratamiento con lentes de contacto produzcan efectos secundarios indeseados sobre la superficie ocular, ya que se espera que dicho tratamiento tenga el mismo efecto que en los humanos. Por otro lado, dado que se espera un proceso inflamatorio tras la cirugía de vitrectomía en uno de los grupos de cobayas, se administrarán antiinflamatorios en caso de que fuese necesario, como por ejemplo Metacam 0.5 mg/kg/día (suspensión oral), evaluando la inflamación ocular mediante biomicroscopía (procedimiento 5).
Medidas para evitar la repetición injustificada de procedimientos	Los procedimientos de este estudio ya se han usado previamente bajo condiciones similares y en los mismos animales en el grpo de investigación. Todos los procedimientos son de carácter leve, excepto la vitrectomía (P4) que se clasifica como moderado. El resto de procedimientos de medida (desde P5 hasta P8) son de carácter no invasivo, por lo que no se espera ningún efecto sobre la salud ocular de los animales. Las medidas de estos procedicimientos (P5-P8) se harán durante 5 días (medida basal y tras 1, 15, 30 y 90 días) para evaluar el efecto a medio plazo de los tratamientos, por lo que el resto de días los conejos no serán sometidos a dichos procedimientos.

Código seguro de Verificación : GEISER-5740-83a2-42e5-469d-a558-3855-bbfc-93ed | Puede verificar la integridad de este documento en la siguiente dirección : https://sede.administracionespublicas.gob.es/valida

ÁMBITO- PREFIJO
GEISER
Nº registro
O00023280e2100023620

CSV
GEISER-5740-83a2-42e5-469d-a558-3855-bbfc-93ed
DIRECCIÓN DE VALIDACIÓN
https://sede.administracionespublicas.gob.es/valida

FECHA Y HORA DEL DOCUMENTO
14/05/2021 12:30:31 Horario peninsular
Validez del documento
Copia

GEISER-5740-83a2-42e5-469d-a558-3855-bbfc-93ed

Código seguro de Verificación : GEISER-5740-83a2-42e5-469d-a558-3855-bbfc-93ed | Puede verificar la integridad de este documento en la siguiente dirección : https://sede.administracionespublicas.gob.es/valida

ÁMBITO- PREFIJO
GEISER
Nº registro
O00023280e2100023620

CSV
GEISER-5740-83a2-42e5-469d-a558-3855-bbfc-93ed
DIRECCIÓN DE VALIDACIÓN
https://sede.administracionespublicas.gob.es/valida

FECHA Y HORA DEL DOCUMENTO
14/05/2021 12:30:31 Horario peninsular
Validez del documento
Copia

GEISER-5740-83a2-42e5-469d-a558-3855-bbfc-93ed

Tabla 1. Justificación del tamaño de la muestra en cada experimento y en el total del proyecto (Añada tantas filas como necesite, pulsando en + a la derecha en la última línea activa)

Experimento nº	1. Número de grupos que se formarán en el experimento	2. Número máximo de grupos en comparación simultánea (p. e. ANOVA)	3. Nivel de significación del test o de los tests a realizar	4. Potencia requerida del test o de los tests	5. Desviación estándar o típica común*	6. Diferencia mínima a detectar**	7. Proporción prevista de pérdidas en el seguimiento	8. Tipo de test que se va a realizar "unilateral o bilateral"	Número de animales por grupo	Número total de animales
1	4	4	0.05	0.80	1	1.8 la desviación típica	0.1		10	40
2	2	2	0.05	0.80	1	1.8 la desviación típica	0.1		6	12
3										
4										
5										
Número total estimado de animales necesarios para el proyecto										52

* Si no se conoce, se puede fijar en 1 y en el apartado siguiente expresar la diferencia que se pide en DT

** Indicar la diferencia significativa entre dos grupos, en términos absolutos o en DT (si se trata de proporciones, expresar esta diferencia en puntos porcentuales)

Observaciones punto 5.

1.- ¿Existe método alternativo?: En este apartado debe indicar las páginas Web relativas a métodos alternativos que ha consultado. Las publicaciones o justificación del proyecto, no son fuentes de métodos alternativos.
Puede consultar en la Web de la UCM el enlace a recursos web de métodos alternativos que le pueden servir de ayuda https://www.ucm.es/reuniones-del-comite

2.- Refinamiento de los procedimientos: reducción del número de animales utilizados y reemplazamiento por otros animales o métodos que no utilicen animales vivos. Indicar las medidas empleadas para mejorar el bienestar animal y reducir posibles situaciones de estrés y/o malestar, incluyendo el empleo de anestesia y/o analgesia

Código seguro de Verificación : GEISER-5740-83a2-42e5-469d-a558-3855-bbfc-93ed | Puede verificar la integridad de este documento en la siguiente dirección : https://sede.administracionespublicas.gob.es/valida

ÁMBITO- PREFIJO
GEISER
Nº registro
O00023280e2100023620
CSV
GEISER-5740-83a2-42e5-469d-a558-3855-bbfc-93ed
DIRECCIÓN DE VALIDACIÓN
https://sede.administracionespublicas.gob.es/valida
FECHA Y HORA DEL DOCUMENTO
14/05/2021 12:30:31 Horario peninsular
Validez del documento
Copia
GEISER-5740-83a2-42e5-469d-a558-3855-bbfc-93ed

Código seguro de Verificación : GEISER-5740-83a2-42e5-469d-a558-3855-bbfc-93ed | Puede verificar la integridad de este documento en la siguiente dirección : https://sede.administracionespublicas.gob.es/valida

ÁMBITO- PREFIJO
GEISER
Nº registro
O00023280e2100023620

CSV
GEISER-5740-83a2-42e5-469d-a558-3855-bbfc-93ed
DIRECCIÓN DE VALIDACIÓN
https://sede.administracionespublicas.gob.es/valida

FECHA Y HORA DEL DOCUMENTO
14/05/2021 12:30:31 Horario peninsular
Validez del documento
Copia

GEISER-5740-83a2-42e5-469d-a558-3855-bbfc-93ed

6. MEDIDAS CORRECTORAS PARA REDUCIR EL DOLOR, EVITAR Y ALIVIAR CUALQUIER FORMA DE SUFRIMIENTO DE LOS ANIMALES A LO LARGO DE TODA SU VIDA, CUANDO PROCEDA

Si necesita más líneas, puede añadirlas pulsando + a la derecha de la última línea activa

Analgésicos (principio activo / Nombre comercial, concentración)	**Dosis, Vía**	**Frecuencia**	
		Nº de veces	**Intervalo**

Anestésicos (principio activo / Nombre comercial, concentración)	**Dosis, Vía**	**Frecuencia**	
		Nº de veces	**Intervalo**
Anestésico general inhalatorio / Isoflurano al 4-5%. Anestesia general. En el caso de las cobayas, todos los procedimientos (desde P4 a P8) se realizarán con anestesia general. Los procedimientos en conejos no requieren de anestesia general ya que no son dolorosos y la manipulación de los conejos puede hacerse sin anestesia (el grupo de investigación ya tiene experiencia previa).	0.5-1 l/min / Inhalación / 1 vez al día	6	Durante la cirugía, medida basal y tras 1, 15, 30 y 90 días.

7. USO DE PUNTOS FINALES HUMANITARIOS

Destino final de los animales

☐**Recuperación** ☐**Reutilización**	☒ **Sacrificio. Método (actuación, medicamento / concentración principio activo, vía, dosis, intervalo de dosis,duración etc.) y nombre de la persona responsable de la eutanasia:** La eutanasia se llevará a cabo una vez acabe el estudio por parte del investigador principal Juan Gonzalo Carracedo Rodríguez. En las cobayas, se hará mediante la inhalación de CO2 al 8% durante un período aproximado de 5 minutos. En los conejos, la eutanasia se realizará mediante inyección intravenosa de pentobarbital sódico (300 mg/kg). Los procedimientos serán realizado por el responsable del procedimiento del estudio.

Si no se realiza la eutanasia, actuación para reducir el sufrimiento a lo largo del resto de su vida:

Criterios de punto final humanitario o de finalización anticipada del estudio o de la eutanasia anticipada del animal*

Explicar detalladamente el criterio para su aplicación: El sacrificio de los animales al final del estudio es necesario ya que los ojos de los animales se van a enuclear para su posterior procesado. Los ojos se procesarán para hacer cortes histológicos que permitan su caracterización morfológica mediante microscopía óptica y electrónica, para calcular la concentración de dopamina y otras moléculas implicadas en el crecimiento del ojo y para localizar los receptores de dichas moléculas. El análisis de todas estas variables, en caso de que los resultados fueran satisfactorios, permitirá conocer los mecanismos oculares que regulan el crecimiento del globo ocular, abriendo una ventana a nuevos tratamientos farmacológicos y ópticos para controlar este crecimiento y así poder evitar el desarrollo patológico de la miopía, la cual puede conducir a la ceguera.

Enlace a página Web INFORMATIVA sobre punto final humanitario https://www.humane-endpoints.info/es

Código seguro de Verificación : GEISER-5740-83a2-42e5-469d-a558-3855-bbfc-93ed | Puede verificar la integridad de este documento en la siguiente dirección : https://sede.administracionespublicas.gob.es/valida

ÁMBITO- PREFIJO	CSV	FECHA Y HORA DEL DOCUMENTO
GEISER	**GEISER-5740-83a2-42e5-469d-a558-3855-bbfc-93ed**	**14/05/2021 12:30:31 Horario peninsular**
Nº registro	DIRECCIÓN DE VALIDACIÓN	Validez del documento
O00023280e2100023620	**https://sede.administracionespublicas.gob.es/valida**	**Copia**

GEISER-5740-83a2-42e5-469d-a558-3855-bbfc-93ed

8. DATOS DE LAS MODIFICACIONES GENÉTICAS (si procede)

Si necesita más líneas, puede añadirlas pulsando + a la derecha de la última línea activa

Nombre de la línea modificada	Modificación / Fenotipo/genotipo *	Severidad

Cualquier línea añadida con posterioridad en el proyecto será clasificada como severa hasta que no se verifique la ausencia de malestar, dolor o sufrimiento en los animales durante el primer año de vida o hasta que no se caracterice y valore la severidad real del fenotipo generado"

* Modificación/Fenotipo: Especificar la modificación, el fenotipo a que da lugar.

9. CONDICIONES DE ALOJAMIENTO, ZOOTÉCNICAS Y DE CUIDADO DE LOS ANIMALES

Estabulación

Aislamiento (si/no)	Si se aísla (duración y justificación)
Sí	Del total de 40 cobayas, solamente se aislarán a las 10 cobayas que pertenecen al grupo que se someterá a la cirugía de vitrectomía para estimular el nervio óptico con luz azul durante los 3 meses del estudio para evitar que la interacción de unas con otras aumente el riesgo de efectos secundarios. De los 12 conejos, todos ellos también se aislarán en jaulas individuales durante los 3 meses del estudio.

Método físico de contención (jaula metabólica, cepo de sujeción…)	Duración	Justificación
Cepo de sujeción: se requiere para introducir la fibra de luz azul diáriamente en el globo ocular de las cobayas con el fin de estimular selectivamente el nervio óptico.	2 minutos al día	

Especificar los requerimientos particulares de manejo (si los hubiera para los animales de este ensayo)

Problemas conocidos relacionados con la reproducción y cría de cualquier especie, raza, estirpe o línea que se vaya a utilizar en el proyecto

No se criará ninguna especie.

Requiere el presente proyecto la modificación de cualquier parámetro medioambiental del animal

Sí, a 2 de los 5 grupos de cobayas se les cambiará su ciclo de 12 horas de luz blanca/oscuridad a un ciclo de 12 horas de luz azul/oscuridad a 1 grupo y 24 horas de oscuridad a 1 grupo. Esto afectará a los ciclos circadianos de las cobayas.

Protocolo de supervisión de los animales (diario, semanal, mensual, momento crítico…)

Diario

Observaciones punto 9

Si es necesario el aislamiento en jaula metabólica /otros métodos hay que justificarlo e indicar medidas paliativas del estrés que esto supone y debería considerarse otro procedimiento e incluirlo en ese apartado y describir el tipo de severidad. Consultar ANEXO IX

EVALUACIÓN RETROSPECTIVA

Código seguro de Verificación : GEISER-5740-83a2-42e5-469d-a558-3855-bbfc-93ed | Puede verificar la integridad de este documento en la siguiente dirección : https://sede.administracionespublicas.gob.es/valida

ÁMBITO- PREFIJO **GEISER** | CSV **GEISER-5740-83a2-42e5-469d-a558-3855-bbfc-93ed** | FECHA Y HORA DEL DOCUMENTO **14/05/2021 12:30:31 Horario peninsular**
Nº registro **O00023280e2100023620** | DIRECCIÓN DE VALIDACIÓN **https://sede.administracionespublicas.gob.es/valida** | Validez del documento **Copia**

GEISER-5740-83a2-42e5-469d-a558-3855-bbfc-93ed

El proyecto será sometido a una evaluación retrospectiva si:

- Utiliza Primates.
- Se incluyen procedimientos clasificados como "severos".
- La realización de procedimientos que conlleven dolor, sufrimiento o angustia severos para los animales y sea probable que dichos efectos sean prolongados y no puedan ser aliviados, cuando por razones excepcionales y científicamente fundadas, se considere necesaria dicha realización.
- Si es solicitado por el Comité de ética.

El plazo de presentación de la evaluación retrospectiva será notificado junto con el Informe Favorable donde se evaluará:

- Si se han alcanzado los objetivos del proyecto.
- El daño infringido a los animales, incluidos el número y las especies de animales utilizados, y la severidad de los procedimientos;
- Cualquiera de los elementos que puedan contribuir a una mejor aplicación del requisito de las 3R (reemplazo, reducción y refinamiento).

Código seguro de Verificación : GEISER-5740-83a2-42e5-469d-a558-3855-bbfc-93ed | Puede verificar la integridad de este documento en la siguiente dirección : https://sede.administracionespublicas.gob.es/valida

ÁMBITO- PREFIJO	CSV	FECHA Y HORA DEL DOCUMENTO
GEISER	**GEISER-5740-83a2-42e5-469d-a558-3855-bbfc-93ed**	**14/05/2021 12:30:31 Horario peninsular**
Nº registro	DIRECCIÓN DE VALIDACIÓN	Validez del documento
O00023280e2100023620	**https://sede.administracionespublicas.gob.es/valida**	**Copia**

GEISER-5740-83a2-42e5-469d-a558-3855-bbfc-93ed

Código seguro de Verificación : GEISER-5740-83a2-42e5-469d-a558-3855-bbfc-93ed | Puede verificar la integridad de este documento en la siguiente dirección : https://sede.administracionespublicas.gob.es/valida

ANEXO I

Clasificación de la severidad de los procedimientos

La severidad de un procedimiento se determinará por el grado de dolor, sufrimiento, angustia o daño prolongado que se prevé que pueda experimentar un animal de forma individual durante el procedimiento.

Sección I: Categorías de severidad.

Sin recuperación: los procedimientos que se realizan en su totalidad bajo anestesia general de la cual el animal no recupera la consciencia, deben clasificarse como "sin recuperación".

Leve: los procedimientos a consecuencia de los cuales los animales es probable que experimenten dolor, sufrimiento o angustia leves de corta duración, así como los procedimientos sin alteración significativa del bienestar o del estado general de los animales, deben clasificarse como "leves".

Moderado: los procedimientos a consecuencia de los cuales es probable que los animales experimenten dolor, sufrimiento o angustia moderados de corta duración, o leves pero duraderos, así como los procedimientos que pudieran causar una alteración moderada del bienestar o del estado general de los animales, deben clasificarse como "moderados".

Severo: los procedimientos a consecuencia de los cuales es probable que los animales experimenten dolor, sufrimiento o angustia intensos o moderados pero prolongados, así como los procedimientos que pudieran causar una alteración grave del bienestar o del estado general de los animales, deben clasificarse como "severos".

Sección II: Criterios de clasificación.

La clasificación de la categoría de severidad tendrá en cuenta cualquier intervención o manipulación de un animal en un procedimiento determinado. Se basará en el efecto más severo que pueda experimentar un animal después de aplicar todas las técnicas apropiadas de refinamiento.

En la asignación a un procedimiento de una categoría particular se han de tener en cuenta el tipo de procedimiento y otros muchos factores, los cuales habrán de considerarse caso por caso.

Los factores relativos al procedimiento deben incluir:
- Tipos de manipulación y manejo;
- Naturaleza del dolor, sufrimiento, angustia o daño prolongado causados por todos los elementos del procedimiento, así como su intensidad, duración, frecuencia y la multiplicidad de técnicas empleadas;
- Sufrimiento acumulativo en el procedimiento;
- Impedimento de expresar el comportamiento natural, incluidas las restricciones en los estándares de alojamiento, zootécnicos y de cuidado de los animales.

En la sección III se establecen tipos de procedimientos atribuidos a cada categoría de severidad sobre la base de los factores relativos al tipo de procedimiento de que se trate. Facilitarán la primera indicación sobre la clasificación que sería la más adecuada para un determinado tipo de procedimiento.

Sin embargo, a efectos de la clasificación final de severidad de los procedimientos, se han de tener en cuenta los siguientes factores adicionales, valorados caso por caso:
- Tipo de especie y genotipo;
- Madurez, edad y sexo del animal;
- Grado de aprendizaje del animal para el procedimiento;
- Si se reutiliza el animal, la severidad real de los procedimientos anteriores;
- Métodos utilizados para reducir o suprimir el dolor, el sufrimiento y la angustia, incluidos el refinamiento de las condiciones de alojamiento, zootécnicas y de cuidado de los animales:
- Uso de puntos finales humanitarios.

Sección III: Tipos de procedimiento atribuidos a cada categoría de severidad sobre la base de los factores relativos al tipo de procedimiento.

1. ***Leve***:

a) Administración de anestesia, salvo para el único propósito de eutanasia:

ÁMBITO- PREFIJO | CSV | FECHA Y HORA DEL DOCUMENTO
GEISER | **GEISER-5740-83a2-42e5-469d-a558-3855-bbfc-93ed** | **14/05/2021 12:30:31 Horario peninsular**
Nº registro | DIRECCIÓN DE VALIDACIÓN | Validez del documento
O00023280e2100023620 | **https://sede.administracionespublicas.gob.es/valida** | **Copia**

GEISER-5740-83a2-42e5-469d-a558-3855-bbfc-93ed

b) Estudio farmacocinético donde se administra una única dosis y se recoge un número limitado de muestras de sangre (totalizando < 10 por cien del volumen circulante) y no se prevé que la sustancia cause ningún efecto nocivo detectable;

c) Técnicas no invasivas de diagnóstico por imagen en animales (por ejemplo resonancia magnética) con la sedación o la anestesia apropiada;

d) Procedimientos superficiales, por ejemplo biopsias de oreja y rabo, implantación subcutánea no quirúrgica de minibombas y transpondedores;

e) Aplicación de dispositivos exteriores de telemetría que únicamente causan al animal un debilitamiento menor o una interferencia menor con la actividad y el comportamiento normales;

f) Administración de sustancia por vía subcutánea, intramuscular, intraperitoneal, por sonda gástrica e intravenosa a través de los vasos sanguíneos superficiales, donde la sustancia solo tiene un efecto leve en el animal, y los volúmenes se encuentran dentro de límites apropiados para el tamaño y la especie del animal;

g) Inducción de tumores, o tumores espontáneos, que no causan ningún efecto nocivo clínico perceptible (por ejemplo nódulos pequeños, subcutáneos, no invasivos);

h) Cría de animales genéticamente modificados que se prevé que dé lugar a un fenotipo con efectos leves;

i) Alimentación con dietas modificadas, que no cubren las necesidades nutricionales de todos los animales y se prevé que causen una anomalía clínica leve en el periodo de estudio;

j) Confinamiento a corto plazo (< 24 h) en jaulas metabólicas;

k) Estudios que implican la privación a corto plazo de compañeros sociales, enjaulado solitario a corto plazo de ratas o ratones adultos de estirpes gregarias;

l) Modelos que exponen al animal a estímulos nocivos que se asocian brevemente con dolor, sufrimiento o angustia leve, y que el animal puede evitar;

m) Una combinación o una acumulación de los siguientes ejemplos puede dar lugar a una clasificación leve:

1º. Evaluación de la composición corporal a través de mediciones no invasivas y restricción mínima;
2º. Supervisión ECG con técnicas no invasivas con una restricción mínima o nula de animales habituados;
3º. Aplicación de dispositivos exteriores de telemetría que no se prevé que causen ningún impedimento a animales socialmente adaptados y que no interfieren con la actividad y el comportamiento normales;
4º. Cría de animales genéticamente modificados que no se espera que tengan ningún fenotipo adverso clínicamente perceptible;
5º. Adición a la dieta de marcadores inertes para seguir el paso de la ingesta;
6º. Retirada de la alimentación durante un periodo inferior a 24h en ratas adultas;
7º. Ensayos en campo abierto.

2. ***Moderado***:

a) Aplicación frecuente de sustancias de prueba que producen efectos clínicos moderados, y extracción de muestras de sangre (> 10 por cien de volumen circundante) en un animal consciente en el plazo de algunos días sin sustitución del volumen;

b) Estudios de determinación de la gama de dosis causante de toxicidad aguda, pruebas de toxicidad crónica/carcinogenicidad, con puntos finales no letales;

c) Cirugía bajo anestesia general y analgesia apropiada, asociada con dolor o sufrimiento posquirúrgicos o alteración posquirúrgica de la condición general. Los ejemplos incluyen: toracotomía, craneotomía, laparotomía u orquidectomía, linfadenectomía, tiroidectomía, cirugía ortopédica con estabilización efectiva y cuidado de heridas, trasplante de órganos con tratamiento efectivo del rechazo, implantación quirúrgica de catéteres, o dispositivos biomédicos (por ejemplo transmisores de telemetría, minibombas, etc.);

d) Modelos de inducción de tumores, o tumores espontáneos, que se prevé que causen dolor o angustia moderados o interferencia moderada con el comportamiento normal;

Código seguro de Verificación : GEISER-5740-83a2-42e5-469d-a558-3855-bbfc-93ed | Puede verificar la integridad de este documento en la siguiente dirección : https://sede.administracionespublicas.gob.es/valida

ÁMBITO- PREFIJO	CSV	FECHA Y HORA DEL DOCUMENTO
GEISER	**GEISER-5740-83a2-42e5-469d-a558-3855-bbfc-93ed**	**14/05/2021 12:30:31 Horario peninsular**
Nº registro	DIRECCIÓN DE VALIDACIÓN	Validez del documento
O00023280e2100023620	**https://sede.administracionespublicas.gob.es/valida**	**Copia**

GEISER-5740-83a2-42e5-469d-a558-3855-bbfc-93ed

e) Irradiación o quimioterapia con una dosis subletal, o con una dosis que de otro modo sería letal, pero con reconstitución del sistema inmunitario. Cabría esperar que los efectos nocivos fueran leves o moderados y que fueran efímeros (< 5 días);

f) Cría de animales genéticamente modificados que se espera den lugar a un fenotipo con efectos moderados;

g) Producción de animales genéticamente modificados mediante procedimientos quirúrgicos;

h) Uso de jaulas metabólicas que impliquen una restricción moderada de movimientos durante un periodo prolongado (hasta 5 días);

i) Estudios con dietas modificadas que no cubren las necesidades nutricionales de todos los animales y que se espera que causen una anomalía clínica moderada en el periodo de estudio;

j) Retirada de la alimentación durante 48 horas en ratas adultas;

k) Provocación de reacciones de escape y evitación cuando el animal no pueda escapar o evitar el estímulo, y que se espera que dé lugar a una angustia moderada.

3. ***Severo***:

a) Ensayos de toxicidad en los que la muerte sea el punto final, o en los que se prevean muertes y se causen estados fisiopatológicos intensos. Por ejemplo, ensayo de toxicidad aguda de dosis única (véanse las directrices de la OCDE sobre ensayos);

b) Ensayos de dispositivos en los que el fracaso pueda causar dolor o angustia severos o la muerte del animal (por ejemplo dispositivos de reanimación cardiaca);

c) Ensayo de potencia de una vacuna caracterizada por la alteración persistente del estado del animal, enfermedad progresiva que causa la muerte, asociada con dolor, angustia o sufrimiento moderado prolongado;

d) Irradiación o quimioterapia con una dosis letal sin reconstitución del sistema inmunitario, o reconstitución con la producción de enfermedad de injerto contra huésped;

e) Modelos con inducción de tumores, o con tumores espontáneos, que se espera causen enfermedad mortal progresiva asociada con dolor, angustia o sufrimiento moderado duradero. Por ejemplo tumores que causan caquexia, tumores óseos invasivos, tumores que dan lugar a diseminación metastásica, y tumores que se permite que se ulceren;

f) Intervenciones quirúrgicas y otras en animales bajo anestesia general que se espera den lugar a dolor, sufrimiento o angustia postoperatorios moderados severos o persistentes, o a una alteración severa y persistente de la condición general del animal. Producción de fracturas inestables, toracotomía sin analgesia adecuada, o traumatismo para producir el fallo multiorgánico;

g) Trasplante de órgano donde es probable que el rechazo del órgano origine angustia o la alteración severa del estado general del animal (por ejemplo xenotransplante);

h) Reproducción de animales con trastornos genéticos que se espera experimenten una alteración severa y persistente de su estado general, por ejemplo la enfermedad de Huntington, distrofia muscular, modelos de neuritis crónicas recurrentes;

i) Uso de jaulas metabólicas que impliquen una restricción severa de los movimientos durante un periodo prolongado;

j) Choque eléctrico ineludible (por ejemplo para producir invalidez inducida);

k) Aislamiento completo durante periodos prolongados de especies gregarias, por ejemplo perros y primates;

l) Tensión de inmovilización para inducir úlceras gástricas o fallo cardiaco en ratas;

m) Natación forzada o pruebas de ejercicio con el agotamiento como punto final.

Código seguro de Verificación : GEISER-5740-83a2-42e5-469d-a558-3855-bbfc-93ed | Puede verificar la integridad de este documento en la siguiente dirección : https://sede.administracionespublicas.gob.es/valida

ÁMBITO- PREFIJO	CSV	FECHA Y HORA DEL DOCUMENTO
GEISER	**GEISER-5740-83a2-42e5-469d-a558-3855-bbfc-93ed**	**14/05/2021 12:30:31 Horario peninsular**
Nº registro	DIRECCIÓN DE VALIDACIÓN	Validez del documento
O00023280e2100023620	**https://sede.administracionespublicas.gob.es/valida**	**Copia**

GEISER-5740-83a2-42e5-469d-a558-3855-bbfc-93ed

This PhD Thesis was focused on the design of soft CLs suitable for the loading and release of therapeutic amounts of drugs useful for the treatment of diabetic-related ocular diseases. Two types of combination products have been developed: soft CLs with atorvastatin and soft CLs with pravastatin. Release profiles of drug-loaded CLs in a 3D printed in vitro model were compared with drug levels in the tear fluid of in vivo animal models. Melanin was incorporated into CLs with the double aim of incorporating drugs into CLs, and endowing CLs with photothermal capacity. This work render drug-CL combination products for topical ocular drug delivery that provide sustained drug levels in the ocular surface. Moreover, in vitro test methods that mimic drug release on the ocular surface have been identified.